NASA-FC-Conf-March 24-25 1964 Vol 2
Cy 1

GEORGE C. MARSHALL SPACE FLIGHT CENTER
HUNTSVILLE, ALABAMA

N67-86145 N67-86155
(ACCESSION NUMBER) (THRU)
(CODE)
(CATEGORY)
FACILITY FORM 602

PROCEEDINGS OF THE CONFERENCE ON DESIGN OF LEAK-TIGHT SEPARABLE FLUID CONNECTORS

March 24, 25, 1964

VOLUME II
of
TWO VOLUMES

National Aeronautics and Space Administration

NASA

REPRODUCED BY
NATIONAL TECHNICAL
INFORMATION SERVICE
U. S. DEPARTMENT OF COMMERCE
SPRINGFIELD, VA. 22161

FC - Form 454 (Revised September 1961)

394

GEORGE C. MARSHALL SPACE FLIGHT CENTER

PROCEEDINGS OF THE CONFERENCE ON DESIGN OF LEAK-TIGHT SEPARABLE FLUID CONNECTORS

March 24 25 1964

Volume II
of
Two Volumes

REPRODUCED BY
NATIONAL TECHNICAL
INFORMATION SERVICE
U.S. DEPARTMENT OF COMMERCE
SPRINGFIELD, VA. 22161

PROPULSION DIVISION
PROPULSION AND VEHICLE ENGINEERING LABORATORY

TABLE OF CONTENTS
FOR VOLUME II

Page

SESSION III

Interaction of Flange, Gasket, and Pipe
S. LEVY, Senior Mechanical Engineer, Advanced Technology Laboratories, General Electric Company. 1

Development and Application of Separable Fluid Connectors for Liquid-Propellant Rocket Engines
C. M. DANIELS, Rocketdyne, A Division of North American Aviation, Inc. 23

Analysis of Pressure Energized Seals
JOHN WALLACH, Mechanical Engineer, Advanced Technology Laboratories, General Electric Company. 97

Design of Static Elastomeric Seals for Cryogenic Temperatures
D. H. WEITZEL, P. R. LUDTKE, and R. F. ROBBINS
Cryogenic Engineering Laboratory, National Bureau of Standards 139

The Development of a New Cryogenic Gasket for Liquid Oxygen Service - Part I,
DR. R. B. GOSNELL, NARMCO Research and Development, A Division of Telecomputing Corporation 167

The Development of a New Cryogenic Gasket for Liquid Oxygen Service - Part II
F. M. WILSON, J. W. FELDMANN, C. R. THOMPSON
NARMCO Research and Development, A Division of Telecomputing Corporation 209

SESSION IV

Experimental Leakage Rate Experiments
F. O. RATHBUN, JR. Mechanical Engineer, Advanced Technology Laboratories, General Electric Company. 249

A Bolted Flange Joint Incorporating a Soft Aluminum Gasket
J. A. ZIMMERMAN, Group Engineer, Titan II Propulsion, Martin Company 288

Preceding page blank

TABLE OF CONTENTS (CONCLUDED)

Page

Bimetallic Seal for Advanced Aerospace Fluid Systems
W. A. PRINCE, Senior Design Engineer, General Dynamics/Astronautics. 307

Design and Test of Marman CONOSEAL Joint
HUB DYKSTRA, Aeroquip Corporation/Marman Division. 331

APPENDIX
List of Industry and Agency Attendees. 389

TABLE OF CONTENTS
FOR VOLUME I

Page

FOREWORD 1

CHAIRMEN AND COMMITTEES 2

SESSION I

Zero Leakage Effort for Saturn Vehicles
H. BERGELER, Deputy Chief, Applied Mechanical Research Branch, MSFC. 3

Statistical Evaluation of Flare Dimensions Obtainable with Current Manufacturing Processes
R. D. BLAKLEY, Chrysler Corporation Space Division . . . 29

The Problem of Stating the Tube Connector Problem
KEN BRAGG, Chief Engineer, Systems and Advanced Components Division, Parker Aircraft Company 45

Five Regimes of Metal-to-Metal Sealing
F. O. RATHBUN, JR., Mechanical Engineer, Advanced Technology Laboratories, General Electric Company. 63

Significant Factors in the Design and Classification of Separable Tube Connectors
E. C. RODABAUGH, Battelle Memorial Institute 89

Elastic Displacements in the Design of Threaded Fittings
J. W. ADAM, Battelle Memorial Institute 123

Helium Leak-Tight Seal - Functional Analysis and Development
B. GOOBICH, Battelle Memorial Institute 157

SESSION II

Recent Developments of Instrumentation and Measurement for Evaluating Separable Tubing Connector and Manufacturing Tooling
W. B. CRUISE and JOHN R. RASQUIN
Methods Research and Development Branch, Manufacturing Division, MSFC. 193

TABLE OF CONTENTS (CONCLUDED)

Page

Laboratory Leakage Measurement Techniques on Separable Connectors
LARRY E. GRIMES, General Dynamics? Astronautics 213
Leakage Measurement and Evaluation
J. W. MARR, Vacuum Engineer, Advanced Technology Laboratories, General Electric Company. 245
Acoustic Radiation Damage in Materials
DR. B. LANGENECKER, U. S. Naval Ordnance Test Station 307
Optical Observations of Sealing Phenomenon
L. G. GITZENDANNER, Consulting Engineer, Advanced Technology Laboratories, General Electric Company. 327

N67-86146

INTERACTION OF FLANGE, GASKET, AND PIPE

BY

S. LEVEY, SENIOR MECHANICAL ENGINEER
ADVANCED TECHNOLOGY LABORATORIES
GENERAL ELECTRIC COMPANY
SCHENECTADY, NEW YORK

THIS PROGRAM WAS SPONSORED BY GEORGE C. MARSHALL SPACE FLIGHT CENTER, NATIONAL AERONAUTICS AND SPACE ADMINISTRATION.

1. Introduction

A fluid connector mechanically joins two sections of pipe and provides a seal against fluid leakage. It must perform these functions for a wide range of environmental conditions.

Ease in design suggests the use of separate parts of the connector for the "joining" and "sealing" functions with a minimum of interaction between them. Such a design approach avoids compromising the "sealing" function by changes intended to improve the reliability of "joining" and vice versa. The necessity to economize on weight and space does not ordinarily permit the complete separation of functions. As a result, it is found that many connectors in use today have constructions such that flange or bolt flexibility relaxes gasket pressure, while gasket creep may result in joint looseness.

As is pointed out in Ref. 1, the first step in the design of a bolted flanged connection, for example, is to select the seal or gasket material and its shape. Sufficient pressure must then be provided on the gasket to hold the joint tight at all times. The load required to do this as well as overcome the internal fluid pressure, is provided by the bolts and determines their size. The flange dimensions must now be chosen to withstand the bolt load. Similar procedures can be described for other types of joints. After the initial design has been determined, it is necessary to evaluate its performance under the many other environmental conditions which may apply. Consideration must be given to tolerances, material availability, cost, LOX sensitivity, and many other factors.

Internal pressure has a major effect on connectors. In many designs it causes a reduction in gasket pressure and, therefore, in seal performance. A typical example is the conventional flange coupling shown in Fig. 1.

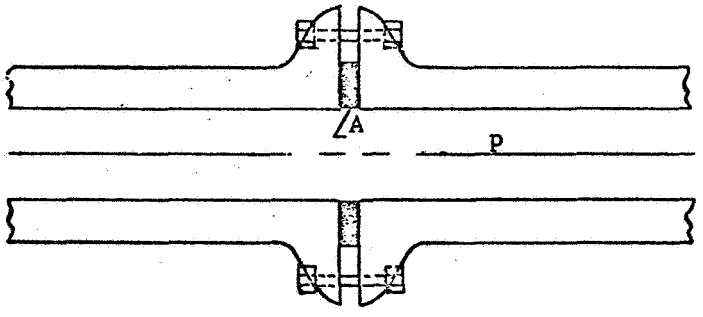

FIG. 1

CONVENTIONAL FLANGE COUPLING

With increasing pressure, p, gasket compression at A decreases. At a sufficiently high pressure, the gasket compression has decreased to be equal in magnitude to the internal pressure. Further increases in internal pressure find the gasket acting as a pressure relief valve with corresponding large-scale

Preceding page blank

leakage. Recognition of the effect of internal pressure on gasket compression has led to many "pressure assisted" seals, a typical example of which is shown in Fig. 2. Such seals are based on Bridgman's "unsupported area" principle (Ref. 2). By allowing the internal pressure to "bulge" the U-shaped seal ring, it is possible to have the seal pressure (at A, for example) increase with internal pressure, p, rather than decrease.

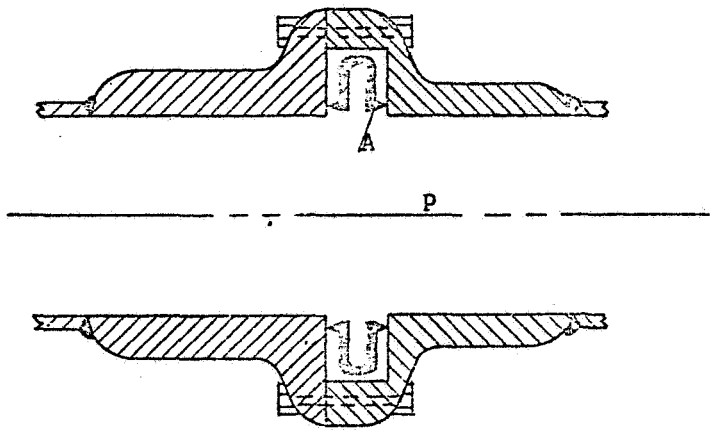

FIG. 2

PRESSURE-ASSISTED SEALS

Temperature changes and temperature transients also have a major effect on connectors. An example of an AN fitting is shown in Fig. 3. A cold fluid starting to flow through the pipe will cool the inside much more rapidly than the sleeve, A, or nut, B. As a result, the contraction of the sleeve and nut will be slower. The sealing pressure will thereby be lowered with increased possibility of leakage. Another example is the flanged connector shown in Fig. 4. Here the flange, A, could

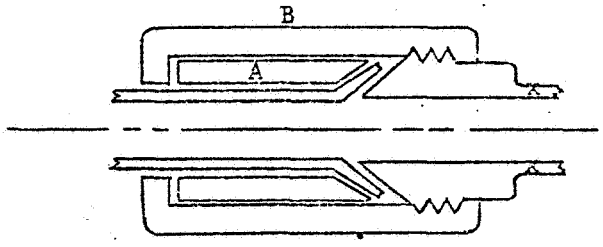

FIG. 3

AN-TYPE FITTING

cool more rapidly than the bolts, B. As a result, the gasket load will be reduced and leakage made more likely. Again, recognition of the effect of temperature change in causing contraction or expansion has resulted in the design of "temperature-compensated" connectors.

In Fig. 5 is shown

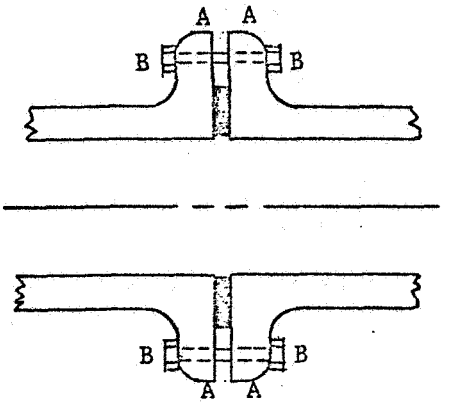

FIG. 4

FLANGED CONNECTOR

a flange connector with a sealant material confined between the flange and an invar ring (Ref. 3). During cooling the sealant contracts proportionately more than the flange material. The invar ring, since it contracts less, tends to compensate for this excess and keep the joint tight. Data on the effect of temperature on the elastic and expansion properties of materials are given in Refs. 4, 5, and 6. Since the coefficients of expansion may vary substantially with temperature, true compensation is seldom achieved.

Bending forces due to vibration or otherwise tend to open one side of the connector and close more tightly the other side.

Other environmental effects include radiation, erosion by the fluid flow, water-hammer, high vacuum, etc.

A successful connector must be capable of withstanding all environmental conditions without coming apart and with essentially zero leakage. To determine if a connector will be adequate, the methods given in the literature must be applied to determine deformations, stresses and leakage flow rates. We will examine some of these methods and how the results thus obtained are combined to determine the overall connector performance.

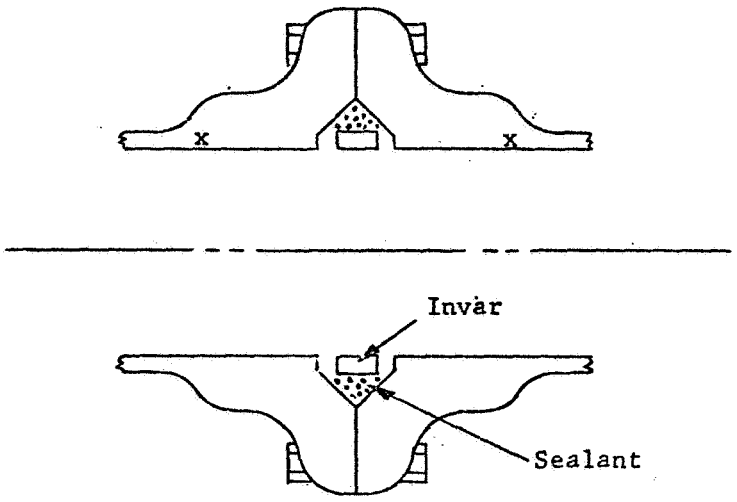

FIG. 5

TEMPERATURE COMPENSATED SEAL

2. Flange Deformation

An excellent discussion of the stresses and deformations of the flanges of connectors is given in Ref. 7. The flanges considered in Ref. 7 have the contact area between flanges entirely within the bolt circle. This reference considers the elastic interaction of flange ring, tapered hub, and pipe. It presents charts which greatly increase the speed of computing maximum stresses. It also presents equations for determining flange rotation and radial expansion. It assumes an axisymmetric loading, with negligible "dishing" of the flange ring. It excludes all types of flange facings where the gasket or contacting flange surfaces have any contact outside of the bolt circle.

Flanges which are in bearing outside of the bolt circle are considered in Ref. 8. In this analysis it is assumed that radial force is resisted by hoop stress in the flange. Axial forces are considered to cause a bending moment in the flange which is resisted by bending stresses in the flange ring in a radial direction. It is assumed that the flange bends about the bolt center circle as if it were fixed there. The elastic interaction of flange ring, tapered hub, and pipe is then considered by requiring deflections and slopes to match at their junctures.

The effect of flange barreling due to pressure and temperature differences is considered in Ref. 9. Ref. 9 presents a simplification of the approach in Ref. 7 by considering the flange and hub to move as a unit without cross-sectional distortion. This approach is a good approximation for sturdy flanges where the length and thickness are comparable.

3. Gasket Compression

From the point of view of mathematical analysis it would be most desirable if the gasket were compressed as a linear spring. The actual relationship is much more complex, as is shown by Fig. 6 taken from Fig. 11 of Ref. 10 for a

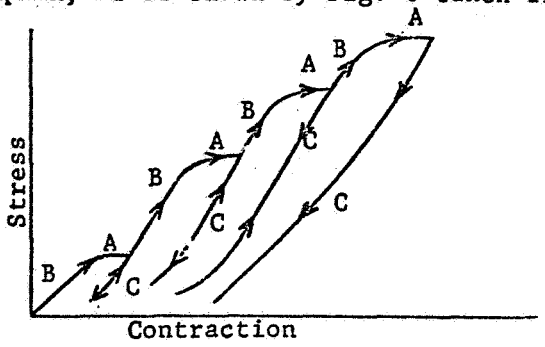

FIG. 6

REPEATED LOAD ON COMPRESSED-ASBESTOS GASKET MATERIAL

compressed-asbestos gasket material. In the regions A we see creep under constant stress. At B we see the curved form of the initial load-shortening curve. At C we see that the curve for retraction differs from the loading curve B and in this case overlaps for reloading. (The overlapping is not always present. See, for example, Fig. 9 of Ref. 10). Other gaskets may include metallic elements that improve the "springiness" and linearity and may include "soft" materials, such as teflon and rubber, that can be squashed substantially to improve the sealing effectiveness.

An important function of the gasket is to be soft enough to provide good sealing while retaining adequate hoop strength to resist "blowing out".

An interesting characteristic of the interaction of flange and gasket is discussed in Ref. 11 for flanges whose contacting area is entirely within the bolting circle. It is pointed out that when pressure is applied "to our knowledge no increase in bolt stress has ever been observed. On the contrary, the bolt stress has been observed to reduce as internal pressure is applied both with solid metal and soft gaskets until the gasket precompression is lost and leakage begins. This effect is due to rotation of the ring flanges under the applied moments and far outweighs the effect of the hydrostatic end force." It seems likely that a similar phenomenon will be present when thermal transients heat the hub much more rapidly than the ring flange.

Creep in gaskets is treated most eloquently in Ref. 12. It is pointed out that one can observe "declines in gross gasket loads of ordinary 1/16-in. compressed-asbestos gaskets...of the order of 68 percent in 20 hours at a temperature corresponding to 350 psi steam." Such creep will have a marked effect on the stress and deformation distribution of a connector and must be considered where extended life is involved. In another comment, W. R. Burrows, remarking on the paper in Ref. 13, stated that "very heavy exchange flanges with 1.23-in. SAE 4140 stud bolts, operating at 400 psi and 650°F, leaked after 24 hours on stream. Measured stud bolt stresses of 50,000 psi had

relaxed to 12,000 psi owing to crushing of the soft-iron gaskets. These gaskets, following custom, had been designed for a bolt stress of 25,000 psi. The actual stress of 50,000 psi crushed the gaskets even at a temperature of 650°F."

At high pressures there is a tendency to use Bridgman-type closures, Ref. 14, which utilize the unsupported-area principle. Many closures of this type have been devised and some are widely used. In some cases the gasket is a hard metal and sealing is accompanied by permanent deformation of either the gasket, the seat, or both. As pointed out in Ref. 14, "at present, even for the simplest types of gaskets, there is no completely reliable design criterion, based on anything other than experience."

In view of the non-linear behavior of almost all good gasket materials, it would appear that reliable designs can best be achieved where the contribution of the gasket "stiffness" to the overall stiffness is small. In this way the uncertainty introduced by this analytically difficult portion of the design can be minimized.

4. Bolt Spacing

Proper bolt spacing depends on flange thickness and gasket flexibility as well as other factors. It is apparent that a given bolting load can be achieved by either a few large bolts or by a greater number of smaller bolts. Factors affecting bolt size and spacing, as pointed out in Ref. 1, are clearance necessary for socket wrenches; strength to withstand over-torquing; adequate spacing to avoid high stress-concentration; and close enough spacing to insure uniform gasket compression. Ref. 1 recommends a bolt spacing of 2-1/4 to 3-1/2 bolt diameters between centers. A somewhat more involved method of analysis is presented in Ref. 10. It considers the flange-gasket combination as a beam on an elastic foundation. In view of the questionable adequacy of neglecting the effect of the hub in increasing the flange ring bending stiffness, this refinement does not seem to have broad application. Bolt spacing is also considered in Ref. 8. It recommends a spacing less than 2.6 times the flange ring thickness to achieve good sealing between bolts. The variety of "rules" for choosing bolt spacing, all of which appear to be successful, indicates that bolt spacing is not a critical design consideration.

5. Interaction of Flange and Gasket

The effect of internal pressure on the interaction of flange and gasket is considered in detail in Ref. 13. Using the analysis for flange deformation in Ref. 7 and assuming the gasket behavior for decreasing load is adequately represented by a linear relationship, a method is provided for considering the loads when (a) assembling the joint, (b) at test pressure, and (c) in service. In Fig. 7, taken from Fig. 2 of Ref. 13, P_3 is the service pressure and P_2 is the test pressure. The line GJ is the limit of bolt load for flange yielding. It shows a decreasing permissible bolt load as the pressure increases. The line OA represents the bolt load to compensate the hydrostatic end force. Line EB represents line OA plus the minimum gasket sealing force. The slope $-\alpha$ of the bolt load curves, CD, FB, MJ, and KL

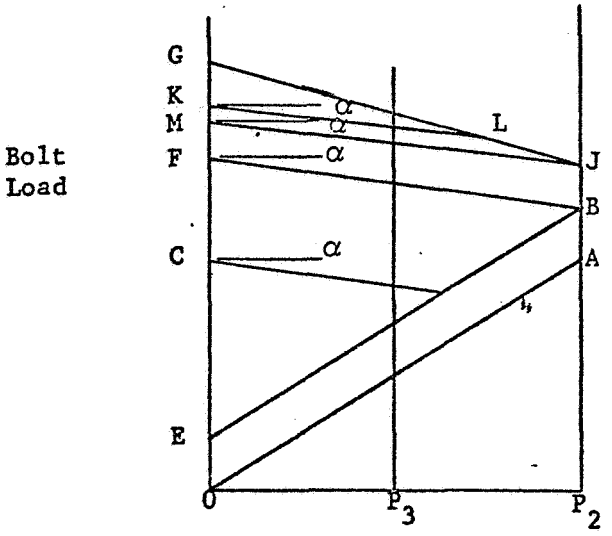

FIG. 7

INTERACTION OF FLANGE, BOLTS AND GASKET

is determined by the interaction of the various stiffnesses. If the bolts are initially tightened to C, leaking will occur at D at a pressure greater than P_3, the operating pressure, and less than P_2, the test pressure. With the bolts initially tightened to F, leaking will not occur, although at B the connection will be on the verge of leaking. With the initial bolt tightening to K, as pressure is increased, the flange begins to yield at L and continues to yield until J is reached. Upon removing load, the bolt tightness returns to M. It may be pointed out that the effect of gasket creep would be to lower the bolt-load curves, such as FB, with time so that they might leak after a short time in service.

6. Hydrostatic End Force

In most connectors one considers a "hydrostatic end force" to load the connector axially. Such a force is assumed in Ref. 7. In the case of a pipe having expansion joints, however, such as found in missile structures, it is not necessarily true that an axial force is present. Similarly, a pipe having closely spaced attachments to a supporting structure may have much reduced "end force" carried by the connector. In Ref. 15 it is pointed out that "in concentrating on the bolted-flange joint itself, it is easy to overlook the fact that there is little hydrostatic end force in pipe lines equipped with slip joints". The correct axial force to be considered in a connector, therefore, depends on interaction between piping and supporting structure and may be temperature dependent. In addition, it is reasonable to provide for a pipe bending moment to be transmitted across the connector. A rather extensive discussion of piping flexibility effects is given in Ref. 16.

7. Closures

Closures for pipes can be plugs in the case of small sizes but must be considered as heads for large sizes. A method for considering a "floating head" (see Fig. 8) is given in Ref. 17. The interaction of A and B is required to give equal radial displacement and rotation of their juncture J. Part A is considered to have no cross-sectional distortion. The analysis is well adapted for use with the flange analysis of Ref. 13 to determine sealing performance as well as stresses and deformation.

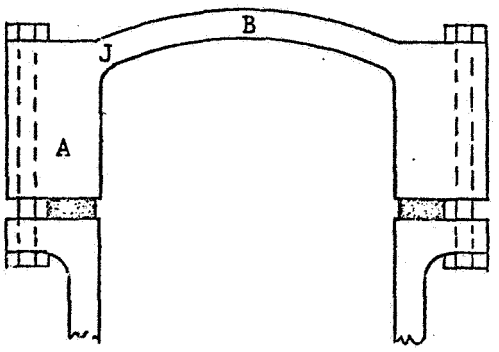

FIG. 8

PIPE CLOSURE

8. Transient Thermal Stresses

During the initial flow through a connector of a fluid which is either hotter or colder than the connector walls, there will exist a transient temperature condition. The inner walls will change temperature more rapidly than the outer walls. In addition, the thinner sections will "heat through" more rapidly than the thicker sections. As a result of these temperature differences, there will be transient stresses and distortions which could initiate leakage. A discussion and general equations for some of the stress and temperature problems are given in Ref. 18. The author points out, however, that "clearly the stress and temperature formulas for hollow cylinders pose difficult problems in evaluation. The roots of the equation have not yet been evaluated. Also, the ratio of outer to inner radius is involved, and a general graphical presentation such as can be made for the case of plates is difficult because of the large number of graphs which would now be required". The results of an approximate solution for the transient temperatures in a cylinder are given in Ref. 22. This approximate solution is particularly adaptable to stress analysis, since it gives the temperature as a power function of the radius. The application of this solution to determining the distortion of glanges is given in Ref. 23. Figure . in Ref. 22 is particularly useful, since it gives the temperature difference from inner to outer wall at the time of maximum temperature difference. Additional information on stresses and temperature distributions is found in Ref. 19.

9. Warped Flanges

Initial lack of flatness in the flanges of connectors can result in leakage if the bolt loads are not sufficient to achieve positive gasket compression at all points on the circumference. The magnitude of permissible initial warping of the flanges is, therefore, governed by the available additional bolt strength and flange strength. Ref. 23 presents equations for computing flange warping displacements due to bolt load and gasket forces. The effect of the pipe in restraining the flange is included in the analysis. It is assumed that the deviation from uniformity of forces and displacements around the circumference of the flange can be adequately approximated by considering them to vary as cos 2θ. Ref. 9 considers warping also by developing the pipe shell as a flat plate. The adequacy of this approximation will depend on the flange and pipe hoop bending strengths and is questioned by Waters in his discussion of the paper.

10. Leakage Flow

The interface between gasket and flange forms a channel for leakage flow. The depth of this channel depends on surface finish, yield strength of the gasket and flange materials, and gasket compression. The interplay of these factors is considered using a statistical approach for determining the effect of gasket compression on the effective flow channel. The magnitude of the flow through such a channel is proportional to the cube of the channel thickness in laminar flow and proportional to the square of the channel thickness in molecular flow. Thus, a reduction in clearance from 100 to 10 microinches reduces the flow by a factor of 100 to 1,000.

11. Fluid Momentum Effects

When the fluid in a pipe is caused to accelerate or decelerate, unbalanced forces are imposed on the piping system. Thus, in the pipe shown in Fig. 9, an acceleration in fluid flow in direction A causes a reaction of the pipe at B in the direction shown. The magnitude of the bending moment and axial force thus imposed on connectors in the piping system will depend on the restraint imposed on the piping system by the supporting structure C. When valves are suddenly opened or closed, these momentum changes are most severe and are described as "water hammer". A discussion of "water hammer" is given in Ref. 22.

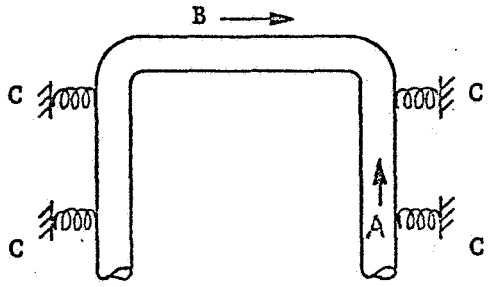

FIG. 9

EFFECT OF FLUID FLOW

Even when the fluid flow is zero, momentum effects are present due to acceleration of the entire booster. (See Ref. 22).

12. Fatigue

In some instances the number of stress cycles at a particular connector may be sufficient to result in fatigue failure. A method for analyzing for fatigue damage is presented in Ref. 19. The method assumes that the stress condition is known versus time for a complete cycle of operation. It takes account of yielding and of the mean and alternating stresses.

13. Discussion

Many methods and considerations have been presented concerning the interaction of flange, gasket seal, and pipe. The optimum configuration of a connector varies widely depending on the service conditions. To consider all of the factors in any particular design requires a large amount of detailed computation. As a result of this, standard forms of connectors have evolved for particular applications in the past, and new forms can be expected to meet the requirements of new environments.

A large amount of careful work has been done in the field of connector design, and this provides a sound base from which to evolve new design methods and to develop and evaluate new materials for new environments.

The missile application of fluid connectors imposes much more severe design requirements because of the range of pressure, temperature and time over which performance is required and the limitations imposed by minimum weight, lox sensitivity, radiation and space environments in general.

When methods and applicable material properties have been assembled, it may be possible to combine them in one, or several, computer programs to yield optimum designs for specified load conditions.

14. References

1. E. O. Waters, D. B. Wesstrom, and F.S.G. Williams, "Design of Bolted Flanged Connections, "Pressure Vessel and Piping Design Collected Papers 1927-1959, ASME, p. 58 (also published in Mechanical Engineering, 1934).

2. P. W. Bridgman, The Physics of High Pressure, 2nd Edition, G. Bell, London, 1949, Chapter II.

3. S. E. Logan, "Temperature-Energized Static Seal for Liquid Hydrogen", Advances in Cryogenics, Vol. 7 (Proceedings of Conference at Ann Arbor, Michigan, 1961), pp. 556-561.

4. R. Michel, "Elastic Constants and Coefficients of Thermal Expansion of Piping Materials Proposed for 1954 Code for Pressure Piping", Pressure Vessels and Piping Design Collected Papers 1927-1959, ASME, p. 442 (also in Trans. ASME, 1955).

5. J. R. Vinson, "Short-Time Properties of Materials as a Function of Temperature," General Electric TIS Report No. 60SD314, Feb. 8, 1960.

6. L. Mantell, Engineering Materials Handbook, McGraw-Hill Book Co., 1958, pp. 18-43 to 18-47, "Low-Expansion Alloys".

7. E. O. Waters, D. B. Wesstrom, D. B. Rossheim and F.S.G. Williams, "Formulas for Stresses in Bolted Flanged Connections", Pressure Vessel and Piping Design Collected Papers 1927-1959, ASME, p. 62 (also publ. in Trans. ASME, 1937, and in more extended form by the Taylor Forge and Pipe Works, "Development of General Formulas for Bolted Flanges").

8. C. K. Coombs, "Circumferential Flange Analysis", General Electric TIS Report No. R56AGT386, July 16, 1956.

9. W. M. Dudley, "Deflection of Heat Exchanger Flanged Joints as Affected by Barreling and Warping", Trans. ASME, Nov. 1961, pp. 460-466.

10. I. Roberts, "Gaskets and Bolted Joints", Pressure Vessel and Piping Design Collected Papers 1927-1959, ASME, p. 102 (also published in J. Appl. Mech., ASME, 1950).

11. D. B. Rossheim and J. J. Murphy, Discussion of paper by I. Roberts, Ref. 10, Pressure Vessels and Piping Design Collected Papers 1927-1959, ASME, p. 115.

12. F.C. Thorn, Discussion of paper by I. Roberts, Ref. 10, Pressure Vessels and Piping Design Collected Papers 1927-1959, ASME, p. 117.

13. D. B. Wesstrom and S. E. Bergh, "Effect of Internal Pressure on Stresses and Strains in Bolted-Flanged Connections", Pressure Vessels and Piping Design Collected Papers 1927-1959, ASME, p. 121.

14. A. R. Freeman, "Gaskets for High Pressure Vessels", Pressure Vessels and Piping Design Collected Papers 1927-1959, ASME, p. 165.

15. H. C. Boardman, Comment on paper, "Stress Conditions in Flanged Joints for Low-Pressure Service" by E. O. Waters and F.S.G. Williams, Pressure Vessels and Piping Design Collected Papers 1927-1959, ASME, p. 162.

16. A.R.C. Markl, "Piping Flexibility Analysis", Pressure Vessels and Piping Design Collected Papers 1927-1959, ASME, p. 419 (also in Trans. ASME, 1955).

17. J. E. Sochrens, "The Design of Floatingheads for Heat Exchangers", Pressure Vessels and Piping Design Collected Papers 1927-1959, ASME, p. 261 (also in ASME Paper 57-A-247).

18. M. P. Heisler, "Transient Thermal Stresses in Slabs and Circular Pressure Vessels", Pressure Vessels and Piping Design Collected Papers 1927-1959, ASME, p. 532 (also in J. Appl. Mech., 1953).

19. "Tentative Structural Design Basis for Reactor Pressure Vessels and Directly Associated Components", distributed by OTS, Dept. of Commerce, PB151987, 1 Dec. 1958 Revision with Addendum No. 1-27 Feb. 1959 (see also NR-S-1 issued March 1961).

20. S. Timoshenko, Theory of Plates and Shells, McGraw-Hill, 1940.

21. S. Timoshenko, Strength of Materials, Part II, D. VanNostrand Co , 2nd Edition, 1941.

22. S. Levy (Editor), Design Criteria for Zero-Leakage Connectors for Launch Vehicles, Vol. 6, Environmental Effects, General Electric Report No. 63GL46, March 15, 1964.

23. S. Levy (Editor), Design Criteria for Zero-Leakage Connectors for Launch Vehicles, Vol. 4, Design of Connectors, General Electric Report No. 63GL44, March 15, 1964.

DEVELOPMENT AND APPLICATION OF SEPARABLE FLUID CONNECTORS FOR LIQUID-PROPELLANT ROCKET ENGINES

by

C. M. Daniels

Rocketdyne
A Division of North American Aviation, Inc.
Canoga Park, California

Preceding page blank

INTRODUCTION TO THE SUBJECT OF STATIC SEALS

A liquid-propellant rocket engine is essentially an assemblage of hydraulic and pneumatic components. Because of this, there are many interconnecting joints which must be sealed with a high degree of reliability by means of static seals. The proper design of these joints presents a formidable array of technical problems to the designer; for example, temperature extremes from -423 to 1700 F, pressure extremes from zero to several thousand psi, high vibration and shock load environment, and corrosive media.

The importance of leak-free and trouble-free static seal joints in spacecraft cannot be overemphasized, especially in the coming era of manned space vehicles requiring extremely high reliability. The consequences of seal leakage are: fire or explosion hazards, freezing of fluids or equipment adjacent to leakage or, in cases of severe leakage, degradation of engine performance because of loss of specific impulse. Any of these things could cause abortion of a mission. An entirely new seal philosophy is being evolved, one in which any leakage at all is intolerable, whereas, a certain amount of leakage was tolerated in unmanned vehicles. Since static seal leakage was not monitored in flight during early ballistic missile development, it is not known how many of the early failures were caused directly or indirectly by seal leakage.

TYPES OF STATIC SEAL JOINTS

There are three main categories of static seal joints in liquid rocket engines. These are:

1. Bolted flanged joints
2. Flared tube fitting joints
3. Threaded bosses

Preceding page blank

In the early design phase of a new engine, each static seal joint should be carefully evaluated for justification of its existence. Obviously, no joint at all, or a welded joint, is vastly superior in reliability to a static seal joint. Sometimes certain joints, originally provided to allow easy removal and installation of components under development, can be eliminated after they have served their purpose and the engine is in production.

TYPES OF STATIC SEALS

The seals that fit into these joints can be categorized further into four types. These are:

1. Pressure actuated
2. Brute force
3. Temperature actuated
4. Spring

TYPES OF SEAL FLUID ENVIRONMENT

Static seals in liquid engines (excluding storable propellants) are required to seal basically three fluid regimes. These are:

1. Cryogenics
2. Hydrocarbon fuel
3. High-temperature turbine gases

ROCKETDYNE STATIC SEAL HISTORY

Table 1 is a resume of the types of static seals that have been used by Rocketdyne over the past 10 or more years. It can be seen that, for an extended period, the spiral-wound gasket was the stalwart design for use in liquid oxygen and turbine gas joints. A suitable replacement was not developed until the advent of the NAFLEX pressure-actuated seal. The NAFLEX concept originated as a special seal design to correct a leakage problem with the LOX cover plate on the gas generator blade valve of the Atlas sustainer engine. Its obvious performance improvement over the spiral-wound gasket led to its wider use.

The NAFLEX-type seal is the standard for all cryogenic, bolted-flange joints on the F-1 and J-2 engines. It is also the standard seal for the J-2 hot-gas, bolted-flange joints.

TABLE 1

ROCKETDYNE FLANGED-JOINT, STATIC-SEAL CHRONOLOGY

Initiated	1952	1954	1955	1956	1956	1957	1958	1959	1961
Engine Model	Redstone 75-110	Navaho G-38	Atlas MA-2	Thor	Jupiter	Atlas MA-3	H-1	F-1	J-2
Oxidizer	Spiral Wound	Spiral Wound	Spiral Wound	Spiral Wound	Spiral Wound	Spiral Wound and NAFLEX	NAFLEX	NAFLEX	Spacer NAFLEX
Fuel	O-Rings	O-Rings	O-Rings	O-Rings	O-Rings	O-Rings	Gask -o- Seal	Gask -o- Seal	Spacer NAFLEX (hydrogen)
Turbine Gas	Silicone O-Rings	Marman J-11	Asbestos Filled, Spiral Wound	Asbestos Filled, Spiral Wound	Asbestos Filled, Spiral Wound	Asbestos Filled, Spiral Wound	Asbestos Filled, Spiral Wound	Copper Filled, Spiral Wound	Spacer NAFLEX

IMPORTANCE OF ALL ELEMENTS WITHIN A JOINT

The design of a static seal joint is dependent upon the correct application and integration of all the elements making up the joint, i.e., fasteners, flanges, and the seal itself. The joint assembly must be capable of maintaining the seal in intimate conformance with the sealing surfaces, and this condition must exist throughout its operating life, regardless of strains, loads, and thermal gradients. That is, the usual goal of optimum weight within safe stresses must be broadened to control of the elastic (and plastic) behavior of the parts. Accurate predictions for the performance of a static seal joint cannot be made before tests are conducted with representative hardware.

This report is limited to a discussion of the static seal itself, based on data derived from test results and operational experience. It is intended to serve as a basis for seal selection, and includes a discussion of design features and deficiencies of the static seals evaluated. Methods for designing the flanges and threaded connectors of a joint are not discussed in detail, since they already are well documented (Ref. 1, 2, and 3).

FLARED TUBE FITTING EXPERIENCE

The AN standard tube flare and fitting was used by Rocketdyne for tube joints in early Rocketdyne engines. This standard was developed before World War II, principally for aircraft hydraulic system use, and was carried over into pneumatic and hydraulic installations in rocket engines. Joints made with aluminum fittings and lines have proven adequate in sealing characteristics but have limited protection in high temperature environments. Aluminum lines and fittings have additional limitations in strength to prevent seizing between parts under over-torque conditions or in usage in extreme environments. Joints made with stainless fittings and lines have proven difficult to seal because of the poor material yield characteristics for the seal surface and the difficulty in quality control of the seal surface of the fittings and tube flares involved. Stainless steel flared tube fittings have a problem of torque relaxation on first installation, whereas both aluminum and stainless fittings may be subject to complete disengagement under extreme vibration conditions.

There are a great many vendors making different flared and flareless tube joint designs, and all make glowing claims about their product. In 1955, Missile Division (now Space and Information Division) of North American Aviation, Inc., conducted a qualification test survey on many of the designs then on the market. They came to the conclusion that none of those tested were any better in performance than the AN standard flare (Ref. 4).

Rocketdyne's search for a better flared joint led eventually to the use of a machined flare (Fig. 1). The machined flare combined the flare and the ferrule, or sleeve, into one machined part, which then was welded into the tube assembly at a safe distance from the flare to prevent warpage. The advantages of the machined flare over the flared tube are as follows:

1. Machining allows a practical method for close control of tolerances in the conical tube sealing surface.

2. The weak point of the tubing at the base of the flare is eliminated.

3. Seizing between the tube and sleeve is eliminated.

4. Greater hoop strength is provided to help prevent seizing between the sleeve (now tube end) and coupling nut.

The production versions of the J-2 and F-1 engines will have no flared tube joints in any functional systems. Bolted flange joints will be used throughout, since they are considered more reliable and offer a method of leakage monitoring.

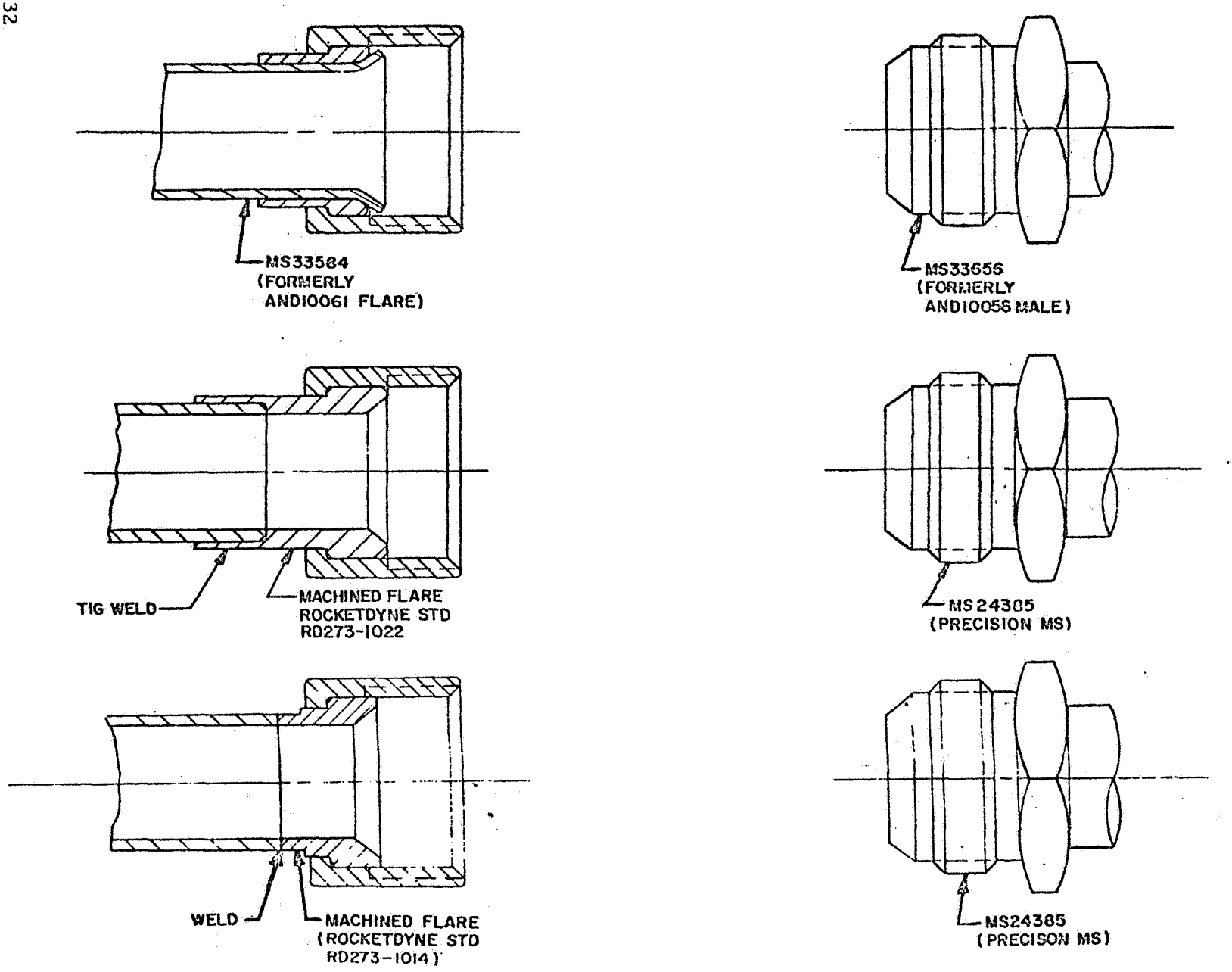

Figure 1. Flared Tube Experience

THREADED BOSS SEAL EXPERIENCE

AN STANDARD BOSS

Rocketdyne experience has shown that the metallic, K-shaped (cross-section)-type seal with Teflon coating (Fig. 2), although having some deficiencies, is the best available for sealing AN standard threaded bosses in cryogenic service. Rubber O-rings should be used for AN standard bosses in hydrocarbon fuel service and for gases within the operating temperature range of rubber.

The poor quality of sealing surface finish in AN fittings adversely affects the performance of any metallic seal, especially those that require the metal of the seal to be forced (by yielding) into the imperfections of the fitting surface to effect a leak-proof seal. Since the K-seal is Teflon coated, it achieves better conformance of its sealing surface to the fitting than an all-metal seal, such as the NATORQ (NAVAN Products Division of North American Aviation, Inc.). The rough finishes of the fittings, however, sometimes cause scuffing of the Teflon during the rotational movement of tightening torque, and result in leakage.

NAFLEX BOSS

Whenever the requirement for sealing a threaded boss other than the AND type arises, the Naflex boss seal is recommended for use (See Fig. 3). It requires that a counterbored seat be machined into the boss instead of the countersunk one as used in the AND standard. However this configuration still has the disadvantage of scuffing of the Teflon during the rotational movement of tightening torque. For this reason the bolted flange joint with NAFLEX seal is preferable over all types of threaded boss connections.

No fully successful seal has ever been found by Rocketdyne for use in a cryogenic-service bulkhead fitting; consequently, this type of fitting is avoided in the design.

(1) AN FITTING K-SEAL (NO. 12100 CR) TEFLON-COATED STEEL

(2) NATORQ NO. VD 261-0002;6061-T6 ALUMINUM ALLOY

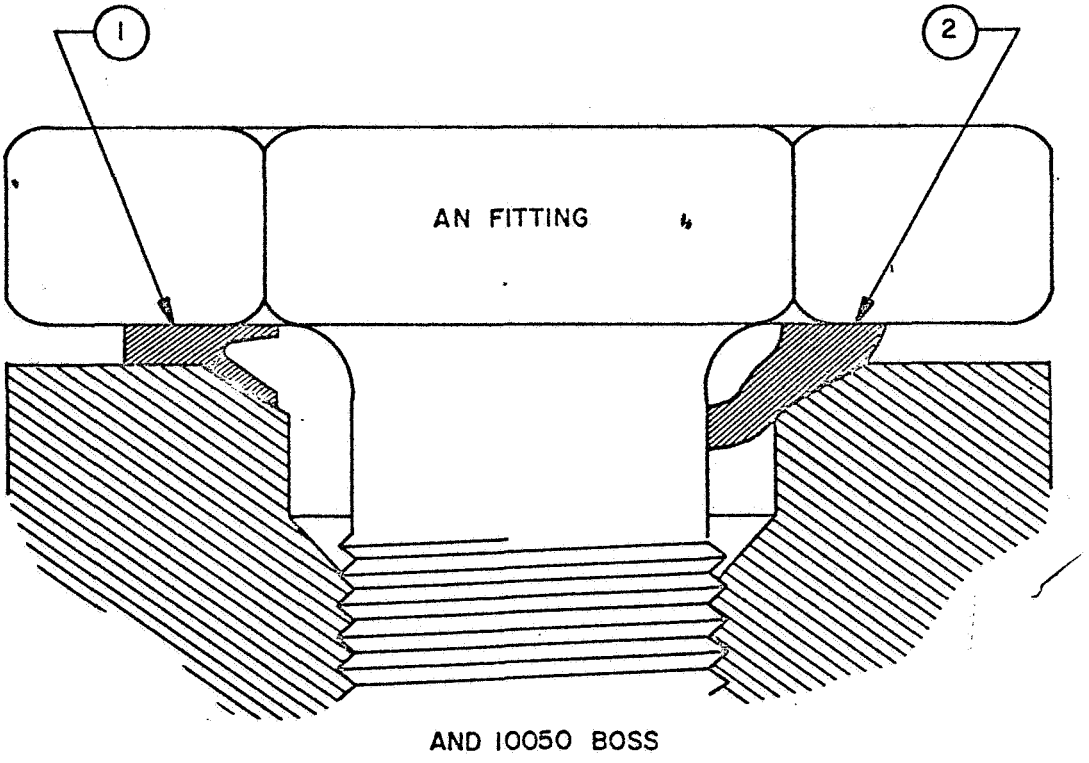

Figure 2. Metallic AN Boss Seals

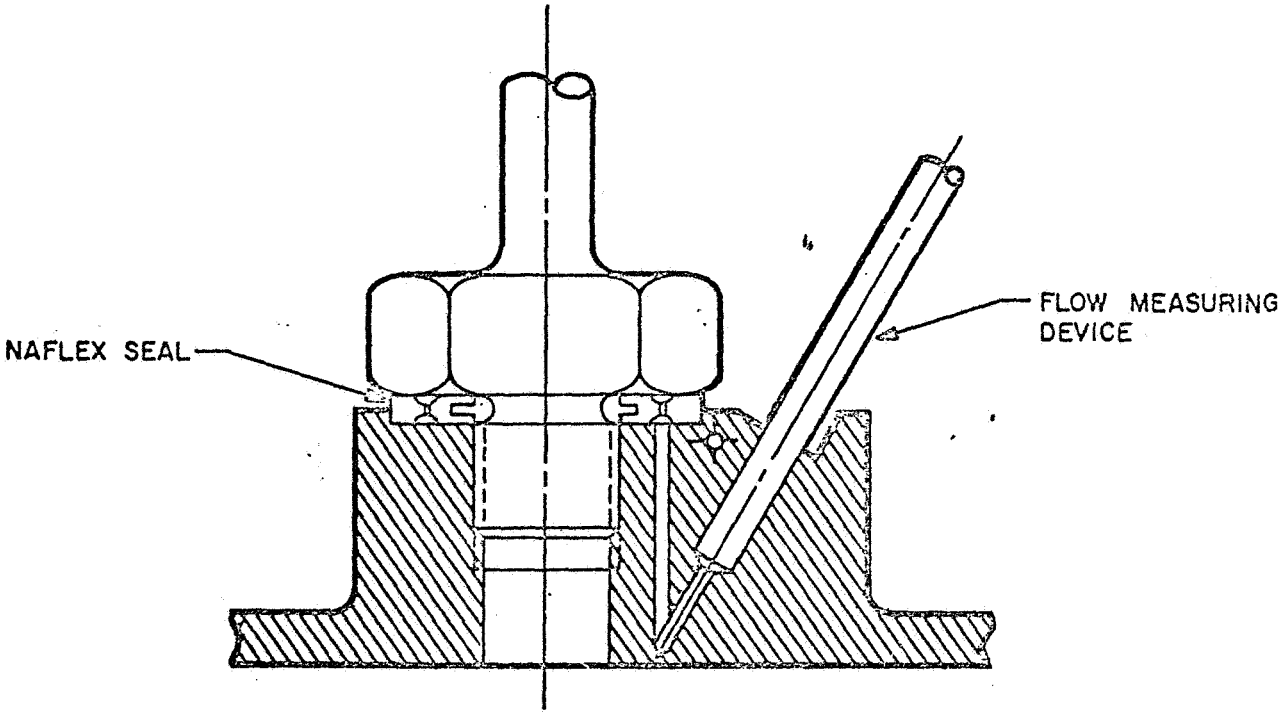

Figure 3. Typical Installation of NAFLEX Boss Seal

N67-86147

HYDROCARBON FUEL SEAL EXPERIENCE

Hydrocarbon fuel is by far the easiest-to-seal fluid regime on an engine. Buna-N rubber O-rings have long been used very successfully. However, with the advent of large-sized hardware, such as used in the F-1 engine, the in-place or gask-o-seal has become more attractive than the O-ring.

The in-place or gask-o-seal is an offshoot of the O-ring, except that the rubber molding is done directly in a groove of a metal part or spacer. In the case of a spacer, which is the type most used in bolted flange applications, the in-place seal is molded into both sides of the spacer (Fig. 4). Bolt holes are located in the spacer outside of the sealing area to match the bolt pattern of the mating flanges. Sealing is accomplished both by initial squeeze of the rubber upon installation in the flanged joint, and extrusion of the rubber by the pressure of the fluid being sealed.

In-place seals are not limited to circular shapes, but can be made in almost any cross-sectional shape. Figure 5 shows a "figure-eight" cross section used on the F-1 engines.

The advantages of the in-place seal over the O-ring, especially in large-sized hardware, are as follows:

1. The thickness of the metal spacer controls the amount of squeeze on the rubber portions of the seal; this allows the use of flat-faced flanges on both sides of the seal, thus obviating the need for machining an O-ring groove in one of the flanges (with its attendant increased dimensional tolerance buildup and cost).

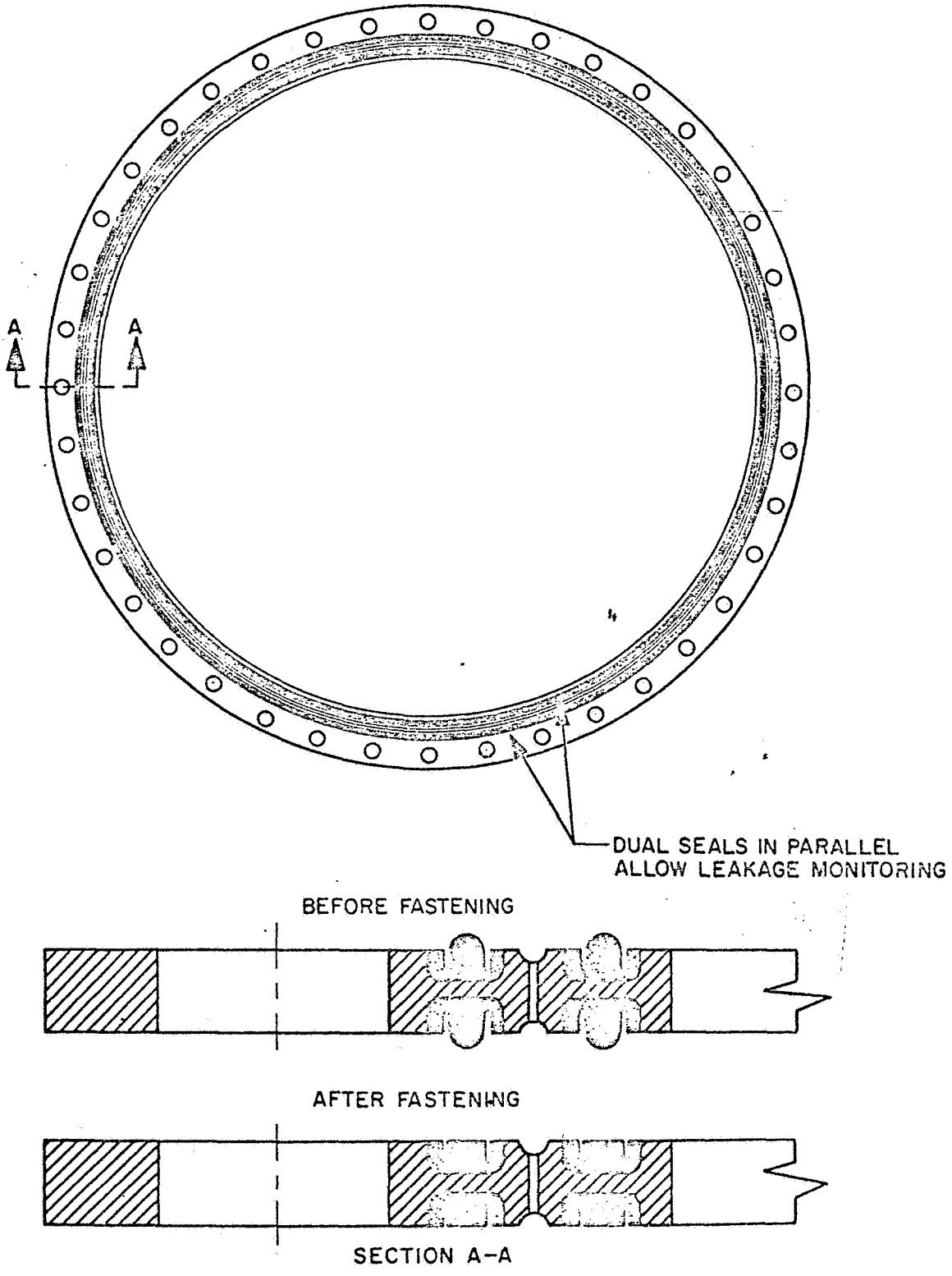

Figure 4. In-Place or Gask-o-Seal

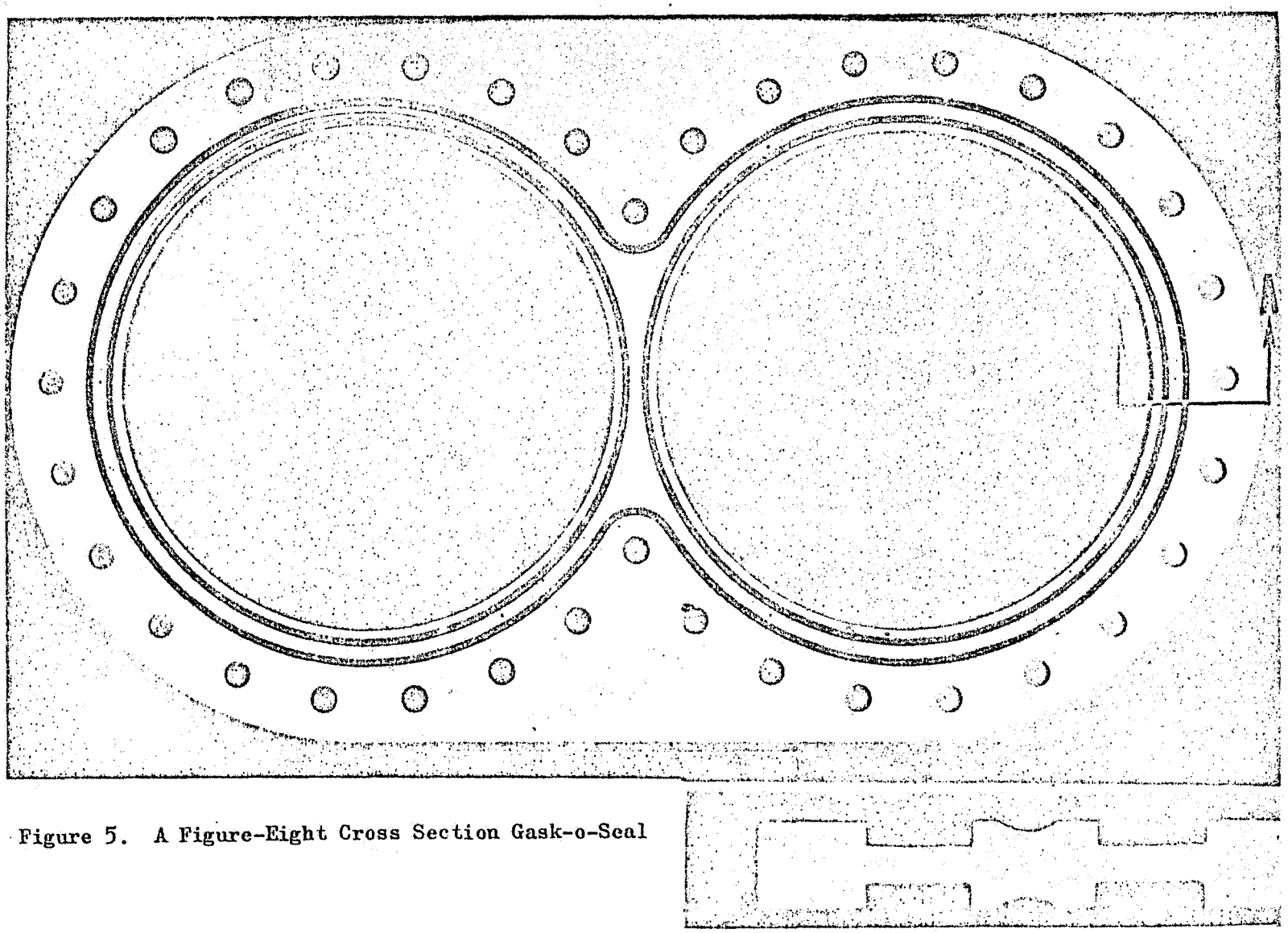

Figure 5. A Figure-Eight Cross Section Gask-o-Seal

2. The in-place seal permits easy installation in large, heavy, and cumbersome hardware, since it can be installed laterally between two flanges, with only enough clearance to slip the seal in or out. This same feature also makes replacement in the field easier.

The gask-o-seal is the standard hydrocarbon static seal used on the F-1 engine, and has demonstrated a high reliability in engine and component testing conducted thus far. It can be adapted easily (and has been on the F-1 engine) for primary seal leakage monitoring by having two seals molded closely together concentrically in the seal plate. A leakage tapoff into the space between these two seals allows leakage monitoring.

For compatibility with trichlorethylene, which is used on the F-1 engine for flushing and cleaning sequences, Viton A is used as the standard elastomer material for gask-o-seals. Further information on the development and design application of gask-o-seals is contained in Ref. 5.

PECULIARITIES OF CRYOGENIC SEALS

The design of a static seal for cryogenic service involves not only the routine seal design problems of any ambient temperature joint, but also the peculiarities of the materials resulting from their behavior at the reduced temperatures. For example, not all metals can be used at cryogenic temperature. Some metals, such as 17-7PH and AM350, become very brittle and notch impact sensitive at the low temperature, and are unacceptable for use. Most nonmetallic, plastic materials commonly used in ambient-temperature seals also become brittle at the low temperature. Fluorocarbons, such as Teflon, Kel-F, and Mylar, are exceptions to this; however, their coefficients of contraction are considerably greater than those for metals. Therefore, when used in conjunction with metals in a seal design, a differential shrinkage condition and disturbance of the sealing interface will exist and possibly cause leakage.

Cryogenic seals present a greater variety of operating principles than any other group of static seals. The basic types are the brute-force gaskets, temperature-actuated seals, pressure-actuated seals, and many hybrids combining the principles of these basic types.

The lack of resilience demonstrated by nonmetallic materials at cryogenic temperatures makes it necessary to apply extremely high loads to simple flat gaskets, even for leak-free operation at low pressures. The use of serrations, narrow radial widths, and other compressive-area-reducing devices on flat gaskets tend to lower the required bolt load; however, extremely high preloads are still required to prevent flange separation and unloading of the "dead" gasket materials.

The more effective cryogenic seals currently available use one or more "boost" principles to overcome the deficiencies of "plastic" material. The combination of spring- and pressure-actuation principles is common to the most efficient seals.

Rocketdyne experience indicates that seals that are capable of "following the flanges" are the most successful. As a result of extreme load conditions in rocket engine systems, some flange movement, separation, and deflection are inevitable. To maintain low or zero leakage under these conditions, a seal must be designed to compensate for this movement, i.e., be pressure actuated, spring loaded or, in some manner, capable of the necessary deflection.

THEORETICAL ANALYSIS FOR FLANGED JOINTS

The function of the static seal is to permit a fluid seal to be effected between two imperfect surfaces. Usually, it is made of a material that will conform readily to the surfaces or is coated with such a material so that, when properly stressed, a barrier will be formed in depressed surface regions to prevent leakage of the contained fluid. Seals that damage the seating surfaces are usually unsatisfactory if the joint has to be broken and remade, since sealing becomes increasingly difficult with each reassembly. Eventually, the seating surfaces must be refaced. From this, it follows that the static seal surfaces should be softer than the flange surfaces.

Ideally, the seal should remain undisturbed throughout the operating cycle. Since this condition is usually impossible to attain, the seal must be capable of sufficient elastic recovery to maintain the leakage barrier. This goal is usually pursued in one of two ways: (1) a relatively nonresilient gasket or seal used in conjunction with extremely rigid flanges and heavy bolting, or (2) a very resilient seal capable of following the deflections of flightweight flanges.

The first approach can be analyzed by the time-honored, classical approach developed by industries other than the aircraft and missile industry. It can be shown theoretically (Ref. 6), that for uniform gasket stress and in the absence of adhesion, leakage will begin when the internal pressure begins to exceed the compressive stress that holds the gasket in contact with the seating surfaces. Therefore, it would seem to follow that if gasket stress is not uniform, the leakage pressure will be substantially lower than the average gasket

compression stress, if radial paths of below-average stress exist. The difficulty of sealing a joint when radial scratches exist in the gasket seating surface is well known. Conversely, if paths of subnormal stress are circumferentially closed loops, it is conceivable that leakage pressures could be achieved which would be higher than the average gasket stress. That is, gasket factors (defined as $m = \sigma_g/p$, where σ_g = gasket stress and p = leakage pressure) should be lower for a flat gasket against a facing consisting of concentric serrations than against a smooth finish. This is supported by experimental evidence (Ref. 7).

MINIMUM SEALING REQUIREMENTS

As indicated above, the minimum requirement for sealing is first to precompress the gasket sufficiently to close up all paths through which mass flow could occur. The load required generally is termed the seating load or the gasket yield load. The next step is to maintain a sealing load such that $\sigma_s = mp$, where m (the gasket factor) is approximately a constant.

In the simplest type of gasketed joint (Fig. 6), the gasket is prestressed in compression by the tensile prestress applied to the bolts. As internal pressure is increased, the gasket stress will diminish until the leakage condition is attained. The relationship, assuming rigid flanges, is as follows:

$$W = A_g \sigma_g + H$$

where

W = bolt load*

H = pressure-separating load

A_g = gasket area

σ_g = gasket stress

It should be noted that this type of joint requires bolting in excess of that required to restrain the separating load by the amount:

$$A_g \sigma_g = A_{gmp}$$

Various approaches are used to attain a more nearly optimum design. Most obvious of these is to reduce W by reducing A_g; i.e., by using a narrower gasket sealing surface such as that shown in Fig. 6.

With a minimum A_g, however, σ_g may be excessive when $p = H - 0$, leading to crushing the gasket or Brinelling the flange. Hence, when the reduction in A_g is carried to the extreme, it becomes necessary to limit the compression of the gasket, as shown in Fig. 8.

An ingenious approach for attaining the minimum W is to use the pressure to generate the gasket sealing load, as shown in the bellows type of Fig. 9.

---

*If the gasket is relatively thin and hard, the bolt load will remain approximately constant, as shown in Ref. 8.

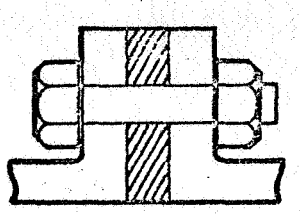

Figure 6. Gasket Prestressed in Compression by Bolt Tensile Prestress

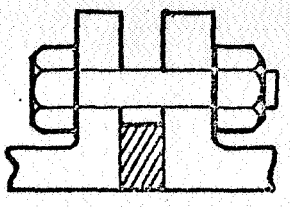

Figure 7. Gasket Prestressed in Compression With Reduced Cross-Sectional Area

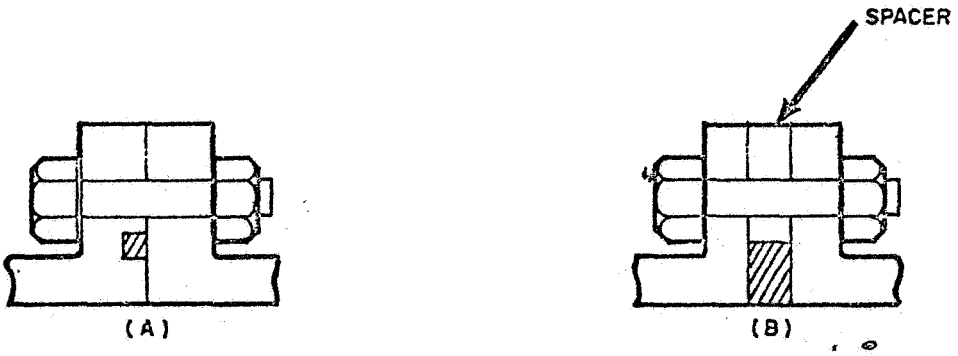

Figure 8. Methods For Limiting Compression of Gasket

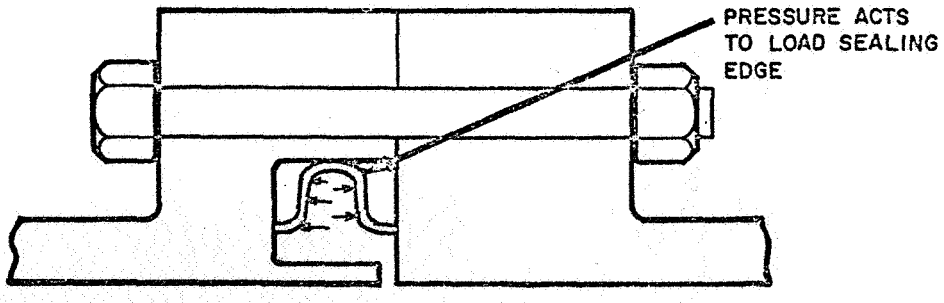

Figure 9. Pressure-Actuated Seal

It can be seen that this type of seal is made possible by the approximately linear relationship between p and the required sealing stress, the latter being obtained by making:

$$\frac{\text{effective bellows area}}{\text{sealing area}} \geq m$$

DESIGN PARAMETERS FOR SEALS

Operating Pressure

The operating pressure, as defined in this report, is approximately the maximum possible pressure obtainable without permanent deformation of the seal structure, or the maximum pressure at which leakage did not exceed 1/10 scim/circumferential inch for those seals that develop excessive leakage before exceeding their structural strength, whichever is lower.

Temperature Range

Cryogenic seals must operate over a wide range of temperatures. Most cryogenic seals are designed for operation between -425 F (liquid hydrogen temperature) and -297 F (liquid oxygen temperature); however, the seals also must be capable of sealing high proof pressures at ambient temperature during component and system checkout. Military specifications require the seal to withstand 160 F temperature while installed, but naturally in cryogenic operation, the seal is immediately chilled. Teflon-coated seals can operate at 400 or 500 F with reduced operating pressure. This pressure reduction is necessary because Teflon tensile properties decrease rapidly at higher temperatures. Soft-metal (i.e., copper, silver) plated seals generally can withstand higher temperatures, but the better performing metal-plated seals use soft plating with a melting temperature of less than 1000 F.

Seal Load Required

The seal load required, i.e., gasket factor or load per inch of circumference, for tight joint makeup shows the advantages of the pressure-actuated and spring-loaded type seals over the brute force gasket types (Table 2). The use of thse seals drastically reduces bolt load which results in a reduction in size or number of bolts, and in flange weight.

Surface Finish Required

Flange finishes quoted in Table 2 are those proved in the test laboratory or recommended by the seal suppliers. These finishes are the minimum (i.e., roughest) finish allowable. It is impractical to machine an exact numerical value of rms finish in production; therefore, correctly machined flanges will range typically from a finer-than-required to the required finish.

The orientation of the tool marks made in facing the flange is as important as the fineness of finish--the finish values quoted are for flanges with their tool marks oriented circumferentially, i.e., not actually complete concentric circles, but rather like a very fine phonograph record surface. Recent tests indicate that, where other methods of machining are used that produce no circumferential tool marks, the finish must be one or two grades better than normally required (example: 8 rms, nonoriented tool marks substitutes for 32 rms circumferential), depending on the type of seal and operating conditions.

TABLE 2. COMPARISON OF THE DESIGN PARAMETERS OF VARIOUS TYPES OF CRYOGENIC STATIC SEALS

	Pressure Actuated			
	Naflex Groove, Type RD261-3010	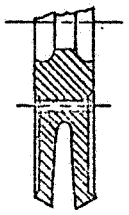 Naflex Spacer Type 404656		K-SHAPED SEAL
Description	Metallic U-Shaped Cross Section With Teflon	Metallic U-Shaped Cross Section With Teflon	Teflon U-Shaped Cross Section With Inner Backup Metallic U Spring	All-Metal, K-Shaped Cross Section; Head of K Controls Leg Deflection
Figure of Merit(3)	332	332	50	12
Operating Pressure, psi	5000(1)	5000(1)	500(1)	500(1)
Temperature Range, F	-425 to ~ 300	-425 to ~ 300	-300 to 160	-425 to ~ 500
Average Seal Load Required, lb/in. of circumference	150	150	~ 30	~ 40
Flange Finish Required, microinch/inch rms (4)	32C	32C	32C	32C
Materials	4340 Steel and Teflon	4340 Steel and Teflon	17-7 Steel and Teflon	Steel With K-6 Coating

(1) MAXIMUM BASED ON STRUCTURAL STRENGTH OR SEAL LEAKAGE

(2) LEAKAGE EXCEEDS 1/10 SCIM/IN. OF CIRCUMFERENCE AT ALL PRESSURES

(3) REFERENCE SECTION OF REPORT THAT DESCRIBES

(4) REFERENCE SECTION OF REPORT DESCRIBING "C" NOMENCLATURE

TABLE 2. CONTINUED

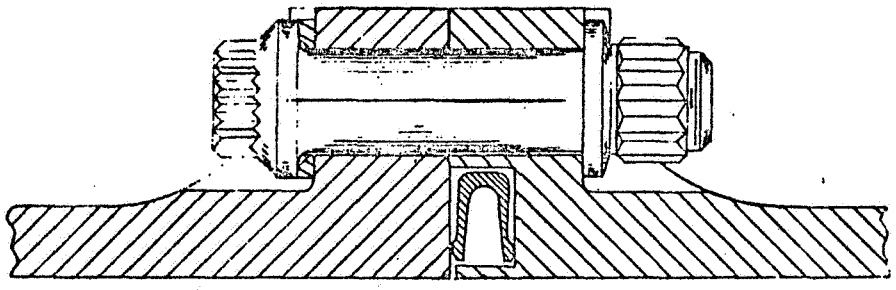

NAFLEX GROOVE

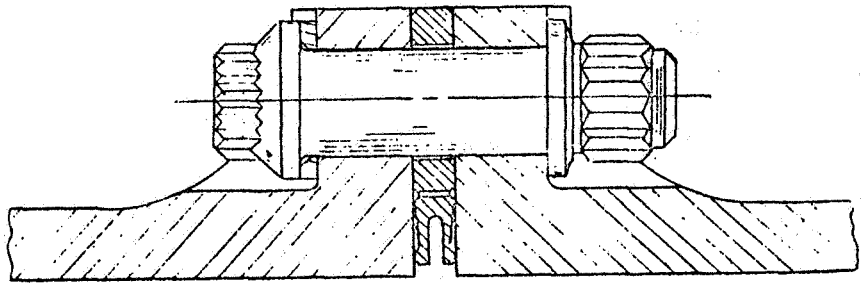

NAFLEX SPACER

ENLARGED VIEW OF
K-SHAPED SEAL

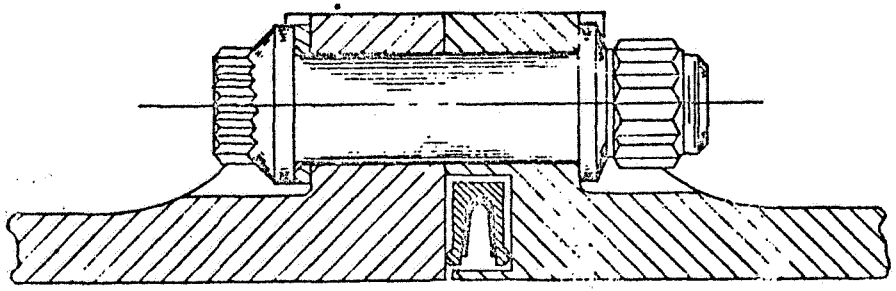

TEFLON U-SHAPED CROSS SECTION
WITH INNER BACKUP METALLIC U SPRING

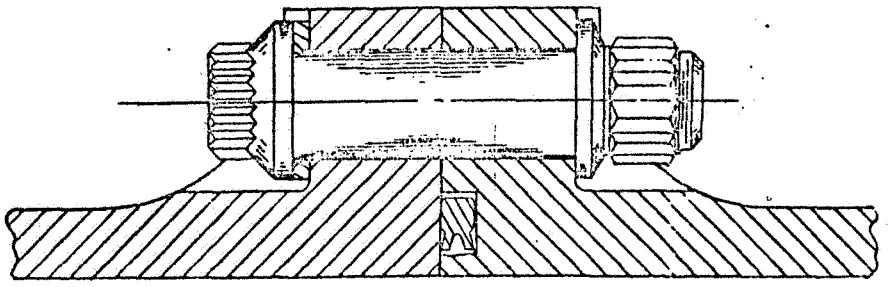

K-SHAPED SEAL

TABLE 2. CONTINUED

	Brute Force			
	Metal O-Ring	Spiral Wound	Bureau of Standards O-Ring	
Description	All-Metal Tube. May be Coated With Teflon and/or Gas Filled	Spiral-Wound Steel Ribbon With Asbestos Filler	An Elastomer Compressed to High Unit Loading	Inconel-X Wire Mesh Wrapped in Thin Aluminum or Inconel Sheet
Figure of Merit	2	0	0.0001	0.0005
Operating Pressure, psi	1000	(2)	1000	2000
Temperature Range, F	-425 to ~ 300	-425 to ≯ 400	-425 to ~ 300	-320 to 1800
Average Seal Load Required, lb/in. of circumference or Gasket Factor	~ 500	4000	6000	3.00 (Gasket Factor)
Flange Finish Required, microinch/inch rms	32C	32 to 125	32	32 to 64
Materials	321 Steel and Teflon	CRES and Teflon or asbestos	Neoprene Hypolon, Viton, etc.	Inconel-X Wire Mesh Wrapped in Thin Aluminum or Inconel Sheet

(2) Leakage exceeds 1/10 scim/in. of circumference at all pressures

TABLE 2. CONTINUED

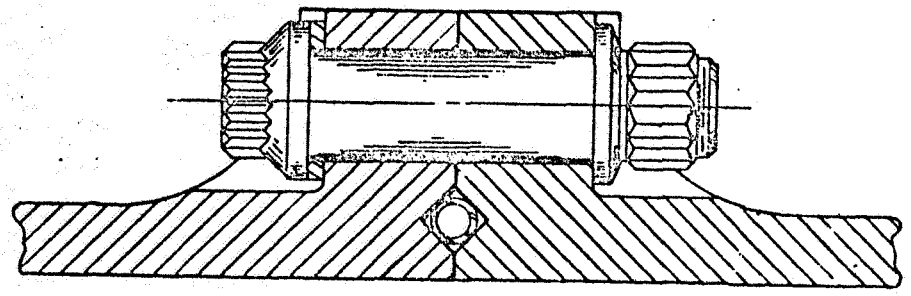

METAL O-RING

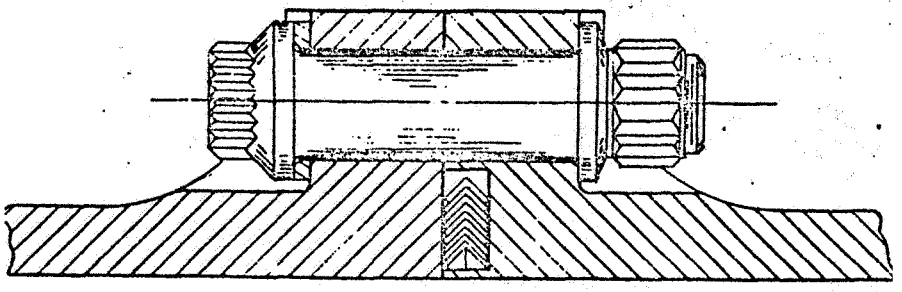

SPIRAL WOUND

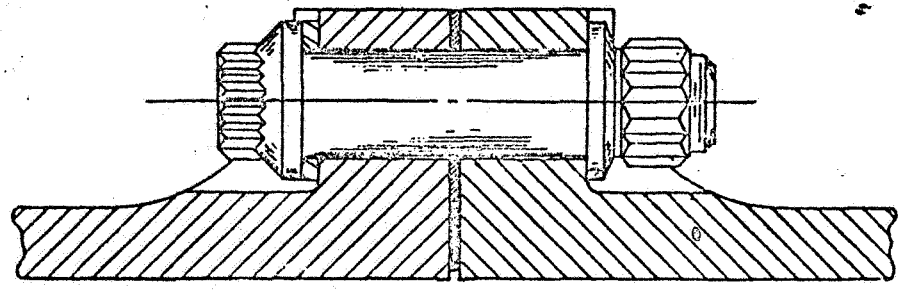

BUREAU OF STDS. O-RING

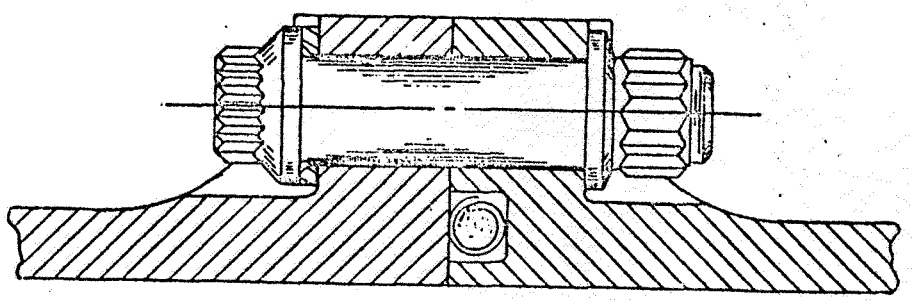

INCONEL-X WIRE MESH WRAPPED
IN THIN ALUMINUM OR INCONEL SHEET

TABLE 2. CONTINUED

	Temperature Actuated		Spring Type		
		Rubber Invar	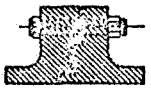 CONICAL SPRING SEAL	X-TYPE SEAL	Miniature Machined Bellows Seal
Description	Metal O-Ring in a Spacer Ring Which Controls Compression	Elastomer Ring With Invar Inside Backup Ring	Conical Spring Seal Squeezed Between Inclined-Plane, Flange Mating Surface	All-Metal, X-Shaped Cross Section	A One-Convolution, Machined, Metal Bellows
Figure of Merit	2.5	0.0011	0.450	2	12
Operating Pressure, psi	2000	2000	2000	200	200
Temperature Range, F	-320 to 1800	-320 to 160	-320 to 1800	-425 to ~ 1000	-425 to ~ 300
Average Seal Load Required, lb/in. of circumference or Gasket Factor	2.00 to 2.500 (Gasket Factor)	1.00 (Gasket Factor)	6.00 (Gasket Factor)	~ 200	~ 30
Flange Finish Required, microinch/inch rms	32C	64 to 125	32 in Sealing Corners, 125 Elsewhere	16 to 32C	16 to 32C
Materials	302 CRES OD Ring; 347 CRES for O-Ring; 410 CRES ID Ring	Elastomer Ring With Invar Inside Backup Ring	All Metallic but Various Combinations can be used; Gasket may be Aluminum or Steel	Inconel-X and Silver Coating	Steel and Kel-F

TABLE 2. CONTINUED

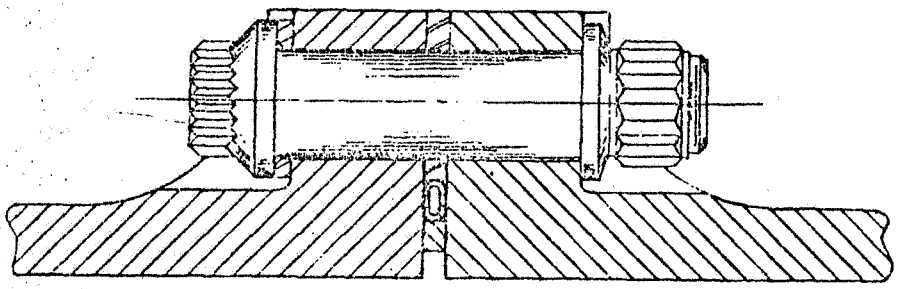

METAL O-RING IN METALLIC SPACER

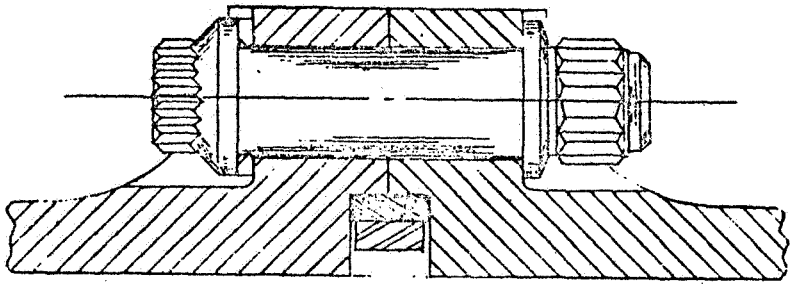

RUBBER INVAR

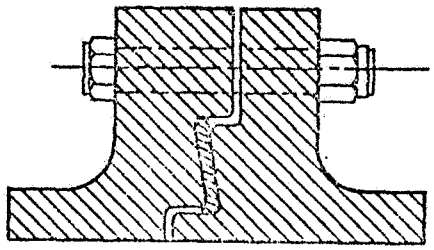

CONICAL SPRING SEAL

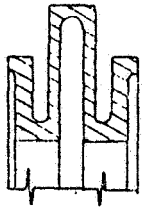

ENLARGED VIEW OF
MINIATURE MACHINED BELLOWS SEAL

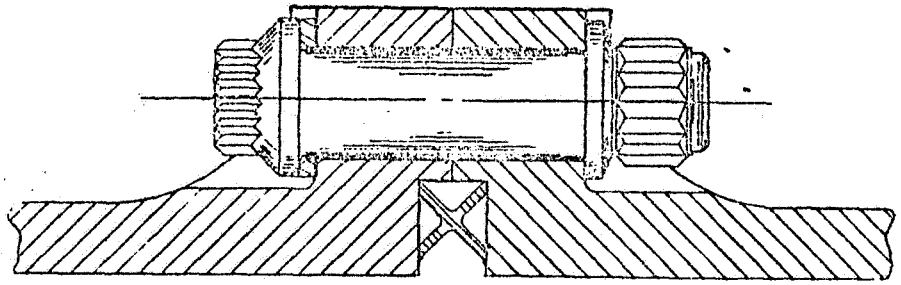

X-SEAL

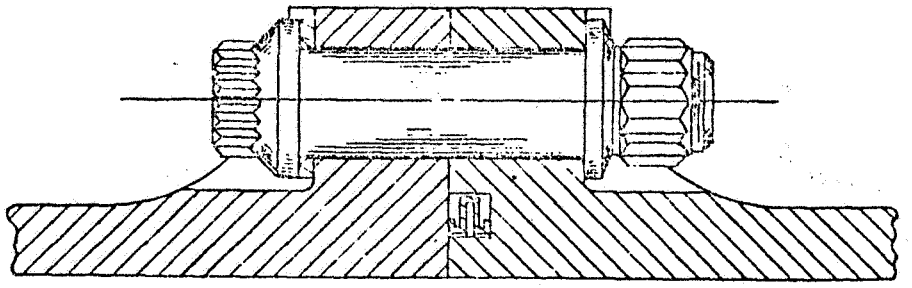

MINIATURE MACHINED BELLOWS SEAL

COMPARISON OF PERFORMANCE OF DIFFERENT SEAL TYPES

PRESSURE-ACTUATED TYPES

Pressure-actuated seals (Table 2) derive their name from the fact that internal fluid pressure acts on the seal legs and tends to increase unit loading, thus providing increased sealing ability as the pressure increases. All of the pressure-actuated seals are spring loaded, to some extent and the proportion of pressure-to-spring loading depends on the seal leg thickness, the length, the material, and the fluid pressure. For example, above approximately 1000 psi, the pressure loading exceeds the spring loading of the standard steel NAFLEX seal.

The static seal commonly employed on Rocketdyne engines are face seals. The sealing member mates with a flat surface on each flange. The efficiency of the seal depends upon the intimacy of contact between the members and the properties of the media to be sealed.

Naflex Seal (Metallic, U-Shaped Cross Section With Teflon Dispersion Coating)

Upon initial installation under ambient-temperature conditions, the relatively soft Teflon coating on a NAFLEX pressure-actuated seal conforms to the surface irregularities of the mating sealing surfaces. The seal then chills down to a low temperature when the cryogenic propellant appears in the fluid system, thus causing differential shrinkage between the Teflon and its mating metal surfaces. The seating load caused by initial deflection of the seal in installation is usually sufficient to prevent leakage at this point in spite of the differential shrinkage; and, as internal pressure is applied, the

seating load is increased proportionally by pressure actuation of the seal legs. Very fine surface finish tolerances and a high degree of mating-surface flatness are required to maintain seal integrity.

Teflon, U-Shaped Cross Section With Inner Backup Metallic "U" Spring

This type pressure-actuated seal has a "U" cross section, of which the Teflon makes up the largest part. The Teflon portion may be either molded or machined from sheet or bar stock. Within the Teflon seal, a metal spring supplies the separating force to the legs. This seal has good sealing ability; however, it has some serious drawbacks. Because of the large amount of Teflon within its cross section, it has a tendency to cold flow under installation and pressure loads, thus relieving its unit loading. High-temperature storage life tends to accelerate this cold-flow process and reduce the seal's service life. It is also weak in hoop stress carrying ability unless backed up by close contact with the flange material around its OD.

All-Metal, K-Shaped Cross Section

This type seal (several different types available commercially) can be obtained machined from one material and either unplated or with a soft metallic plating. It also may be obtained with a thin dispersion coating of Teflon. The platings or coating are used to aid in seal leg conformance to mating flange surface finish. Because of the short, thin legs inherent in its design, the seal is quite sensitive to deflection (squeeze), and may be deflected only a few mils before yield stresses are exceeded. Although, it is small in cross section, thus allowing installation in space-tight areas, this seal does not attain sufficient deflection to take up the tolerances inherent in the grooved-joint makeup without taking a permanent set. This yielding causes a

degradation in its sealing ability, and cannot be used again after removed from a joint. Fine surface conditions in the mating flange are required, i.e., 8 to 16 rms finish, for any reasonable degree of success. The highly loaded seal contact points tend to Brinell the mating flanges, thus making subsequent seal installations in the same groove worthless.

BRUTE FORCE TYPES

Metal O-Rings

The only similarity between rubber and metal O-rings is in their shape. Rubber O-rings are completely elastic when used within their temperature limits, and have outstanding performance as ambient-temperature fluid seals. The metal O-ring is really a brute force seal whose surface must be plastically deformed in a manner similar to a gasket to effect a seal and, therefore, retains only slight resilience compared to the rubber O-ring. As the pressure of the fluid to be sealed increases, causing flange separation and/or rotation, the metal O-ring loading is reduced, causing eventual leakage. Because of their small cross-sectional area, metal O-rings can be used in space-cramped installations; however, they require rigid flanges and high bolt loading to be successful.

Metal O-rings are available in a large variety of sizes, wall thicknesses, materials, coatings, and in pressurized or vented condition. In general, the best performance is given by small (cross-sectional)-size, thin-wall, stainless-steel, Teflon-coated, pressurized, or plain metal O-rings. The Teflon-coated version performs better than either the bare or plated types. Pressurized or plain O-rings should be used

if sufficient bolt loading is available. The vented O-rings should not be used for liquid oxygen because of the possibility of contact between liquid oxygen and contamination in the interior of the ring.

Spiral-Wound Gaskets

This type seal consists of spirally wound steel ribbon of chevron cross-sectional shape, with asbestos or Teflon filler between turns. After being wound tightly, the ends of the steel ribbon are welded to adjacent turns on the ID and OD, thus forming a seal assembly. Spiral-wound gaskets are used widely in the petroleum and chemical industries where flange weight and consequences of small amounts of leakage are not critical. They also have been used for some time in LOX service on missiles at moderate and low pressures; however, the increased emphasis on leakage elimination, higher pressures, larger sizes, and the advent of manrated systems have all contributed to an increase in performance requirements which this gasket cannot meet.

Spiral-wound gaskets require extremely high bolt loads (approximately 3000 lb/in. of circumference) to compress them at installation (Table 2), and tests have shown leakage at very high rates in cryogenic applications. The asbestos filler used in some of these gaskets contains liquid oxygen impact sensitive materials (latex and wax), and should not be used in liquid oxygen service. Because of the fabrication technique used in these gaskets, they are virtually impossible to clean. The Teflon-filled gaskets cannot be liquid oxygen cleaned between the wraps of metal and Teflon after assembly of the gasket and, therefore, are less desirable than seals which can be cleaned on all surfaces.

Gaskets are made in various stiffnesses (spring rates) by varying the tension of the wrapping. The stiffer gaskets are recommended for the higher pressures. They also can be made in various shapes, but their use in shapes other than circular is likely to prove unsatisfactory in all but low-pressure (100 psi) applications, because of unequal radial deflections under pressure.

Various shortcomings have been encountered in spiral-wound gaskets. The relatively loose thickness tolerance, in addition to variations in wrapping, leads to considerable variation in compression load. Another difficulty encountered is the tendency of the stainless-steel ribbon to indent the flange sealing surfaces, particularly aluminum flanges.

Spiral-wound gaskets with soft copper filler between turns are used in the turbine exhaust system of early versions of the F-1 engine; however, these are being converted to NAFLEX® seals on later models.

Bureau of Standards O-Ring

Reference 9 presents the experiences of the National Bureau of Standards (NBS) Cryogenic Laboratory (Boulder, Colorado) with use of elastomeric O-rings used as gaskets in cryogenic service. In their design, the O-ring is not used in its classical sense, i.e., extrusion caused by pressure differential across the seal, but rather squeezes out between flanges in a manner similar to a crush-type gasket. Because of the enthusiasm shown by NBS for this type seal, Rocketdyne undertook a test program to verify the test results.

The conclusion drawn from Rocketdyne tests was that the NBS design was inferior in performance to the NAFLEX seal. Test results indicated that:

1. The best performing elastomeric O-rings require 1000% higher bolt loads than the NAFLEX pressure-actuated seal.
2. The best elastomeric O-rings do not perform as well as the NAFLEX seal at pressures above 500 psi.
3. The elastomeric O-ring exhibited most of the performance characteristic of a typical crush gasket, i.e., extremely high loadings required to seal; sudden and severe leakage when seal is disturbed; leakage, when initiated, continues at a high rate; and leakage increases exponentially with increasing pressure.

The best O-ring test results were obtained with an 0.070-inch neoprene seal loaded to approximately 5600 pounds per linear inch of seal. This extremely high loading was required to compress the O-ring to the NBS-recommended 80 to 90%. Sealing performance varied by 30 to 50% between two identical neoprene O-rings tested at the same conditions. The neoprene O-rings generally showed no leakage below 1000 psi; however, on most tests after leakage was once initiated, it continued until internal pressure was reduced to half the pressure required to produce the initial leak. Actual leakage at the higher pressures was very severe, and can be attributed to the seal's poor resilience at low temperatures. When pressurized, the flange tends to bend away from the seal. The bolts also start stretching as pressure is increased, resulting in decreased squeeze on the O-ring. The O-ring material lacks the resilience to spring back when the squeeze is reduced; therefore, the compressive load decreases rapidly, and severe leakage results.

A neoprene O-ring, which was tested at reduced loading (approximately 3800 pounds per lineal inch), performed about half as well as the best O-ring. Another significant result was the large reduction in internal pressure required to reseat the seal after it had leaked. O-rings of several other materials were tested. Hypalon O-ring performance showed it to be a poor second to the neoprene. Third poorest performance was obtained with the common Buna-N O-ring. The worst O-ring was the Viton A type. This seal showed extreme leakage at relatively low pressure, and was the only material to fail structurally.

Another undesirable characteristic of these highly loaded elastomers is the "nibbling off" of material around the edges of the ring. These particles could easily contaminate a "LOX clean" system and clog small orifices and screens.

Other potential detrimental features (for which no tests were made) of the elastomeric O-ring are:

1. Aging, in long-term storage
2. Creep, caused by the high compressive stresses
3. Complete disintegration, in high-radiation environment

Any one of these defects could cause severe leakage because of the change in material properties and subsequent unloading of the sealing member.

The deficient sealing performance, the excessively high bolt loads, and the poor recovery characteristics of the elastomeric O-ring eliminate it from consideration as a cryogenic seal until better cryogenic-compatible elastomers are developed.

Inconel-X Wire Mesh Wrapped in Thin Aluminum or Inconel Sheet

In the fabrication sequence of this seal, its aluminum shell starts out as a flat, donut-shaped disk which is rolled around the mesh filler. When installed in a joint, the aluminum is soft enough to fill in minor flange-face imperfections.

This seal performed fairly well during laboratory testing in which flange rotation or separation were not involved. When flange separation does come into play, its performance is much poorer than the Naflex seal.

TEMPERATURE-ACTUATED TYPES

Metal O-Ring in Metallic Spacer

This seal is a metal O-ring bounded by solid, metallic spacer rings as its ID and OD. By using materials having different coefficients of contraction in the three components of the seal, a radial squeeze can be exerted on the O-ring at cryogenic temperature because of the differential shrinkage. This squeeze is intended to offset the effect of any flange rotation or separation, and thus maintain a high seating load on the seal. However, this seal still has the requirement for high bolt loading to compress the metal O-ring. Tests indicated that the radial squeeze does not compensate for flange rotation or separation to any great extent.

Rubber-Invar Seal

Information is given in Ref. 10 concerning the development of a promising temperature-sensitive seal consisting of a Neoprene W gasket backed by an Invar insert. It uses a temperature drop accompanying the confinement of a liquid gas to stress the gasket and maintain a positive static seal at temperature down to -297 F. The gasket stress increases as the temperature drops, and is independent of the assembly installation load.

In tests conducted by Rocketdyne, sealing performance of this type seal with aluminum flanges was very good. This seal, however, has two inherent disadvantages which precluded its use. The mating flanges must be aligned so that there is close concentricity of mating grooves; otherwise, installation of the seal is difficult or even impossible. The second drawback is that the components or ducts utilizing the seal cannot be installed or removed from a system installation in a lateral direction without moving the adjacent ducting in an axial direction.

SPRING-TYPE SEALS

Conical Spring Seal

This type joint (Table 2) consists of a male and female flange and a frustrum of a cone-shaped gasket. A quick-disconnect, V-band coupling can be used to retain the flanges or, in the case of high-pressure separating forces, bolted flanges can be used. The initial gasket slope is greater than the slopes of the mating flange faces, since the vertical distance between flange lips is less than the cross-sectional height of the gasket. As the flanges are clamped together, the gasket begins sealing radially against the mating flange lips while the inclined flange surfaces are brought to bear against the gasket

sides and prevent gasket column buckling. The mechanical-advantage leverage involved induces a plastic flow condition on the sealing edges of the gasket. Theoretically, since the gasket is preloaded, the joint should be capable of some flange separation.

This seal was evaluated by Rocketdyne 5 years ago. At that time, this design had not been adapted to the heavier flanges required for high-pressure, large-diameter, rocket engine components. Our test joints were one of the first attempts to accomplish this. For this reason and the fact that the special flange configuration required was peculiar to the conoseal only and not readily adaptable to other types, further evaluation was stopped in spite of encouraging initial test results.

X-Type Seal

Several, special, "X" cross-section seals were tested at cryogenic conditions. The seals were machined from Inconel-X and silver plated. They were found to be completely unsatisfactory because of excessive leakage, and the seal legs Brinelled the flange surfaces, thus making it necessary to resurface them for reuse.

Miniature, Machined Bellows Seal

This type seal is actually a metallic, machined bellows with a sealing edge on each end (Table 2). Because of its pressure balancing areas, this seal has very little pressure actuation and, therefore, is almost entirely spring loaded. Its low spring rate allows a large leg deflection for its size, as compared with other seals of similar design. Its very small cross-section allows installation in space-cramped areas. Two types were tested, one Kel-F coated and one with a soft metallic plating. The plastic-coated seal performed better than the metallic-plated version, but both leaked sufficiently to be dropped from further

consideration. Since the seal has a low spring rate and very little pressure actuation, very fine surface finishes, and flatnesses and parallelism of the flanges are required to effect a seal.

STATIC SEAL FIGURE OF MERIT

Since, by using the gasket-factor technique, it is difficult to compare the performance of a very resilient seal that is capable of following the deflections of flightweight flanges and that of a relatively non-resilient gasket or seal with extremely rigid flanges, a new method of rating seals was developed utilizing a dimensionless parameter called static seal figure of merit. The static seal figure of merit is made up of the parameters most significant to seal performance, and the magnitude of the number is directly proportional to the relative performance of the seal.

$$\text{Static seal figure of merit} = \frac{P \cdot S}{L}$$

where

P = maximum pressure at which leakage with liquid nitrogen is less than 1/10 scim/linear inch of circumference at the sealing edge*, or the maximum operating pressure--whichever is lower

S = distance the seal will spring back when the initial squeeze is relaxed (also may be defined as resilience or elastic recovery), measured in mils.

*Seal performance was determined by functional leakage tests with a cryogenic fluid pressurized in a seal test joint (Fig. 10 and 11) Leakage trapped in a manifold outboard of the test seal was passed through a flowrator. "Zero leakage"--an oft misquoted term-- is virtually unattainable, since even welded joints or solid metal walls may be found to leak when tested with very sensitive instruments

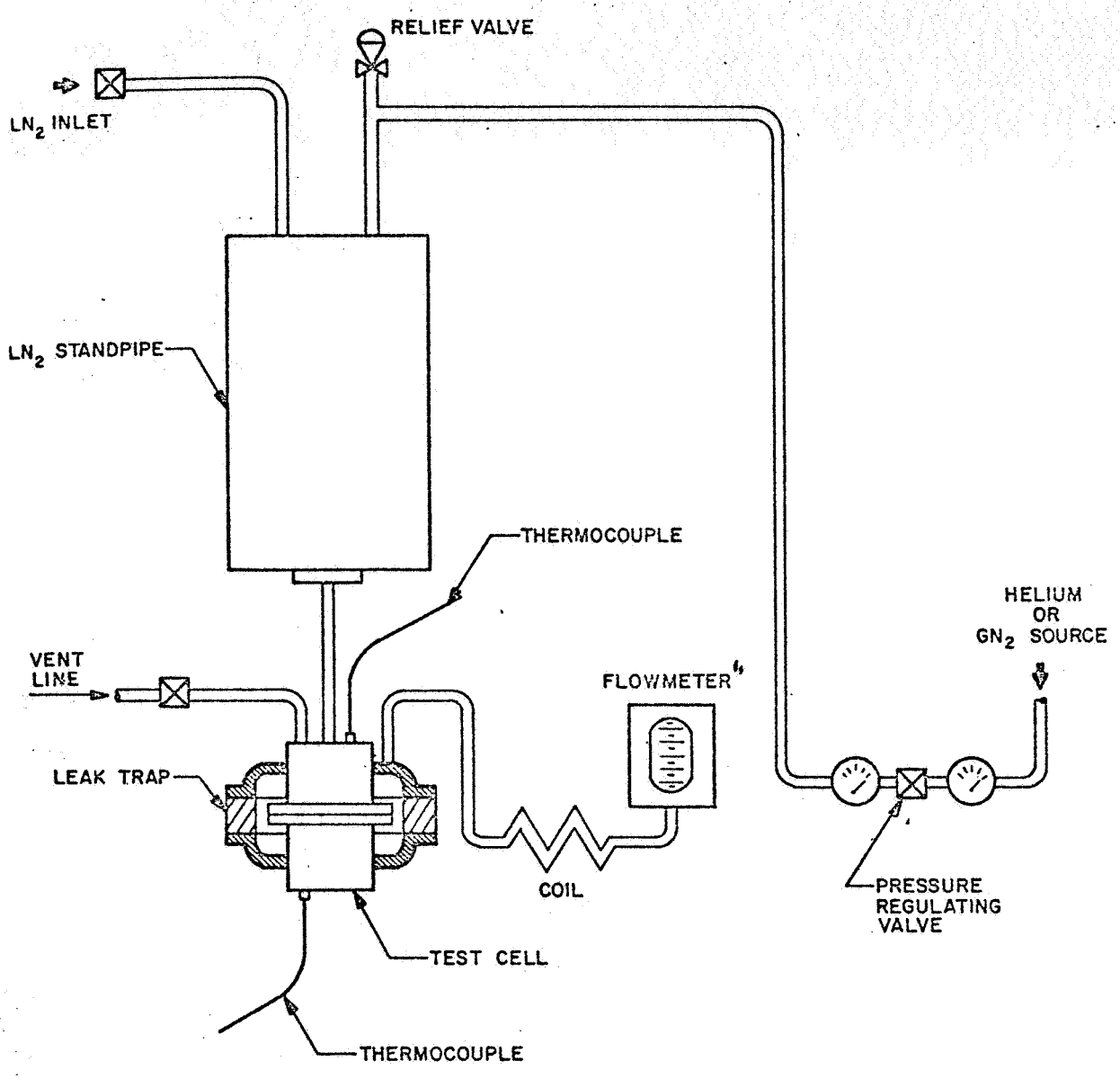

Figure 10. Schematic of Laboratory Seal Test Apparatus

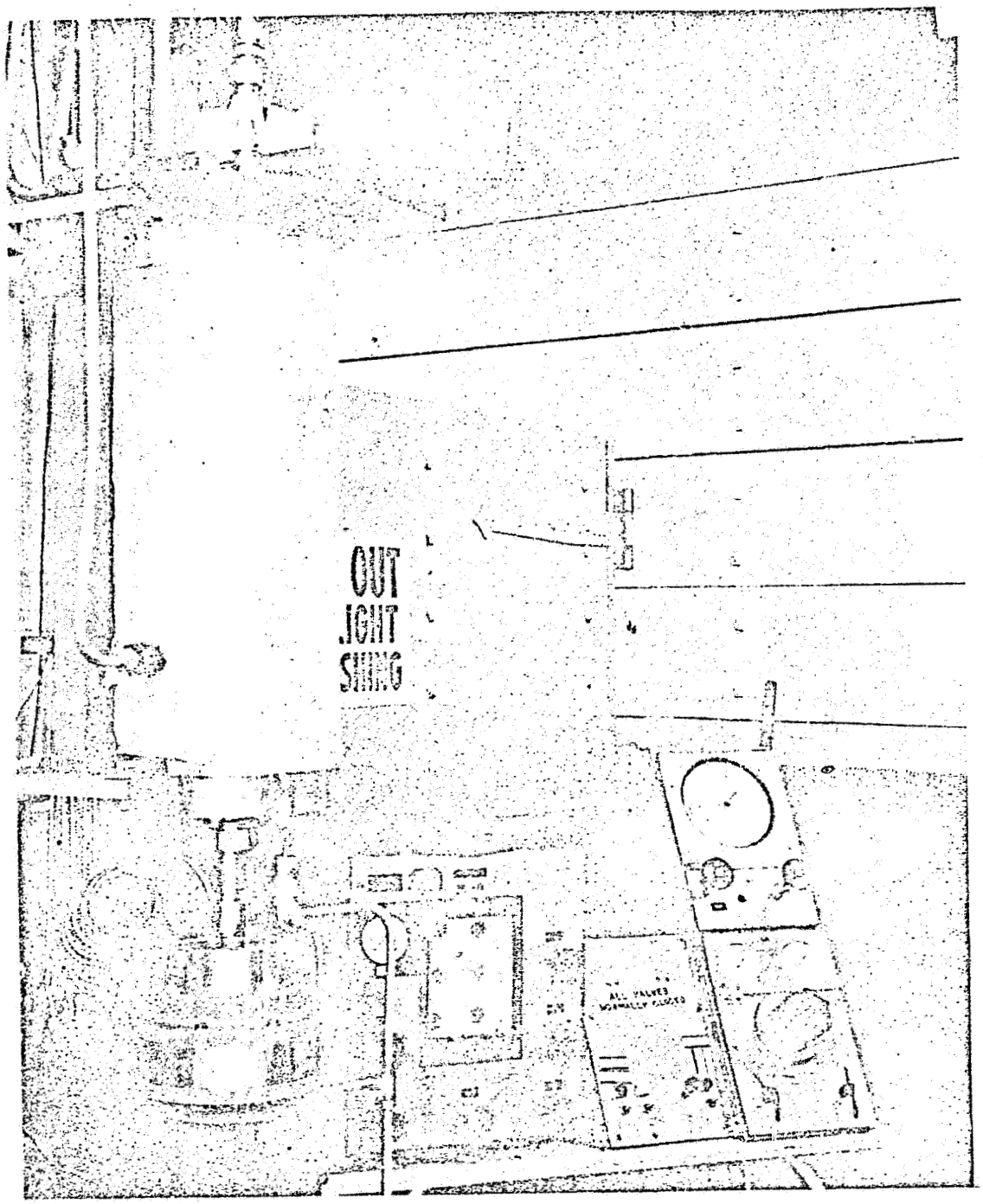

Figure 11. Photo of Seal Lab Test Apparatus

L = the initial load required to make a tight seal measured in pounds/circumferential inch at the seal contact point

The figure of merit is most important when selecting seals for use at pressures above 100 psig. At lower pressures and in heavy flanges, seal selection is often not so critical.

DESIGN PHILOSOPHY OF NAFLEX SEAL

GENERAL

The standard, pressure-actuated NAFLEX seal in cross section is essentially a metal "U", with the slot opening radially inward. The tips of the legs, which contact the flange surface, are covered with a thin Teflon film, which is deformed plastically to conform to flange surfaces. The initial loading, produced by the elastic spring leg, provides a leak-proof joint over a wide range of pressures. Flange and bolt loads, caused by the seal compression are negligible, in comparison with most other seals or gaskets.

The Rocketdyne-designed, pressure-actuated seals are composed of two basic components: (1) soft plastic gasket, and (2) the metallic seal leg. Almost any plastic material, when compressed to high stresses, produces an effective seal; however, as a joint is cooled to cryogenic temperature, the plastic material shrinks at a different (and usually greater) rate than the joint, thus causing the gasket to unseat and lose compressive stress. Plastic materials subjected to high stresses for long durations tend to creep or cold flow. Further loss of gasket load occurs, as a result of flange separation, when the joint is pressurized. The metallic member of the seal compensates for all of the preceding shortcomings of the plastic gasket. The resilience of the metal leg, which in effect is a cantilever spring, corrects for shrinkage, cold flow, and creep. A decrease in leg deflection caused by these effects produces only a relatively small decrease in load applied to the plastic. The increased load caused by seal pressure actuation also tends to balance out the higher load required on the gasket to seal at higher internal pressure.

In theory then, the most efficient cryogenic seal design must be one that combines the maximum of elasticity with the minimum of plasticity. However, practical considerations in the design of seals limit the application of this theory. For example, the elasticity which may be designed into a pressure-actuated seal leg is dependent upon the length and thinness of the leg, but these, in turn, are limited by bending stress and minimum seal seating load requirements. Similarly, the plasticity is dependent upon the thickness of the plastic coating, which may not be reduced below a certain minimum or the plastic will not conform to irregularities in the flange flatness and surface finish.

NAFLEX seals come in various configurations, such as the groove, spacer, and inverted types (Fig. 12.). The spacer-type NAFLEX seal design was conceived to satisfy the NASA requirement for primary seal, leakage-monitoring capability. The flat spacer portion of the seal, between the primary seal legs and the ID of the bolt circle, provides a secondary or leakage-monitoring seal. This is strictly a gasket-type seal with approximately 1000-psi unit load applied over a minimum of 0.12-inch, radial-width ring. Since the cryogenic seals are completely coated with Teflon, the Teflon supplies a soft seat for the secondary seal area. Leakage past the primary seal is trapped by the secondary seal, and vented off to a leak meter, through a hole in the mating flange. Small holes are drilled through the seal to join both cavities between primary and secondary seals, thus obviating the need for vent holes in both mating flanges. The secondary seal is not intended to be a redundant seal; it is intended to provide sealing ability at pressures no higher than 50 psi. In the case of hot-gas NAFLEX seals, a soft metallic (copper or silver) coating performs the same secondary seal function as the Teflon does on the cryogenic seal. Figure 13 is a photo of the cross section of a typical Naflex spacer seal.

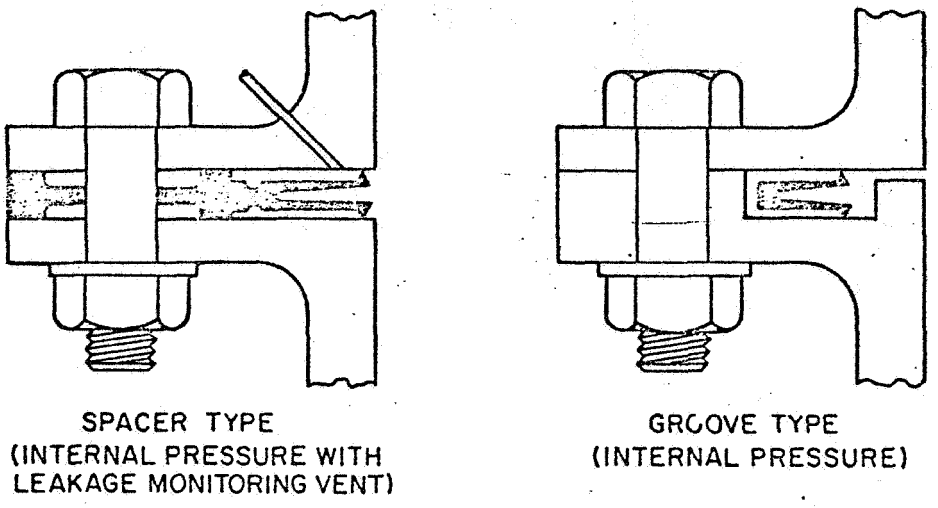

Figure 12. Various NAFLEX Seal Configurations

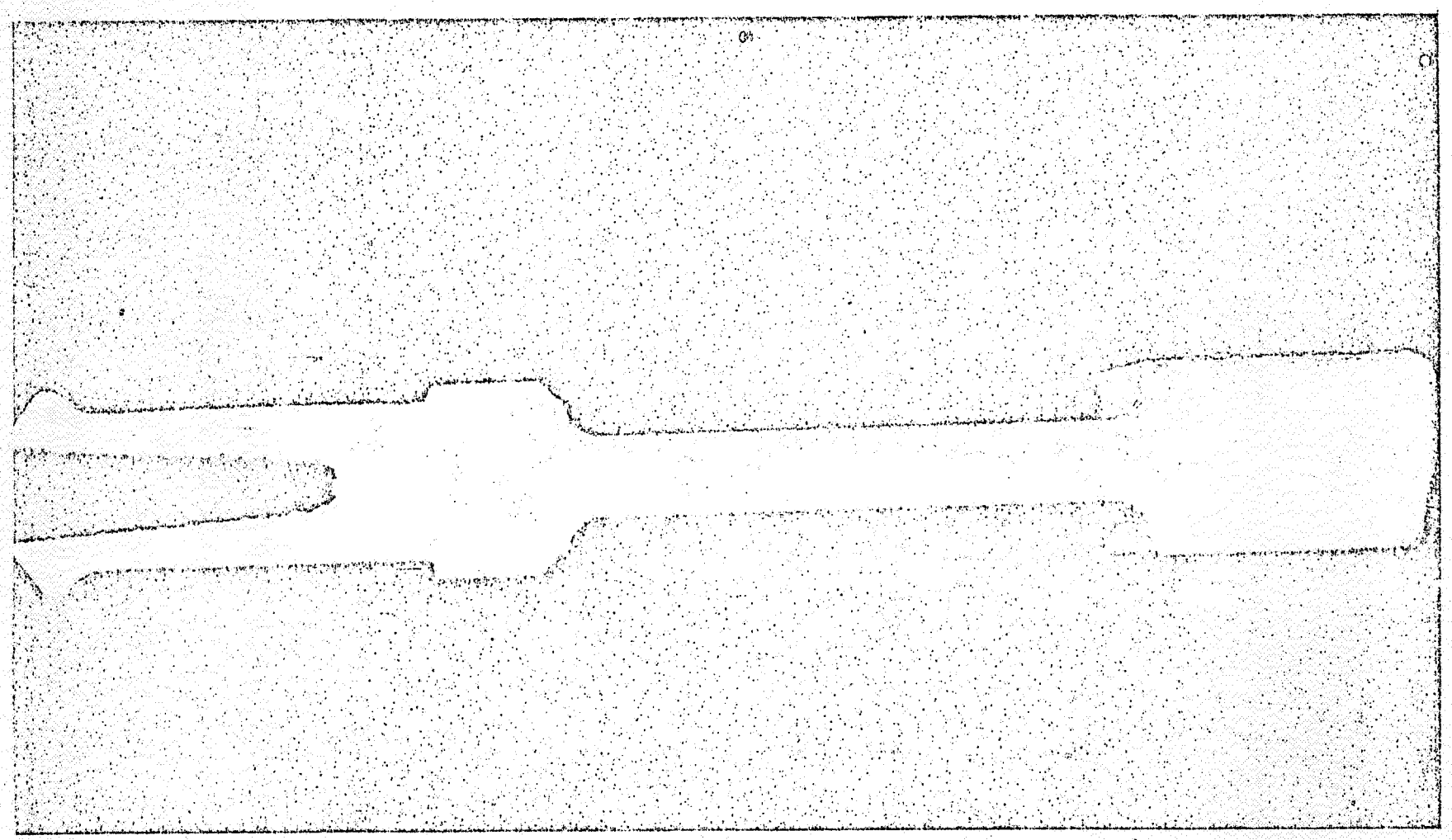

Figure 13. Cross Section of a Typical NAFLEX Spacer Seal

MATERIALS SELECTION

Metals

NAFLEX seals were fabricated of many materials during the early development phases. Those that received the most attention are discussed below.

A-286 alloy steel was the first choice on the basis of good low-temperature ductile properties; however, the large variation in tensile properties inherent with heat-treated A-286 steel caused erratic seal performance. No further consideration was given this material.

17-7PH (precipitation hardened) alloy steel seals were fabricated, and passed functional seal tests, with the exception of impact at cryogenic temperature. The seal was cooled to cryogenic temperature by immersion in liquid nitrogen and, immediately upon removal, an impact load was applied manually with a nonmetallic hammer. Several seals split along a high-stress plane, and repeated tests produced the same results. This material was eliminated from further consideration.

4340 alloy steel was the final high-strength material investigated. This material has superior tensile properties, and has passed the impact test at cryogenic temperature. The lack of corrosion resistance is a problem with 4340 steel; however, the use of electroless nickel plate provides adequate corrosion resistance. All seal data mentioned in this report was obtained from tests with 4340 steel seals.

Inco 718 nickel alloy is in the process of evaluation. It has strength properties comparable to 4340 steel and improved low-temperature notch sensitivity. It is inherently corrosion resistant and, therefore, requires no plating.

Teflon

Teflon proved to be the best plastic material for cryogenic, static-seal applications during the initial development phase; however, earlier models of NAFLEX seals used a pressure-sensitive Teflon tape as the sealing member. The tape had several disadvantages. Because of limitations in the width of tape roll available, a 12-inch-diameter seal was the largest seal that could be covered without lap joints. A lap joint proved undesirable, not entirely from a leakage standpoint, but because the lap acted as a "stress riser" to initiate tape splitting. Difficulities also were experienced with adhesion of the Teflon tape to the seal surfaces.

Development of the steel NAFLEX seal made possible the use of the Teflon dispersion coating. Aluminum seals cannot now be dispersion coated with Teflon because the Teflon bake process requires temperatures which alter the heat treatment of the aluminum.

Teflon dispersion coating is a multiple-layer enamel system applied with a spray paint process; the application techniques used by the coater determine the quality of the coating on the finished part. The actual processing of the Teflon coating is specified by a Rocketdyne process specification.

Problems associated with measurement of the thickness of the Teflon coat were resolved by the addition of an over-all width dimension to be measured on the finished seal. Thus, coating thickness on each side of the seal will be within tolerance if each side receives the same number of coats. TFE (tetrafluoroethylene) Teflon was the first Teflon dispersion coating used on the seals; however, FEP (fluorinated ethylene propylene) Teflon 100, a recent development, appears to be a superior material. Tensile properties of FEP are similar to TFE; but, FEP is a true thermoplastic and, while being processed, melts and flows to form a smooth continuous surface. TFE particles only fuse together, but do not melt. It is intended that FEP coating supersede TFE for all seals when suitable processing controls (process specifications, etc.) have been established and coating vendors have developed their techniques to a higher level.

COMPONENT TESTS

The NAFLEX seal has undergone an extensive series of component tests during the last 5 years. These tests usually are conducted in a component test cell in which the seal is installed with flanges identical to those used on engine hardware, and with sufficient length of tube on each flange end to allow even distribution of flange bending moment into the tube. Figure 14 shows some typical flange test cells. These tests subjected the seal to the normal design conditions of pressure, temperature, deflection, and environment.

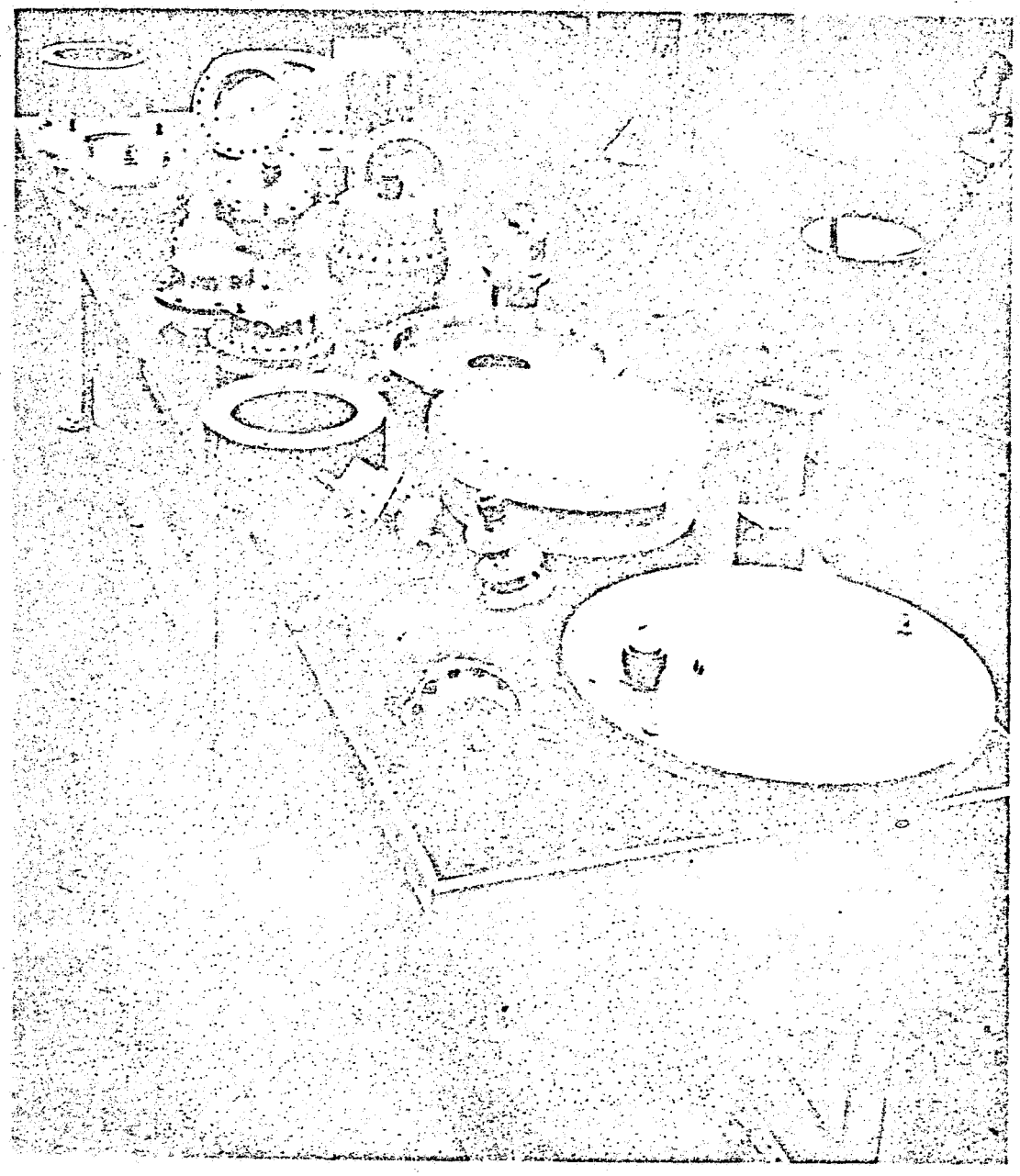

Figure 14. Typical Static Seal Test Cells

Functional Tests

The nominal-condition tests subject the seal at the average static conditions (temperature, pressure, and deflection) at which the majority of seals operate. All tests were conducted to a nominal 2000 psi maximum. The test temperatures were -320 to -290 F, using liquid nitrogen to simulate liquid oxygen. Many tests were made with helium to simulate seal performance with liquid hydrogen. Test results with this prototype indicated no leakage.

Seal Tolerance Extreme Tests

Two seals, one representing the highest seating load and one representing the lowest seating load produced by the extremes of design tolerances, were tested in each of the three sizes (1.5-, 4-, and 17-inch diameter).

These seals all pass the liquid nitrogen functional leakage tests without difficulty. Their satisfactory performance with high loading shows that the Teflon-coated sealing edge is not overstressed, and that there will be no excessive cold flow to affect operation of the seal.

The low-loading seal also performed satisfactorily, which shows that the Teflon coating is loaded high enough to seal, even at the lightest loading conditions.

Life-Cycle Tests (Reusability)

A test series was conducted to demonstrate that the NAFLEX seal would operate satisfactorily for the maximum required life.

The first part of the test series consisted of 100 installation cycles of the seal in a standard installation simulating repeated usage.

The second part of the test series subjected the seal to 500 pressurizations ranging from 0 to 2160 psig to simulate a maximum possible number of proof-pressure cycles any one seal is likely to receive.

The third part of the series consisted of 1/2 million pressure cycles ranging from 1440 to 2160 psig at -320 F. These tests duplicated the fluctuations of pressure that can exist in a typical propellant feed system. This portion of the series was expected to be the most critical, because it subjects the seal to an extended series of stress cycles that will promote fatigue failures if there is any inherent seal weakness.

The 4340 steel, tapered-leg seal passed all phases of the life-cycle test series without structural failure and, subsequently, passed functional leakage tests. Seals representing the tolerance extremes of the steel seal design successfully passed the entire series of tests.

Pressure Surge Tests

The seals were subjected to extreme pressure surges that were produced by pressurizing a stand pipe (Fig. 15) to 100 or 200 psig with liquid nitrogen and opening a quick-acting propellant valve located in the line between the stand pipe and test joint. This procedure consistently produced pressure peak surges over 1000 psig and some as high as 5000 psig.

The NAFLEX seals showed no structural damage after three surge test cycles, and no leakage was recorded during or after the surge tests.

Proof-Pressure Tests

Seals were tested in a very rigid fixture to determine the actual proof-pressure limits on the seal determined by seal structural strength. Standard hydrostatic pressure test techniques were used.

The seals were pressure tested to 6000 psig without any measurable dimensional changes. Critical points (Fig. 16) that were measured were the over-all width and the width at the leg midpoint; changes in either would have indicated that the stress in the seal legs had exceeded yield at the midpoint. The seal's resistance to permanent set indicates that the leg stress did not exceed the material's yield in a significant portion of the seal leg. The flange faces undoubtedly tend to support the seal legs when they balloon at midpoint, and thus reduce the leg stress. Extremely light flanges would not support the legs; however, light flanges could not be used at high pressures.

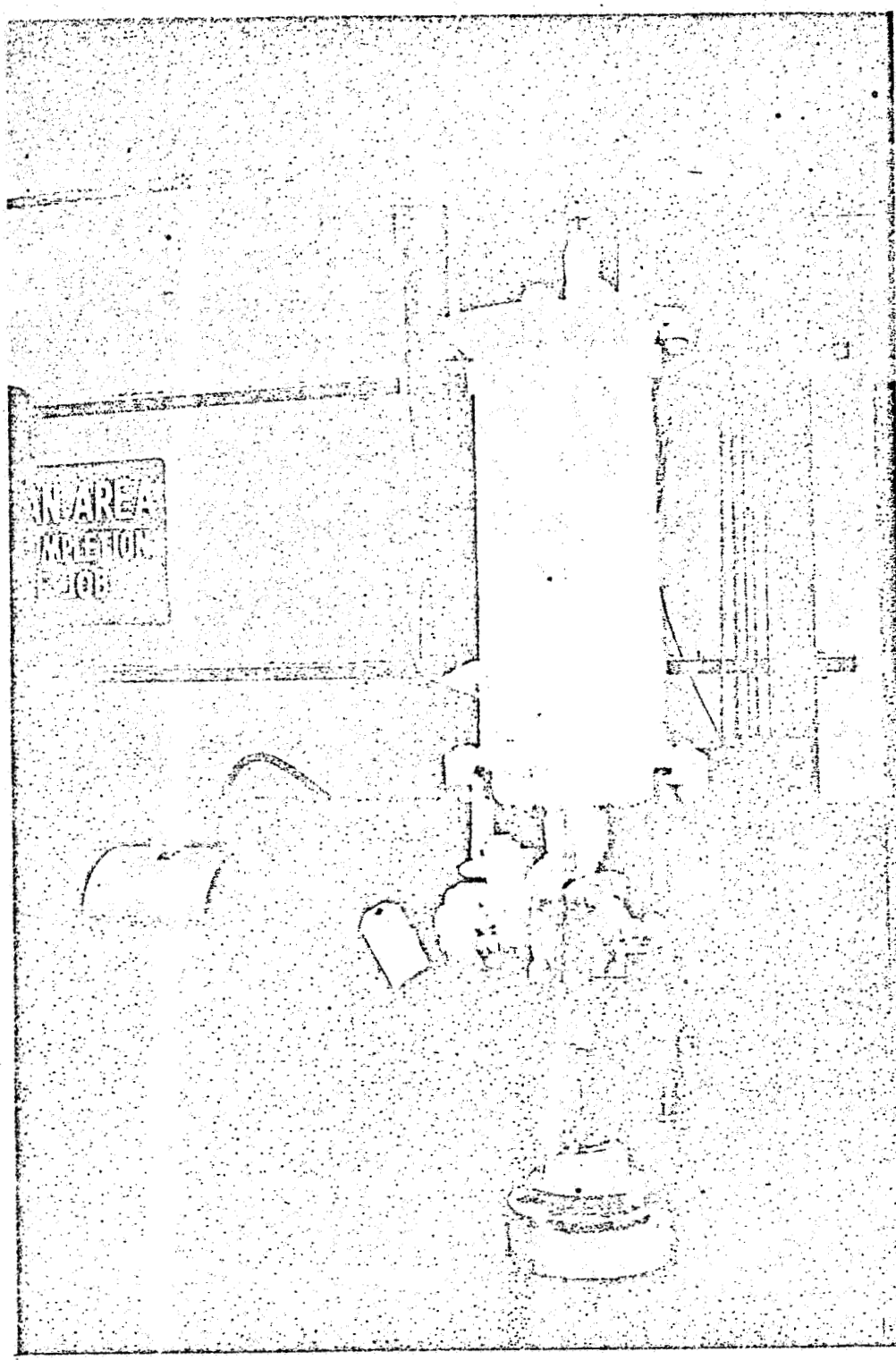

Figure 15. Pressure Surge Test Lab Setup

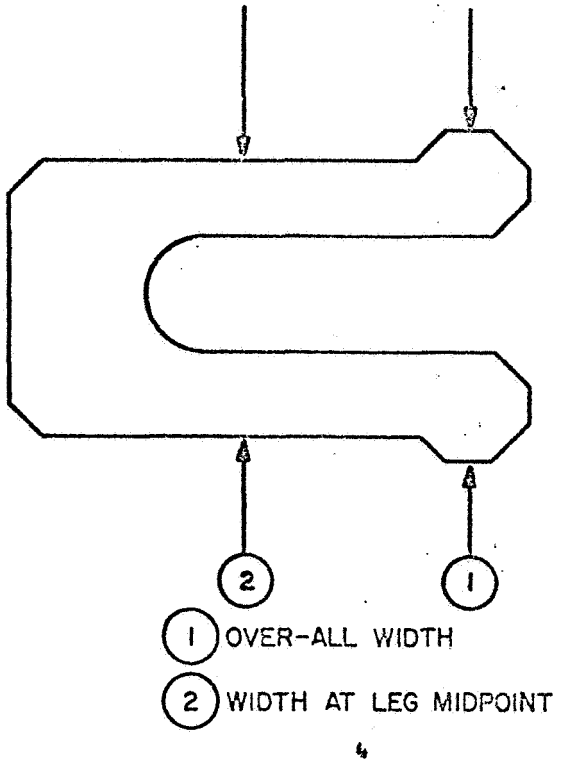

Figure 16. NAFLEX Seal Cross Section

Seals made to the tolerance extreme that produces the thinnest leg were pressurized to structural failure. The failure was evidenced by sudden and severe leakage. In every instance, the pressures required to produce this leakage were in excess of 22,000 psig. At this pressure, the flanges were seen to separate about 3/32 inch.

The dispersion-coated (Teflon) NAFLEX seal showed no sign of leakage up to 20,000 psig.

Based on these proof-pressure tests, the steel, groove-type, NAFLEX seal, when operating at 2000 psig, has a Functional Safety Factor of 3 and a Structural Safety Factor of 11. Functional Safety Factor is defined as the ratio of the maximum safe operating pressure to the operating pressure. Structural Safety Factor is the ratio of the pressure required for structural failure to the operating pressure.

Accelerated Aging

One of the most critical problems associated with any Teflon sealing system is that of cold flow. The Teflon must be highly stressed to seal at cryogenic temperature; however, this same high stress at ambient temperature may over stress the Teflon and cause cold flow. The tensile strength at ambient temperature is approximately 3000 psi and, at cryogenic temperature approximately 20,000 psi; this indicates the extreme change in physical properties of Teflon at the two temperature extremes.

To determine the effects of Teflon aging, the cold flow is accelerated by placing the seal, while installed in a test fixture, in an oven at 160 F for 48 hours. A cryogenic functional test is performed on the seal before and after the aging process. The results are compared, and detailed measurements taken to evaluate the effects of the test. The NAFLEX seal has passed this test.

Performance Tests at Off-Design Conditions

Flange Defect Leakage. NAFLEX seals were tested in flanges with scratched surfaces. Leakage is caused by scratches which are easily detectable with a fingernail and which run in a noncircumferential direction. The larger the scratch, and the closer to radial its direction, the greater the leakage will be.

Flange surface defects are also detected, during the low-pressure gaseous nitrogen checkout with soap solution detector, by formation of bubbles or fuzz.

Flange and Groove Surface Finish. Tests with cryogenic seals have been conducted with various finishes; however, in every case, at least a 32-rms finish was required to prevent leakage. In addition, the lay of the tool marks is important, and should be concentric with the sealing lip of the seal. Tool marks that cross the seal edge promote leakage by offering a direct channel for leakage flow past the sealing edge. Rocketdyne's standard flange finish requires that a "C" be used to indicate that tool marks are to lay in a concentric or circular pattern such as those produced by facing with a lathe (Ref. 11).

Tests were conducted with a 16-rms ground finish and an 8-rms lapped finish. The results indicated that, to meet all service requirements, the only alternative to a 32C finish is the 8-rms finish.

Out-of-Parallel Surfaces. Tests with the NAFLEX seals were conducted in flange pairs purposely out of parallel. A 3.6-inch-ID joint was assembled with shims to produce progressively 0.002-, 0.003-, and 0.004-inch nonparallel surfaces. The seals performed well up to 0.004-inch, which was not a limit but only the extreme of the tests made.

Flange Swiveling Tests. Tests with NAFLEX seals were conducted in a joint modified so that one flange could be swiveled, with respect to the other, around their longitudinal axis.

The seals were tested at pressures ranging from 150 to 250 psig at -320 F, with liquid nitrogen in the joint. The joint was cycled through an angle of 15 to 30 degrees while pressurized. No leakage was recorded, even during the swiveling. Four hundred cycles (800 angular movements) on each seal were performed without any signs of damage to the Teflon coating.

These results suggest the possibility of using NAFLEX seals in swivel joints.

LOX Impact. Sensitivity to LOX impact was a major disadvantage of the Teflon tape used on the original NAFLEX seals. The problem was not in the Teflon film itself, but rather in the pressure-sensitive adhesive that was used on the tape. The first Teflon tape was sensitive to 20 ft-lb of energy impacts. An improved type was sensitive to 40 ft-lb impacts. The Teflon dispersion coating is insensitive to LOX impact.

Shock Tests. Tests were conducted to determine whether the candidate seal materials were subject to failure because of thermal and mechanical shock. Several prototype seals were tested to extremes of temperature range (-320 to 160F) without thermal shock failure. Mechanical shock was applied to the test part after chilling to -320 F. The physical impact was delivered with a rubber mallet. The 17-7PH seal was the only seal that did not pass this test; it showed a typical brittle impact fracture. Other materials tested were 2024 aluminum, and A-286 and 4340 steels.

Although 4340 steel is less ductile than several other steels at cryogenic temperatures, there have been no brittle failures on these seals in any of the many tests conducted at temperatures down to -425 F, or during the life cycle tests (1/2 million pressures cycles at -320 F).

Load Deflection. Tests were conducted with an Instron machine* to determine (1) the load vs deflection curve for steel seals, (2) the load at the installed deflection for these seals, and (3) the empirical coefficient used to modify the theoretical leg deflection equations for leg design purposes.

Typical load deflection curves for representative types of NAFLEX seals are shown in Fig. 17.

Environmental Tests. Military specifications require that components be subjected to extremes of environment (i.e., high humidity, salt spray, 160 F and -65 F) for specific periods of time, and then be capable of passing functional tests.

Satisfactory results were obtained with production-type seals that were installed in seal test joints and given functional tests before and after the environmental tests.

The Teflon dispersion coating on the NAFLEX seal acts as an excellent protective coating. On some of the seals, certain areas cannot be adequately coated or inspected; therefore, the seals are nickel plated for corrosion protection before the Teflon coating is applied.

---

*A type of tensile test machine designed for low-load-range tests

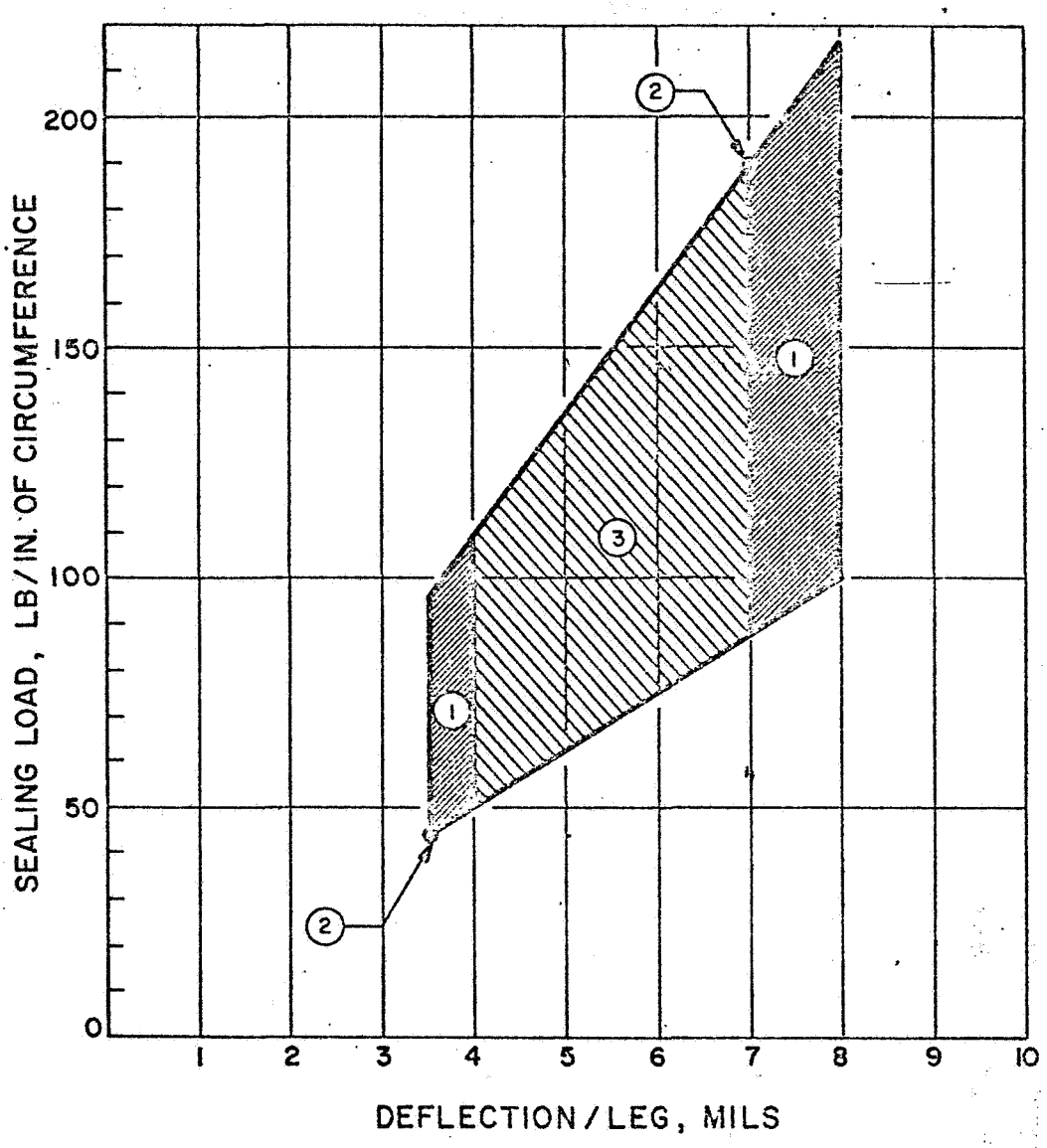

(1) DEFORMATION OF TEFLON ON PRIMARY SEALING SURFACE OF NAFLEX SEAL LEG

(2) MAXIMUM AND MINIMUM LOADS PER INCH OF CIRCUMFERENCE ON SEAL LEG AS A RESULT OF TEFLON DEFORMATION AND MANUFACTURING TOLERANCES

(3) ENVELOPE OF EFFECTIVE SEALING LOAD

Figure 17. Typical Load vs Deflection Envelope for the NAFLEX Seal

LEAKAGE MEASUREMENT TECHNIQUES

LABORATORY

Seal gas leakage during laboratory testing is monitored by (1) water displacement, (2) rotometer (flowmeter), or (3) soap bubbles, with the water displacement method being the most common.

Laboratory testing procedure consists of bringing the test fixture to the desired temperature, pressurizing the fixture to the desired pressure, and then measuring the volume of water displaced by the gas leakage that occurs over a span of 1 minute. With this setup, any volume of leakage from 0.2 to 500 scc can be measured.

The present laboratory water displacement setup consists of an inverted, calibrated burette (Fig. 18), with provisions made for venting leakage to the burette from the seal test setup.

The water displacement method gives a measurement of total leakage per given period of time, i.e., it is not an instantaneous leakage rate measurement. If a rate of leakage is desired, the burette setup (Fig. 19) can be replaced with a rotometer. The rotometer (gas flowmeter) has a leakage measuring capability of 80 to 5000 sccm, and indicates leakage rates instantaneously.

When a nonquantitative check for low-pressure leakage (100 psig maximum) at room temperature is required, a soap solution is applied to the area under investigation. If a leak is present, a foam (fuzz) will appear. The leakage rate is indicated by the size of the bubbles in the foam, and the rate at which they are formed. The soap solution method is used only to determine if a leak exists; any quantitative estimate of the leakage depends entirely on experience.

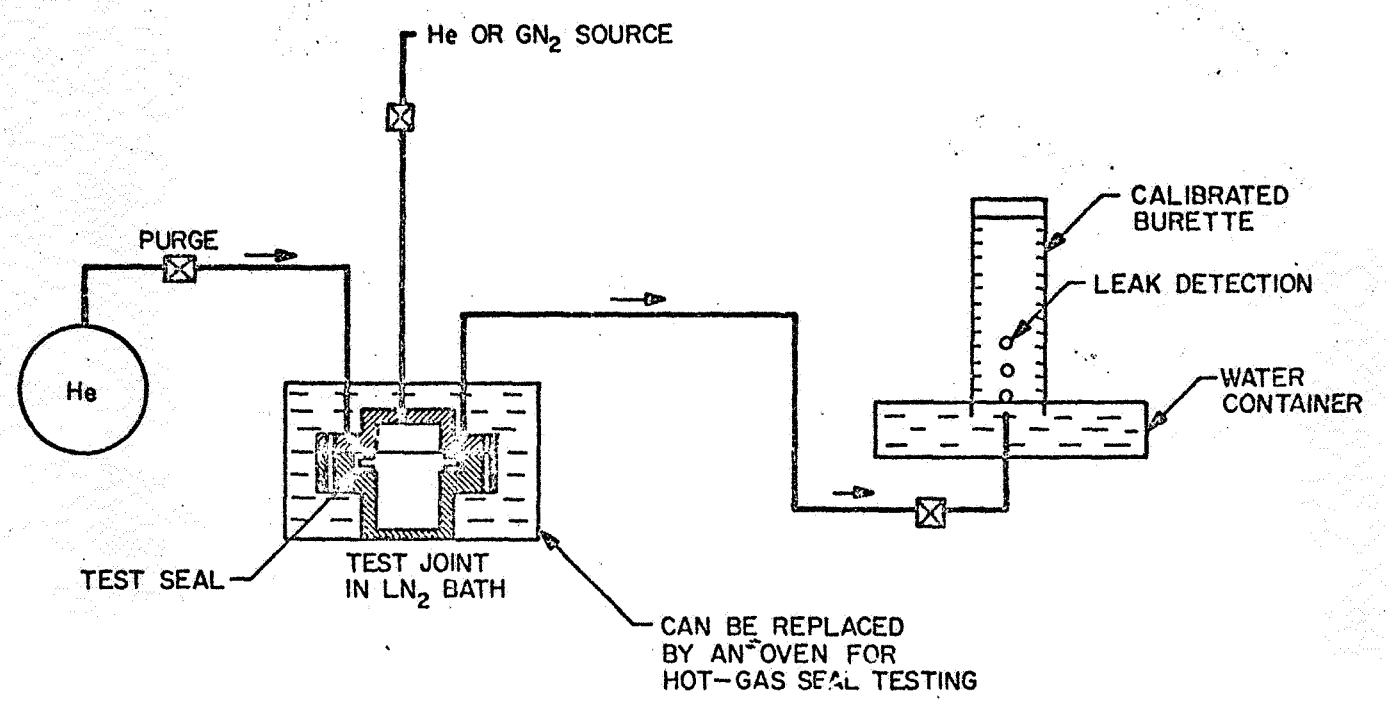

Figure 18 Schematic of Water-Displacement Leakage Measurement Method

An alternative for the soap check method is to immerse the fixture in water, and watch for the appearance of bubbles.

Few tests have been run using the helium mass spectrometer for determining NAFLEX seal leakage. This device has a range of 2×10^{-10} to 2×10^{-5} scc/sec helium, and all tests resulted in leakages in excess of the maximum reading of the spectrometer. All of the seals used were tested by the water displacement method prior to the mass spectrometer tests, with no leakage resulting.

Tests with the mass spectrometer consist of pressurizing the fixture to 50 psig helium, and pulling a vacuum of 5×10^{-5} mm Hg between the primary and secondary sealing surface. Leakage past the primary sealing surface is pulled through a sensor, and the leakage rate recorded.

Prior to delivery of each engine, each engine system is first isolated and leak checked with the pressure gage lockup method; i.e., the system is pressurized with a gas and held, with any drop in pressure indicating leakage. Then, each joint is leak checked with a gas flowmeter (MAECO flowmeter). The range of this instrument is from 10 to 13,000 sccm.

STATIC ENGINE TEST

Hastings-Raydist gas flowmeters (modified) are used during engine firing to detect leakage. This type of flowmeter (Fig. 19) compares the electrical output of directly heated conduits, which form

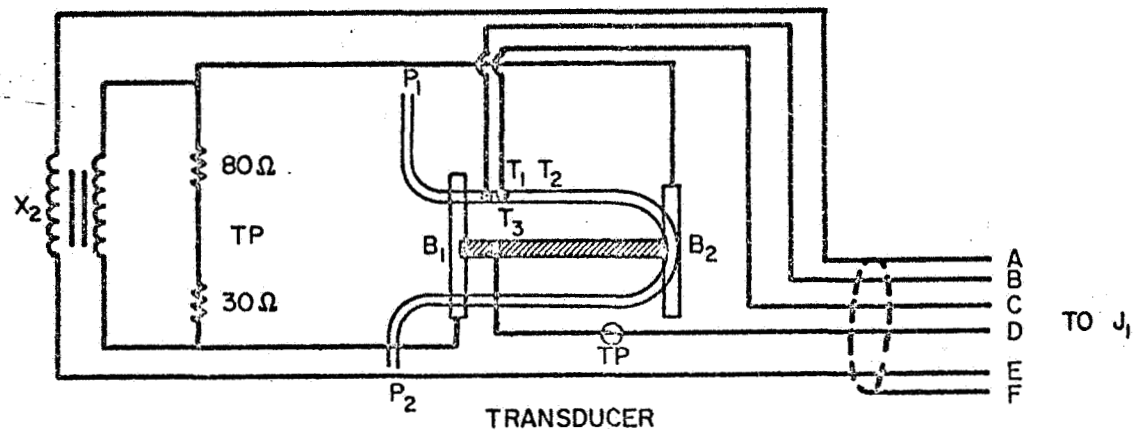

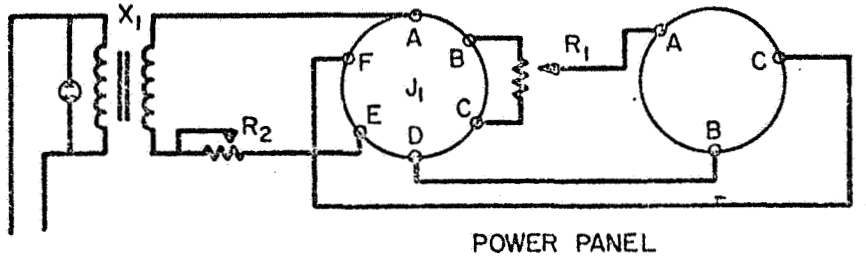

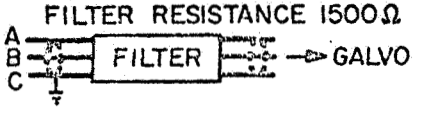

P_1	= GAS INLET
P_2	= GAS OUTLET
▨	= REFERENCE TUBE
T_1, T_2, T_3	= THERMOCOUPLES
R_1	= ZERO ADJUST
R_2	= CURRENT ADJUST
TP	= CURRENT TEST POINTS
B_1, B_2	= ELECTRICAL CONTACT BAR
X_1	= REGULATING TRANSFORMER
X_2	= STEPDOWN TRANSFORMER

Figure 19. Hasting-Raydist Gas Flowmeter Schematic

elements of a thermopile, to measure the cooling effect of the fluid passing through the conduit. The capacity of the flowmeters is 80 to 1600 sccm, with an accuracy within 10% under lab conditions. However, this device is sensitive to vibrations and temperature changes, and its accuracy and reliability under engine firing conditions is still under investigation.

The principle of operation of the Hastings-Raydist meter is identical to that of the flightweight Radiation Technology Inc., unit developed by NASA/MSFC.

CONCLUSIONS

Static seals no longer can be taken for granted, and treated as insignificant components. They now must be given as much engineering evaluation as any other component in an engine system.

Careful consideration must be given to all elements within a static seal joint; a successful design is one blending the attributes of flanges, threaded fasteners, and the seal itself.

Of all the cryogenic seals evaluated thus far by Rocketdyne, the NAFLEX seal has been the most successful.

Although the NAFLEX seal is capable of sealing hydrocarbon fuel joints, the gask-o-seal offers equal reliability at a lower cost and is less sensitive to flange surface imperfections.

The high temperature NAFLEX seal (i.e., copper or silver plated in lieu of Teflon), although not comparable in sealing performance to the cryogenic NAFLEX, is the most successful hot gas seal yet evaluated by Rocketdyne.

Definition of "zero" or minimum leakage requirements for a separable connector must be closely evaluated to balance the leakage hazards involved with the cost and practicability of development, manufacture, assembly, and quality control.

REFERENCES

1. Modern Flange Design, Bulletin 502, 2nd Edition, Taylor Forge & Pipe Works, Chicago, Illinois, 1950.

2. Korn, A. H.: "Torque-Stress-Load Relationship In Bolts and Screws," Product Engineering, March 1943.

3. Design of Piping Systems, 2nd Edition, The M. W. Kellogg Co., N.Y., John Wiley & Sons, Inc.

4. North American Aviation Report No. 2290, Fitting-Tubing and Line Support Program, Test Program Under AF33(600)-28469, August 1955.

5. Jordan, J. and T. J. McCuistion: "The In-Place Seal," Product Engineering, 18 April 1960.

6. Roberts, I.: "Gaskets and Bolted Joints," Journal of Applied Mechanics, June 1950.

7. Dunkle, H. H.: "Effect of Different Machined Finishes on the Sealability of Gaskets," Valve World, No. 2, 1954.

8. Doughtie, V. L. and W. J. Carter: "Bolted Assemblies," Machine Design, February 1954.

9. Weitzel, et al.: Elastomers For Static Seals at Cryogenic Temperature, Paper D-6, 1960 Cryogenic Engineering Conference.

10. Logan, S.: Static Seal For Low Temperature Fluids," Jet Propulsion, p 334-340, July 1955.

11. Rocketdyne Standard RP260-1011, Groove Dimensions, Pressure Actuated Seal.

Question: In your evaluation using the figure of merit, most elastomers would assume a compression set; they will deform plastically. Your variable in this figure of merit equation is resilience, the ability of the material to resume its former shape. In your evaluation of elastomer seals, did you use your initial load figure in the figure of merit for the S-variable, or did you have a compression set and then try to measure the resilience?

Answer: The load used to squash the seal to make up the joint is the load we used, the initial one before it is chilled down.

Question: So, if you use a second calculation, the figure might possibly be higher for most elastomers?

Answer: Most elastomers do not have any recovery at cryogenic temperatures.

Question: After the initial load?

Answer: That is right.

Question: So, the figure would then be higher, if you relaxed your load and applied it again, and took a second measurement of the recovery.

Answer: Possibly, yes.

Question: Then you are referring to the permanent set that might come from the first application of load.

Answer: That is correct.

Comment: I think the use of the figure of merit is a very good device. However, I would like to suggest that you modify it. In using the factor S, the figure of merit is directly proportional to the factor S, and it is based on the assumption that the seal must have some spring-back. However, some of the seals you have shown us do not function on the basis of elastic spring-back. If you were to modify factor S and evaluate it on the basis of the system that you back-off your connectors before you encounter leakage, then perhaps your figure of merit would be a more accurate measure. As it is, you are comparing an elastic seal that

does not depend on it; and, of course, the figure of merit for the elastic seal is always going to be higher.

Reply: Which seals did not have an elastic deflection?

Comment: Well, the conical spring washer is not as dependent upon elastic spring-back because it is a radial seal. I think that, with any of the group of boss seals that you mentioned, spring-back is a secondary factor. Elastomer seals are also less dependent on spring-back, especially if you employ, as you have shown in your diagrams, an independent method of preloading your flange connection, so that the seal is actually acting independent of the ability of the flange to take operational loads.

Reply: The seals that do not have much spring-back will cost you in weight if it takes a lot of bolt-loads to make up the joint and hold it rigidly.

Comment: I did not mean that; in using the figure of merit, I think it would be a more accurate evaluation if the factor S was changed to consider the distances of back-off before leakage is encountered. The way the factor S is presently used, it is really an accurate evaluation for all of the fields that you have shown. It is accurate for spring-actuated fields and pressure actuated fields, but it is not accurate for the other types.

Comment: I question the validity of using the figure of merit as stated. It seems that P, the pressure at leak, should enter as a high power since this is certainly the most important consideration. Therefore, $\frac{P^2S}{C}$ should be a more realistic form. In addition, if "zero leak" was defined as 10^{-6} CC/sec/lin inch instead of 0.1 scim, the figure would apply to hydrogen systems. I question whether some of the pressure actuated seals would have a high figure if these changes were made.

Reply: I think that would spread them even more.

Comment: It depends on whether the seal, for instance a Naflex seal, could satisfy 10^{-6} CC/sec. leakage criteria.

Comment: The figure of merit, as defined, is applicable only to a few types of seals and is not appropriate for temperature energized seals, some other types of radially seated seals, or for all types of pressure energized seals.

The spring-back factor S attempts to account for ability to follow flange movements but does not reflect the temperature induced radial spring deflections established in the insert ring and flange members with the invar-elastomer temperature energized seal. To apply compression recovery of an elastomer at low temperature is incorrect, for this overlooks the basic principle of this class of seal. High flange loading is not required. Normal flange loads are required to retain the pressure end loads; less than 50 lb/lin in seats the seal (as with the Naflex seal).

In many instances, pressure energized seals improve as the pressure is increased. The "P" factor in the figure of merit does not provide for this.

N67-86148

ANALYSIS OF PRESSURE ENERGIZED SEALS

BY

JOHN WALLACH, MECHANICAL ENGINEER
ADVANCED TECHNOLOGY LABORATORIES
GENERAL ELECTRIC COMPANY
SCHENECTADY, NEW YORK

THIS PROGRAM WAS SPONSORED BY GEORGE C. MARSHALL SPACE FLIGHT CENTER, NATIONAL AERONAUTICS AND SPACE ADMINISTRATION.

1.0 CANTILEVER-TYPE PRESSURE-ENERGIZED SEALS

1.1 Introduction

Static seals for use with pipe flanges where high internal pressures are encountered are usually pressure-energized. High internal pressures cause flange separation and unless the initial bolting stresses are very high may reduce the seal-to-flange face contact pressure to a point where leakage occurs. The use of high bolt stresses means larger bolts and flanges and a resultant increases in weight. In order to avoid this weight increase and maintain a sufficiently large seal-to-flange sealing pressure, the seal is designed so that an increase in pressure results in an increase in the sealing force.

The flanges are designed to preload the seal to furnish a minimum seal-to-flange sealing force for zero internal pressure. Otherwise the effect of the flange on the seal is minimized. A typical design has the seal sitting in a recess in the flange, see Fig. 51.1. The difference between the free height of the seal and restrained height results in a preloading of the seal. The restrained height is also affected by the bolt load and resulting compression in the flange faces. However, this effect is small as compared to the difference between the free height and the depth of the recess.

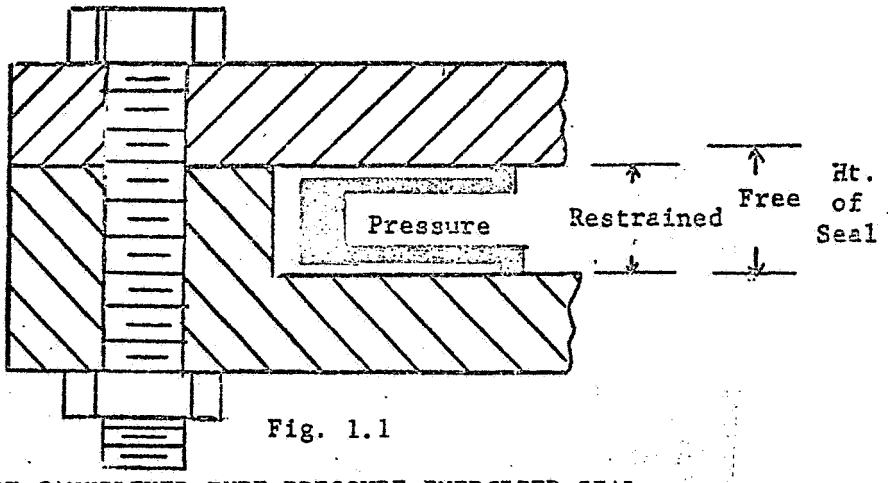

Fig. 1.1

INSTALLATION OF CANTILEVER-TYPE PRESSURE ENERGIZED SEAL

Therefore, the effect of the bolt load on the seal is secondary. The bolt pre-load need only be sufficient to keep the flange faces in contact under all loading conditions.

The sealing of the fluid depends primarily on the seal-to-flange sealing force. As the flange and seal are usually both made of a high-strength metal, the seal lip contacting the flange is often covered with a softer material such as Teflon. The plastic flow of this softer material effects the seal. The minimum sealing force required is determined by the properties of this material.

An analysis is needed to determine the sealing force characteristics for various types of pressure-energized seals. In this section various seal designs are analized to determine the deflection, stress, and sealing force, and to generate design formulas and methods. A number of generalized designs

Preceding page blank

are chosen which are representative of the seals in use in the missile industry. The mathematical models combine simplicity and design accuracy. Because of the recessed flange face the seal analysis considers only the seal and neglects the surrounding structure.

1.2 Nomenclature

		Units
a,b	Constants	
E	Modulus of elasticity	psi
h	Thickness of seal leg	inches
H_F	Free height of seal	inches
H_R	Restrained height of seal	inches
I_c	Area moment about the radial centroidal axis	in^4
k	Axial distance from seal centerline to outside surface of seal leg	inches
ℓ	Length of seal leg	inches
L	Axial length of web	inches
p	Pressure	psi
r	Radius of seal	inches
r_1	Inside radius of seal	inches
r_2	Inside radius of web	inches
r_3	Mean radius of seal web	inches
R	Edge load or reactive load	lb/in
R_s	Sealing force	lb/in
t	Web thickness	inches
x	Length along beam (seal leg)	inches
y	transverse deflection	inches
δ_D	Differential radial motion of seal lips	inches
δ_r	Radial deflection	inches
μ	Coefficient of friction	
ν	Poisson's ratio	
σ	Maximum stress	psi
ϕ	Angle	radians

1.3 Design of Seals

Three general types of pressure-energized seals are analyzed and discussed in this section. For each type of seal considered, a design procedure, design equations, and curves for a typical seal showing the seal's characteristics are presented. The analysis for each seal is given in the appendix, Section 51.5, of Ref. 1. In addition to the design equations, included in the appendix of Ref. 1 are the equations for the seal leg deflection and stress, and the seal-to-flange sealing force.

The seal cross-section, as shown below, consists of a web and two legs with a small lip on the end of each leg. All of the cross-sectional dimensions are usually much smaller than the inside radius of the seal, and the seal legs are much more flexible than the web. Therefore, the seal is analyzed as three separate parts: Two identical legs and the web. The web designs considered are represented by one model, and the legs are represented by three different models:

1. Seal with Straight Leg of Constant Width (Section 1.3.1)
2. Seal with Straight Leg of Linearly Varying Thickness (Section 1.3.2)
3. Seal with Straight Leg of Constant Width without Lip (Section 1.3.3)

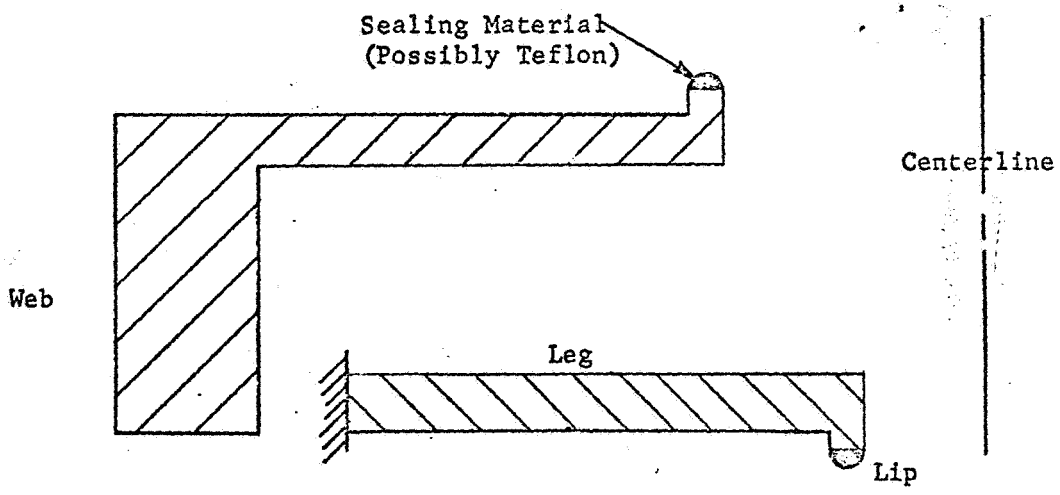

FIGURE 1.2 Cross-section of Cantilever Type Pressure Energized Seal

The characteristics of each of these models have been analyzed and with the use of typical dimensions are illustrated in Section 1.3.6. Based on the needs of a particular application, one of the seal leg designs may be chosen by a comparison of their characteristics.

The chosen seal configuration may then be designed by using the design procedures as outlined in this section. In each case it is assumed that the seal body material and its properties, the required sealing force, the maximum allowable stress, and the inside seal radius are known. The seal body materials used are usually steel or aluminum for their structural properties, provided they are compatible with the fluid contained. In any case the material could be specified and its modulus of elasticity and Poisson's ratio either known or readily determined. The required sealing force is determined from a consideration of the flange faces, sealing material on the seal lip, and pressure and properties of the retained fluid. The method of determining this sealing force is discussed in Volume 3 of Ref. 1. The maximum allowable stress is determined by the designer based on the seal material and application. The inside radius of the seal is usually slightly larger than the inside radius of the pipe and depends primarily on the flange design. The seal leg design is based on the above considerations.

The seal web is primarily a structural member, but it also has a direct effect on the sealing abilities of the seal. Radial motion between the seal lip and flange face will break a seal effected between the lip and flange and may cause leakage. Therefore, in the seal web design, consideration is given to the radial growth of the seal due to internal pressure and differential thermal growth of the flanges and seal. The seal is not as stiff as the flanges and will tend to grow more radially when pressurized. Relative motion between the seal and flange may result from different amounts of thermal expansion of the seal and flange, and it may occur due to a differential thermal growth of the flanges. If one flange grows more than the other, the seal will have to rotate about an axis normal to its cross-section, Figure 1.2, in order to follow the motion of the flanges. Otherwise the seal lip must slip on the flange face.

Making the seal and flange of the same material will tend to eliminate the problem of differential thermal expansion of the seal and flange. However, during thermal transients there is still the possibility of the seal and flange being at different temperatures. A stiffer seal web will decrease the differential radial growth of the seal and flange due to internal pressure, but will also make the seal cross-section more difficult to rotate about its own axis. Therefore, the web design is a balance between the need to limit the growth due to pressure and the ability to accommodate the flange motion. Also, consideration should be given to the design of the recess in the flange face. It is possible to limit the radial motion of the seal by using the flange recess as a backing to the seal web.

The depth of the flange recess where the seal sits, see Figure 1.1,

is one of the prime factors determining the sealing force. As shown in the figure, if the restrained height of the seal, H_R, is less than the free height of the seal, H_F, the seal is axially compressed. This axial compression is essential when installing the seal in order to insure seating the seal and preventing leakage at low pressures. As an axial tensile load is applied to the flanged joint, the flanges will separate and the restrained height of the seal increases. If this tensile load is applied prior to the pressurization of the joint, it is important that the restrained height remains less than the free height, otherwise the seal will separate from the flange. If the flanged joint is pressurized as the tensile load is applied, the pressure will force the seal leg to follow the flange separation. In this case, it is important to match the seal-leg deflection characteristics to those of the flanges so that the required sealing force is maintained. A decrease in the sealing force may cause leakage, and an increase may cause damage to the sealing material on the seal lip. In this section the restrained height of the seal is assumed known. The determination of the restrained height comes from the load-deflection analysis of the flanged joint. Each type of flanged joint may require a different analytical approach. Included in Ref. 1 are analyses of some design examples illustrating different approaches, Section 13. Then the seal leg itself can be designed on the assumption that the flange face is flat. If the soft material coating were not used, it would be necessary to deform the seal lip plastically or to deform the seal leg to follow the contour of the asperity.

The seal leg cross-section shown in Figure 1.2 indicates that the seal leg is a circular flat plate. Also, in some seal designs the seal leg is a conical shell. However, in most seal leg designs the leg length is sufficiently smaller than the inside radius to analyze the leg as a beam. This procedure is used in this report, but not without justification. A set of curves are included in Ref. 1 showing the error incurred by applying beam theory to a particular seal leg. These errors are generally negligible for design purposes.

1.3.1 Seal with Straight Leg of Constant Width

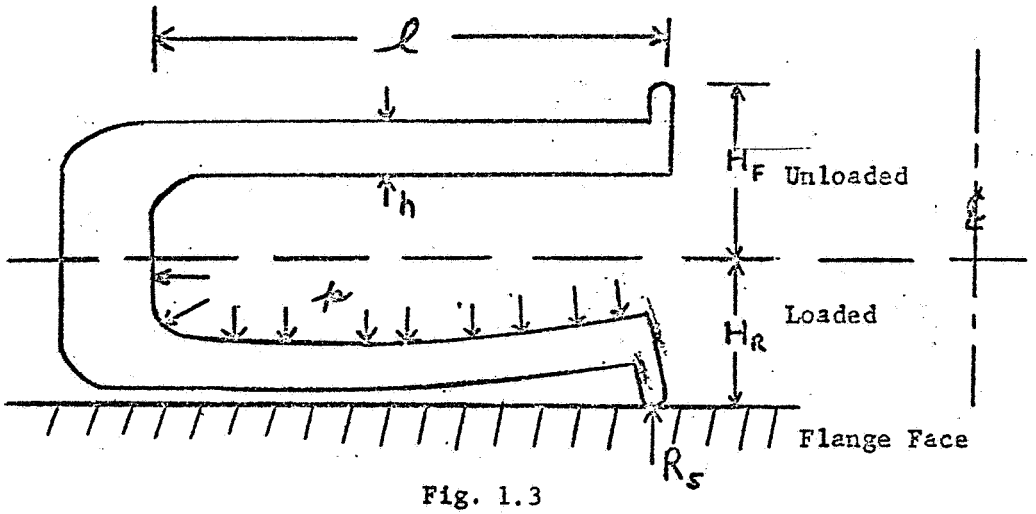

Fig. 1.3

SEAL CROSS-SECTION

The leg is analyzed as a built-in beam of length, ℓ, loaded by a uniform load p and deflected a distance y_ℓ by a simple support. The distance y_ℓ is the difference between the free height, H_F, and restrained height, H_R. The analysis determining the equations for the leg deflection and stresses, and the sealing force, R_s, is in the appendix, Section 51.5.1 of Ref. 1.

The dimensions for the cross-section are determined from the design equations of Section 51.5.1. Having determined the modulus of elasticity, Poisson's ratio, the minimum sealing force and maximum allowable stress, select one or more reasonable values of the length to thickness ratio, ℓ/h, and calculate y_ℓ from equation (1).

$$y_\ell = -\ (4R_s/E)\ (1-\nu^2)\ (\ell/h)^3 \qquad (1)$$

Calculate ℓ from equation (2)

$$\ell = \frac{6y_\ell E}{(1-\nu^2)\ (\ell/h)\left[4\sigma_m - 3p(\ell/h)^2\right]} \qquad (2)$$

Choose the most reasonable values of h and ℓ using design judgment.

If the seal leg is at an angle ϕ to the flange face, see Fig. 1.4, equation (1) changes to the following:

$$y_\ell = -\ (4R_s/E)\ (1-\nu^2)\ (\ell/h)^3 \cos\phi \qquad (3)$$

Equation (2) is the same as before, but the value of y_ℓ is changed to

$$y_\ell = -(H_F - H_R)/\cos \phi \qquad (4)$$

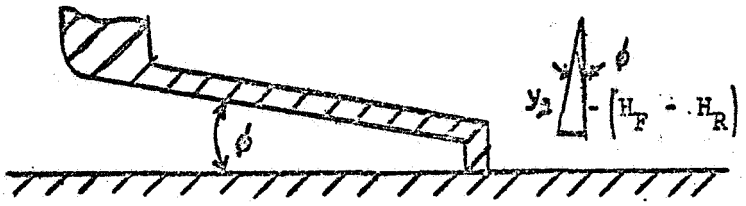

FIGURE 1.4 Seal Leg

The web design formulas are given in Sec. 51.5.4 of Ref. 1. The web length is chosen as short as possible consistent with the overall structural requirements of the seal, see Section 1.3.4. The web thickness should be equal to or greater than the leg thickness at the web end of the leg. It must also be equal to or larger than the thickness calculated using equation (5). r_3 is the mean web radius.

$$t = p\, r_3/\sigma_m \qquad (5)$$

1.3.2 Seal With Straight Leg of Linearly Varying Thickness.

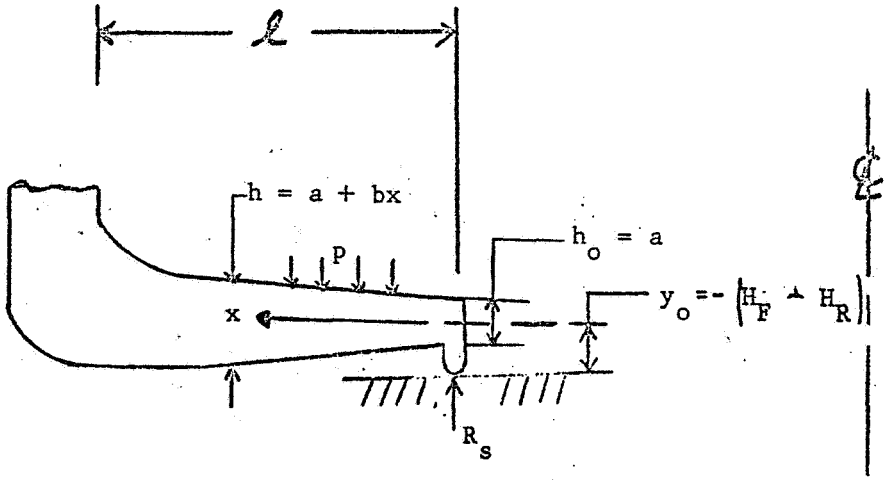

Fig. 1.5

TAPERED SEAL LEG

As in Section 1.3.1, the seal leg is analyzed as a built-in beam loaded by a uniform pressure load p and deflected a distance y_o by a simple support. The leg deflection and stress, sealing force and design equations are derived in the appendix, Section 51.5.2 of Ref. 1.

The design method begins with the specification of the modulus of elasticity, Poisson's ratio, minimum sealing force and maximum allowable stress. The initial deflection of the sealing end, y_o, required to give the minimum sealing force, R_s, is given by equation (6).

$$y_o = \frac{dR_s}{2b^3}\left[\frac{b\ell(2a + 3b\ell)}{(a + b\ell)^2} - 2\log(1 + b\ell/a)\right] \tag{6}$$

Substituting equation (6) directly into the equation for the maximum bending stress results in a relationship relating a, b, and ℓ.

$$\sigma_m = \frac{3\ell}{(a + b\ell)^2}\left\{p\ell - 2R_s + \frac{p\left[\frac{b\ell}{(a + b\ell)^2}(6a^2 + 9ab\ell + 2b^2\ell^2) - 6a\log(1 + b\ell/a)\right]}{b\left[\frac{b\ell}{(a + b\ell)^2}(2a + 3b\ell) - 2\log(1 + b\ell/a)\right]}\right\} \tag{7}$$

This is too complex to solve in general terms for either a, b, or ℓ. To make the equation more tractable, assume a value for the leg thickness at both ends, a and h_ℓ.

$$h_\ell = a + b\ell$$

Another relation between b and ℓ is obtained from the above equation which may be solved for b.

$$b = (h_\ell - a)/\ell \qquad (8)$$

Substitution of values of a and h_ℓ reduces equation (7) by allowing numerical evaluation of the natural logarithm terms. Further substitution of equation (8) for b and all the other known parameters reduces equation (7) to a polynomial in ℓ. This equation can then be solved for ℓ and b can be determined from equation (8).

The calculated values may be unreasonable, in which case other values should be tried for a and h_ℓ. As an alternate procedure, σ_m may be unspecified and calculated for chosen values of a, b, and ℓ. Any calculated value of σ_m less than the maximum allowable is acceptable.

The web design is the same as that for the case described in Section 1.3.1. See also Section 1.3.4.

1.3.3 Seal with Straight Leg of Constant Width Without Lip

The seal is similar to the seal described in Section 1.3.1 except there is no lip at the end of the seal legs. The seal is effected between the seal leg and flange face. As the leg is usually at a small angle to the flange face, decreasing the restrained height, H_R, of the seal or increasing the internal pressure, p, causes the point of sealing to move closer to the seal web, see Figure 1.6.

As in Sections 1.3.1 and 1.3.2 the seal leg is analyzed as a built-in beam. The portion of the leg from $X = \ell_i$ to ℓ is in simple compression. A free-body diagram of this section shows that the end shears and moments must be zero. Therefore, the end moment on the other section of the leg ($x = 0$ to ℓ_i) must be zero and the end shear is only due to the reaction of the flange face, R_s. This means the sealing between the seal and flange is effected only along the line of contact (into the paper on Figure 1.6) at ℓ_i. For further information on the seal characteristics see Section 51.5.3 of Ref. 1.

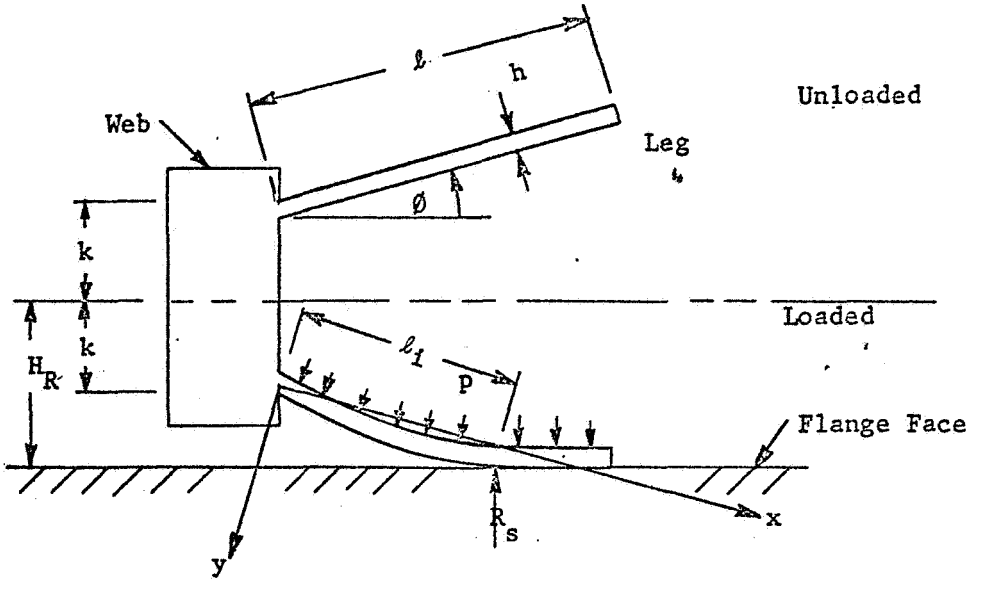

FIGURE 1.6

Cross-section of Seal with Straight Leg
of Constant Width Without Lip

The design of the seal begins with a choice of material and determination of the minimum sealing force, R_o, required. The web design is the same as that for the seal described in Section 1.3.1 and is discussed in Section 1.3.4. The leg design is an iterative procedure beginning with the selection of the lengths H_r, k, and y_ℓ. Then calculate the minimum leg length required using equation (8).

$$\ell_o = - \frac{3\, y_\ell\, (H_r - k)}{\sqrt{y_\ell^{\,2} - 4\,(H_r - k)^2}} \qquad (8)$$

This is the active leg length ℓ_1 when the internal pressure is zero. Unless the leg length is greater than ℓ_o the seal leg will not effect a seal with the flange face at assembly.

Next calculate the seal leg thickness h.

$$h = \sqrt[3]{- \frac{216\,(1 - \nu^2)\, y_\ell\, R_o\, (H_R - k)^4}{E \left[y_\ell^{\,2} - 4\,(H_R - k)^2 \right]^{3/2}}} \qquad (9)$$

Then calculate the minimum active leg length ℓ_m.

$$\ell_m = \frac{(H_r - k) \sqrt[4]{216\, y_\ell^{\,2}\, R_o / P_m}}{\left[y_\ell^{\,2} - 4\,(H_r - k)^2 \right]^{3/8}} \qquad (10)$$

This is the active leg length when the internal pressure is a maximum (P_m). If the calculated dimensions do not constitute an acceptable design, choose other values of H_r, k and y_ℓ and repeat the calculations until an acceptable design is obtained. Where a number of iterations are required or a number of seals are to be designed, it is suggested that curves be plotted for equations (8), (9), and (10).

1.3.4 Radial Motion of the Seal Lip

As a separate design problem, the radial motion of the seal lip due to internal pressure and the rotation of the seal section is considered in this section. Both problems may be considered irrespective of the leg configuration and are, therefore, not included as part of the design consideration of a specific leg.

Each of the seals considered is loaded by a radial force proportional to the internal pressure and internal seal area. The radial growth of the seal is greater than that of the adjacent flanges because of its much lower stiffness. It is assumed that the flanges are rigid compared to the seal and therefore the seal radial growth may be taken as the radial growth of the seal relative to the flange face. This relative radial motion of the seal lip may prevent the forming of a good seal and cause leakage. It is probable that there is some minimum allowable value for which leakage will not occur.

The radial deflection of the seal due to internal pressure is determined in Sec. 51.5.5 of Ref. 1. The analysis leads to an equation which sets an upper limit on the web length L. When the leg design has been completed, all of the parameters except the allowable radial deformation, δ_r, will have been determined. This parameter will be determined from tests and experience.

$$L = 2h\ell / \left[(p r_1^2 / E\delta_r) - t \right] \quad , \qquad (11)$$

Another cause of relative motion between the seal lip and flange face is any differential radial growth of the flange faces. A non-uniform temperature-distribution or the use of dissimilar metals in the flange faces will result in a differential radial growth of the flange faces. The result is a moment applied to the seal by forces acting at the seal lips. These forces are equal to the coefficient of friction times the normal sealing force, R_s. Therefore, as the differential radial growth of the flange faces increases, the forces required to twist the seal increase and a point is reached where the frictional couple is unable to further twist the seal. At this point the seal lip must slip on the flange face and leakage may occur.

The sequence of design calculations assumes design of the seal leg prior to the web. Therefore, in designing the web the rotational rigidity of the seal is considered. Having calculated the differential radial growth of the flanges and determined the maximum allowable relative motion between the seal lip and flange face from tests and experience, the differential radial motion of the seal lips, $\Delta\delta_D$, may then be calculated. $\Delta\delta_D$ must be at least as large as the difference between the differential radial growth of the flanges and the maximum relative motion between the seal lip and flange face. Then the desired total area moment of the seal section may be calculated from equation (12).

$$I_c = 4\mu R_s H_R^2 r_2^2 / E\delta_D \qquad (12)$$

This is the sum of the area moments of the seal legs and web. As I_c varies as the square of the web length, L, it may be possible to achieve the desired I_c by only verifying L.

The maximum bending stress due to the applied couple is a circumferential stress and the maximum is at the upper and lower seal surfaces, $\pm H_R$.

$$\sigma_m = E\delta_D / 2r_2 . \qquad (13)$$

Other design approaches are possible using the equations in the appendix, Section 51.5.6 of Ref. 1.

1.3.5 Summary of Seal Characteristics

Pressure energized seals may be grouped according to the shape of the seal leg. Three major types have been considered.

1. Seal with Straight Leg of Constant Width
   Section 1.3.1

2. Seal with Straight Leg of Linearly Varying Width
   Section 1.3.2

3. Seal with Straight Leg of Constant Width Without Lip
   Section 1.3.3

The seal web is usually a ring which is much stiffer than the seal leg. Therefore, the seal legs and the web have been considered separately.

Of particular importance in the design of pressure energized seals is the sealing force obtained as a function of the internal pressure. Also, the maximum stress in the seal leg is important. Both of these parameters have been calculated as a function of pressure for the three types of seal legs. The results are included in Sec. 51.5.9 of Ref. 1 for each type of seal leg and are summarized in this section. Typical seal dimensions were chosen. Most of the dimensions for the three types of seals considered are identical and the others are equivalent. This makes it possible to compare the seal leg characteristics directly.

The curves of sealing force versus pressure, Fig. 1.7, show that the slopes of the constant width seal legs are the same with or without the lip and are steeper than that for the tapered leg. Also, from Fig. 1.8 it is seen that the slope of the curve for a tapered leg is a function of the taper. The curves also show that the initial sealing force ($p = 0$ psi) is higher for the tapered leg and a function of the taper. The ability to vary the initial sealing force and slope of the curve in the case of a seal with a tapered leg is a desirable factor in seal design. Another factor in favor of the tapered leg is that the stresses are lower, Fig. 1.7.

The seal web is primarily a structural member and does not directly affect the sealing properties of the seal. However, the sealing properties are indirectly affected. The web must be sufficiently rigid to limit the radial displacement of the seal lip when pressure is applied. Excessive radial motion of the seal lip relative to the flange face may cause leakage. Also, the web must not be too rigid so that the seal may rotate and allow for differential radial motion of the flange faces without slippage. If the seal is stiff in rotation of its cross-section the frictional couple from the flange faces will not be large enough to rotate the seal and the seal lip must slide on the flange face. This slippage may cause leakage.

The radial growth of a pressure energized seal as a function of internal pressure and inside radius is given in Fig. 1.9. The seal leg configuration and dimensions of case 2 were used. The web axial length was taken as one-half the leg length, and the web thickness was calculated based

Fig. 1.7 SEALING FORCE VERSUS PRESSURE FOR SEAL LEG DESIGNS

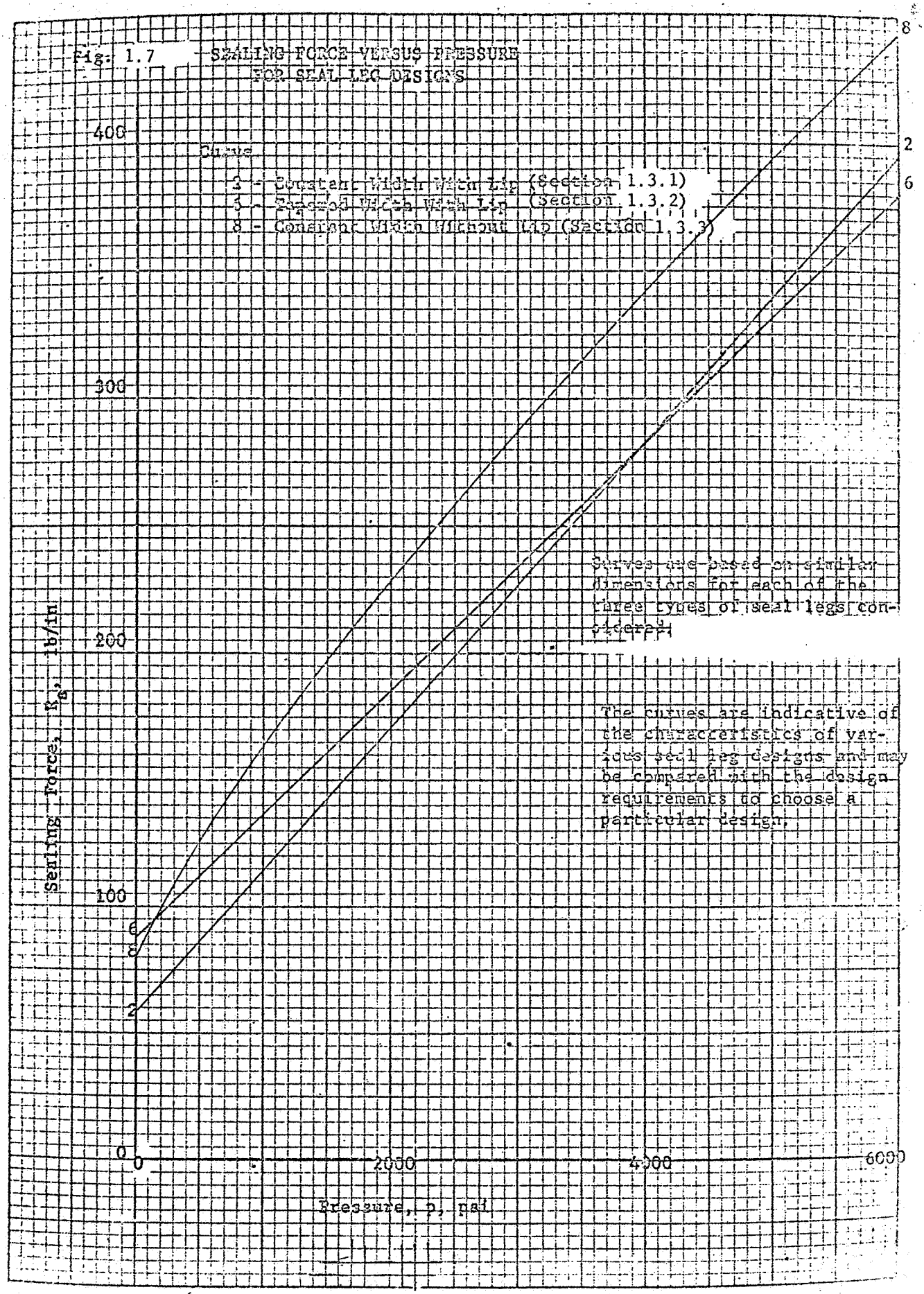

FIG. 1.8

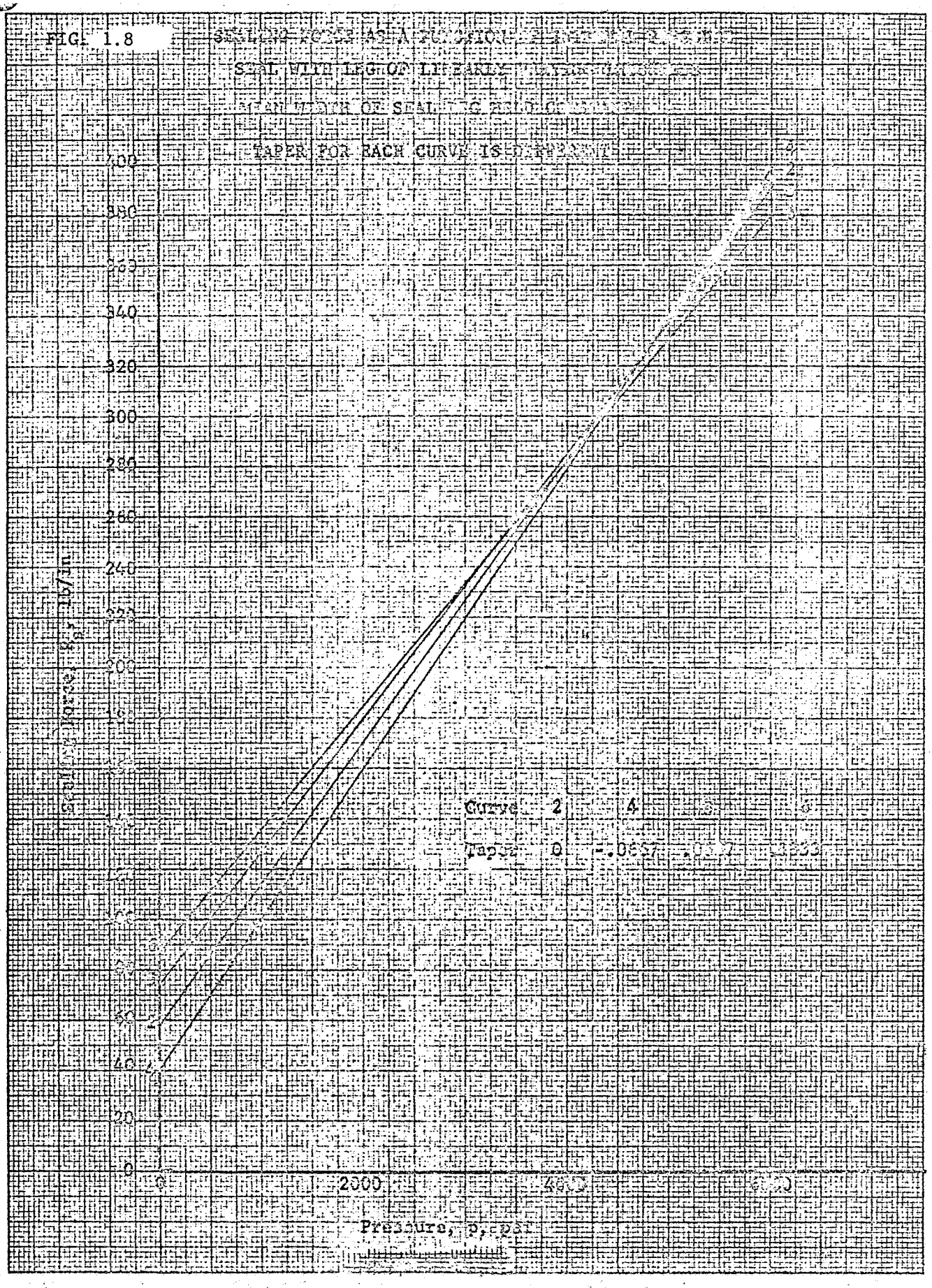

Fig. 1.8 MAXIMUM STRESS AT BASE OF SEAL LEG VERSUS PRESSURE

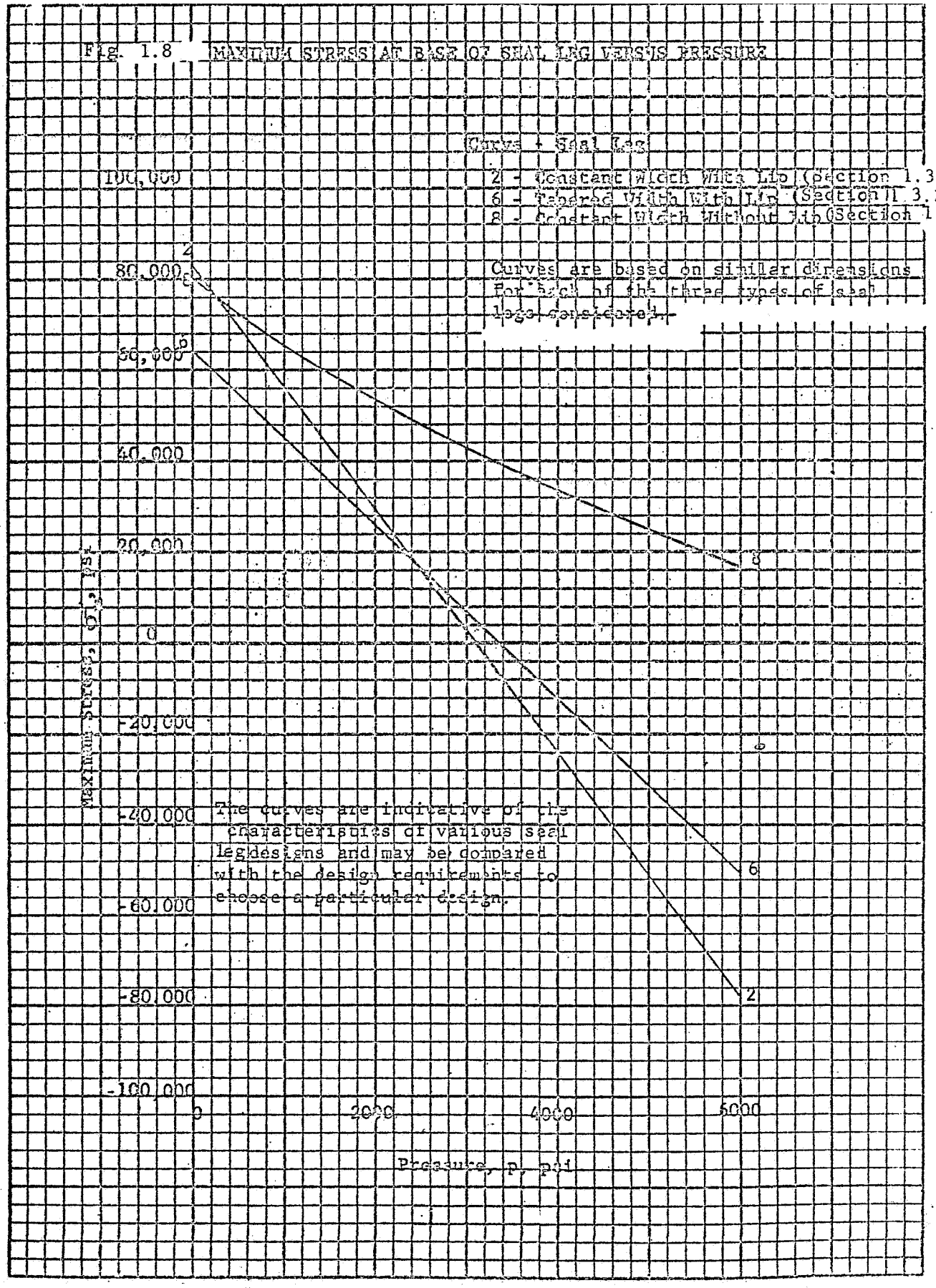

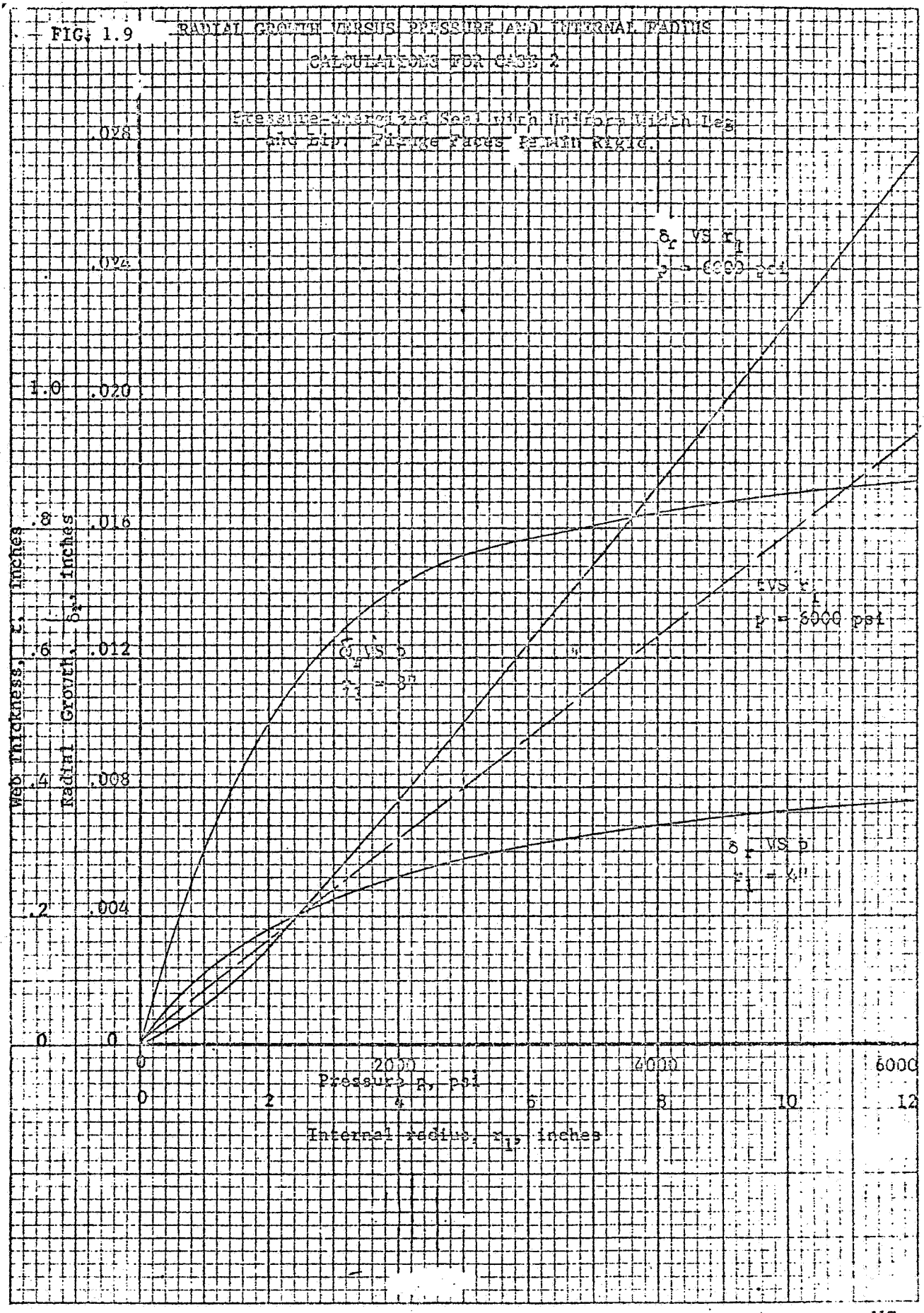

FIG. 1.9 RADIAL GROWTH VERSUS PRESSURE AND INTERNAL RADIUS
CALCULATIONS FOR CASE 2

Pressure-Energized Seal with Uniform Width Legs
and Flat, Plane Faces Pressed Rigid.

on an allowable hoop stress of 80,000 psi. For an internal pressure of 6000 psi the web thickness becomes very large for larger radii. At these pressures and radii a better design may be to use a small web thickness and have the flange recess support the seal radially. A very wide seal web could also be used with flat flange faces so that the web is a spacer between the flange faces and the bolts pass through the web.

1.5 Conclusions

A pressure-energized static seal may be chosen and designed using the formulas and procedures in this section. The desired sealing-force characteristics and gross flange deformation must be known. These are determined from a consideration of the flange face surface and seal lip coating, and an analysis of the complete flanged joint and pipe. The type of seal leg is chosen by making a comparison of the seal leg characteristics with the required characteristics. Then the seal leg and web are detailed using the design formulas given in this section.

The seal leg with a linearly varying thickness and a lip on the sealing end is the best design of those considered. This is due to the ability to change the slope of the sealing-force-versus-pressure curve by changing the leg taper. The uniform-thickness seal leg with a lip on the end is a special case of the tapered leg. The other case considered, uniform-thickness leg without a lip on the sealing end, has no advantages in its sealing-force characteristics and has less advantageous stress characteristics.

The radial motion of the seal lip may be a cause of leakage. From a consideration of the flange face and seal coating material, an allowable maximum radial motion of the seal lip relative to the flange face is determined. The seal web dimensions may then be chosen to limit the radial seal growth due to internal pressure. If the web dimensions become too large, it may be necessary to limit the radial growth with a back-up ring or the flange recess. Stiffening the seal web to limit the radial motion due to internal pressure will limit the seal's ability to comply with differential radial growth of the flange faces. In order to prevent relative motion of the seal lip with respect to the flange face when there is differential radial growth of the flange faces, the seal cross-section must rotate about its centroid. If the seal is too stiff in rotation, the frictional couple applied by the flange faces will be too small to rotate the seal, and slippage will occur. Either type of slippage of the seal lip on the flange face is a possible cause of leakage.

The ability of a seal to comply with a small radial scratch in the flange surface will depend on the seal lip coating. The increase in internal pressure needed to maintain the minimum sealing force in the bottom of the scratch by deforming the seal leg is extremely large even for a scratch whose width is equal to the length of the seal leg. It is possible to make the seal leg comply with gradual flange face irregularities such as flange warpage, but small sharp irregularities require the use of a soft coating on the seal lip.

The use of beam theory to analyze the seal components that are more closely approximated by a circular plate or conical shell was justified in Reference 1, Section 51.5.8. Calculations of the sealing force were made using beam theory, plate theory and shell theory. Curves of the error using beam theory instead of plate theory show that the error is less than ten percent for a ratio of outside radius to inside radius of 1.2 or less. The curves of the error using beam theory instead of shell theory show that the error is less than ten percent for a radius ratio of 1.15 or less and an angle of 15 degrees or less. The error increases more rapidly as the angle increases than as the radius ratio increases.

2.0 HOLLOW METALLIC O-RINGS

2.1 Introduction

Metallic O-rings have been used extensively as static seals under extreme temperature and pressure conditions. They are made of metal tubing formed into rings by welding the two ends together. A spacer or recessed flange must be used to limit the compression of the O-ring. When the connector is assembled, the O-ring is squeezed to the desired thickness and also expands radially so that it is tight against the back-up material provided by the spacer or the flange. The O-ring is often coated with a material such as Teflon or silver that can flow into the asperities of the flange and make a leak-tight joint.

There are three basic types of O-rings; the difference in their construction is evident from the following figure;

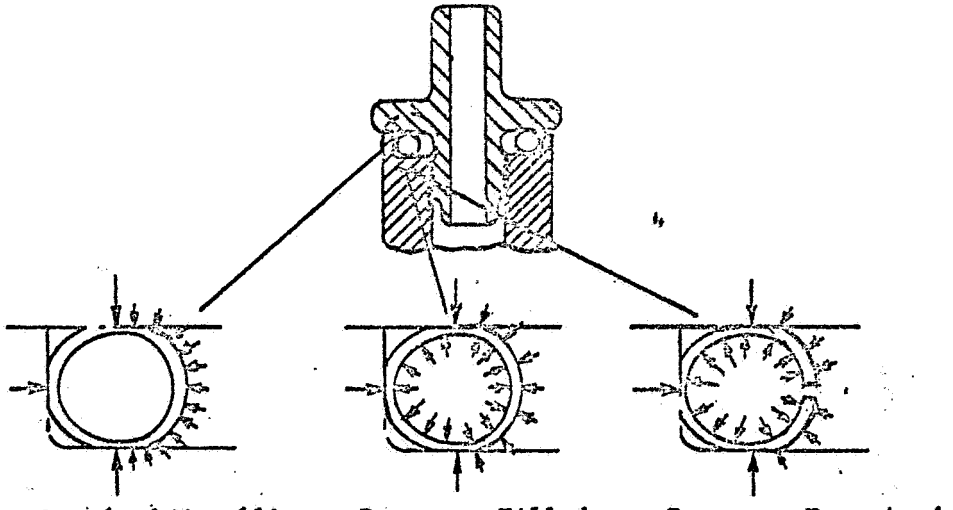

FIGURE 2.1 Three Common Types of Metallic O-ring

The standard O-ring is the most common of the three. The sealing force is derived from the initial compression and maintained by the resiliency of the O-ring. At high pressures there is the danger that the internal pressure may become larger than the sealing stress. Furthermore, the high pressure may cause the O-ring to buckle. The pressure-filled O-ring is filled with an inert gas at usually about 600 psi. At high temperature this gas expands and tightens the seal, while at low temperature it has the reverse effect. Because of the enclosed gas, the pressure-filled O-ring can withstand higher pressure before buckling would occur. The pressure-energized O-ring has holes drilled in the tube wall, and the pressure inside the ring is the same as the pressure in the system; therefore, the higher the pressure in the system, the greater is the sealing force.

A general elastic analysis of O-rings is given in Ref. 1. This is not only a prerequisite to a more general elastic-plastic analysis but also yields some useful information which is applicable despite the presence of plastic deformation in the practical application of O-rings. Among the conclusions are:

(1) Within the elastic theory, all three types of O-rings behave similarly. In particular, they all may have the same pressure-energizing effect.

(2) The use of a retaining ring or other mechanical back-up is desirable because it increases the pressure-energizing effect considerably.

O-rings currently in use are compressed to such an extent that large permanent deformation occurs. Because of the plasticity and large deformation effect, a theoretical analysis of the O-ring behavior becomes extremely difficult. Based on very much simplified assumptions, some considerations of the plastic behavior of O-rings are given in Section 2.4. The results obtained include

(1) A conservative estimate of the sealing force.

(2) An estimate of the decrease of the sealing force when the flanges tend to separate as a result of differential thermal expansion, external loads, etc.

(3) An estimate of the area of contact between the O-ring and the flange.

2.2 Summary of the Results of Elastic Analysis of O-rings

One of the primary requirements of face seals such as metallic O-rings is to maintain sufficient sealing pressure between the O-ring and the flange surfaces. In order to find out the variation of sealing pressure with the bolt load, the internal and external pressure, and so forth, we need to know the load-deflection relations. The deflection parameters of importance are the shortening of vertical diameter of the tube δ_V and the increase of the outside diameter of the O-ring δ_H. The elastic load-deflection relations for the four basic types of loading are obtained in Section 52.4 of Ref. 1 and are summarized as follows:

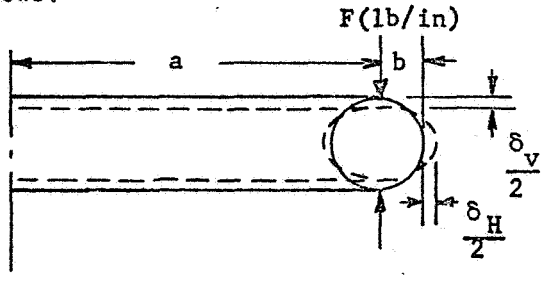

FIGURE 2.2 Axial Load

$$\frac{F}{\delta_v} = \frac{D}{b^3\left[0.149 - \dfrac{0.141}{1 + 14.4/\mu^2}\right]} = \text{Spring constant of the O-ring} \quad (14)$$

$$\frac{F}{\delta_H} = \frac{D}{b^3\left[0.137 - \dfrac{0.141}{1 + 14.4/\mu^2}\right]} \quad (15)$$

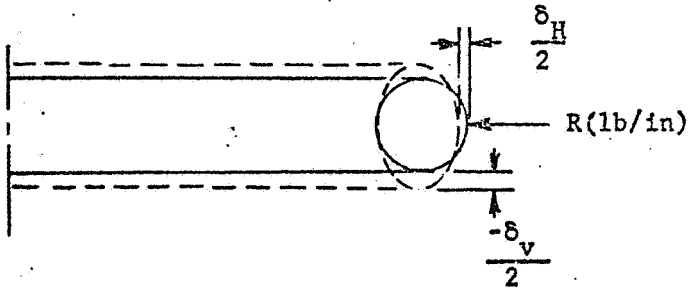

FIGURE 2.3 Radial Load

$$\frac{R}{\delta_v} = -\frac{D}{b^3\left[0.193 - \dfrac{0.199}{1 + 14/\mu^2} + \left(\dfrac{\nu}{\pi\mu m}\right)\left(\dfrac{h}{b}\right)\right]} \quad (16)$$

$$\frac{R}{\delta_H} = -\left(\frac{b}{a}\right)\frac{Eh/a}{0.318 + 2/(1 + 14/\mu^2)} \quad (17)$$

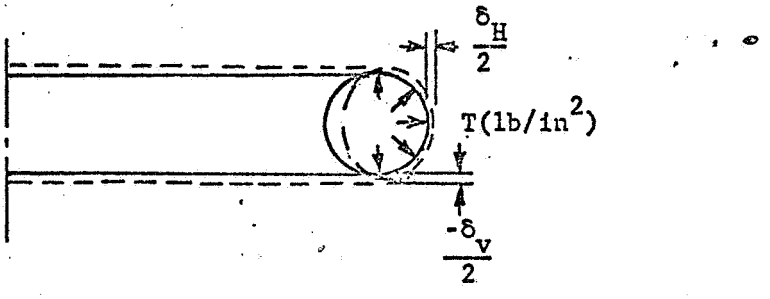

FIGURE 2.4 Pressure Load on Half of Cross-Section

$$\frac{T}{\delta_v} = -\frac{D}{b^4\left[0.25 - \dfrac{0.232}{1 + 14/\mu^2} - 0.636\left(\dfrac{h}{b}\right)\left(\dfrac{\nu}{\mu m}\right)\right]} \quad (18)$$

$$\frac{T}{\delta_H} = \frac{Eh}{a^2\left[0.636 - \dfrac{1.18}{1 + 14/\mu^2}\right]} \quad (19)$$

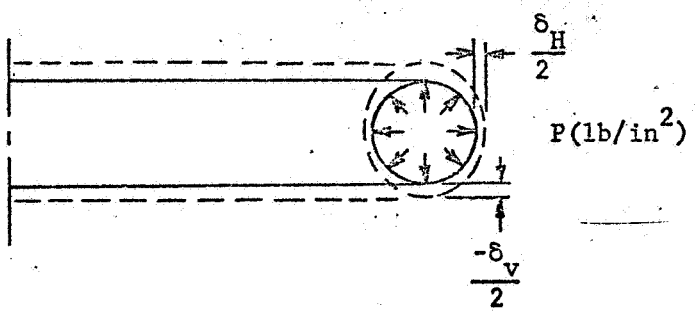

FIGURE 52.5 Pressure Load on Entire Cross-Section

$$\frac{P}{\delta_v} = \frac{-Eh}{2b^2(1 - \nu/2)} \tag{20}$$

$$\frac{P}{\delta_H} = \frac{Eh}{ab(1 - 2\nu)} \tag{21}$$

where $D = \frac{Eh^3}{12(1 - \nu^2)}$ = bending rigidity

$\mu^2 = 12(1 - \nu^2)b^2/ah$

h = wall thickness

E = Young's modulus

ν = Poisson's ratio

$m = \sqrt{12(1 - \nu^2)}$

The way in which these four types of loading can be combined to represent the total load for each type of O-ring is illustrated by the examples of Section 2.3.

In the above load-deflection relations μ appears as an important parameter. The physical significance of μ is discussed in Ref. 1. For most O-rings, μ is small. Our results are restricted to $\mu^2<10$. Among these load-deflection relations, Eq.(14) is of primary importance since it gives the spring constant of the O-ring.

In addition to the load-deflection relations, we would also like to know the stresses in the ring under load so that overstressing does not occur. The stress and moment resultants under the four basic loadings are given in Section 52.4 of Ref. 1.

2.3 Illustrative Examples

We shall illustrate the application of the results of the preceding section by considering O-rings of the following sizes:

(1) 5 O.D. x 1/4 x 0.012 wall, type 321 stainless steel

(2) 20 O.D. x 1/4 x 0.012 wall, type 321 stainless steel

The parameter

$$\mu^2 = 12(1 - \nu^2)(b^2/ah)^2$$
$$= \begin{cases} 2.96 & \text{(5" O-ring)} \\ 0.185 & \text{(20" O-ring)} \end{cases}$$

The bending rigidity

$$D = Eh^3/12(1 - \nu^2) = 4.75 \text{ lb-in}$$

From Eq. (14) the spring constants of the O-rings are

$$\frac{F}{\delta_v} = \frac{D}{\left(0.149 - \dfrac{0.141}{1 + 14.4/\mu^2}\right) b^3}$$
$$= \begin{cases} 18800 \text{ lb/in}^2 & \text{(5" O-ring)} \\ 16400 \text{ lb/in}^2 & \text{(20" O-ring)} \end{cases}$$

If a unit compression load of F = 90 lb/in is required to seat the O-rings, the groove depth should be smaller than the O.D. of the O-rings by the amount

$$\frac{90}{18800} \text{ in (5" O-ring)}$$

$$\frac{90}{16400} \text{ in (20" O-ring)}$$

For this loadings, the bending stress is predominant. The maximum stress occurs at the top and bottom of the O-ring. σ_ϕ is hoop stress and σ_θ is circumferential stress.

$$(\sigma_\phi)_{max} = \frac{6M_\phi}{h^2} = \frac{6Fb}{h^2}\left[\frac{1}{\pi} - \frac{2}{3\pi(1 + 14.4/\mu^2)}\right] \tag{22}$$
$$= \begin{cases} 1.32 \times 10^5 \text{ psi} & \text{(5" O-ring)} \\ 1.47 \times 10^5 \text{ psi} & \text{(20" O-ring)} \end{cases}$$

$$|\sigma_\theta|_{max} = 0.3\,|\sigma_\theta|_{max} \tag{23}$$

These are indeed very high stresses and outer fibres of the O-ring would have yielded locally. But plastic flow will be contained by the neighboring elastic regions so that the load-deflection relations obtained previously will still hold approximately.

Suppose that after the O-rings are installed, fluid under a pressure of 300 psig passes through the connector. We would like to know the O-ring compression F for

(1) Standard O-rings

(2) Pressure-energized O-rings

The load on the standard O-ring is now a combination of the basic loadings as shown when friction is neglected.

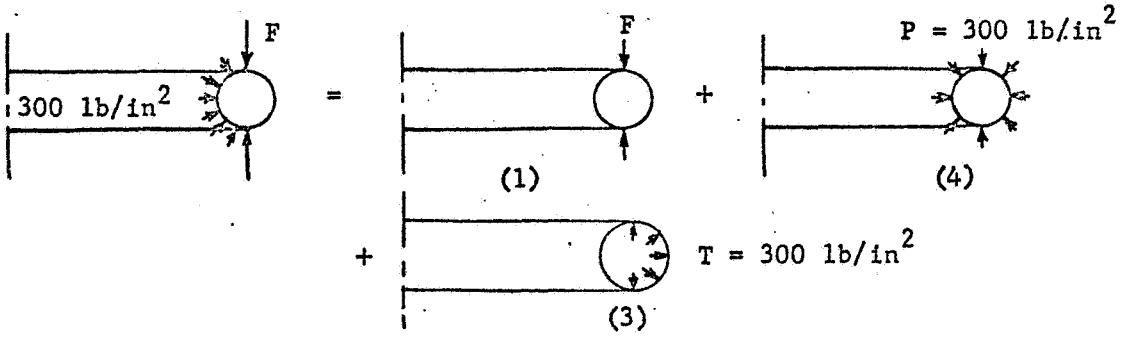

From Eq. (20) we obtain the shortening of the vertical tube diameter under loading (4) as

$$\delta_v = \frac{-2Pb^2(1 - 0.3/2)}{Eh}$$

$$= 2.22 \times 10^{-5} \text{ in.}$$

The extension of the vertical tube diameter under loading (3) is, from Eq. (18),

$$-\delta_v = \frac{Tb^4\left[0.25 - \dfrac{0.232}{1 + 14/\mu^2} - 0.636\left(\dfrac{h}{b}\right)\dfrac{\nu}{\mu m}\right]}{D}$$

$$= \begin{cases} 1.52 \times 10^{-2} \text{ in. (5" O-ring)} \\ 1.72 \times 10^{-2} \text{ in. (20" O-ring)} \end{cases}$$

The combined effect of loading (3) and (4) is that the vertical diameter of the tube would extend by the amount

$$1.52 \times 10^{-2} - 2.22 \times 10^{-5} = 1.52 \times 10^{-2} \text{ in. (5" O-ring)}$$

$$1.72 \times 10^{-2} - 2.22 \times 10^{-5} = 1.72 \times 10^{-2} \text{ in. (20" O-ring)}$$

Since the bolts clamping together the flanges are much more rigid than the O-ring, these would-be extensions of the vertical tube diameter are almost completely restrained. The corresponding increase in O-ring compression is equal to

$$\text{(spring constant) x (extension restrained)} = \begin{cases} 0.0152 \times 18800 = 296 \text{ lb/in (5" O-ring)} \\ 0.0172 \times 16400 = 323 \text{ lb/in (20" O-ring)} \end{cases}$$

The maximum stress due to loading (4) is small compared with that due to loading (3). For loading (3) it can be seen from Eqs. (36) in Section 52.4 of Ref. that the ratio between the bending stress and the membrane stress is

$$\frac{6M_\phi/h^2}{N_\phi/h} = 0(\mu) = 0(1) \text{ for both O-rings}$$

where 0 stands for order of magnitude

Therefore, the bending stress and the membrane stress are of equal importance. It can also be seen from the stress equations that the ratio of bending stress for loading (1) and (3) is of the order of

$$0\left(\frac{F}{Tb}\right) = 0(1/b)$$

Therefore, an internal pressure of 300 psig adds a great deal to the stresses in the O-ring. This is all the more important, since considerable addition of the stress is in the form of membrane stress. This indicates that an O-ring of much thicker wall should be used. Notice that doubling the wall thickness would reduce the membrane stress approximately by half and the bending stress by three quarters. The spring constant of the O-ring, however, becomes eight times as large.

In considering the effect of internal pressure in the above, we have not considered the relief of O-ring compression due to bolt and spacer extension. Given the bolt and spacer dimensions, this can be calculated readily. However, the spring constant of most O-rings is so small compared with that of the bolts and spacer, that the relief of O-ring compression is usually negligible.

For a pressure-energized O-ring the load is a combination of the basic loading (1) and (3)

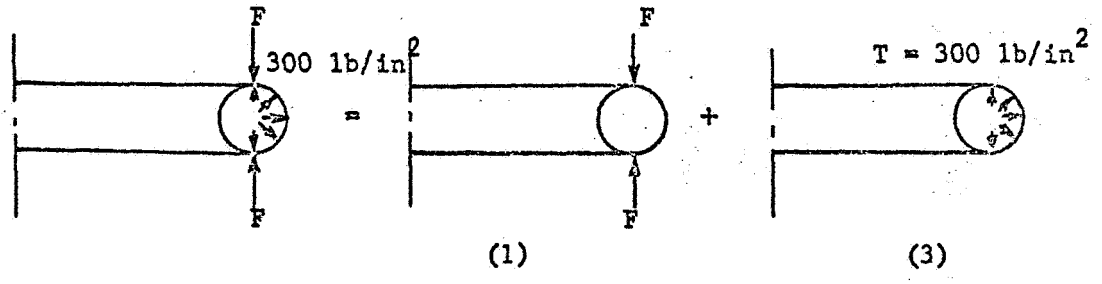

This differs from the load on a standard O-ring shown on Page 28 only in the absence of the basic loading (4). Since it is seen in the preceding case that the basic loading (4) does not add much to either the deflection or stresses of the O-ring, the conclusions reached for the standard O-rings apply also to the pressure-energized O-rings. This is a very surprising conclusion, since it shows that within the small-deflection elastic theory the standard O-ring has self-energizing action just as the vented "pressure-energized O-rings."

Another important conclusion can be obtained by reversing the direction of pressure in loadings (3) and (4) for the standard O-rings. It can be seen that in this case the O-ring compression decreases with the increase of external pressure. In other words, the pressure-energized O-ring is entirely ineffective against external pressure unless a back-up ring is used.

We shall consider next that in addition to initial seating compression and internal pressure, the ring is backed up by the flange (or a back-up ring) which exerts a reaction force on the O-ring. Suppose that the inside diameter of the flange is to be equal to the outside diameter of the compressed O-ring so that during initial seating the flange (or back-up ring) will not react on the O-ring. What should be the inside diameter of the flange? If the O-ring is then subjected to 300 psig internal pressure, what is the reactive force between the O-ring and the flange (or back-up ring), and what is the change in O-ring compression? From Eq. (15) we see that during initial seating the outside diameter of the O-ring increases by the amount

$$\delta_H = \frac{b^3 F\left[0.137 - \dfrac{0.141}{1 + 14.4/\mu^2}\right]}{D}$$

$$= \begin{cases} 0.00418 \text{ in. (5" O-ring)} \\ 0.00500 \text{ in. (20" O-ring)} \end{cases}$$

Therefore, the inside diameter of the flange should be 5 + 0.00418 in. for the 5" O-ring and 20 + 0.00500 for the 20" O-ring.

When an internal pressure of 300 psig is now applied, the outside diameter of the O-ring would tend to increase if it were not restrained by the flange. Since the flange is much stiffer than the O-ring, we may assume that these would-be expansions of the O-ring are completely suppressed. The result is that there is a circumferential pressure R lb/in between the O-ring and the flange (or back-up ring) as well as an increase ΔF of the O-ring compressions. The forces R and ΔF can be determined from the condition that

$$\delta_H = \delta_V = 0$$

due to the combined action of R, ΔF and the 300 psig internal pressure.

We have already found

$$\left(\delta_V\right)_{300 \text{ psig}} = \begin{cases} -0.0152 \text{ in. (5" O-ring)} \\ -0.0172 \text{ in. (20" O-ring)} \end{cases}$$

From Eq. (19) we have

$$\left(\delta_H\right)_{300 \text{ psig}} = \frac{a^2(300)\left[0.636 - \dfrac{1.18}{1 + 14/\mu^2}\right]}{30 \times 10^6 (0.012)}$$

$$= \begin{cases} 0.00227 \text{ in. (5" O-ring)} \\ 0.0518 \text{ in. (20" O-ring)} \end{cases}$$

Also

$$(\delta_v)_{\Delta F} = \begin{cases} \Delta F/18800 \text{ (5" O-ring)} \\ \Delta F/16400 \text{ (20" O-ring)} \end{cases}$$

and from Eq. (15)

$$(\delta_H)_{\Delta F} = \frac{(\Delta F)b^3\left[0.137 - \dfrac{0.141}{1 + 14.4/\mu^2}\right]}{4.75}$$

$$= \begin{cases} \Delta F/21500 \text{ (5" O-ring)} \\ \Delta F/18000 \text{ (20" O-ring)} \end{cases}$$

Similarly from Eqs. (16) and (17) we obtain

$$(\delta_v)_R = -\frac{R(1/8)^3\left[0.193 - \dfrac{0.199}{1 + 14.4/\mu^2} + \left(\dfrac{0.3}{3.3\pi\mu}\right)\left(\dfrac{0.012}{0.125}\right)\right]}{4.75}$$

$$= \begin{cases} -R/15400 \text{ (5" O-ring)} \\ -R/13200 \text{ (20" O-ring)} \end{cases}$$

$$(\delta_H)_R = -\frac{0.318 + 2/(1 + 14/\mu^2)}{30 \times 10^6 (0.012)(1/8)/a^2}$$

$$= \begin{cases} -R/10800 \text{ (5" O-ring)} \\ -R/1330 \text{ (20" O-ring)} \end{cases}$$

Therefore, from the equations

$$(\delta_v)_{300 \text{ psig}} + (\delta_v)_{\Delta F} + (\delta_v)_R = 0$$

$$(\delta_H)_{300 \text{ psig}} + (\delta_H)_{\Delta F} + (\delta_H)_R = 0$$

we obtain

$$R = 732 \text{ lb/in}$$

$$\Delta F = 1180 \text{ lb/in}$$

for the 5" O-ring and

$$R = 98.5 \text{ lb/in}$$

$$\Delta F = 404 \text{ lb/in}$$

for the 20" O-ring.

Of course, the O-ring would have failed under such heavy load. The result indicates

(1) The use of a back-up ring is desirable since it increases the O-ring compression.

(2) Clearance between the O-ring and back-up ring may be needed to avoid overstressing.

(3) As far as increasing the O-ring compression is concerned, the reaction of the back-up ring is more effective than the internal pressure. This indicates that, for sealing against external pressure, the tendency of the external pressure to relieve the O-ring compression is more than compensated by the reaction of the back-up ring. Therefore, O-rings can be used to seal against external pressure, provided a back-up ring is used.

2.4 Some Considerations of the Plastic Behavior of Hollow Metallic O-rings

Most of the hollow metallic O-rings currently in use operate in the plastic range. A satisfactory elasto-plastic analysis is very complicated. Some consideration of their plastic behavior are presented in this section based on very much simplified assumptions. The results obtained include:

1. A conservative estimate of sealing force.
2. An estimate of the decrease of the sealing force when the flanges tend to separate as a result of differential thermal expansion, external loads, etc.
3. An estimate of the area of contact between the O-ring and the flange.

They seem to correlate well with the limited experimental data available.

2.4.1 Yielding Load and Estimate of Sealing Force

At the beginning of the process of tightening the connector, the compression is small and the O-ring behaves elastically. The elastic solution presented in Section 2.3 is valid. It was shown that the predominating stresses are bending stresses. Therefore, for simplicity we shall neglect the membrane stresses completely. The maximum bending moments occur at the outer and inner surfaces of the top and bottom of the O-ring.

$$M_\phi = \frac{Fb}{\pi}$$
$$M_\theta = \nu M_\phi \qquad (24)$$

The corresponding maximum stresses are

$$\sigma'_\phi = \frac{6Fb}{\pi h^2}$$
$$\sigma'_\theta = \nu \sigma'_\phi \qquad (25)$$

where $M\theta$, $M\phi$ are bending moments per unit length of meridianal section and a section perpendicular to the meridian, respectively

F is the compressive force
b is the tube radius of O-ring
h is the wall thickness of O-ring
ν is Poisson's ratio of O-ring material

According to Mises' yield criterion, initial yielding at these points begins when

$$\sigma_\phi \sqrt{1-\nu+\nu^2} = \text{yield strength of material in tension test, } Y \qquad (26)$$

or, the installation force causing the O-ring to begin yielding as

$$F_{yield} = \frac{\pi h^2 Y}{6b\sqrt{1-\nu+\nu^2}} \qquad (27)$$

Further increase of load will spread the plastic zone both outward and in depth. The load deflection curve will begin to deviate from a straight-line. The deflection will still remain small since the plastic deformation will be contained by the neighboring elastic material. With further increase in load the plastic zone will finally penetrate the wall thickness at the top and the bottom of the O-ring. The material at these points will have very small bending rigidity and behaves more or less like a hinge. It can be easily shown

that the bending moment causing the hinge to occur is 3/2 times the moment of initial yielding if the small effect of work-hardening is neglected, i.e.

$$M_{hinge} = 1.5M_{yield} = \frac{1.5b}{\pi}F_{yield} = \frac{h^2 Y}{4\sqrt{1-\nu+\nu^2}} \tag{28}$$

We shall call the load at which the plastic hinge occurs the hinge load. It should be expected that for loads greater than the hinge load, the deflection of the O-ring increases very much faster even though unrestricted deflection still does not occur because one hinge alone does not transform the O-ring to a "mechanism". Referring to a typical load deflection curve we are saying that F_{hinge} corresponds to the point A

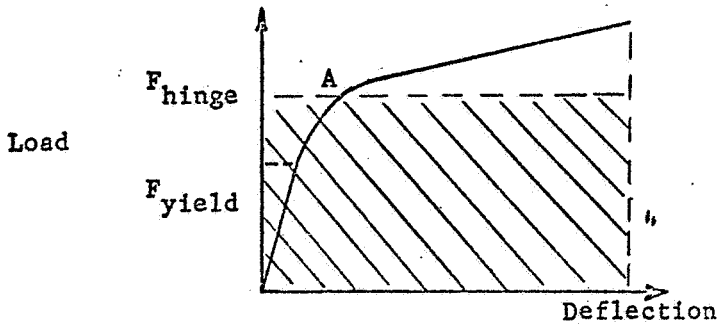

Fig. 2.6 Load-Deflection Curve of an O-ring

A rough estimate of F_{hinge} can be made that, similar to the bending moment

$$F_{hinge} = 1.5\ F_{yield} = \frac{\pi h^2 Y}{4b\sqrt{1-\nu+\nu^2}} \tag{29}$$

Referring to Fig. 2.6, it can be seen that F_{hinge} as given above serves as a good lower estimate of the sealing force for most O-ring applications.

A load-deflection diagram for a 1/8 in. tube size, 0.010 in. wall, type 321 stainless steel O-ring is given in Reference 2. It shows that the load-deflection curve begins to deviate from a straight line at a load of approximately 75 lb/in and large deflection begins to occur around a load of 120 lb/in. If we take F_{yield} as 75 lb/in, Eq. (43) gives us the yield limit of the material in tension as:

$$Y = \frac{(75)(6)(1/16)\sqrt{1-0.3+(0.3)(0.3)}}{\pi(0.01)^2} \simeq 80{,}000 \text{ psi}$$

If we take 120 lb/in as F_{hinge}, then

$$F_{hinge} = 120/75\ F_{yield} = 1.6\ F_{yield}$$

which seems to correlate well with Eq. (29).

2.4.2 Spring Constant of O-ring When Flanges are Separating

After the O-ring is installed a conservative estimate of the sealing force is given by Eq. (29). The sealing force decreases if the flanges tend to separate from each other due to differential thermal expansion, adverse external loads, etc. The amount of decrease of the sealing force depends on the resilience of the O-ring. If the effect of the change of the geometry of the O-ring is negligible then it is a fundamental hypothesis of the theory of plasticity that the spring constant of the O-ring during unloading is approximately the same as the elastic spring constant of the O-ring. Indeed, this fact is substantiated by the load-deflection diagram of Reference 2. The elastic spring constant of most O-rings is given by Eq. (14). For a non-pressure-energized O-ring the decrease in sealing force due to separating of flanges is therefore

(spring constant of O-ring as given by Eq. (14)) x (amount of separation)

2.4.3 Area of Contact Between O-Ring and Flange

In the following we shall present a simple method of estimating the area of contact between the O-ring and the flanges based on energy considerations. The work done by the compressive load can be approximated by the shaded area in Fig. 2.6, i.e.

$$(F_{hinge}) \times (\text{O-ring compression, } \delta) \tag{30}$$

Assume that all this work is done in flattening a portion of the O-ring and that in the flattened portion, the moment is at the fully plastic moment (M_{hinge}). This part of the work is given approximately as

$$2M_{hinge}\theta \cong 4M_{hinge}\sin^{-1}\frac{c}{2b} \tag{31}$$

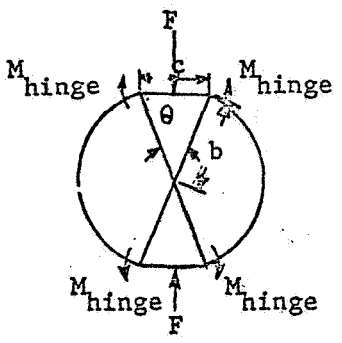

Equating the work given by Eqs. (3) and (31) and making use of Eqs. (28) and (29) we obtain the following relation between the width of the area of contact c and the amount of O-ring compression δ

$$\frac{c}{2b} = \sin\left(\frac{\delta}{b}\right)\left(\frac{\pi}{4}\right) \tag{32}$$

For a 1/8 in. tube diameter O-ring compressed 0.035 in , the width of area of contact is

$$c = 1/8 \sin \left(\frac{0.035}{1/16}\right)\left(\frac{\pi}{4}\right)$$

$$= 0.053 \text{ in.}$$

which seems to correlate well with the measured value of

$$c \tilde{=} 3/64 \text{ in.} \tilde{=} 0.047 \text{ in.}$$

on one of the O-rings available to us.

The average sealing stress is of course the sealing force divided by the area of contact. However, the sealing stress is far from being uniform over the area of contact and the maximum sealing stress is much greater than the average stress. The distribution of sealing stress has the general shape of the shaded area in the following figure.

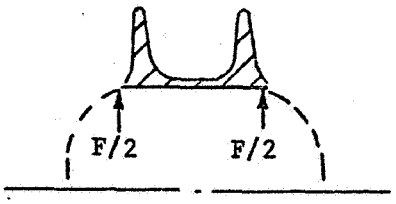

This is necessary because the flattened portion of the O-ring is at approximately constant moment and in order to maintain a constant moment the sealing force has to concentrate near the edges of the area of contact.

REFERENCES

1. "Design Criteria for Zero-Leakage Connectors for Launch Vehicles, Vol. 5, Pressure Energized Seals", B. T. Fang (Ed.), March 15, 1963, prepared for NASA on Contract NAS 8-4012 by General Electric Co.

2. United Aircraft Products, Inc., "Handbook of United Metallic O-Rings", Bulletin No. 59619A, Dayton, Ohio, 1959.

Question: Have you made an experimental verification of these load deflection equations?

Answer: We did not run any tests; however, there is data available in literature for O-rings, and this was checked and seemed to check fairly well. In the other case, no checks have been made.

Comment: I asked the question because we have (IIT) done some work in this area and have found that because of the equations involved, many of the dimensions appeared raised to various powers. If you do not know the exact dimensions, you can get large errors. Just taking nominal dimensions from catalogs is not usually good enough. While the method itself is quite applicable, you must be careful about what dimensions are used so that these methods can be used to predict accurate results.

Reply: I agree. You must use accurate dimensions for substitution in the equations. It was not our intent to use information from catalogs to predict behavior; those dimensions were used just to show the use of the equations.

Question: How does a pressure energized gasket perform when pressure is low and, at the same time, high cyclic bending moments are applied to the connector? Do you get abrasion of the sealing surfaces in that transient period?

Answer: No, we do not get abrasion of the sealing surface. We consider just the structural member and the response of the structural member. The coating that you place on it is something else.

Question: Have you made an experimental verification of these load deflection equations?

Answer: We did not run any tests; however, there is data available in literature for O-rings, and this was checked and seemed to check fairly well. In the other case, no checks have been made.

Comment: I asked the question because we have (IIT) done some work in this area and have found that because of the equations involved, many of the dimensions appeared raised to various powers. If you do not know the exact dimensions, you can get large errors. Just taking nominal dimensions from catalogs is not usually good enough. While the method itself is quite applicable, you must be careful about what dimensions are used so that these methods can be used to predict accurate results.

Reply: I agree. You must use accurate dimensions for substitution in the equations. It was not our intent to use information from catalogs to predict behavior; those dimensions were used just to show the use of the equations.

Question: How does a pressure energized gasket perform when pressure is low and, at the same time, high cyclic bending moments are applied to the connector? Do you get abrasion of the sealing surfaces in that transient period?

Answer: No, we do not get abrasion of the sealing surface. We consider just the structural member and the response of the structural member. The coating that you place on it is something else.

N67-86149

DESIGN OF STATIC ELASTOMERIC SEALS FOR CRYOGENIC TEMPERATURES

by

D. H. Weitzel, P. R. Ludtke, and R. F. Robbins
Cryogenic Engineering Laboratory
National Bureau of Standards
Boulder, Colorado

Preceding page blank

DESIGN OF STATIC ELASTOMERIC SEALS FOR CRYOGENIC TEMPERATURES*.

D. H. Weitzel, P. R. Ludtke, and R. F. Robbins
National Bureau of Standards
Boulder, Colorado

1. Introduction

Elastomers have properties which make them ideal for numerous seal applications. Elastomeric O-ring seals enjoy unparalleled and well deserved popularity in almost every area of science and technology. The requirement that a seal remain tight when cycled between room temperature (or higher) and temperatures approaching absolute zero may, however, be considered extraordinary. Very few solids experience more drastic property changes over this temperature interval than do elastomeric polymers. It has often been assumed, therefore, that elastomers are not suitable seal materials for cryogenic temperature applications.

To test the validity of this assumption has been the objective of a continuing study at the National Bureau of Standards Cryogenic Engineering Laboratory for the past three years. Many elastomeric O-ring seals have been tested in flanges of varying design, and highly effective seals for cryogenic applications have resulted. Instead of demonstrating that elastomers are intrinsically unsuitable for low temperature seals, it has been shown that elastomeric O-rings offer simple and reliable solutions for this as well as more conventional sealing problems.

It goes without saying, of course, that the unusual properties of elastomers, and the drastic changes in these properties which occur at low temperatures, must be considered in their use for cryogenic seals. A typical elastomer will change its unstressed linear dimensions by about two percent between room temperature and 76K. It will change from rubbery to stiff or brittle in the neighborhood of 200K; during this "glassy state transition" the modulus of elasticity may change by a factor

* Work supported by Air Force Materials Laboratory, United States Air For

Preceding page blank

of 1000 or more. The contraction between the brittle transition temperature (T_g) and a cryogenic temperature will normally be much greater than that of the flange material. Thus it is possible for an O-ring to actually shrink away from the flange, leaving a gap instead of a seal. Elastomeric polymers are unique materials which behave in a characteristic manner at room temperatures (where the seal is made) and in an entirely different manner at cryogenic temperatures (where the seal is expected to maintain good performance).

A complete or even typical cataloging of the relation between physical properties and temperature throughout the region of interest would be of great value. This is an almost totally unexplored area, however, and it soon became apparent that we would not be able to base cryogenic seal designs on accurate or well known information. An experimental approach was therefore taken in the design of seals, and an attempt was made to augment this with measurements of properties which were judged to be most significant.

Two essential parts of a mechanical joint are (1) a conformable material which flows under pressure and (2) a mechanical fastener for applying force and holding the joint together. Our objective is to attain the sealing integrity and strength of a weld or reinforced solder joint without losing the convenience of a mechanical connection. Let us examine the two essential parts of a mechanical joint with this objective in mind. We will then be in a position to think critically about cryogenic temperatures and elastomers.

The sealing integrity depends on the conformable material and a sealing pressure which forces it into intimate contact with the surface irregularities. The strength of the joint depends on the mechanical fastener. The sealing pressure may also come from the fastener or, with better design, may come from the pressure of the confined fluid. Many good designs make an initial seal with the help of force from the fastener, after which the seal is energized by the pressure of the enclosed fluid. An elastomer O-ring normally operates in this manner, as shown in figure 1. This extremely simple and effective action is the key to the unmatched success of elastomeric O-ring seals.

Another popular way to use the fluid pressure to energize a seal is illustrated in figure 2. Here the initial seal is obtained by light loading which flexes a metal body. After this the fluid pressure acting

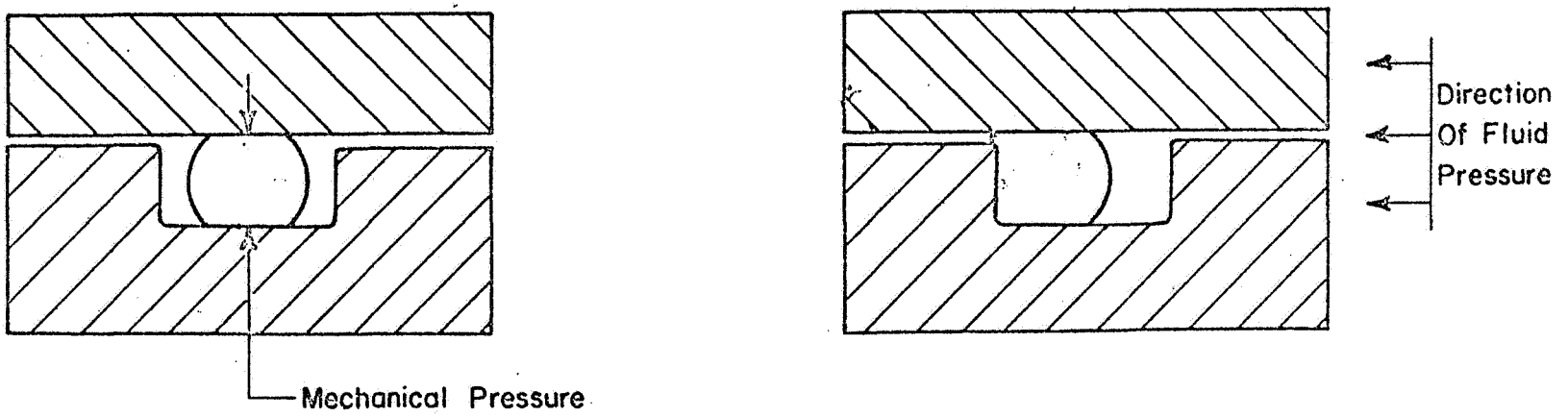

FIG 1. Elastomer O-Ring, Nominal Operatio

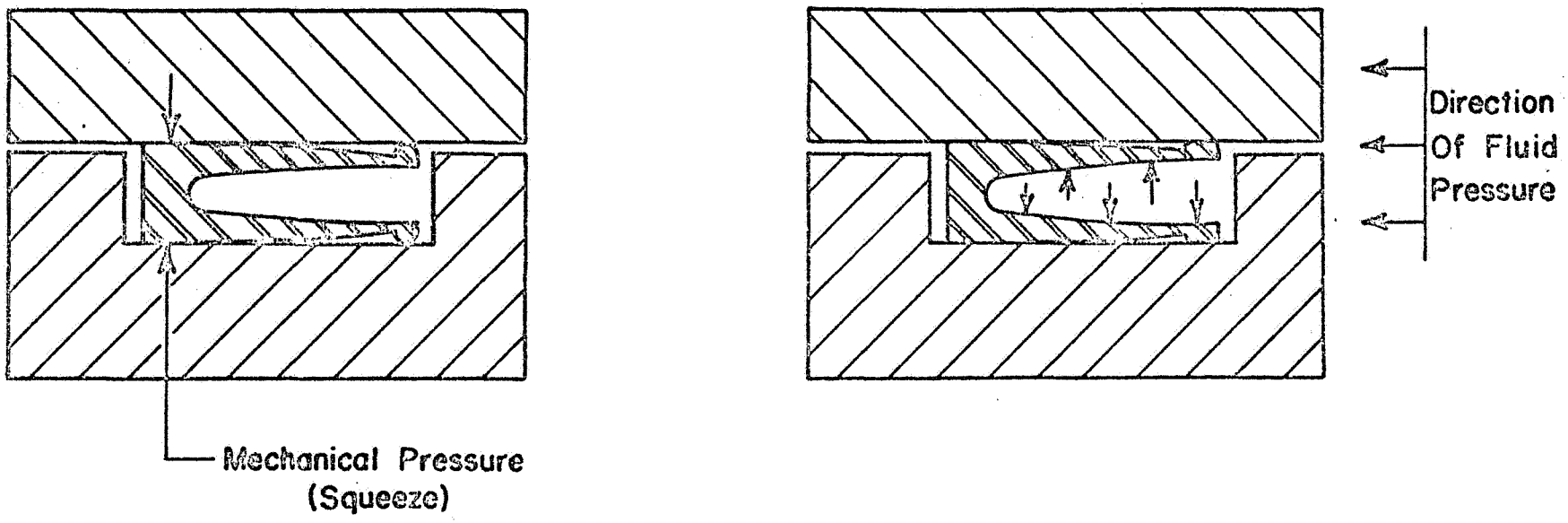

FIG 2. Pressure Actuated Metal Body Seal

on the area inside the body results in a force which is concentrated on the sealing edges. The sealing edges or lips are usually coated with a soft metal or plastic. This type of seal is particularly effective in small sizes, but it is expensive and requires very accurate flange surfaces. It's main advantage is light flange loading and the ability to follow axial movement without drastic reduction in sealing force. Its weakness lies in the small amount of material which flows to make the seal; this makes it susceptible to minute surface imperfections, as well as to unseating which may result from relative motion between the sealing surfaces. Such motion may be caused, for example, by different contraction rates between the flanges and the seal body.

When considering elastomers for cryogenic static seals we are thinking primarily of the first of the two essential parts of a mechanical joint, i.e., the conformable material. Without worrying about efficient flange or fastener design, the first part of our investigation consisted of experiments designed to see what the elastomer itself would do when used as a sealing medium and then cooled below its brittle point. The seal will unquestionably be good at room temperature. What is questionable concerns behavior when the seal is cooled from room temperature to the cryogenic region. Specifically, we should like to know:

(1) If the seal leaks, at what temperature and pressure does the leak begin?

(2) What physical changes cause the seal to leak?

(3) Which of the available elastomer compounds perform best?

2. O-Ring Seal Experiments

It was easily shown that elastomeric O-rings can make excellent seals at cryogenic temperatures. The first successful seals used a "brute force" approach, as shown in figure 3. A tongue and groove type of flange was used, giving the closely confined O-ring an 80 to 90 percent linear compression followed by about five percent volume compression. High flange loading was necessary (on the order of 10,000 lb/in of circumference) but the seals were helium leak detector tight at 1000 psig and 20K. When vibrated on a shaker table at 70K they remained tight[1]. The better compounds, moreover, emerged from this drastic treatment with no visible sign of material failure, although some compression set was usually observed.

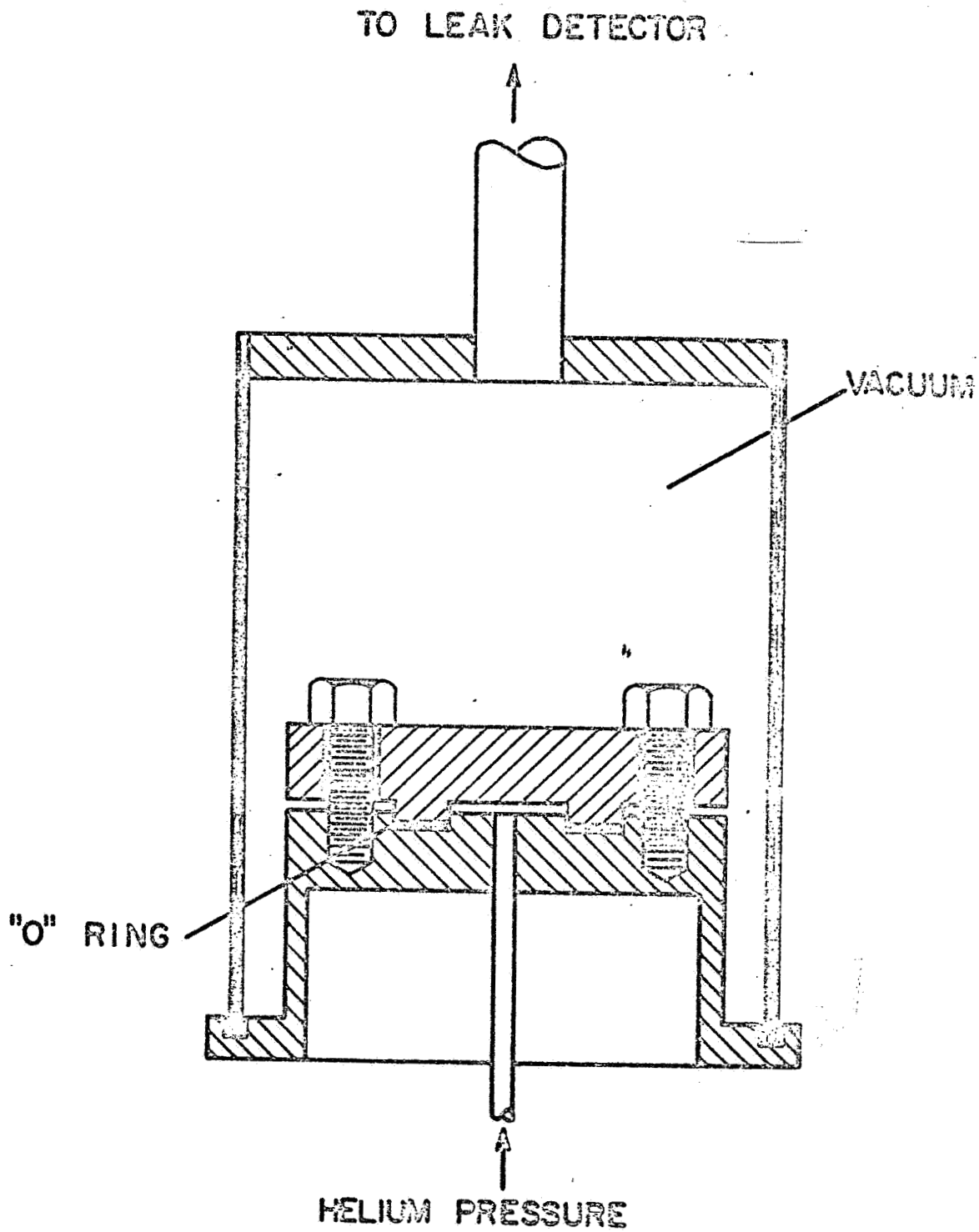

FIG 3. High Compression Torque and Groove

The next step was an effort to reduce flange loading and simplify flange design by eliminating the tongue and groove[2], as shown in figure 4. This also resulted in successful seals and these could be maintained with lower flange loads than had been used in the tongue and groove design. Further reduction in flange loading was achieved by using an O-ring of smaller cross section. When the 0.139 inch cross section O-rings were replaced with O-rings having cross section diameters of 0.070 inches, good seals were obtained with flange loading around 6000 lb/in of seal circumference. These tests were performed with stainless steel flanges 3/8 to 1/2 inch thick which flexed enough to provide a degree of incidental spring loading on the compressed O-ring, a feature which helped to maintain the sealing force. This feature was further exploited by the flange design shown in figure 5.

Here an O-ring of 0.070 inch cross section was lightly stretched around a retaining sleeve which snugly fit the I.D. of the flanges. The flanges were dimensioned to flex appreciably under the bolt load required to compress the O-ring. With this arrangement for positioning and partly confining the O-ring, it was possible to obtain reliable seals with flange loads as low as 2000 lb/in of seal circumference.

These tests demonstrated principles to be employed in the use of elastomeric O-rings as simple crush gaskets for seals at cryogenic temperatures:

(1) Compress as small a cross section as is practical.

(2) Compress to the minimum thickness which does not result in material failure.

(3) Spring load the compressed elastomer in some effective way.

At the same time it was recognized that the tests demonstrated principles only, that the flange designs used in the testing were not optimum and in some cases not even practical, and that no discriminating comparison of the performance of various elastomers had been made. We proceeded next to make a systematic comparison of the performance of various elastomers, and then to seek the most practical and efficient flange designs for use of these materials.

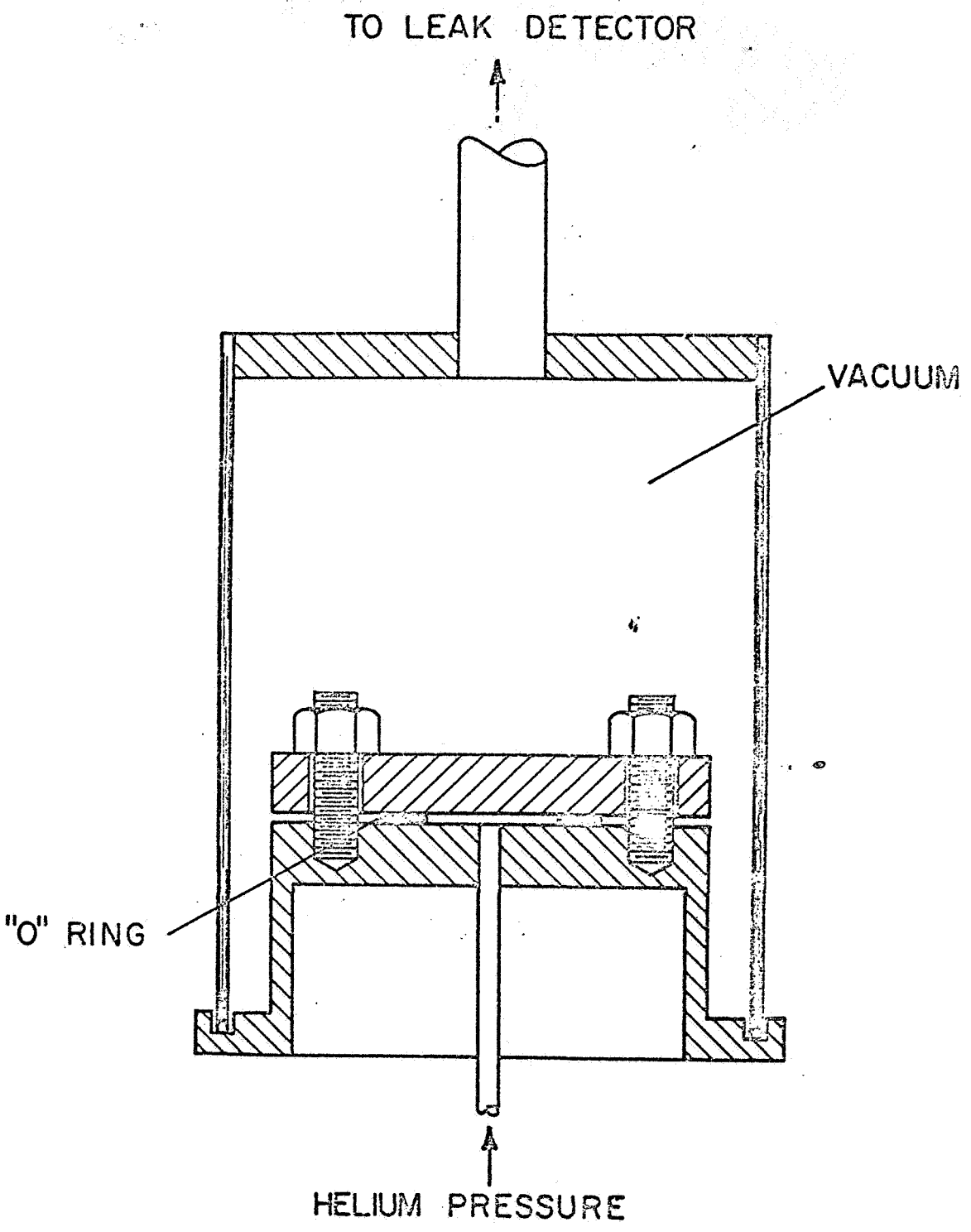

FIG 4. Flat Flange Test Fixture

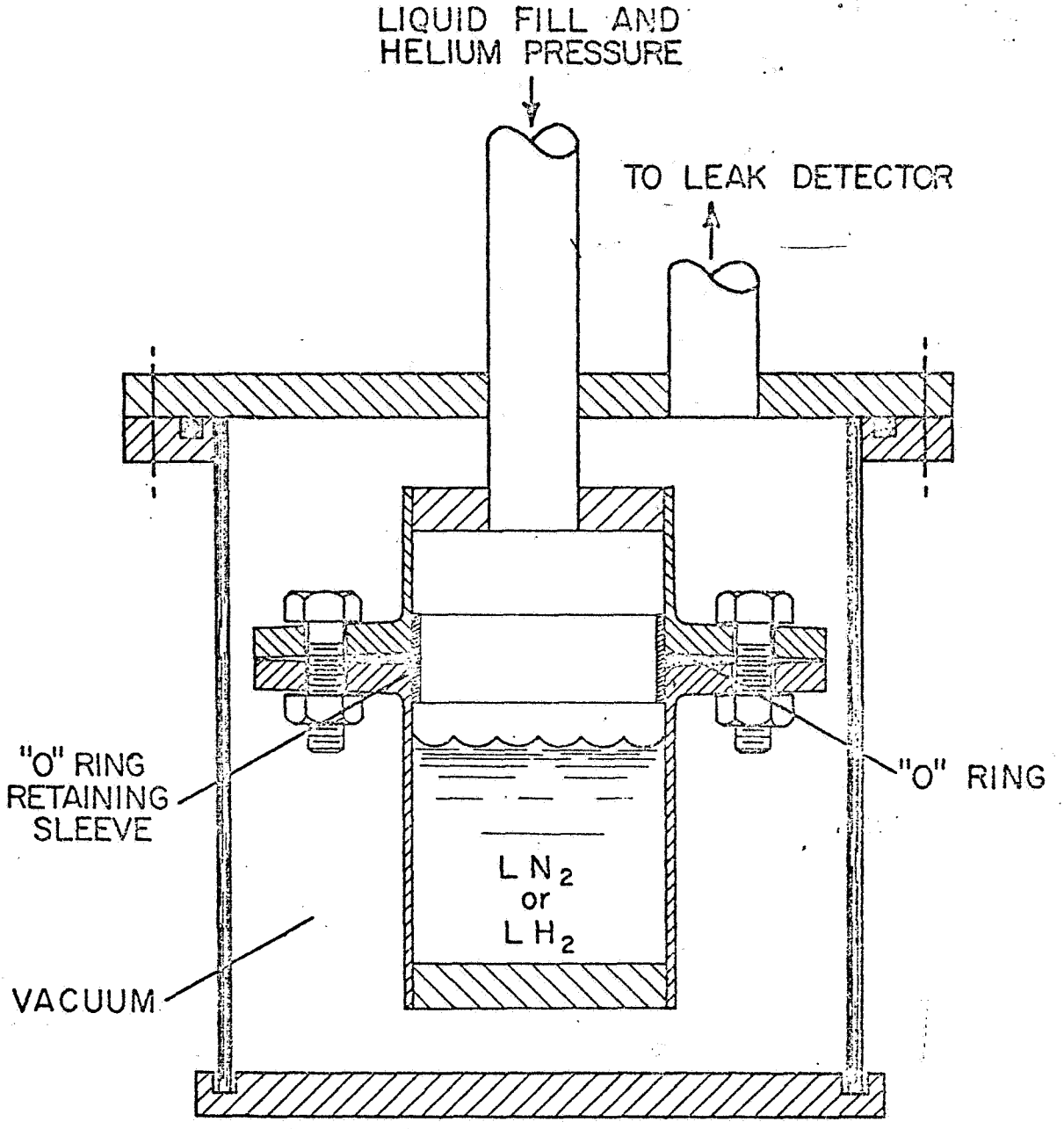

FIG 5. Flat Flange and Retaining Sleeve

3. Force Decay Seal Tester

An apparatus was designed to critically compare the performance of various elastomers when highly compressed at room temperature, then cooled to cryogenic temperatures while maintaining a seal. Conditions of the test were such that most of the seals would leak, with the temperature at which a leak occurred serving as an index of merit. The apparatus is shown in figure 6. Compressive force was applied through washer type strain gauges placed in a bellows filled with liquid nitrogen during cooldown.

Initial compressed thickness of the O-ring was maintained as constant as possible by making critical parts of the apparatus of invar and placing invar pillars between the loading bolts. This maintained a constant separation between the main flanges and eliminated most of the spring loading, so that we were able to obtain a record of the force which the compressed elastomer exerted against the flanges during an initial relaxation period before cooldown and during cooldown to 76K. Thus parameters obtained for use in comparing the various elastomers were:

(1) The temperature and pressure at which a leak occurred.

(2) The force at which a leak occurred.

(3) The force decay during initial relaxation.

(4) The force lost during cooldown.

Data were plotted with the help of an x, y recorder, giving us graphs such as those shown in figure 7. Three successive cooldowns were made for each material which showed promise, with seals separating high vacuum from helium pressures of 100 to 1000 psig.

Detailed results of this work are given elsewhere[3]. For our present purpose we can summarize by saying that about 50 different samples divided into 10 groups representing all of the basic elastomeric polymers were tested with this apparatus, giving about 25 graphs similar to those we have seen. From a study of this information we were able to reach several conclusions regarding the use of elastomers for cryogenic seals. Among these were the following:

(1) Even with constant flange separation and a minimum amount of spring loading, some elastomers are capable of maintaining high sealing forces when cooled far below their brittle transition temperatures.

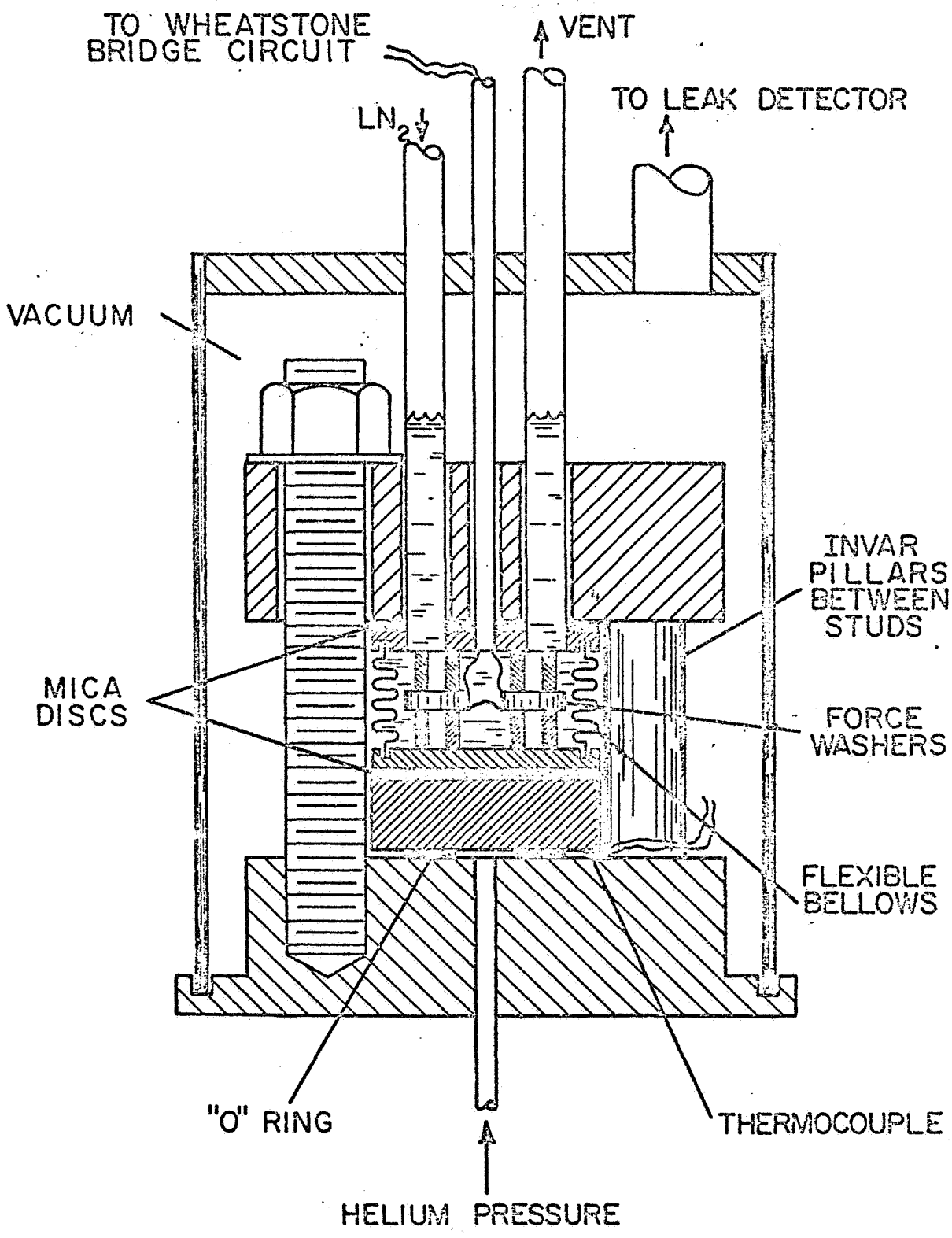

FIG 6. Force Decay Test Fixture

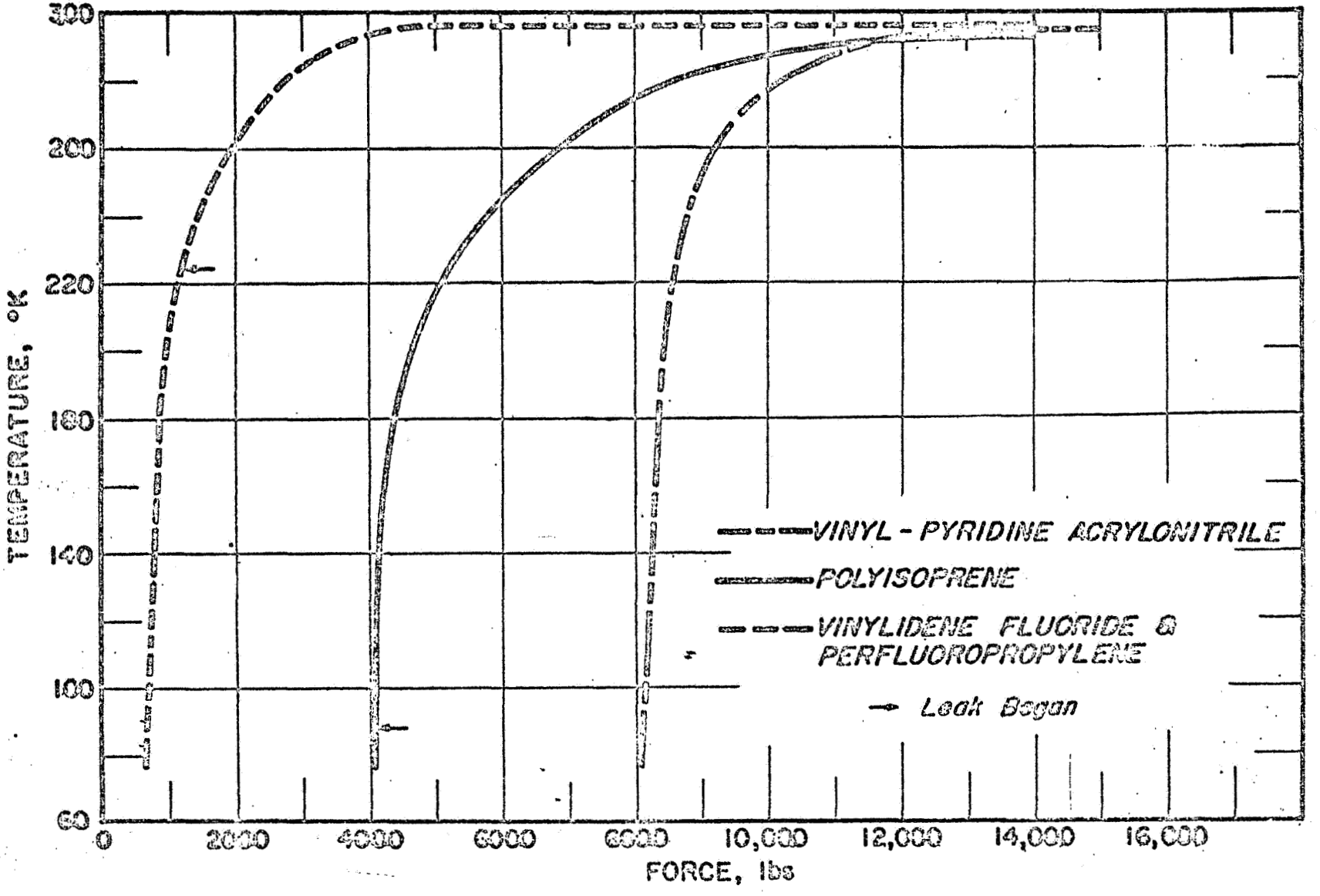

Figure 7 Force decay during cooldown

(2) With high compression and small final thickness most of the force decay occurs during an initial relaxation period of about six hours at room temperature. The amount of this initial relaxation is a fair indication of the effectiveness of the material for cryogenic seals.

(3) Best seals were obtained with compounds of natural rubber, polyisoprene, polybutadiene, vinyl pyridine-acrylonitrile, neoprene, and butadiene-acrylonitrile. Several others, including one experimental silicone, also showed promise.

(4) Many of the seals leaked while the elastomer was still maintaining considerable net force (three to five thousand psi) against the flange surfaces. This apparently was the minimum sealing force which had to be maintained. The reason for this was not obvious, and led to an investigation of sealing and unseating mechanisms.

4. Seal Interface Studies

Since the contraction rate of the brittle elastomer is several times as high as that of the confining flanges, temperature changes which occur below T_g will introduce thermal strains parallel to the flange surfaces, and may even cause lateral motion or sliding along the interfaces. Relative motion at the interfaces will result in "unseating" of the seal unless there is plastic flow or deformation to prevent this. The seals which leaked while the net sealing pressure was still high were probably operating in this way. A "constant force" experiment was designed to study this problem and to find ways of reducing the required sealing force.

The central part of the constant force apparatus is shown in figure 8. Force was applied to the flanges at what would normally be the bolt circle, but instead of using bolts a hydraulically loaded testing machine was used to maintain a constant compressive force during cool-down. A specially designed dewar, not shown in the figure, surrounded the apparatus for cooling by slow addition of liquid nitrogen. The O-ring was positioned around a machined step on the bottom flange; the top flange had a circular recess which fit the step with 0.002 inches diametral clearance. Thus the O-ring was confined at its I.D. and forced to extrude outward when compressed.

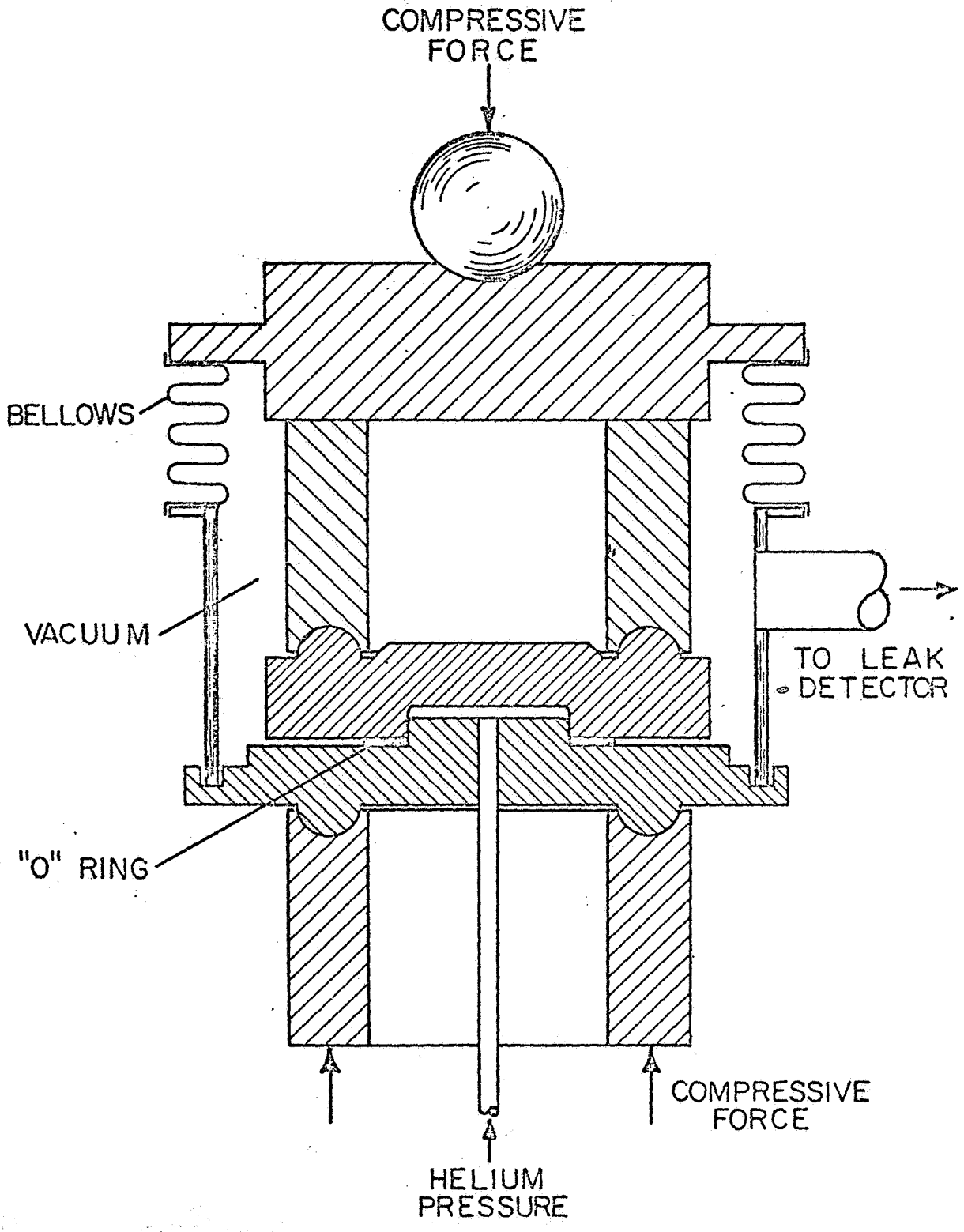

FIG 8. Constant Force Seal Test Apparatus

With this equipment and a selected control group of one inch diameter by 0.140 inch cross section O-rings we determined the minimum force required to maintain tight seals at 76 K with 1000 psig helium on the inside and high vacuum on the outside. The minimum constant force required for the better materials was 5000 to 6000 pounds, which is equivalent to about 1200 pounds net force per linear inch of O-ring, or a net pressure of 4000 to 5000 psi on the compressed O-ring surface. This agreed with results obtained with the force decay apparatus, and led to attempts to lubricate the interfaces with a thin layer of material which would flow plastically at cryogenic temperatures.

To pursue this idea we used a sandwich configuration consisting of two foil or film washers with the O-ring between, as shown in figure 9. Films of polytetrafluoroethylene, lead, aluminum, and indium were tried with neoprene O-rings. Three mil thick indium foil proved to be highly successful when used in this way. Flange loading was reduced by a factor of three, and more reliable seals than ever before were obtained. A net flange load of only 400 pounds per inch of seal circumference was required to separate 1000 psig at 76 K from high vacuum with leakage less than 10^{-6} atm cc/sec. Net pressure on the sealing surfaces was reduced to about 1500 psi. It might be mentioned also that the step in the flange was designed for external rather than for internal pressure, as shown in sketch A of figure 10. If the back-up step had been on the outside of the O-ring, as shown in sketch B, the seal could probably have been maintained with even less flange loading.

The indium-elastomer sandwich seals were tested in the constant force apparatus with O-rings of natural rubber, neoprene, polybutadiene, ethyl-acrylate, vinylidene fluoride perfluoropropylene, and chlorosulfonated polyethylene. All performed exceptionally well. Neoprene-indium was also tested in the force decay fixture. While at 76 K this seal was shocked by dropping the heavy fixture on a concrete floor from a height of several inches, a treatment which very few previous seals had sustained without developing leaks. The neoprene-indium seal could not be made to leak by this type of shock treatment.

The elastomer indium sandwich makes effective use of indium's ability to cold flow. A very thin layer of indium remains compressed between the elastomer and the flange surface and continuously fills any openings which tend to form as the surfaces move relative to one another. In this way indium functions as an O-ring lubricant or grease, but one which does not become brittle at cryogenic temperatures. The advantage over plain indium is that there is no continuous cold flow because of frictional

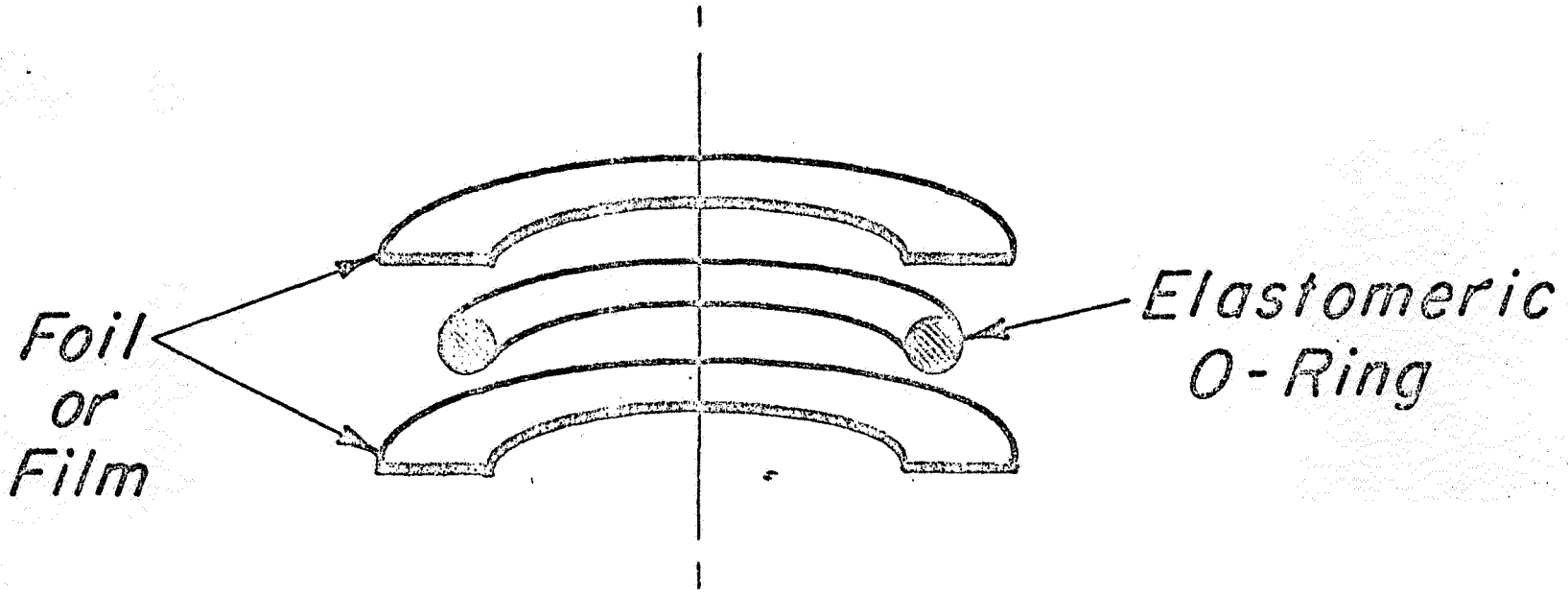

FIG 9. Sandwich Seal Configuration

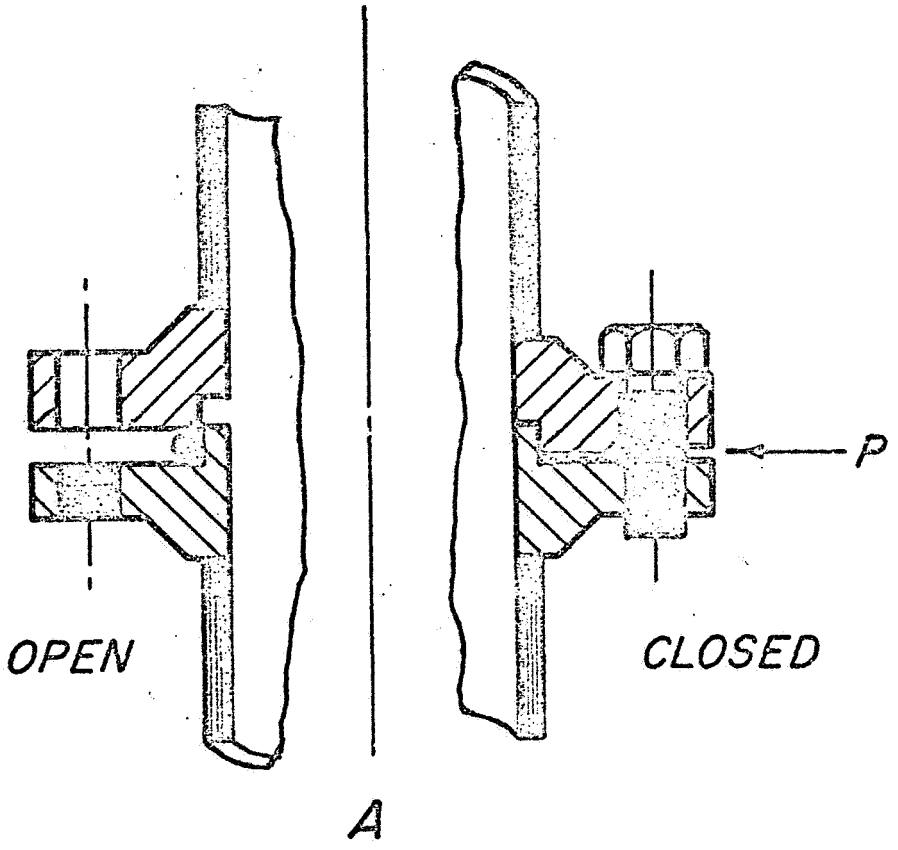

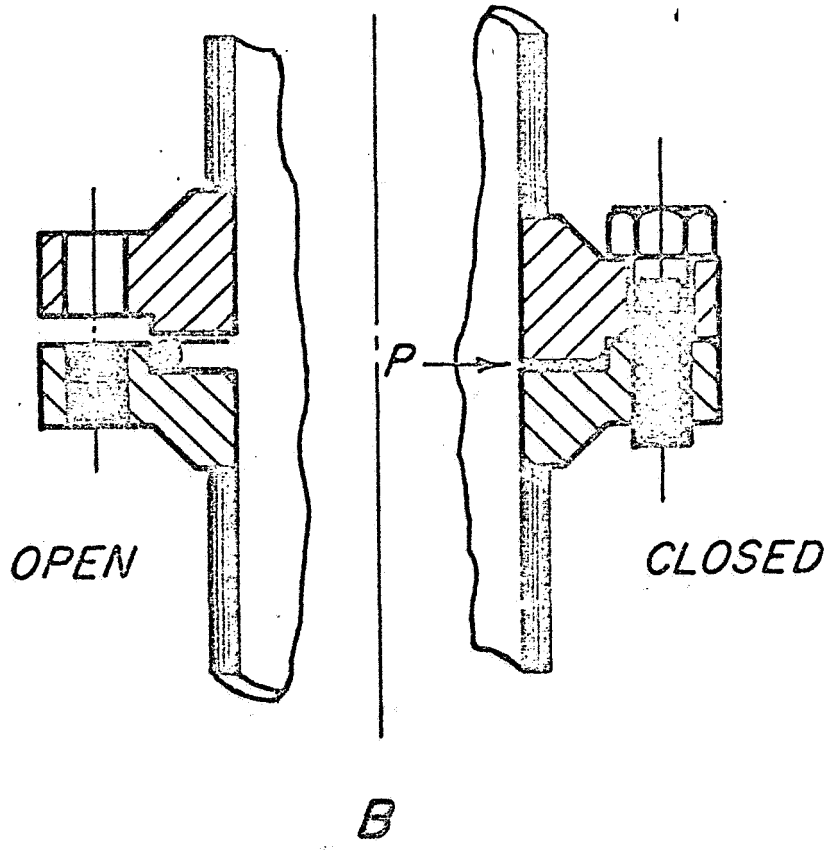

FIG 10. Stepped Flanges

forces on the extremely thin layer of indium which remains between the flange and O-ring. In addition, each time the elastomer warms to its brittle point it comes to life like a compressed spring and reseats the seal. Thus we have a technique for adding elasticity to indium.

With the aid of these two experiments, one showing force decay and seal performance at constant flange separation, the other giving seal performance at constant flange loads, we can restate the principles to be kept in mind for use of static elastomeric seals at cryogenic temperatures. These are:

(1) Choose an elastomer which can be given 80 to 90 percent linear compression without material failure. This requirement is easily met by the elastomers which performed best in the above tests.

(2) Compress at least part of the elastomer cross section 80 to 90 percent, and choose the cross section to give a final compressed thickness no greater than 0.010 inch.

(3) Spring load the compressed elastomer, or use the pressure of the confined fluid, or take advantage of differential thermal contraction (or use two or all of these) to maintain a net sealing pressure of about 5000 psi on the sealing area. This does not require heavy flanges nor high bolt loads because the sealing area can be made small. A seal width of 0.050 inches, which should be ample, will experience a compressive load of 5000 psi with a flange load of only 250 pounds per inch of seal circumference.

(4) If the interface between the elastomer and the flange is lubricated with a thin layer of indium the required net sealing pressure can be reduced to as little as 1500 psi.

5. Design Suggestions

We have described a number of experimental flange and elastomer combinations which were developed to test various aspects of the performance of elastomeric O-rings as seals at cryogenic temperatures. Several of these designs were found to make very satisfactory high pressure to high vacuum seals and can be used for many practical low temperature applications.

In conclusion, however, we would like to suggest a few designs which utilize principles which the experimental flanges have helped us to establish. For light weight flanges and low bolt loads one can use:

(1) An O-ring of convenient cross section, but requiring high compression on only a small sealing area.

(2) Spring loading.

(3) Pressure actuation.

(4) Temperature actuation.

For good connector design, one should have:

(1) Simple, symmetrical flanges.

(2) Easy trouble-free assembly.

(3) Solid metal to metal flange contact for transmission of loads through the joint.

Figure 11 shows a stepped flange which can be dimensioned to apply high compression to any desirable fraction of the O-ring cross section. The step can of course be reversed, as shown at B, which is better for vacuum or external pressure, and also holds the O-ring better during assembly of the joint. These stepped designs depend for spring loading on flexing of the flanges before metal-to-metal contact. They are neither pressure nor temperature actuated, and the flanges are not symmetrical, but they are simple and those which we have tested have been reliable.

Figure 12 shows a flange and insert assembly which uses two O-rings in a design analogous to the usual spring loaded and pressure actuated seal. This design has solid metal-to-metal contact for transmitting loads through the joint and does not depend on flange flexing for spring loading. Flanges are simple, symmetrical, and light weight, with bolt loads controlled by the spring constant of the insert beams. This is a good design which combines most of the desirable features which we have enumerated.

Figure 13 shows another method for tucking away part of the cross section of the O-ring and applying a controlled spring load to the remainder, which is used to make the seal. If the beams point out, as shown, the O-ring can be positioned on the O. D. of the insert but the seal is oriented for external rather than internal pressure. For high internal pressure the insert should be reversed as shown in figure 14.

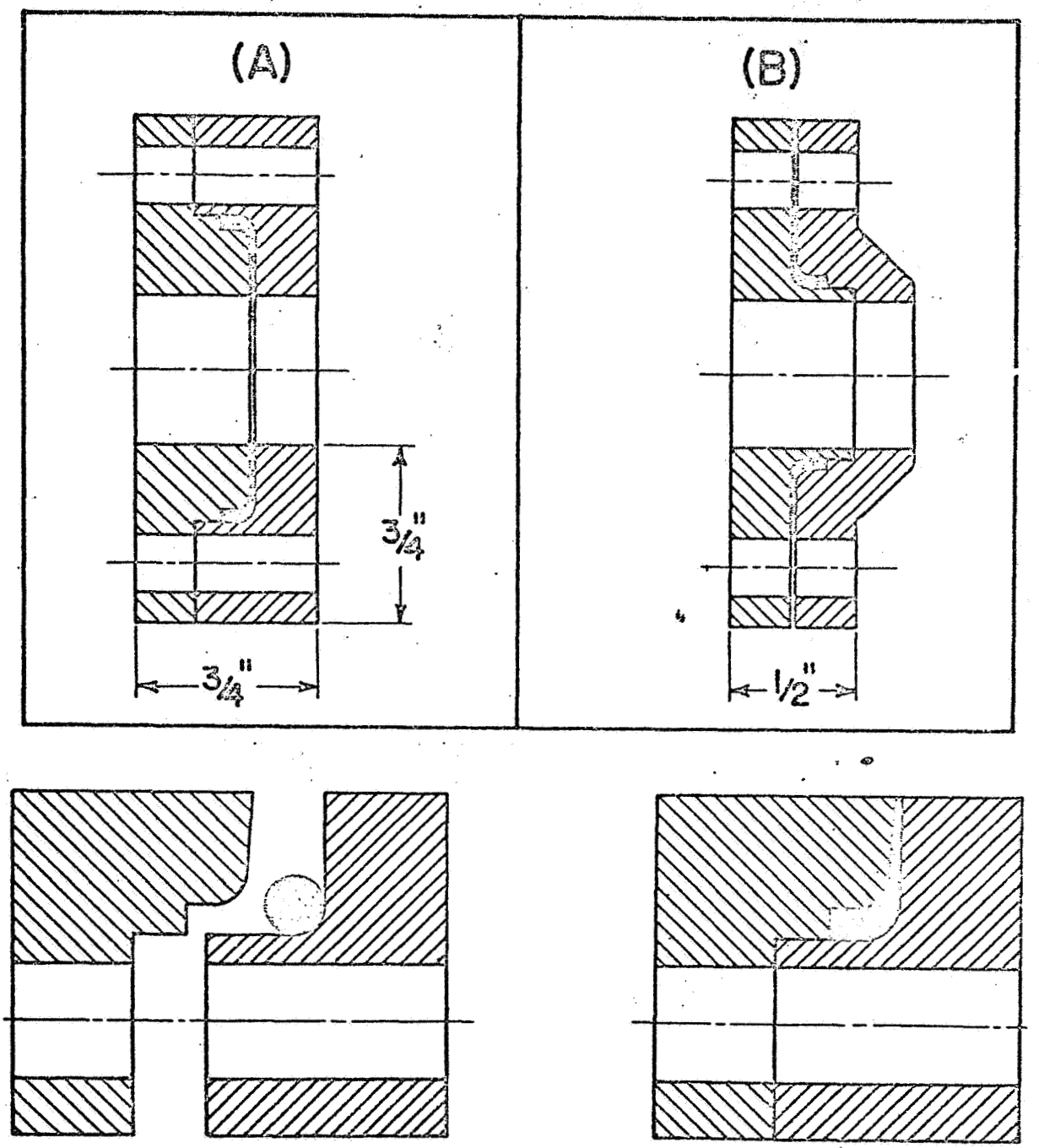

FIG 11. Stepped Flanges With Cross Section Control

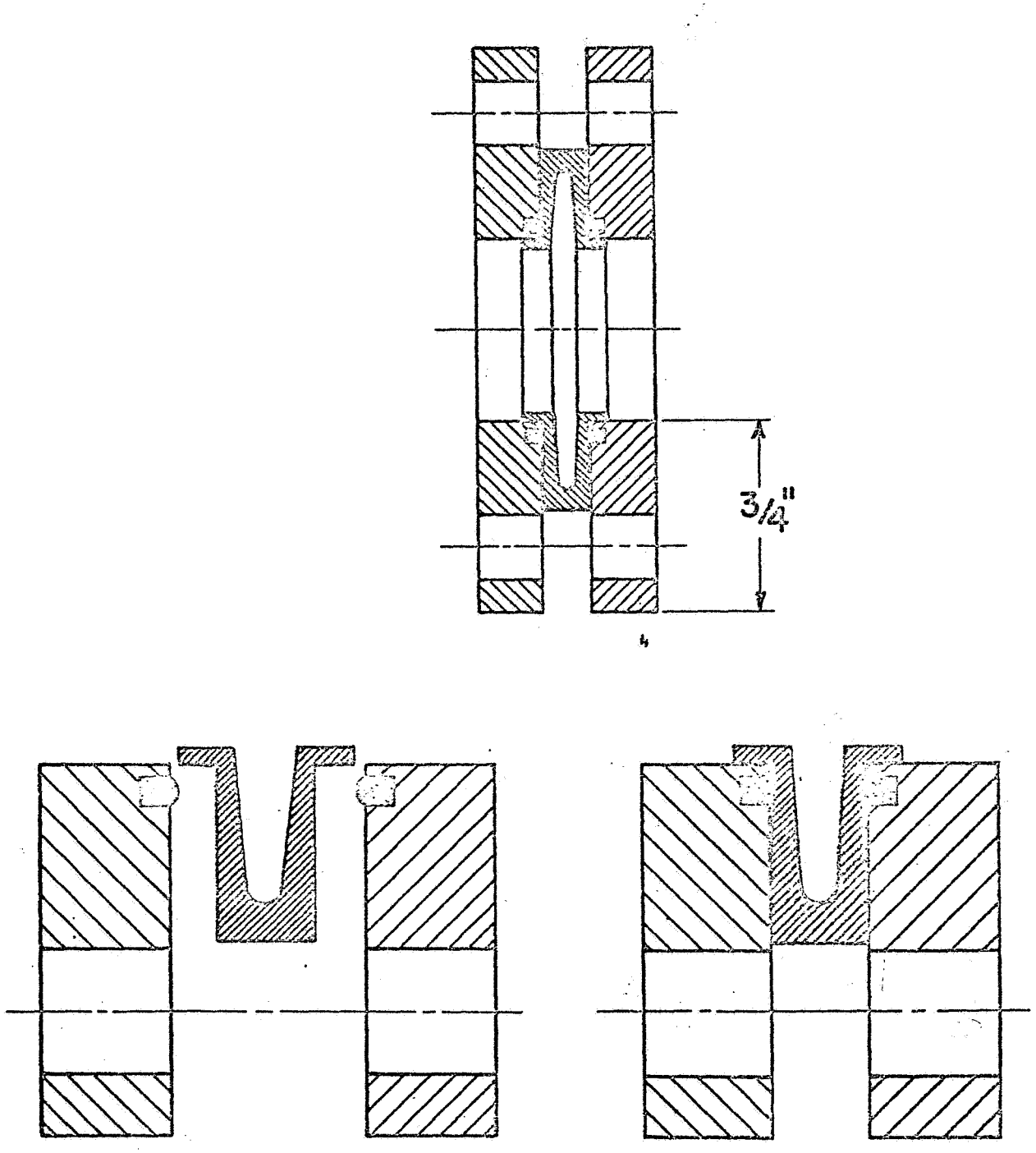

FIG 12. Elastomer Seal, Spring Loaded and Pressure Actuated

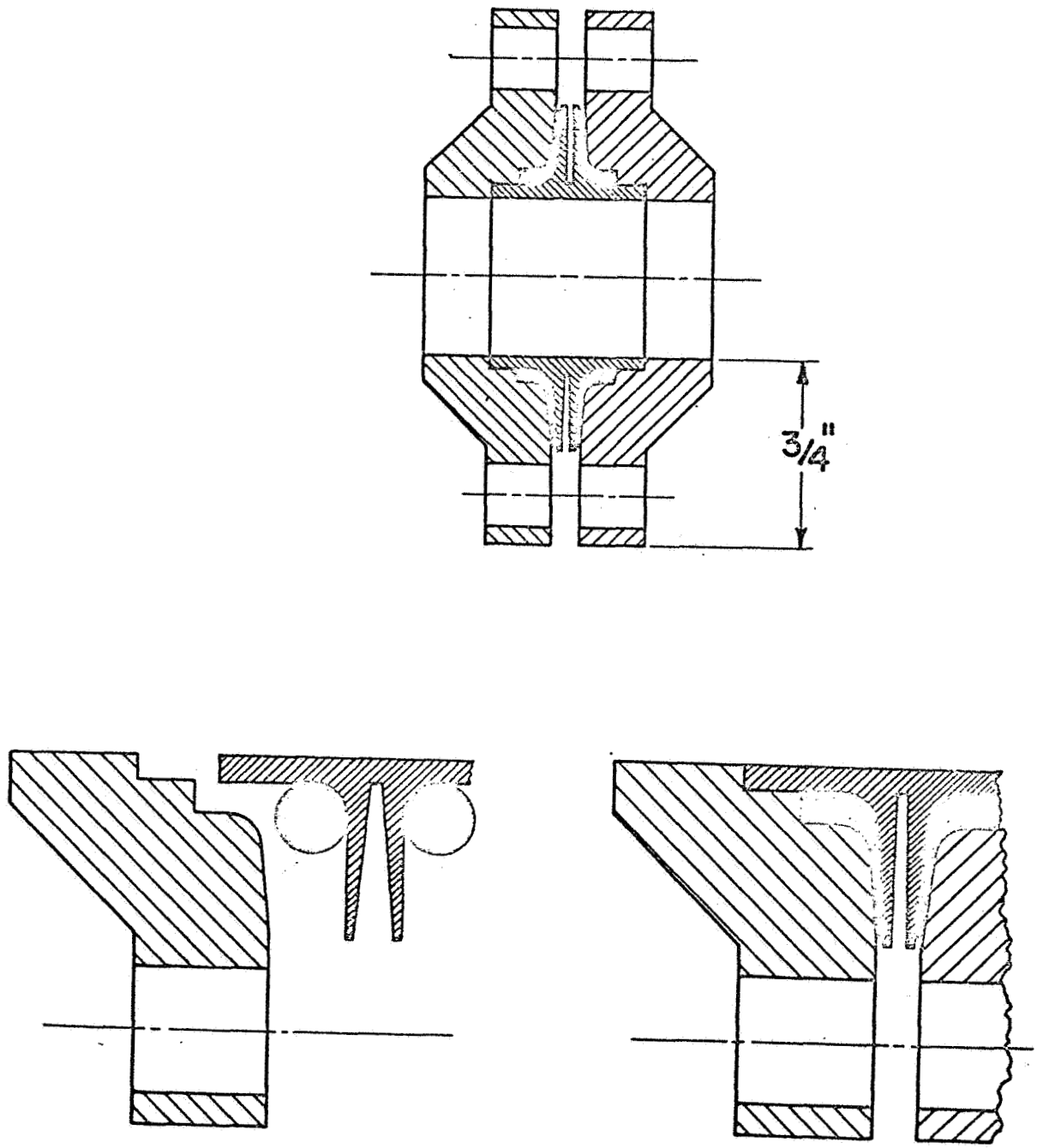

FIG 13. Spring Loaded Seal for External Pressure

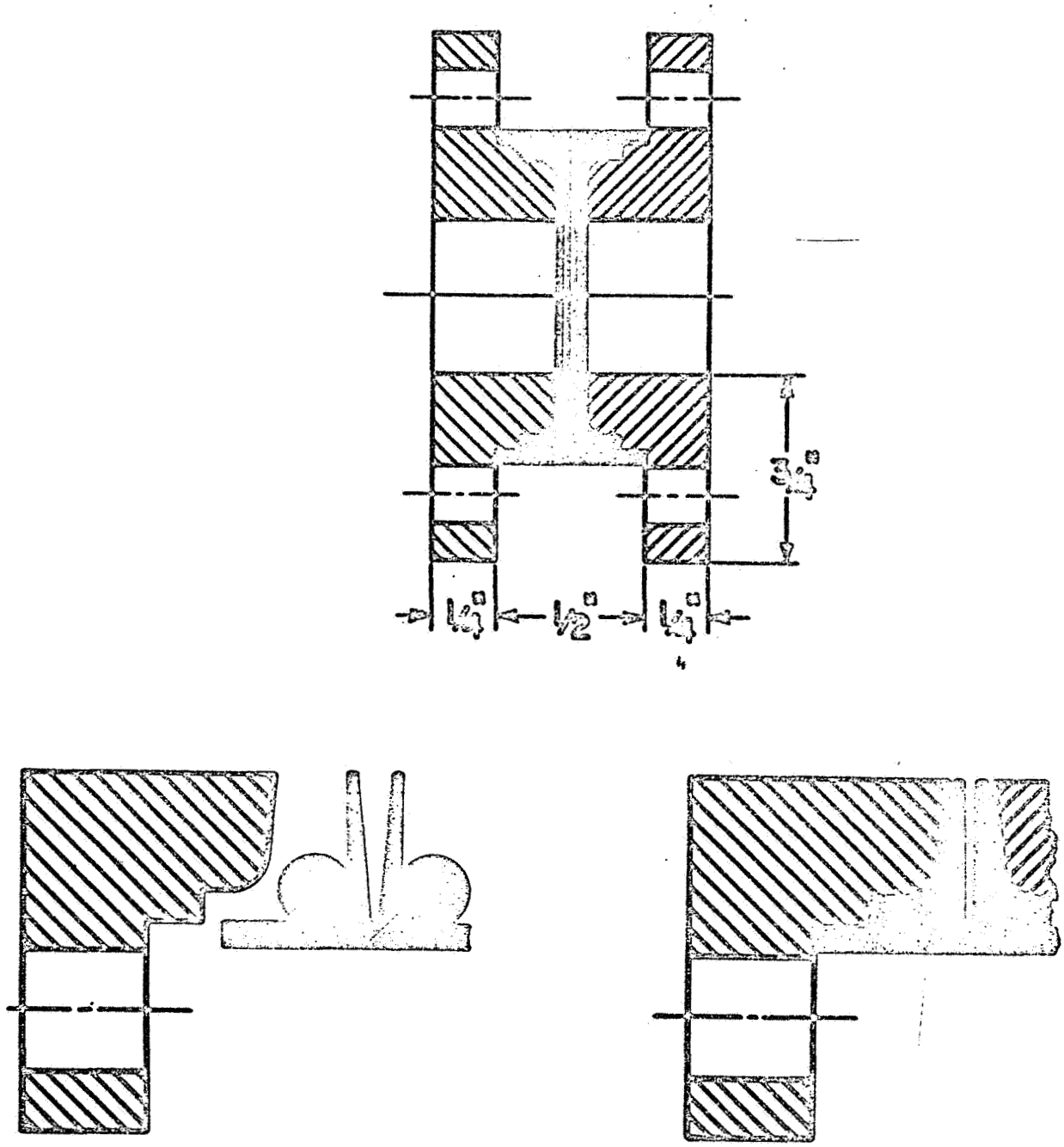

FIG 14. Spring - Loaded Seal for Internal Pressure

A third possibility is shown in figure 15 which spring loads the elastomer through hoop compression of a ring-shaped insert. This design is compact and allows low bolt loads because it utilizes the mechanical advantage of an inclined plane to compress the insert ring and elastomer. It is not suitable for diameters less than about four inches, however, because in these the insert ring may yield in compression before deflecting enough to make room for the elastomer, and subsequently will not have sufficient springback to maintain an effective sealing pressure. *

Materials for these spring loading inserts should be chosen primarily on the basis of elastic properties and yield strength, with thermal expansivity a secondary consideration. If the O-ring is positioned on the O. D. of the insert the seal will tighten during cool-down if the insert shrinks less than the flange. If the O-ring is on the I. D. of the insert, temperature actuation results if the insert shrinks more than the flange.

These and other designs are being studied at the NBS Cryogenic Engineering Laboratory. We are convinced that elastomers should not be overlooked when considering the problem of leak tight separable connectors for service at cryogenic temperatures.

6. Bibliography

1. Weitzel, D. H., R. F. Robbins, G. R. Bopp, W. R. Bjorklund, Elastomers for Static Seals at Cryogenic Temperatures, Advances in Cryogenic Engineering 6, p. 219, K. D. Timmerhaus, Editor, Plenum Press, 1960.

2. Robbins, R. F., D. H. Weitzel, R. N. Herring, The Application and Behavior of Elastomers at Cryogenic Temperatures, Advances in Cryogenic Engineering 7, p. 343, K. D. Timmerhaus, Editor, Plenum Press, 1961.

3. Weitzel, D. H., R. F. Robbins, P. R. Ludtke, Y. Ohori, Elastomeric Seals and Materials at Cryogenic Temperatures, Aeronautical Systems Division, Technical Data Report 62-31, Parts II and III, 1962 and 1963.

---

* Threaded holes between the bolt holes in the flanges are used to disassemble the seal by jacking against the insert skirt.

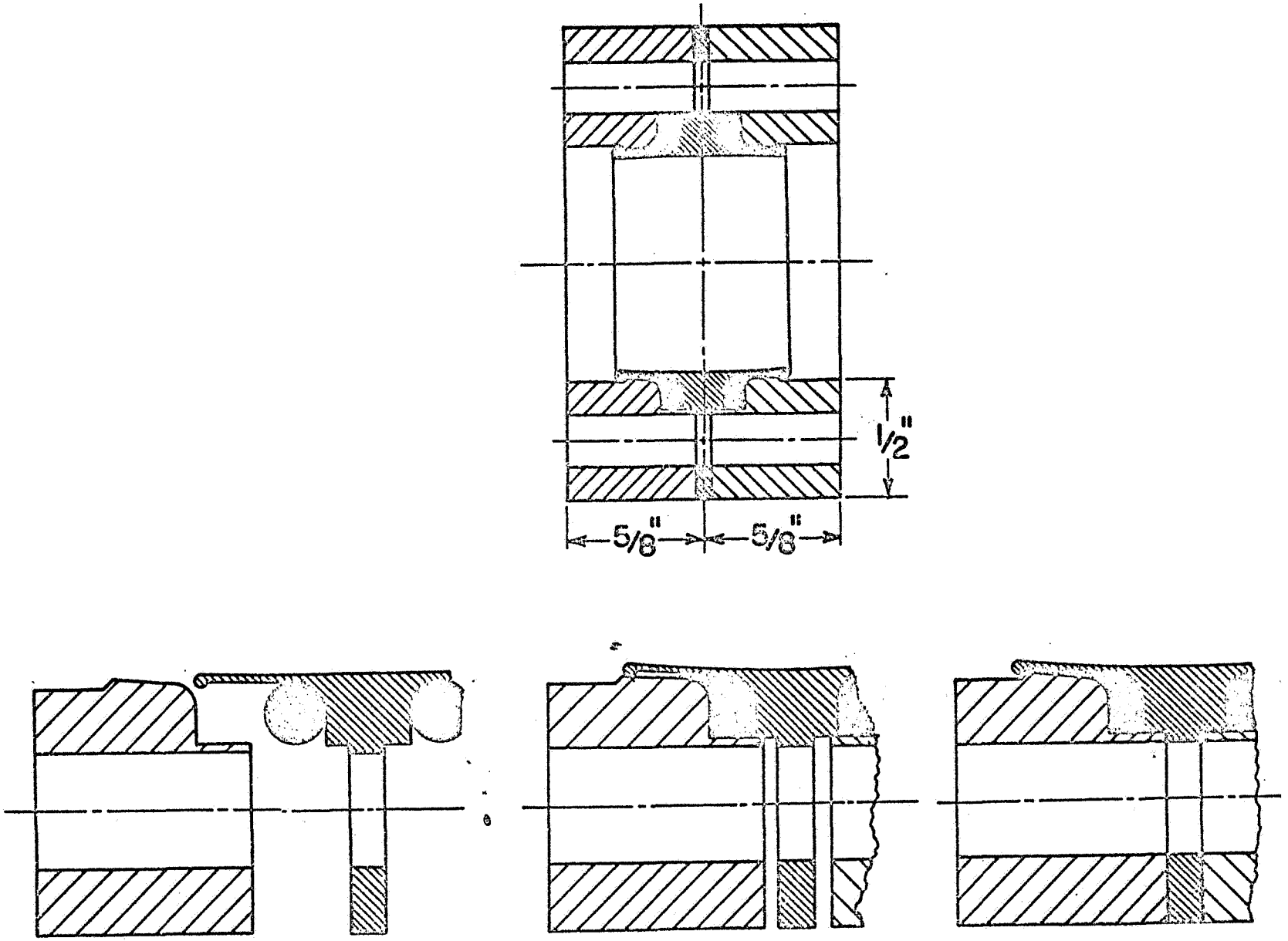

FIG 15. Spring Loaded Seal With Hoop Insert

N67-86150

THE DEVELOPMENT OF A NEW CRYOGENIC GASKET FOR LIQUID OXYGEN SERVICE

PART I

By

Rex. B. Gosnell, Ph.D.

NARMCO RESEARCH & DEVELOPMENT
A Division of Telecomputing Corporation

This program was sponsored by the George C. Marshall Space Flight Center National Aeronautics and Space Administration.

INTRODUCTION

A particularly critical and unique liquid oxygen gasketing problem has been encountered by the George C. Marshall Space Flight Center during the development of the Saturn launch vehicle. Only a marginal solution to this problem has been achieved so far. The need for an improved cryogenic gasket, especially designed for Saturn liquid oxygen use, resulted in their sponsorship of this program.

In surveying the possibilities for elastomers which retain a degree of real flexibility at cryogenic temperatures, only two present themselves as candidates, namely the polyurethanes and the fluorocarbon polymers. For liquid oxygen service, it is indeed most fortunate that one of these types of materials is LOX compatible. If the fluorocarbon polymers were subject to the embrittlement observed with many other elastomers, the problem of a flexible, LOX compatible material would be considerably more serious than it is now.

A number of gaskets and gasket materials that are compatible with liquid oxygen are available commercially. However, exhaustive testing by the Marshall Space Flight Center has revealed that many of these products do not possess the physical properties needed to maintain a tight seal in the lightweight flanges favored for launch vehicle applications. These shortcomings are also demonstrated by test data obtained during this investigation. Some of the key requirements for a material in this specialized application include:

(1) Little or no cold flow or creep under load at ambient temperature.

(2) Little or no compression set at ambient temperature.

(3) Retention of some degree of flexibility at cryogenic temperature.

(4) Generally good sealing characteristics at ambient and cryogenic temperatures.

(5) Complete resistance to reaction upon impact in LOX.

Also, it would be most desirable if this gasket could be reuseable.

This paper presents information on the tests which were used in the evaluation of gasket materials along with the results of these tests, and how they indicated the proper design of a new gasket. Data is presented which show the improvements realized with the newly developed gasket.

GASKET EVALUATION

The specimen chosen for all evaluation testing was in the form of a flat gasket with an O.D. of 2.06" and an I.D. of 1.31". This specimen gave a flange contact area of 2 square inches. Most specimens were from 80-90 mils in thickness.

All specimens were evaluated in a test which was termed "load decay." This test was designed to establish how well the material was able to maintain its resistance to compression. The test was an exaggerated one with very high flange pressure and was designed to magnify cold flow problems in a gasket material. Specimens which resist cold flow and had sufficient tensile strength to resist material failure, performed well in this test. The specimen was loaded to 15,000 psi between two flat flanges in a hydraulic press with tight check valves enabling the plotting of the decay of the load or the pressure exerted by the compressed gasket. The load was followed for a period of thirty minutes and a typical cure is presented in Figure 1.

Notice that the compressibility and compression set are also recorded in this test. The curve shown in Figure 1 refers to the commercial SBR-asbestos material now used for most Saturn LOX gasketing applications. This product is marginal in its sealing properties, and it requires elaborate pretreatment with a chlorofluorocarbon polymer oil to minimize its potential reactivity with liquid oxygen.

Materials with poor performance are readily identified by their sharp drop in load as illustrated in Figure 2. This curve was obtained on an asbestos filled fluorocarbon elastomer specimen. The filler level was 37% by weight. Notice the high compression set measured 24 hours after releasing the load.

The fact that different fillers may not have an equivalent effect at the same level is indicated in Figure 3. This family of curves was obtained with specimens containing various levels of zinc oxide. The levels between 0 and 34% were not pursued for reasons mentioned later.

Several specimens were prepared by molding Teflon powder with various levels of chopped fiberglass filler. The effect of filler level on the load is shown in Figure 4. Also shown in Figure 4 are three commercial cryogenic gasketing materials. Typical of all the glass filled Teflon systems is a compression set of about 30 percent. This test demonstrates the serious cold flow problem of this type gasket.

At this point it became evident that the degree of resistance to cold flow required in this situation would not be attained with any known filled or fiber reinforced fluorocarbon polymer without seriously compromising other important physical properties. This led us to a laminated gasket design, consisting of

alternating plies of a woven fabric and a suitable fluorocarbon film. After the application of heat and pressure the resulting laminate has real reinforcement and the woven structure effectively inhibits cold flow, but sufficient void content is allowed to remain to provide some compressibility. A typical load decay curve for a fluorocarbon polymer and 112 glass fabric laminate is shown in Figure 5.

Table I is a listing of the compressibility and compression set data obtained from the load decay testing. Notice that most of the commercial gaskets suffer considerable compression set.

In addition to obtaining cold flow information from load decay with high flange pressures, the compressive modulus of gasket candidates were obtained at more realistic flange pressures. Furthermore, the gasket specimens were load cycled ten times to 3000 psi in order to observe changes in the compression modulus resulting from compression set or flow. Stress-strain curves were obtained during this cycling which were conveniently used to calculate the compressive modulus in each cycle. Because most of the change occurs between the first and second cycle, tabulation of modulus values are made on the first, second and tenth cycle.

The equipment used consists of two plates mounted on an Instron testing machine, with gasket deflection measured by an extensometer driven by an appropriate linkage, (see Figure 6). For cryogenic testing, the entire fixture was immersed in liquid nitrogen. A typical Instron chart is shown in Figure 7. This chart was obtained with a 40% glass filled Teflon gasket. A number of modulus values for various materials are shown in Table II. Notice the excellent values obtained for the fluorocarbon polymer - 112 glass laminate.

A summary of the modulus values for the various types of gaskets is shown in the form of a bar graph in Figure 8. Note that the filled fluorocarbon elastomer has high compressibility at room temperature but becomes quite hard at -320°F. The glass fiber filled Teflon is not as severe in its modulus change but the fluorocarbon polymer laminate is outstanding in this regard. The -320°F moduli of the laminate systems are not far different from the room temperature moduli. This performance is brought about by certain features of the laminate introduced by the special laminating procedure mentioned previously. This procedure consists of the layup of glass fabric and the fluorocarbon polymer film and lamination at a temperature sufficient to produce some flow but not high enough to give complete saturation of the fiber bundle. This characteristic results in a material with a springlike compressibility which is not subject to drastic changes in modulus with decreasing temperature.

This difference in bundle wetting at different laminating pressure was demonstrated by placing polished edges of a series of Teflon laminates prepared at temperatures from 500°F-700°F, in a penetrant dye solution for 20 minutes. At the end of this time, the laminates were removed from the solution and wiped dry. The extent of lateral penetration of the dye into the laminate was measured and found to be a function of the laminating temperature. Lesser penetration was observed at 700°F due to the lower resin viscosity and the resulting improved wetting ability of the binder.

Teflon FEP can be used to fabricate laminates with pressing temperatures from 500°F-700°F. Generally 100 psi is sufficient. Other fluorocarbon materials can also be used with the appropriate temperatures including the elastomeric systems of the type composed of copolymers of vinylidene fluoride and tetrafluoroethylene or trifluorochloroethylene. Other polymers include the polytrifluorochloroethylene based systems which can be pressed from 400°F-450°F and it is possible to use these polymers in combination with the elastomeric systems to achieve greater flexibility of the gasket at room temperature. Compressive moduli for these systems is presented in Table III.

Hysteresis loops were also obtained on the test specimens and were of considerable value in demonstrating differences in compression set and flow. Shown in Figure 9 are the hysteresis loops obtained on cycling a 25% glass filled Teflon system typical of a number of commercial cryogenic gasketing materials. Compare these with the loops shown in Figure 10 for the Teflon 112 glass fiber laminate which almost completely obey Hook's law.

The actual sealing characteristics of materials was also studied. Two aspects of the sealing ability were studied, the first of which was to establish what flange pressure was required to maintain a seal against an internal gas pressure. The gasket was loaded to 1500-psi flange pressure and then the small volume inside the gasket was pressurized to 200 psi. The flange pressure was then gradually decreased until a leak was observed on a pressure monitoring gauge. A small leak was readily detected because of the small volume inside the gasket. It was noted that almost all gaskets were similar at -320°F and the minimum flange pressure to prevent a leak was about 200-250 psi. The similarity of performance in this test led us to another method of evaluation consisting of the determination of the flange deflection which can take place before a leak occurs.

It can be easily understood how this feature in a gasket would be of importance. A good gasket will maintain a seal even though the flange may move under a stress. A safety factor would be available for thermal contraction as well. The expression of the flange deflection before a leak occurs is tabulated in Table IV, with the values expressed in terms of a coefficient which is the flange deflection per unit thickness of the gasket. Note that many of the commercial materials have values of 0.020 or less, while the fluorocarbon-glass fabric gaskets have values as high as 0.040 to 0.050.

With continued studies of the effect of changing each of several processing variables upon the compressibility of gasket composites, it became apparent that interpretation of slight differences in compressibility were required. With the original testing device it was felt that these small differences could not be detected within the limits of the experimental error. This experimental error

became significant due to a measuring system which was somewhat complex and will not be discussed in this presentation. A more effective device was designed and its simplicity actually contributed to a greater accuracy. This fixture is shown in Figure 7. Stress-strain curves were obtained with this device which were felt to be quite reliable.

Typical curves are shown in Figures 8 and 9, which compare Fluorolube treated asbestos-rubber and a typical Teflon FEP laminate.

Further work with these gasket systems is continuing and will be reported in Part II of this presentation.

CONCLUSIONS

It has been demonstrated that the greatest problem with gaskets using binders of fluorocarbon polymers, is their high cold flow or creep characteristics. Various methods of restricting cold flow have been evaluated but only one shows indications of success. The promising approach is the use of a laminated composite with a fluorocarbon polymer binder. A desirable feature of this composite is the incomplete wetting of the fiber bundle which results in temperature-independent springlike compressibility.

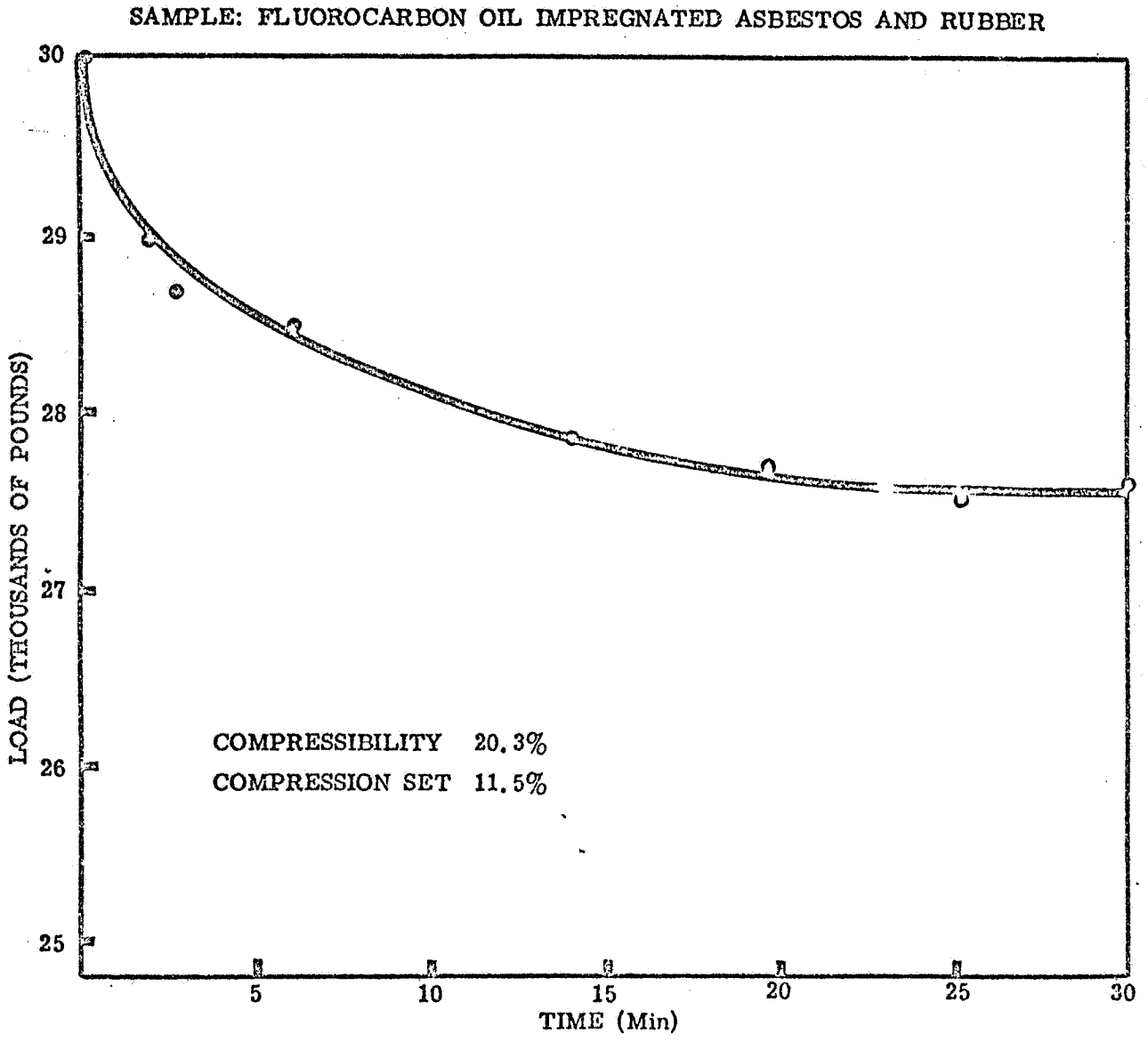

Figure 1. Load Decay Curve

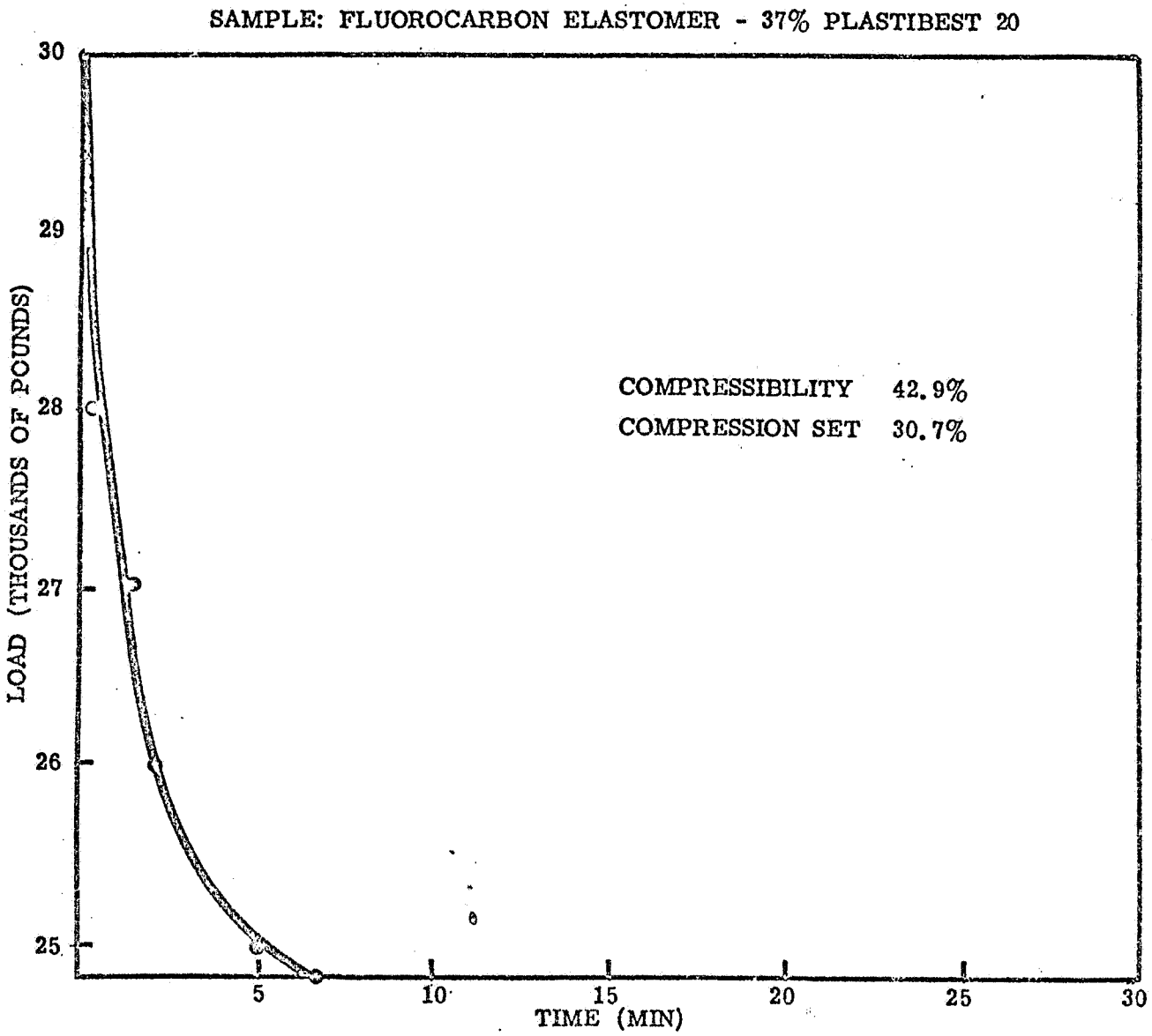

Figure 2. Load Decay Curve

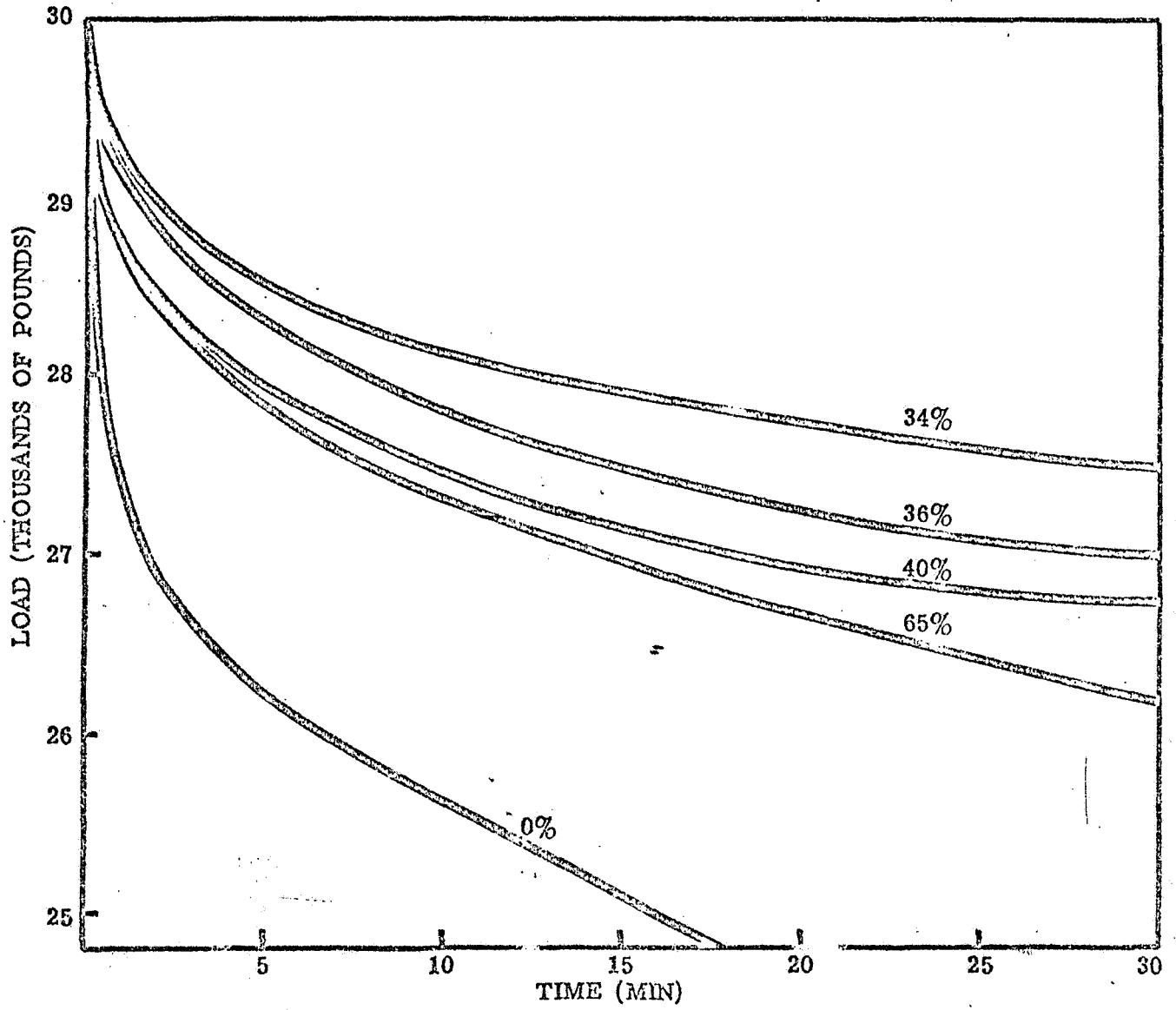

Figure 3. Family of Load Decay Curves - Zinc Oxide Filled Fluorocarbon Elastomer

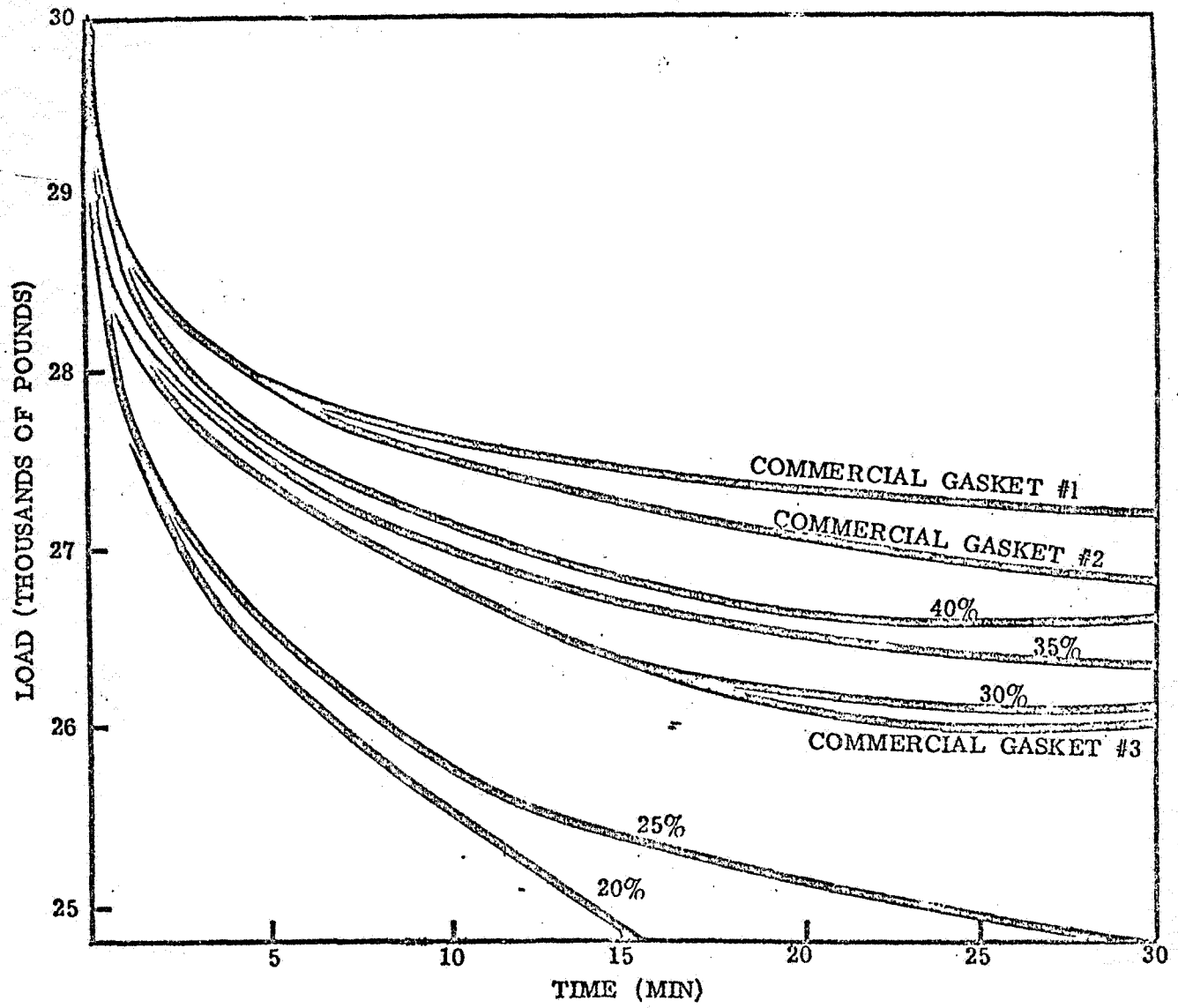

Figure 4. Family of Load Decay Curves for Various Filler Levels of Fiberglass-Teflon Gaskets

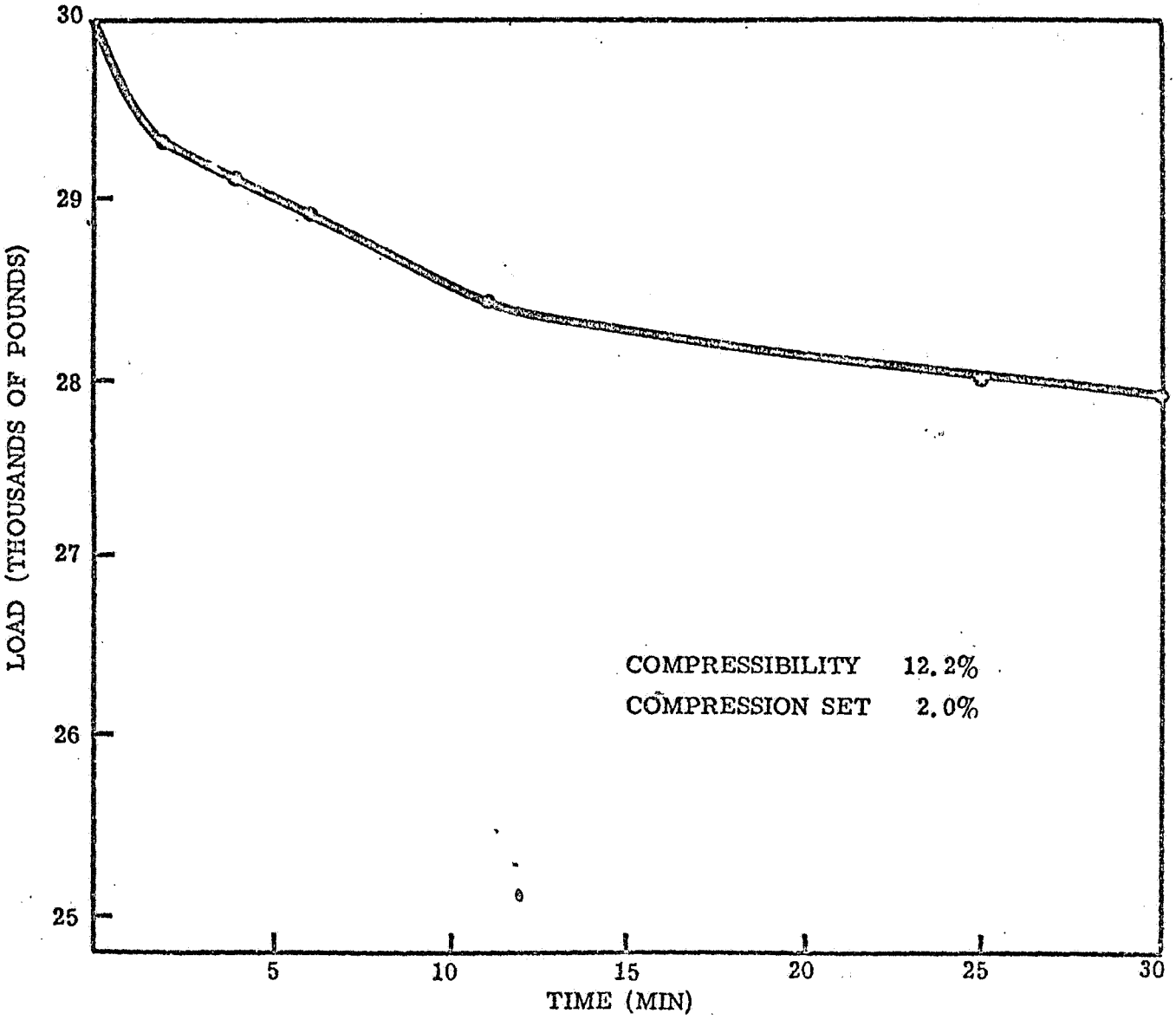

Figure 5. Load Decay Curve of Teflon and 112 Glass Fabric Laminate

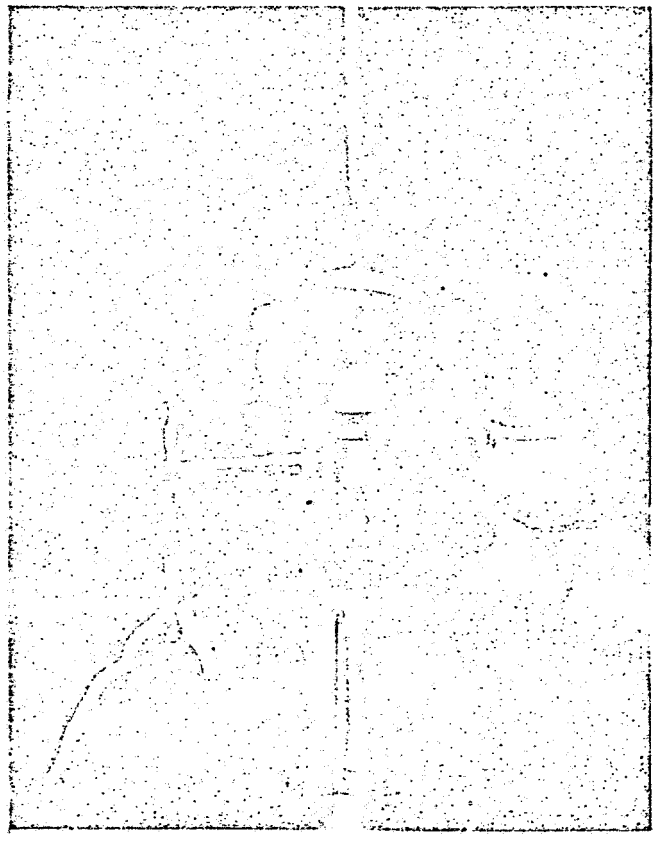

Figure 6. Test Fixture with Extensometer Installed, and 1/8" Thick Sample Prepared for RT Test

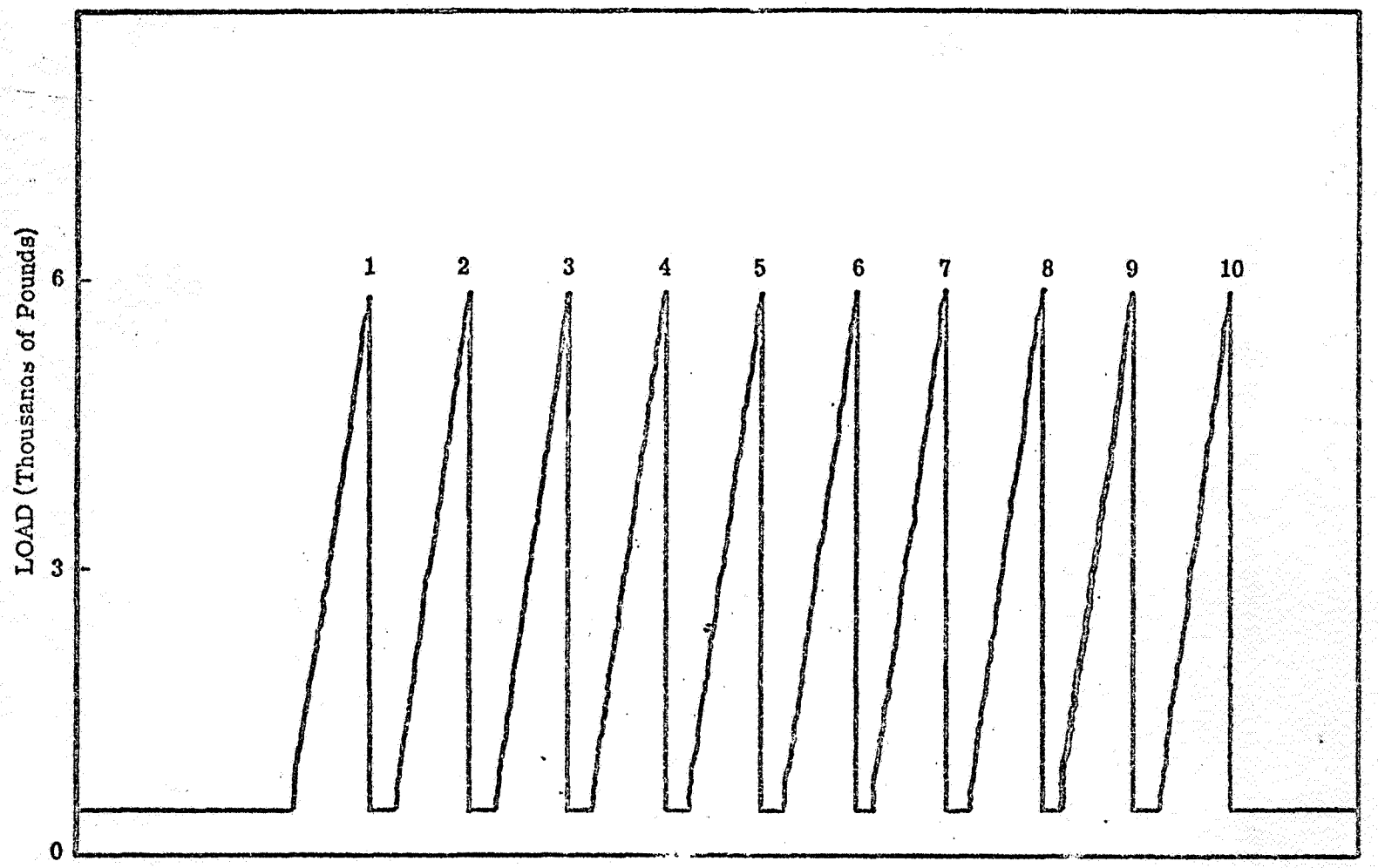

Figure 7. Instron Record of Stress-Strain, Teflon-40% Fiberglass at -320°F (0.090")

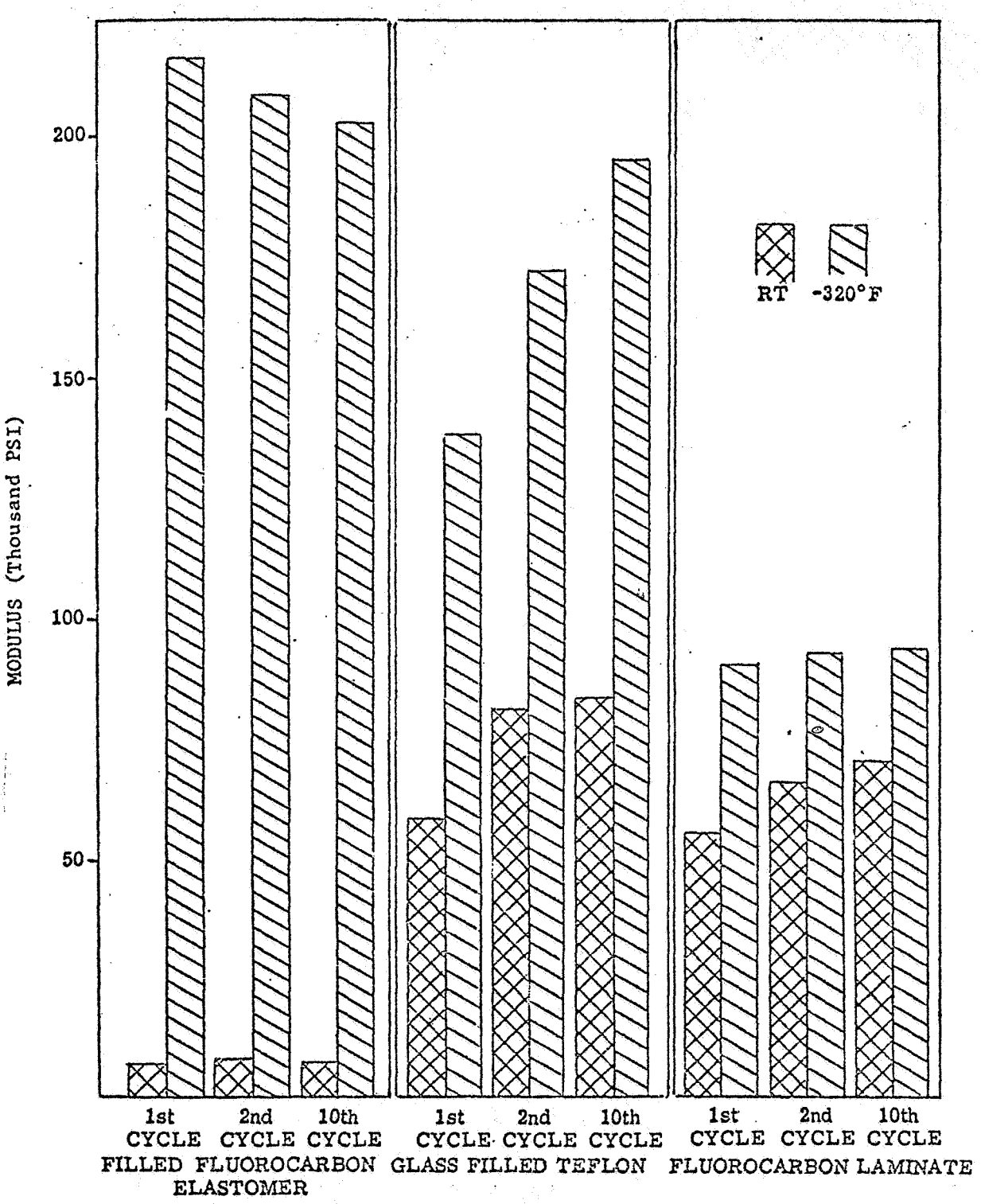

Figure 8. Comparative Compressive Moduli of Three Types of Fluorocarbon Composites Upon Cycling at RT and -320°F

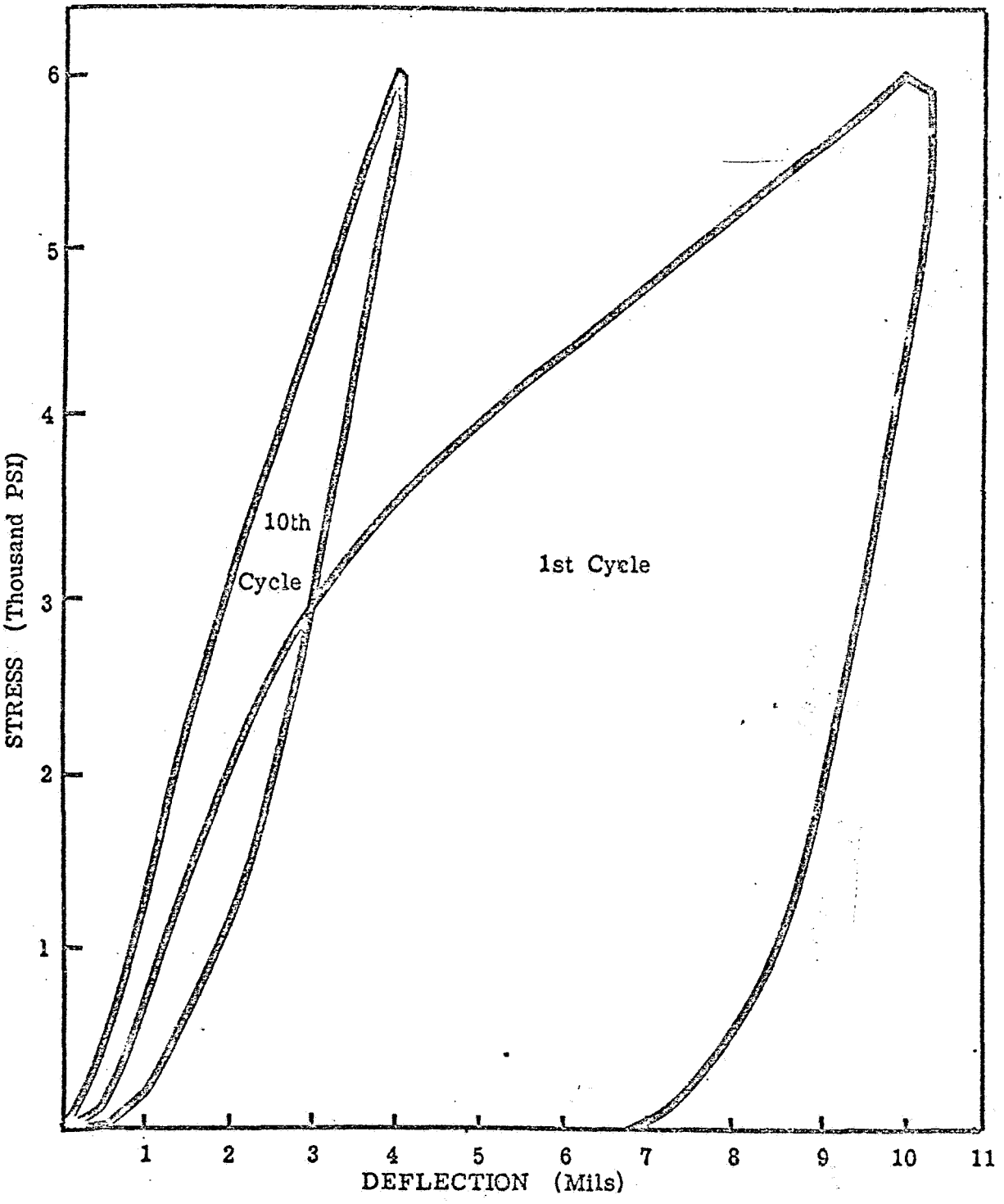

Figure 9. Compressive Hysteresis Curves for 25% Glass Filled Teflon at Room Temperature

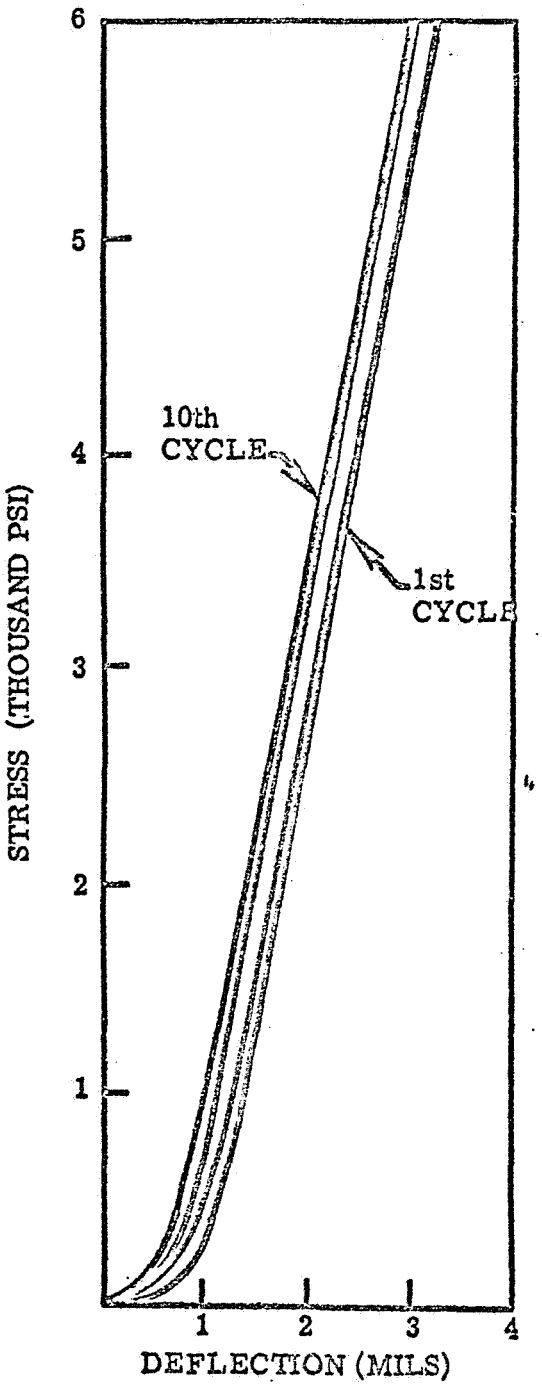

Figure 10. Compressive Hysteresis Curves for Teflon - 112 Glass Laminate at Room Temperature

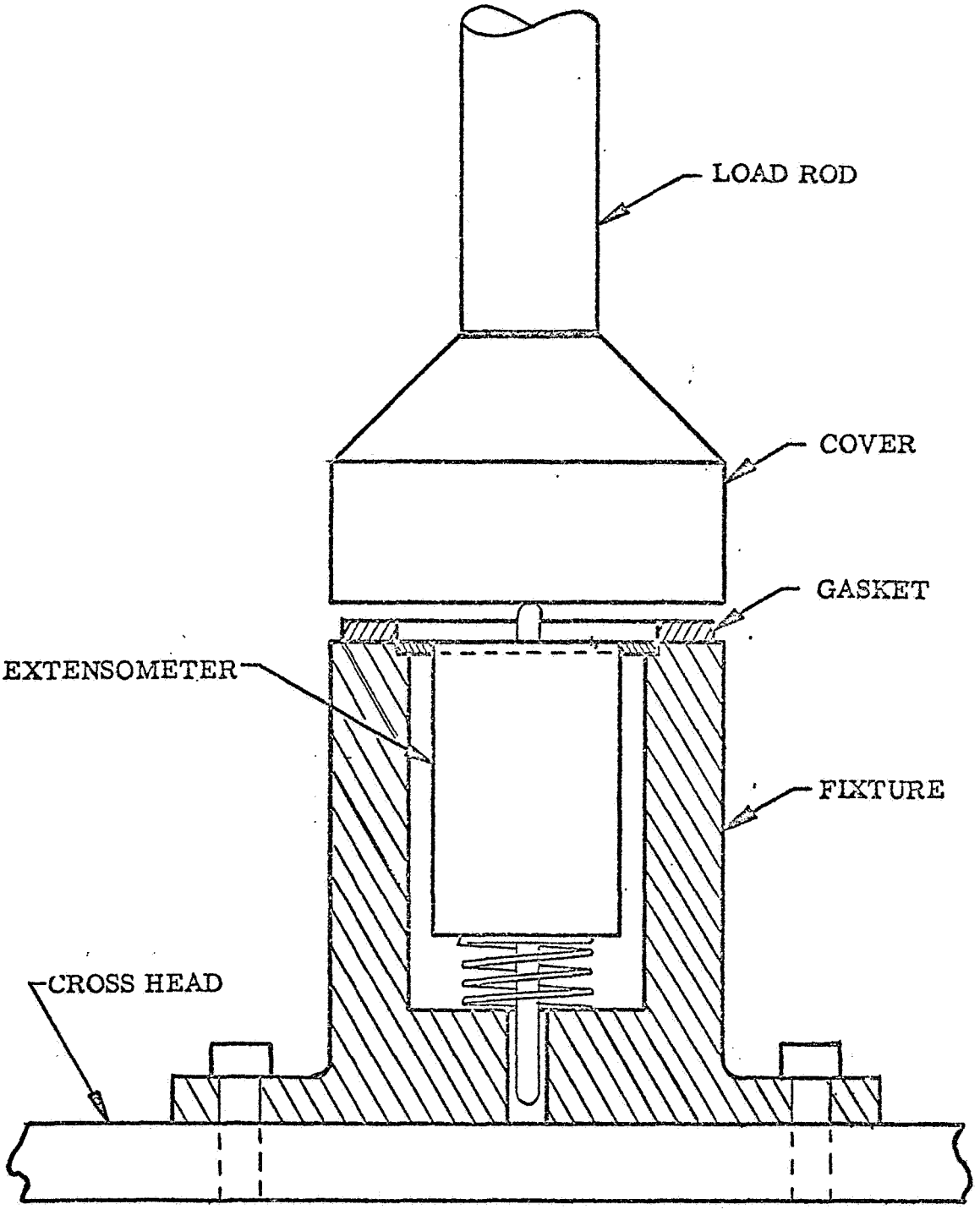

Figure 11. Compression vs. Deflection Test Fixture for 2.06 O.D. Gaskets

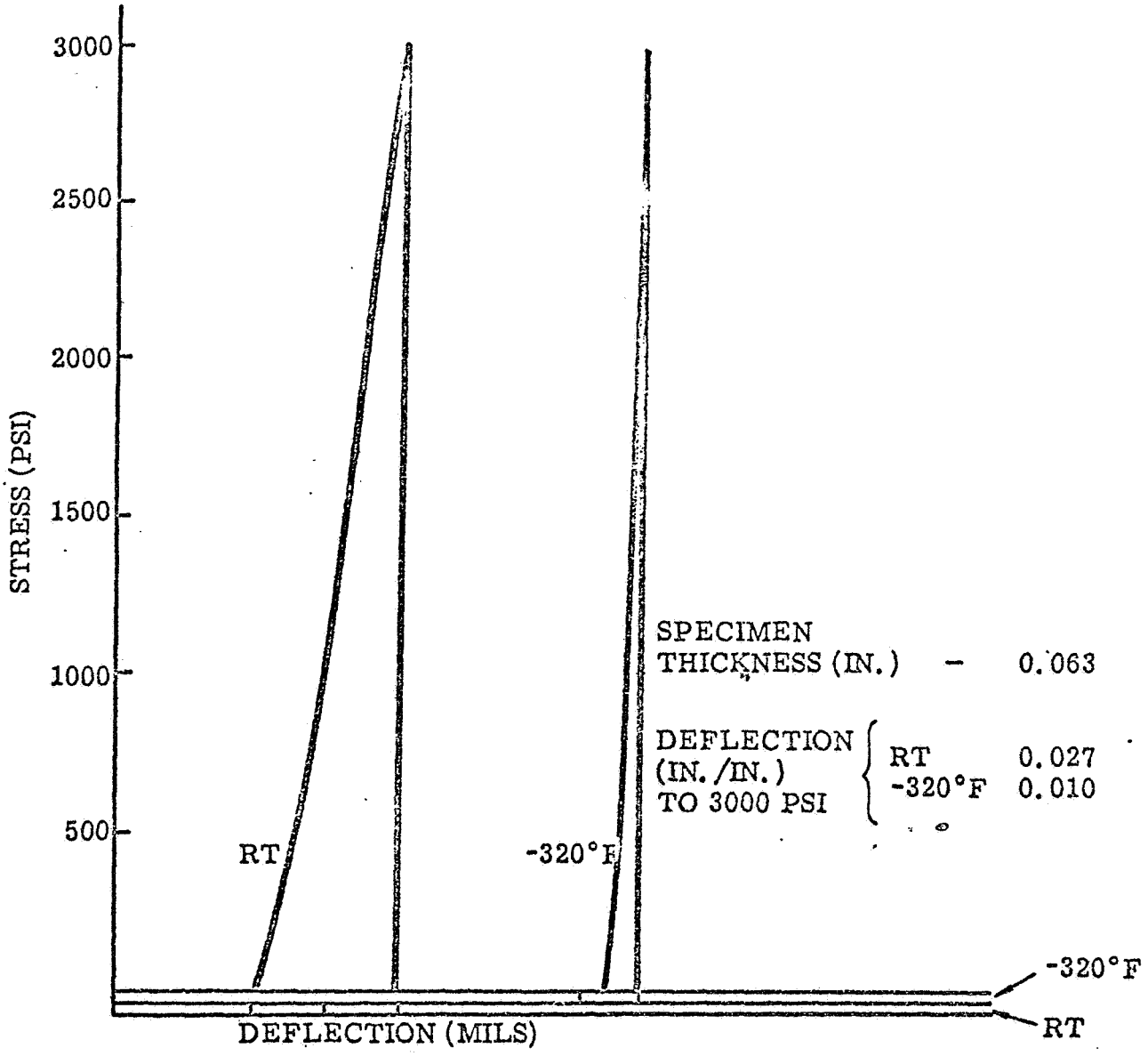

Figure 12. Stress-Strain Curves for Fluorolube Treated Asbestos-Rubber.

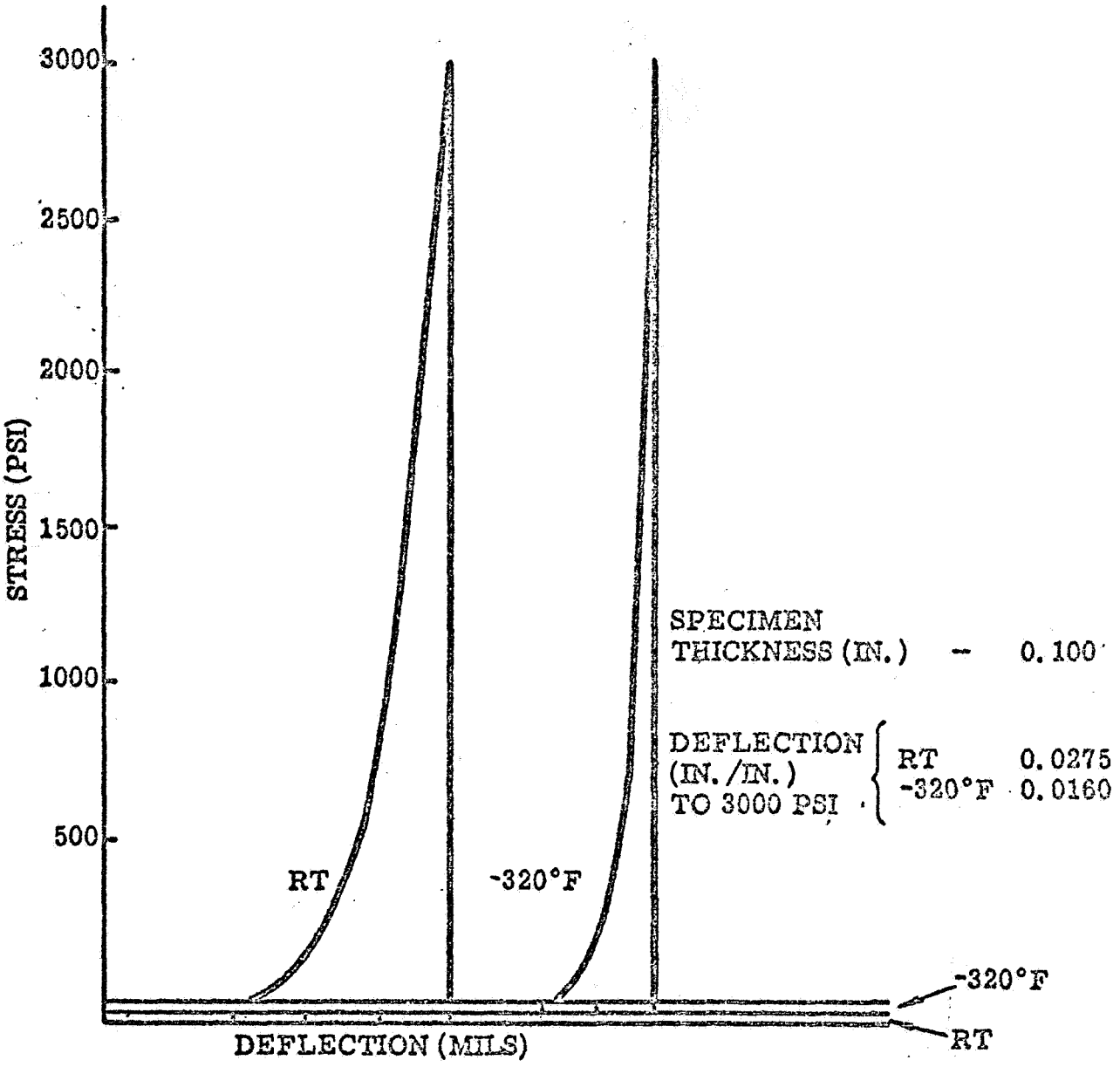

Figure 13. Stress-Strain Curves for Polytrifluoro-chloroethylene Glass Fabric Laminate

TABLE I

COMPRESSION-COMPRESSION SET ON GASKET MATERIALS

MATERIAL		COMPRESSIBILITY	COMPRESSION SET
Fluorocarbon Oil Impregnated Asbestos-Rubber		20%	12%
Glass Filled Teflon Gaskets	#1	47%	30%
	#2	52%	24%
	#3	34%	22%
Fiberglass-Teflon	40% Fiberglass	50%	40%
Unfilled Polyfluorocarbon		44%	30%
Encapsulated	#1	46%	34%
	#2	49%	38%
55% ZnO-Fluorocarbon Elastomer		46%	4%
Teflon-112 Glass Laminate		12%	2%

TABLE II

COMPRESSIVE MODULUS OF VARIOUS TYPES OF GASKETS

MATERIAL	RT MODULUS			-320°F		
	1st Cycle	2nd Cycle	10th Cycle	1st Cycle	2nd Cycle	10th Cycle
Filled Fluorocarbon Elastomers						
3% ZnO	10,000	10,000	10,000	167,000	163,000	163,000
Fiberglass Filled Teflon						
20%	57,600	68,900	71,400	143,000	175,000	173,000
30%	57,100	72,100	72,100	140,000	154,000	154,000
40%	61,300	83,000	87,000	140,000	151,000	150,000
Commercial #1	55,500	62,700	67,100	95,000	123,000	126,000
Commercial #2	51,500	60,800	66,000	132,000	136,000	130,000
Commercial #3	50,000	63,000	70,100	113,000	113,000	118,000
Fluorocarbon Oil Treated Asbestos Rubber	35,000	54,000	60,000	175,000	180,000	190,000
Laminate						
#1	52,100	63,900	67,700	87,600	89,600	93,300
#2	69,200	76,600	78,300	72,800	73,900	74,500

TABLE III

COMPRESSIVE MODULI OF LAMINATES

LAMINATE	RT MODULUS			-320°F MODULUS		
	1st Cycle	2nd Cycle	10th Cycle	1st Cycle	2nd Cycle	10th Cycle
Asbestos Paper and Teflon	52,100	63,900	67,700	87,600	89,600	93,900
112 Glass Fabric and Fluorocarbon Polymer	63,100	71,500	75,300	69,500	75,600	81,300
112 Glass Fabric and Teflon	69,500	77,000	79,100	78,900	78,900	84,000
112 Glass Fabric 50% Fluorocarbon Elastomer 50% Fluorocarbon Polymer	47,000	48,800	49,800	96,300	99,000	100,100
181 Glass Fabric Teflon	60,700	60,800	65,000	77,400	77,900	78,800

T A B L E IV

FLANGE DEFLECTION BEFORE LEAK

Material	Flange Deflection per unit thickness of Gasket	
	RT	-320°F
Filled Fluorocarbon Elastomer	>0.5	0.020
Unfilled Fluorocarbon Polymer	0.051	0.023
Teflon	0.064	0.026
Fluorocarbon Asbestos & Rubber	0.079	0.014
Encapsulated	0.035	0.021
Glass Filled Teflon #1	0.056	0.025
#2	0.064	0.018
#3	0.059	0.023
25% Fiberglass	0.068	0.022
Laminates		
Fluorocarbon Polymer-112 Glass	0.062	0.041
Teflon 112-Glass	0.041	0.034

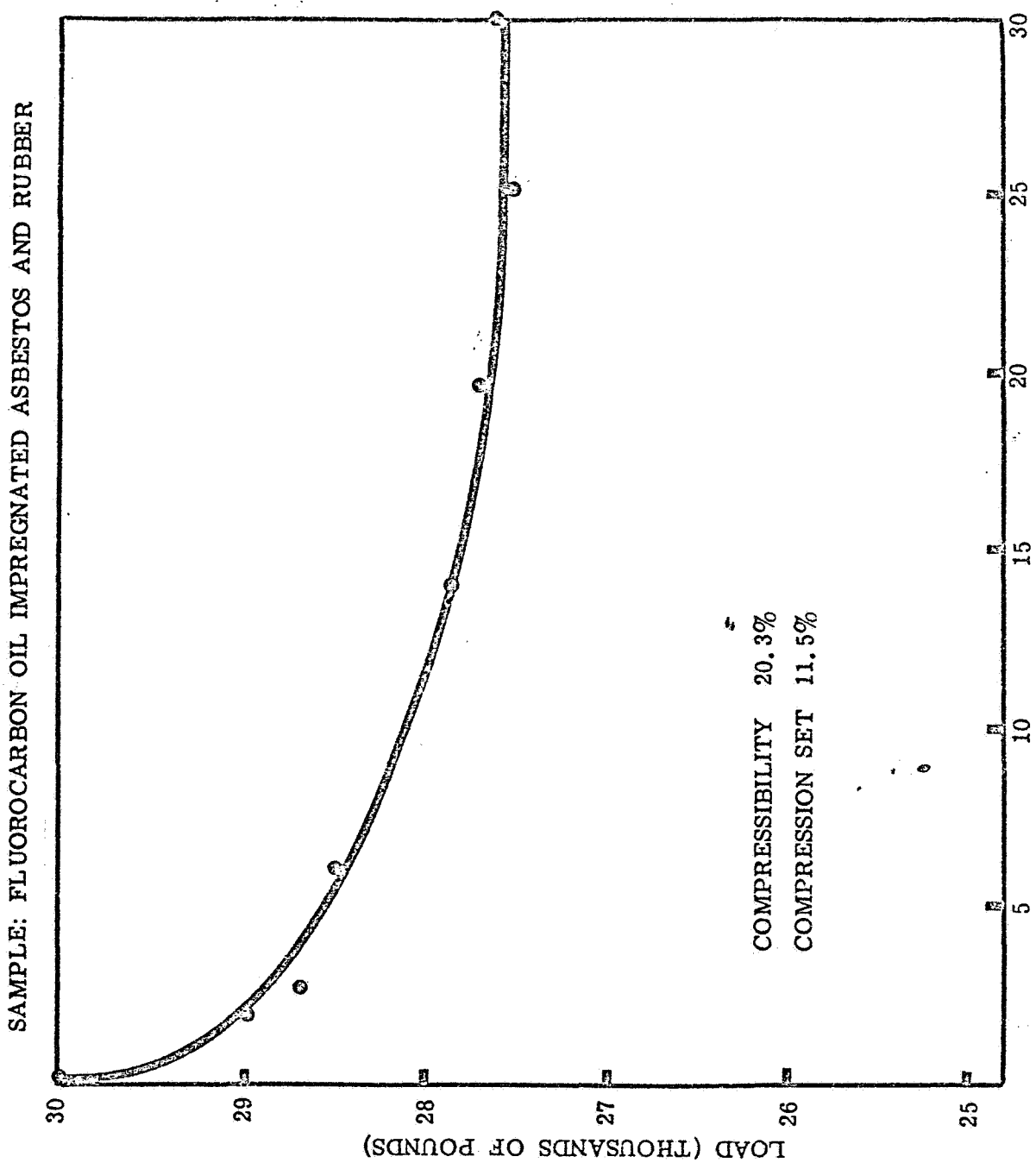

Figure 1. Load Decay Curve

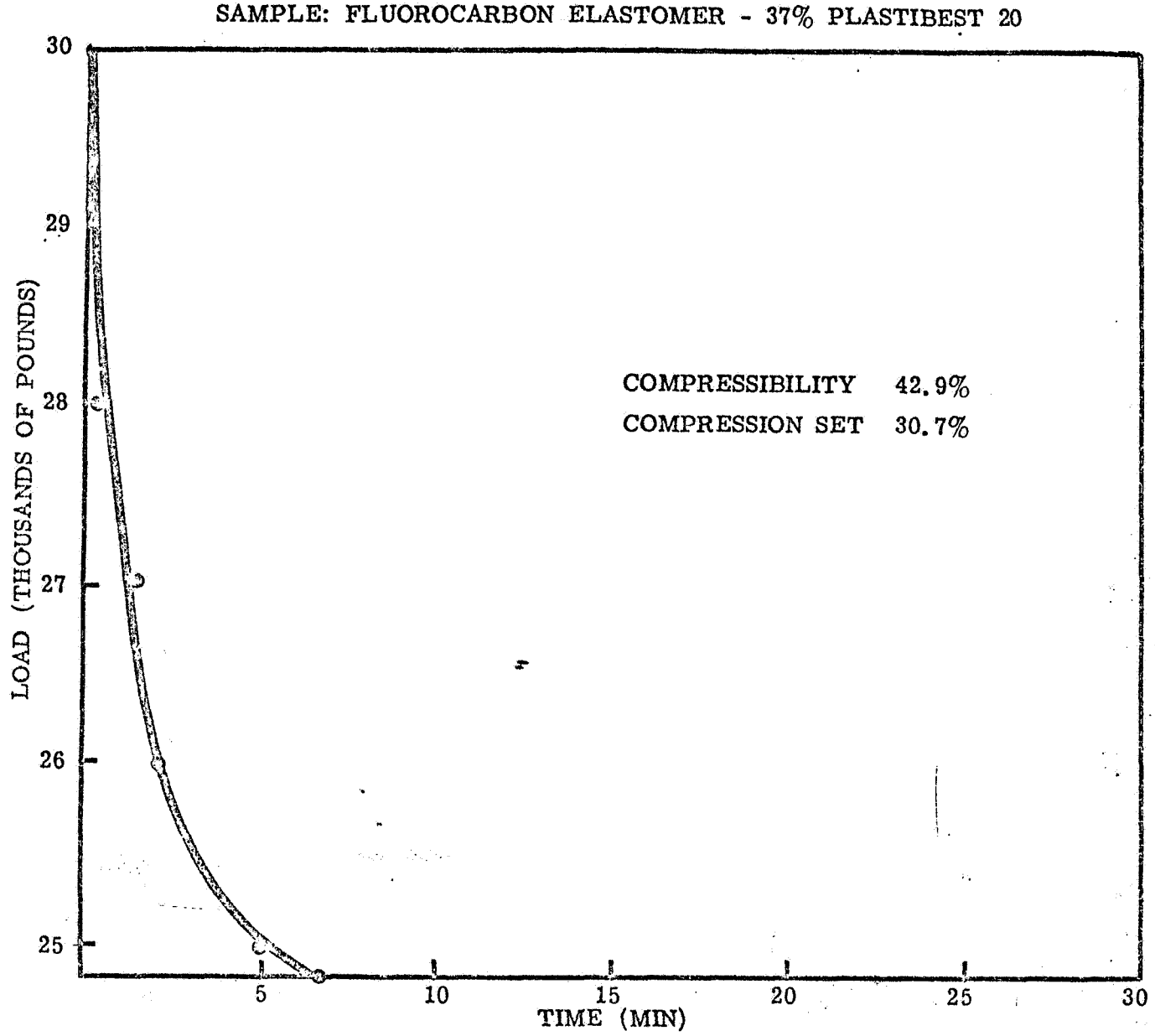

Figure 2. Load Decay Curve

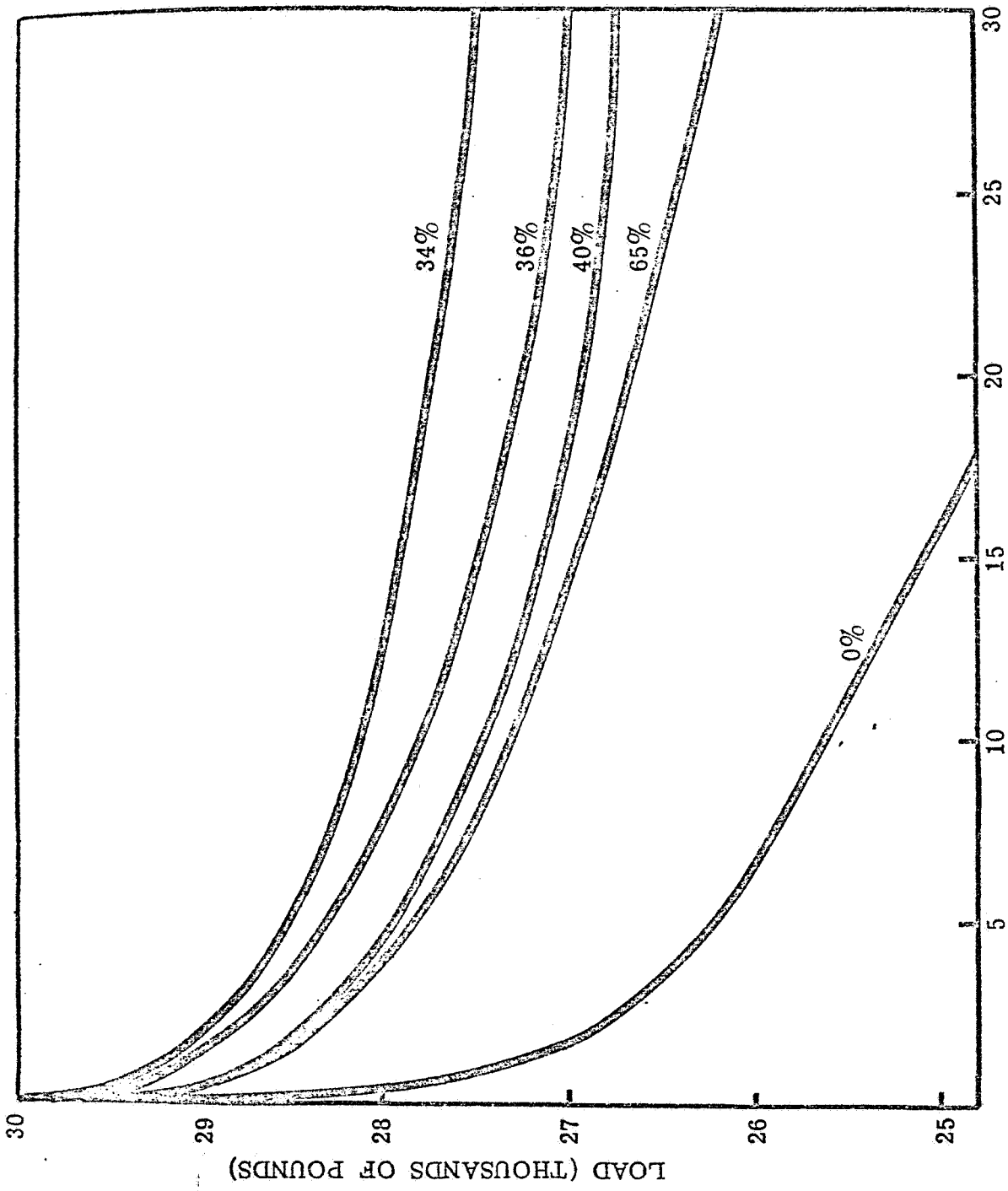

Figure 3. Family of Load Decay Curves - Zinc Oxide Filled Fluorocarbon Elastomer

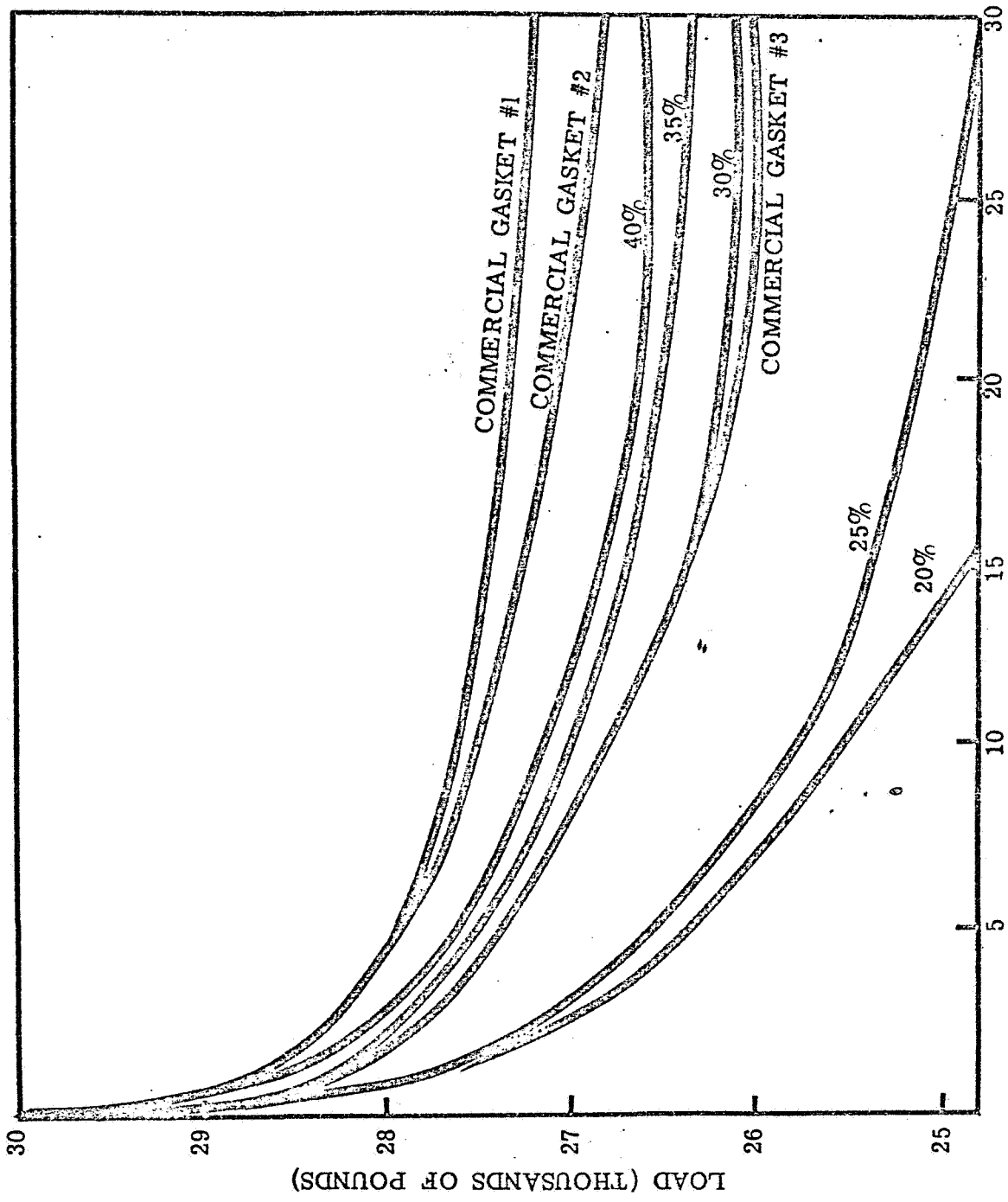

Figure 4. Family of Load Decay Curves for Various Filler Levels of Fiberglass-Teflon Gaskets

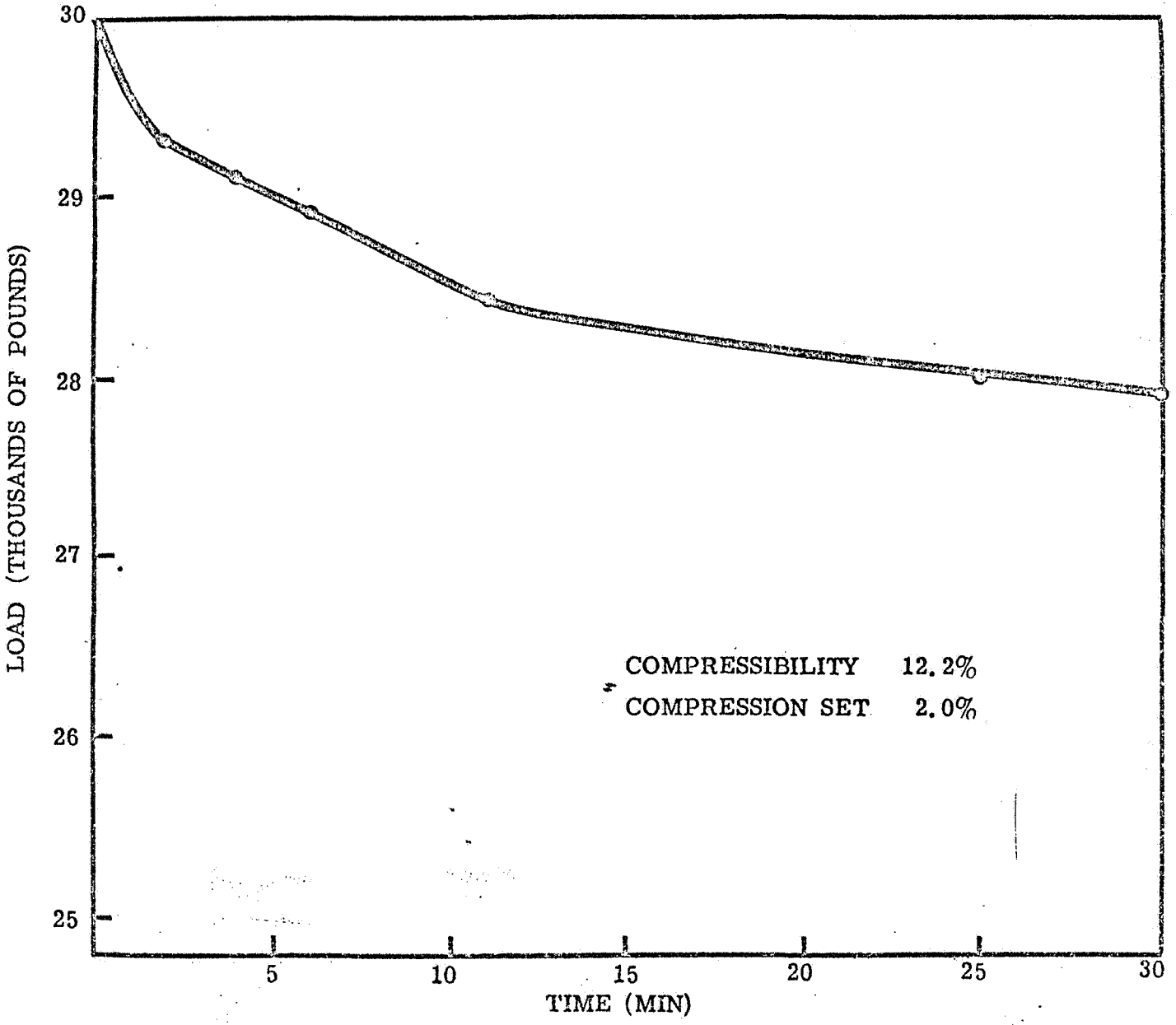

Figure 5. Load Decay Curve of Teflon and 112 Glass Fabric Laminate

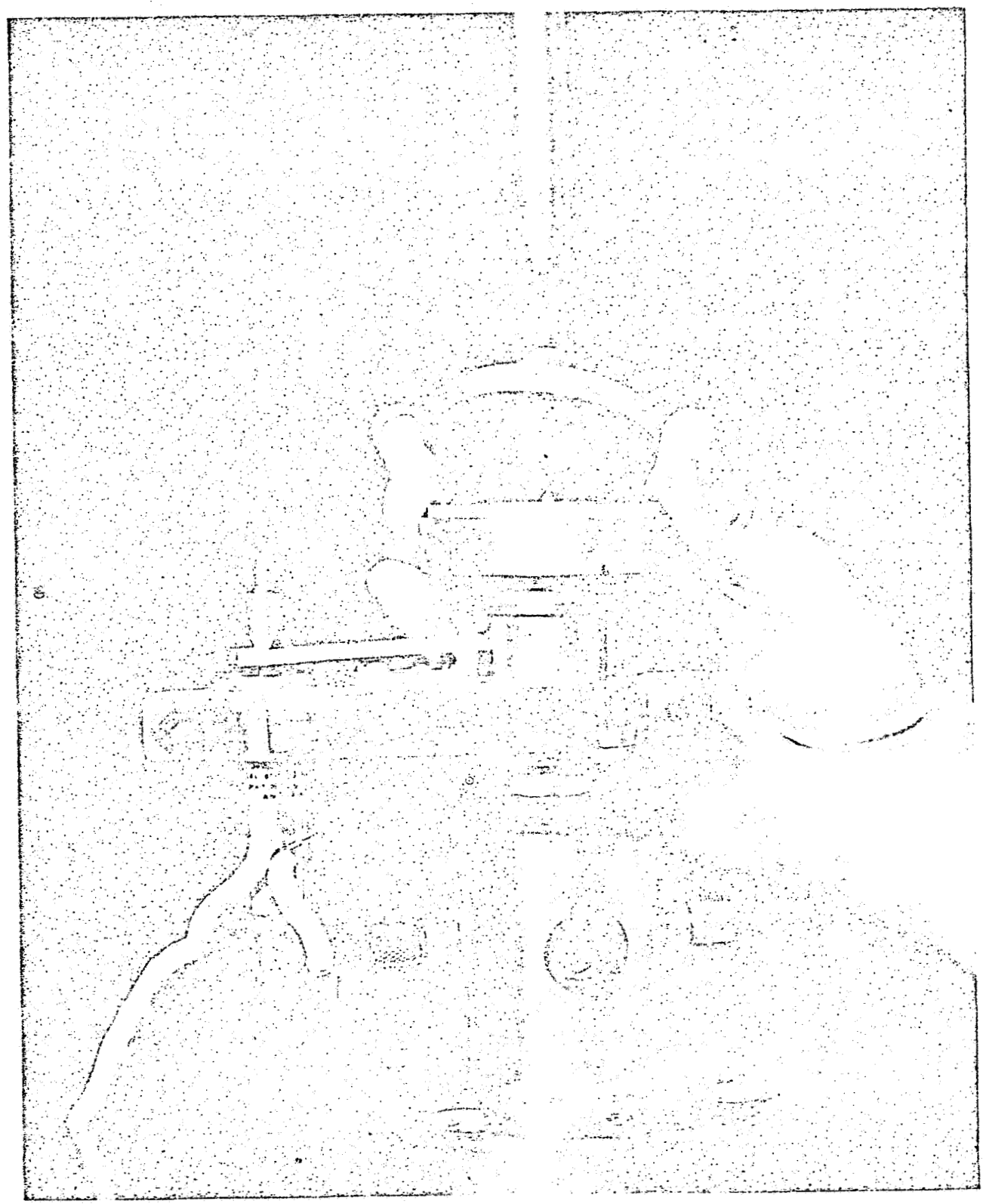

FIGURE 6.

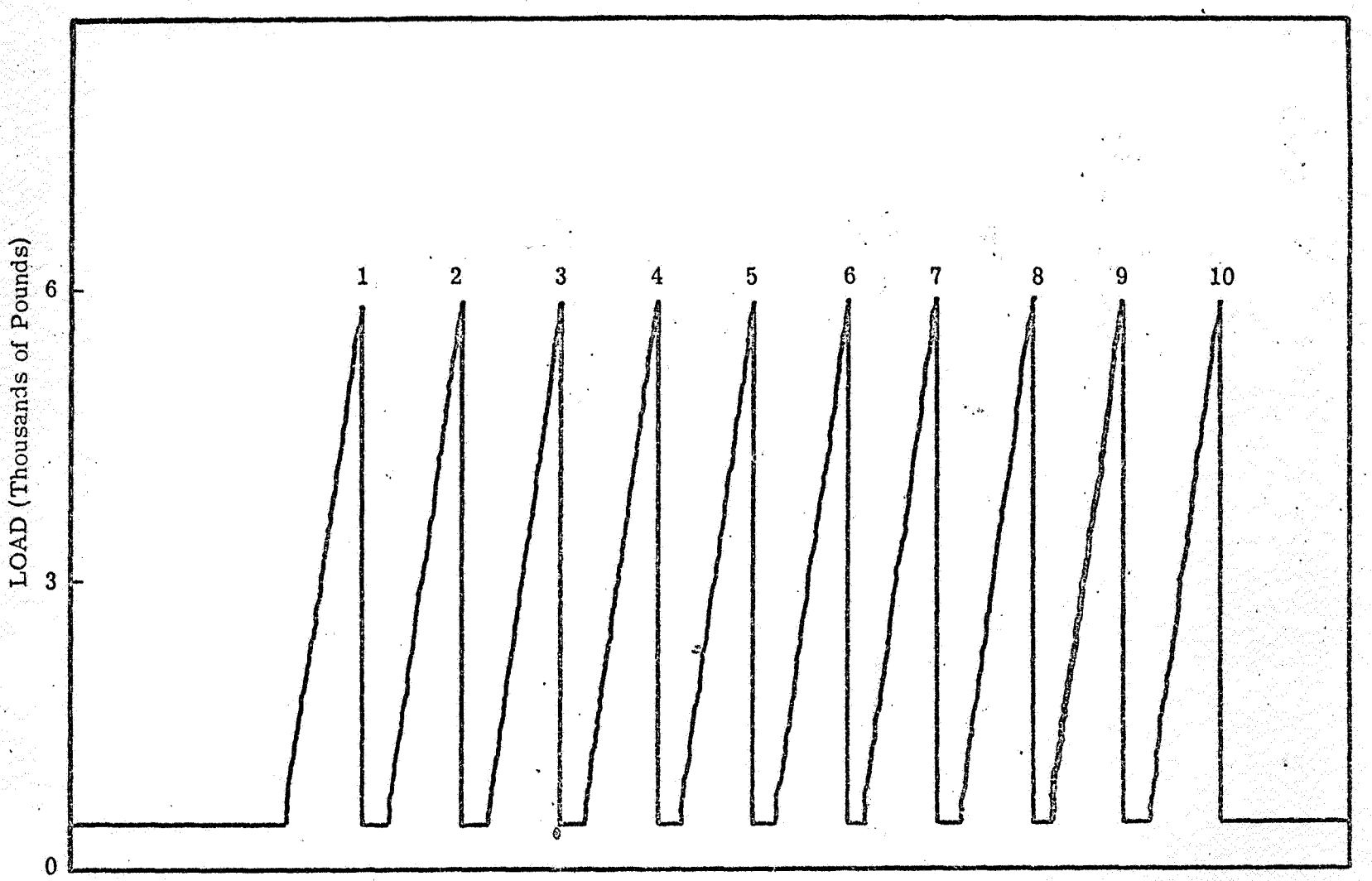

Figure 7. Instron Record of Stress-Strain, Teflon-40% Fiberglass at -320°F (0.090")

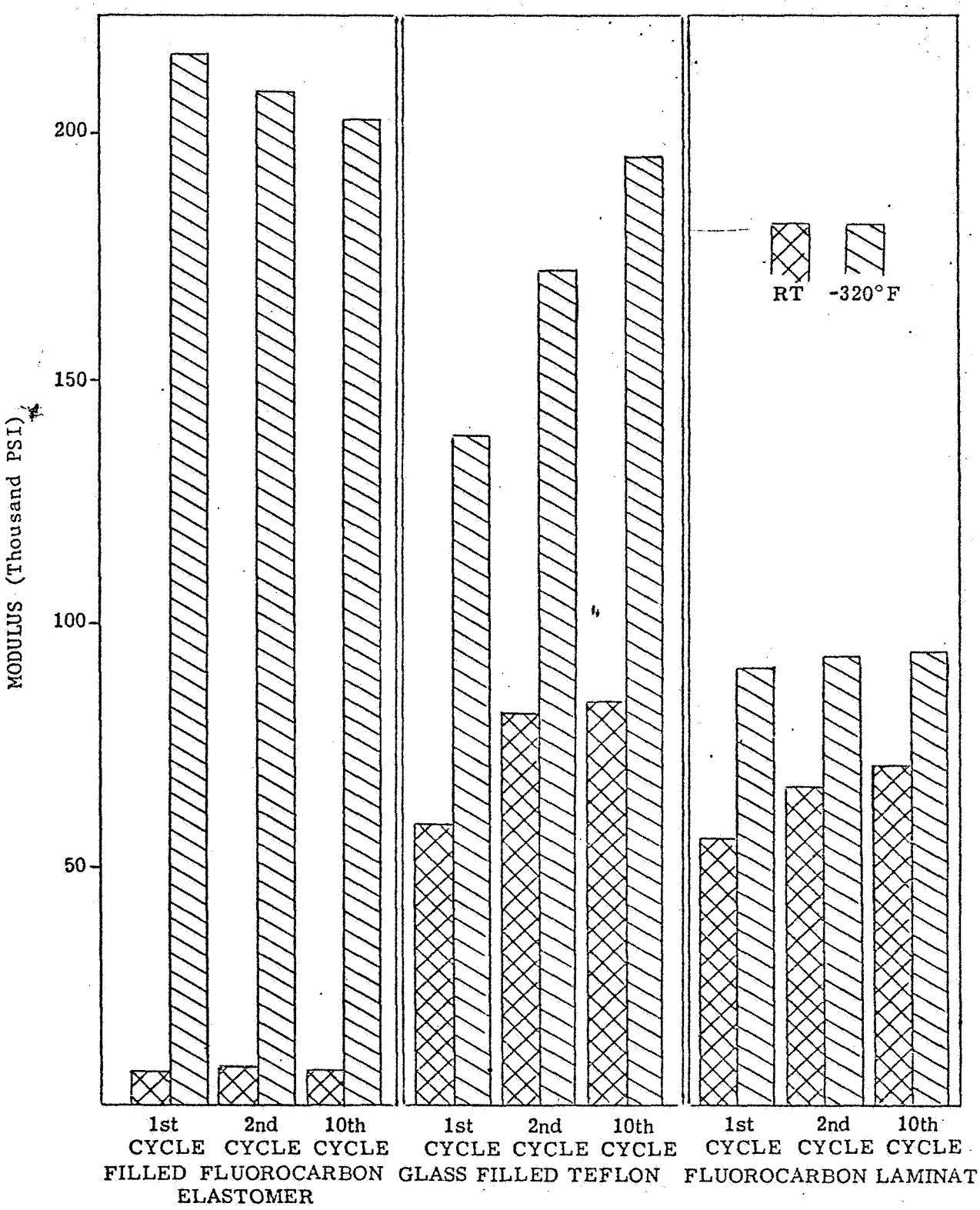

Figure 8. Comparative Compressive Moduli of Three Types of Fluorocarbon Composites Upon Cycling at RT and -320°F

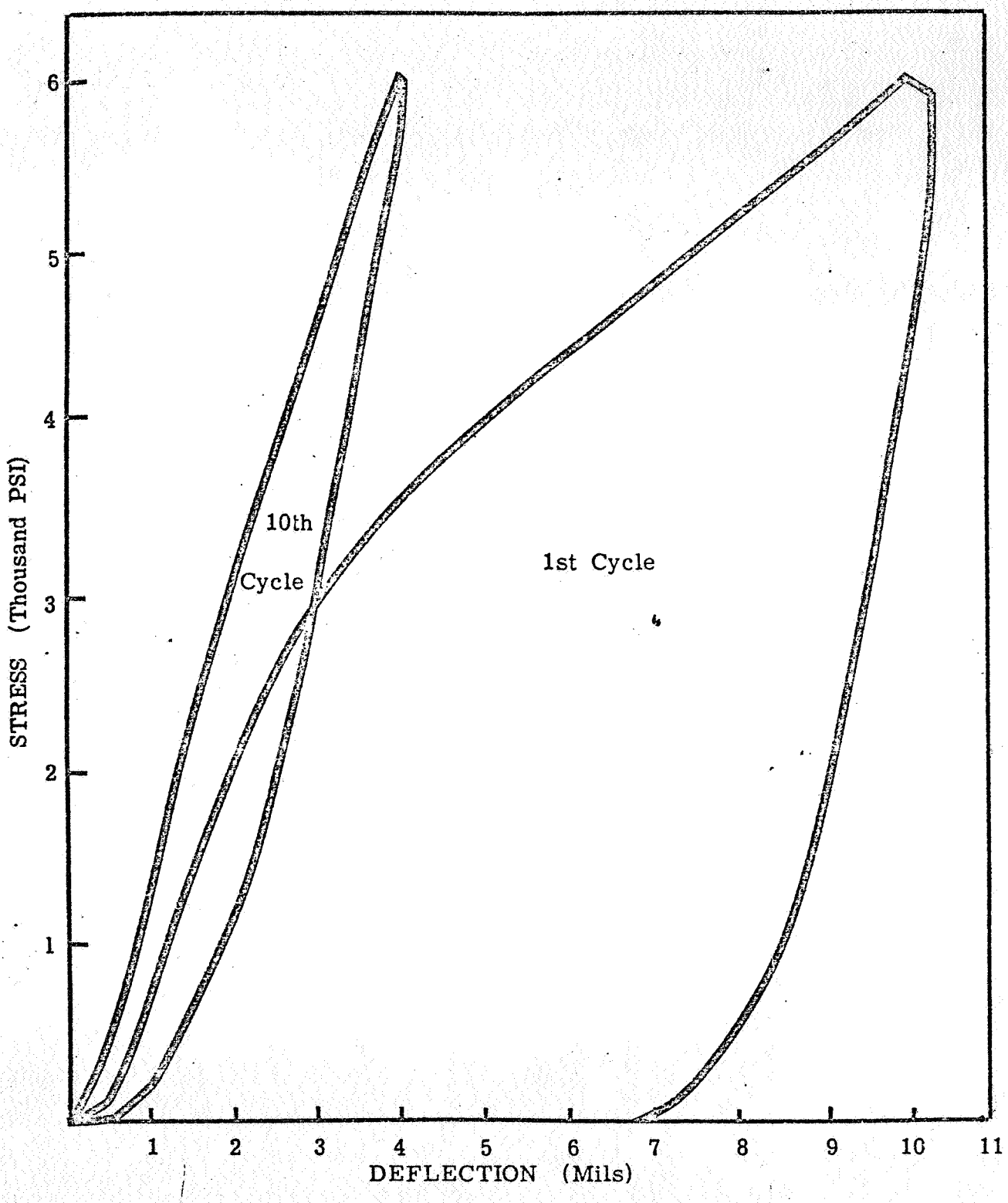

Figure 9. Compressive Hysteresis Curves for 25% Glass Filled Teflon at Room Temperature

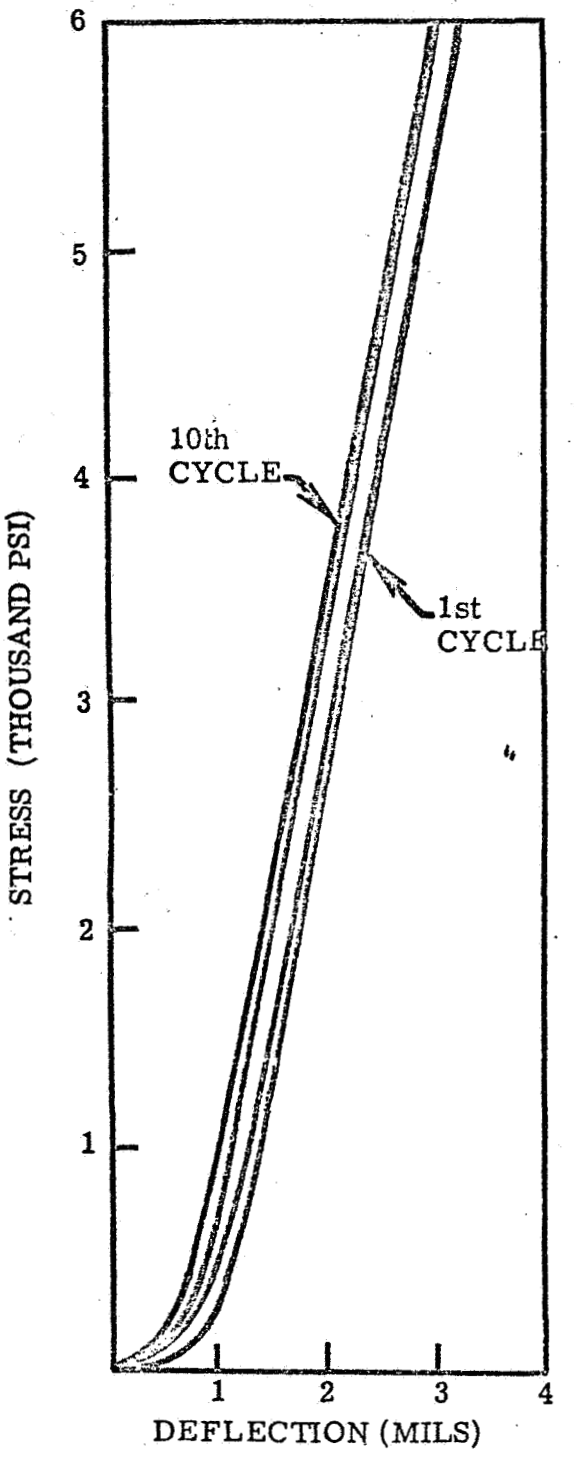

Figure 10. Compressive Hysteresis Curves for Teflon - 112 Glass Laminate at Room Temperature

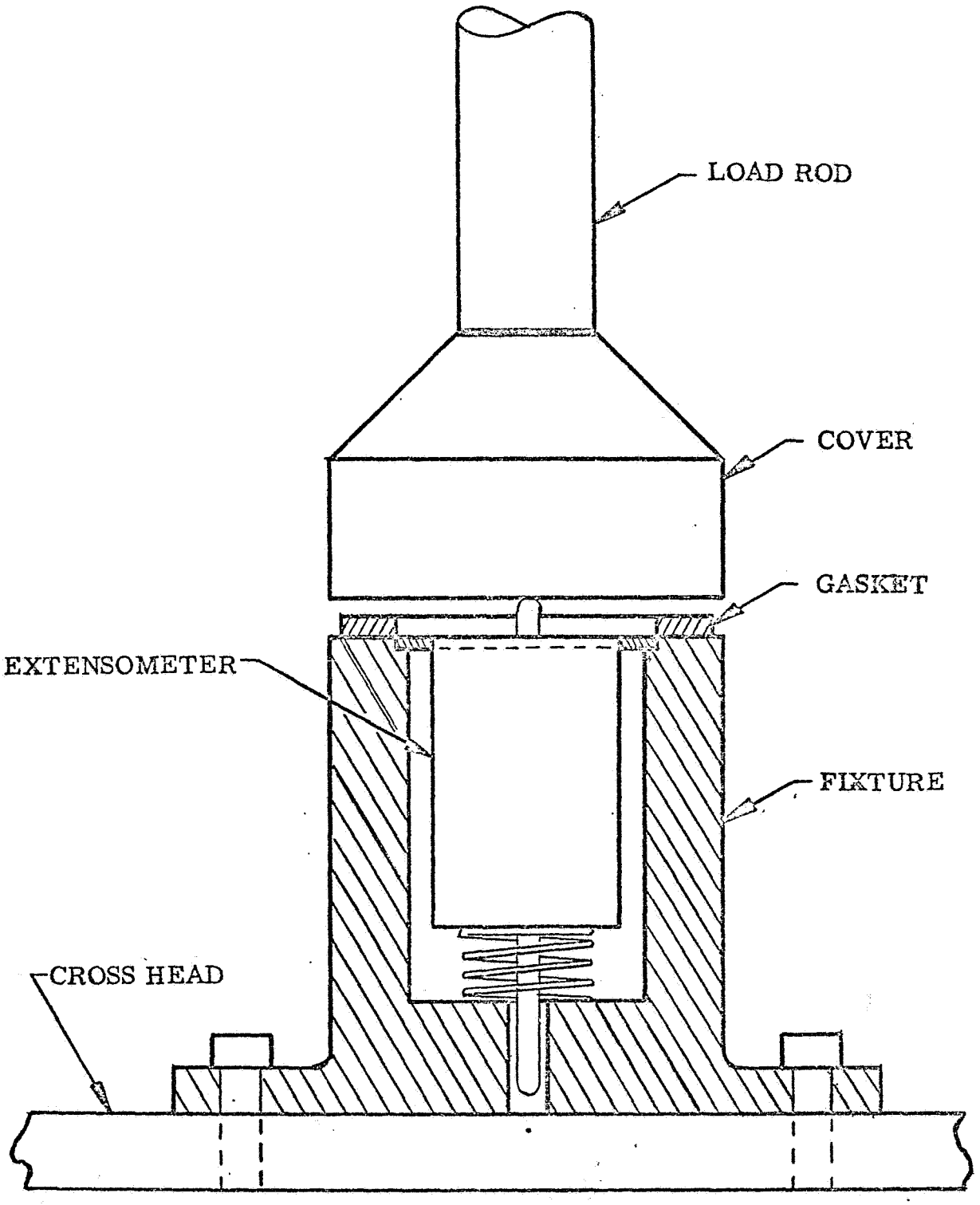

Figure 11. Compression vs. Deflection Test Fixture for 2.06 O.D. Gaskets

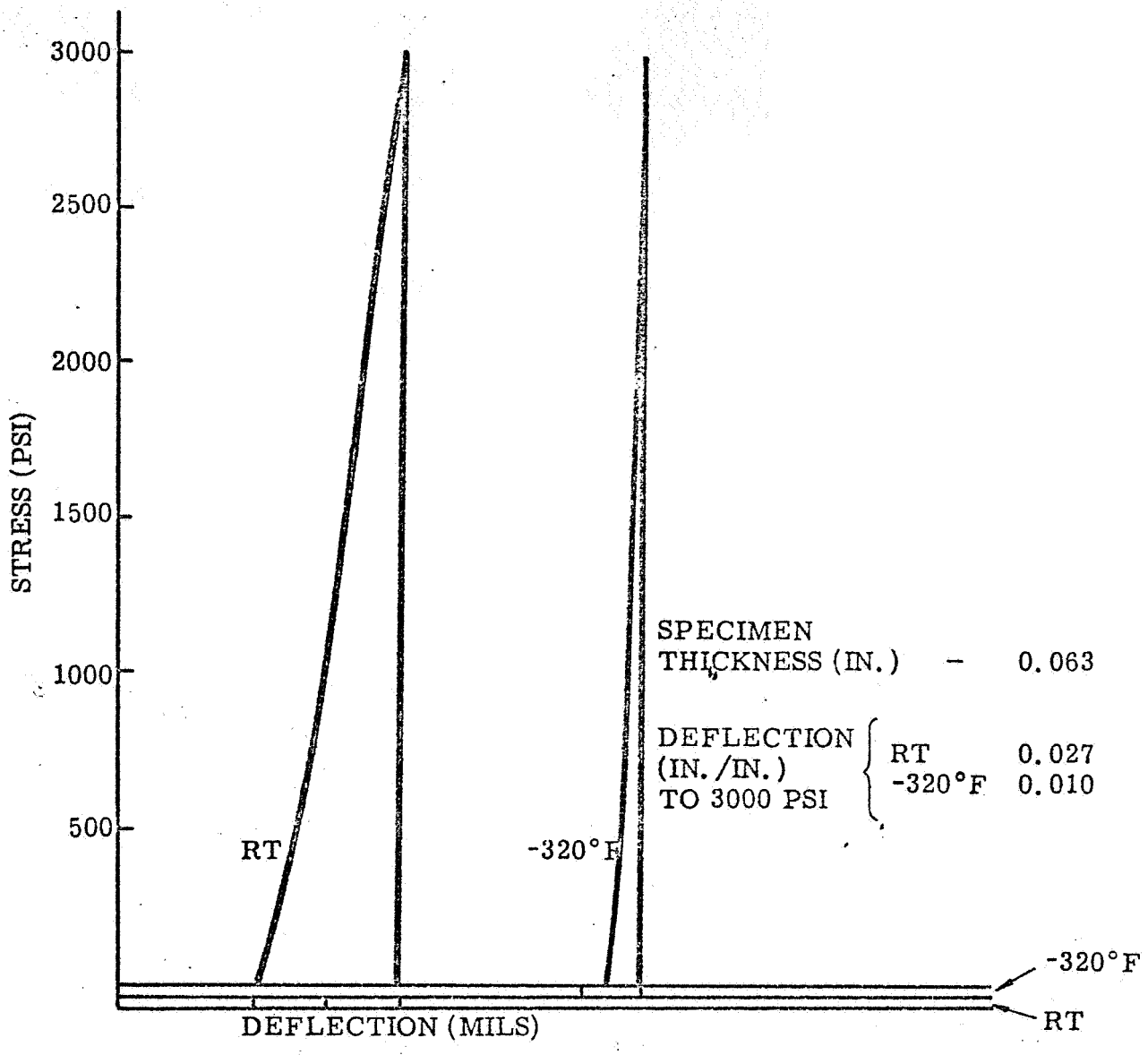

Figure 12. Stress-Strain Curves for Fluorolube Treated Asbestos-Rubber

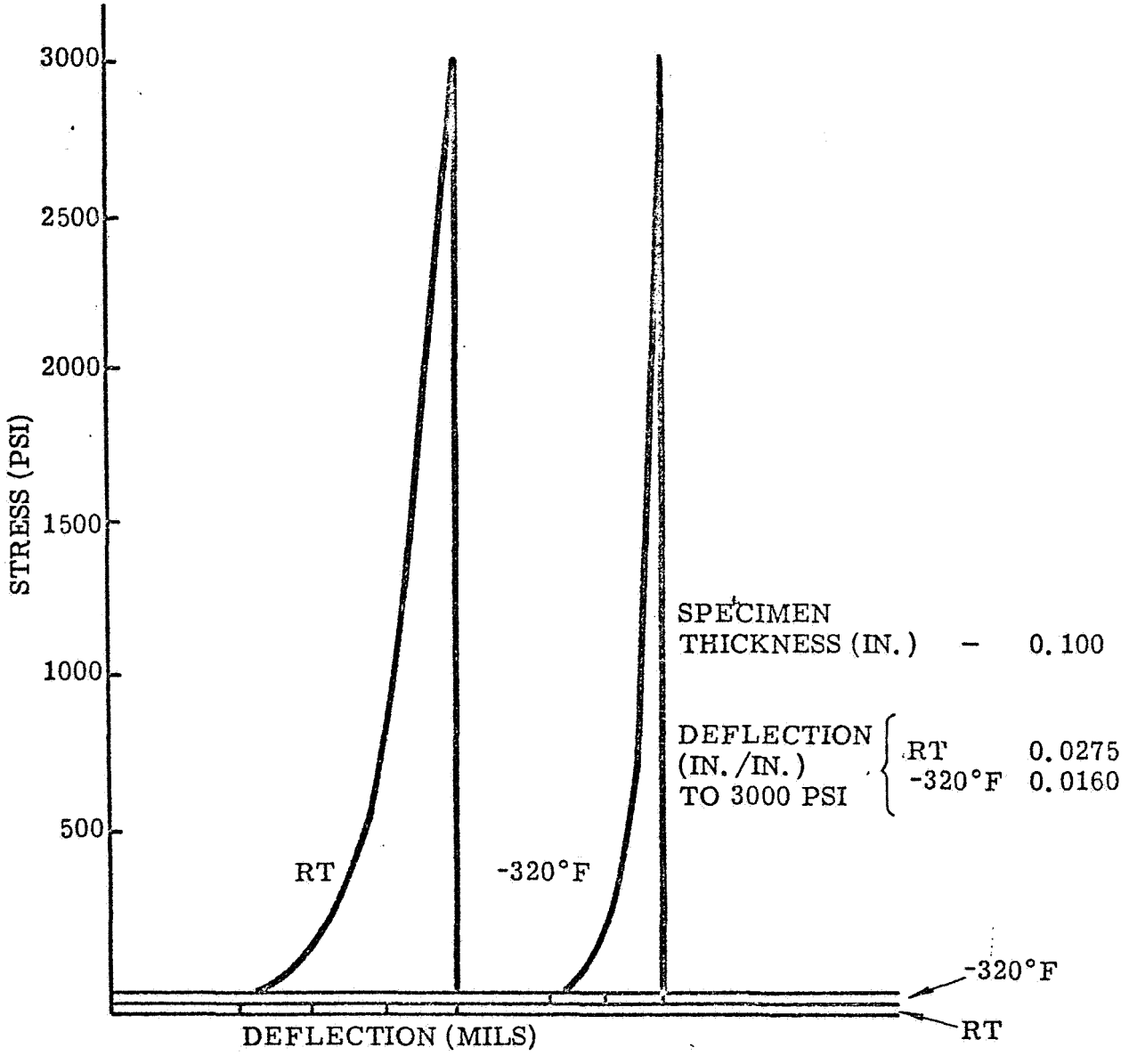

Figure 13. Stress-Strain Curves for Polytrifluoro-chloroethylene Glass Fabric Laminate

T A B L E I

COMPRESSION-COMPRESSION SET ON GASKET MATERIALS

MATERIAL		COMPRESSIBILITY	COMPRESSION SET
Fluorocarbon Oil Impregnated Asbestos-Rubber		20%	12%
Glass Filled Teflon Gaskets	#1	47%	30%
	#2	52%	24%
	#3	34%	22%
Fiberglass-Teflon	40% Fiberglass	50%	40%
Unfilled Polyfluorocarbon		44%	30%
Encapsulated	#1	46%	34%
	#2	49%	38%
65% ZnO-Fluorocarbon Elastomer		46%	4%
Teflon-112 Glass Laminate		12%	2%

TABLE II

COMPRESSIVE MODULUS OF VARIOUS TYPES OF GASKETS

MATERIAL	RT MODULUS			-320°F		
	1st Cycle	2nd Cycle	10th Cycle	1st Cycle	2nd Cycle	10th Cycle
Filled Fluorocarbon Elastomers						
3% ZnO	10,000	10,000	10,000	167,000	163,000	163,000
Fiberglass Filled Teflon						
20%	57,600	68,900	71,400	143,000	175,000	173,000
30%	57,100	72,100	72,100	140,000	154,000	154,000
40%	61,300	83,000	87,000	140,000	151,000	150,000
Commercial #1	55,500	62,700	67,100	95,000	123,000	126,000
Commercial #2	51,500	60,800	66,000	132,000	136,000	130,000
Commercial #3	50,000	63,000	70,100	113,000	113,000	118,000
Fluorocarbon Oil Treated Asbestos Rubber	35,000	54,000	60,000	175,000	180,000	190,000
Laminate						
#1	52,100	63,900	67,700	87,600	89,600	93,300
#2	69,200	76,600	78,300	72,800	73,900	74,500

T A B L E III

COMPRESSIVE MODULI OF LAMINATES

LAMINATE	RT MODULUS			-320°F MODULUS		
	1st Cycle	2nd Cycle	10th Cycle	1st Cycle	2nd Cycle	10th Cycle
Asbestos Paper and Teflon	52,100	63,900	67,700	87,600	89,600	93,900
112 Glass Fabric and Fluorocarbon Polymer	63,100	71,500	75,300	69,500	75,600	81,300
112 Glass Fabric and Teflon	69,500	77,000	79,100	78,900	78,900	84,000
112 Glass Fabric 50% Fluorocarbon Elastomer 50% Fluorocarbon Polymer	47,000	48,800	49,800	96,300	99,000	100,100
181 Glass Fabric Teflon	60,700	60,800	65,000	77,400	77,900	78,800

T A B L E IV

FLANGE DEFLECTION BEFORE LEAK

Material	Flange Deflection per unit thickness of Gasket	
	RT	-320°F
Filled Fluorocarbon Elastomer	>0.5	0.020
Unfilled Fluorocarbon Polymer	0.051	0.023
Teflon	0.064	0.026
Fluorocarbon Asbestos & Rubber	0.079	0.014
Encapsulated	0.035	0.021
Glass Filled Teflon #1	0.056	0.025
#2	0.064	0.018
#3	0.059	0.023
25% Fiberglass	0.068	0.022
Laminates		
Fluorocarbon Polymer-112 Glass	0.062	0.041
Teflon 112-Glass	0.041	0.034

Question: In the experiment where you used teflon in the glass laminate and you backed off the flange to see how far you could go before leakage occurred, what levels of leakage did you have before the flange was backed off, and how much after the leakage started? Were you talking about the levels of leakage that we generally speak of when discussing fluid seals?

Answer: Possibly not. We did not use a mass spectrometer to detect low rates of leakage, and we could observe no pressure drop. When a leak did occur, it was catostrophic.

Comment: I asked this because we leak-checked some of the glass impregnated teflon and found that under no stress level at a one atmosphere pressure differential were we able to get the leakage below 10^{-3} atm cc/sec.

Reply: I suspect that this is a matter of lateral penetration; Mr. Wilson will discuss this in the next paper.

Question: How do you define compressibility as used in your tables? What was the degree of wetting for the tests shown in the bar braph?

Answer: The degree of wetting was approximately 30% content by weight. Compressibility is simply the compression under load as measured in comparison with no load.

Question: IIT has been doing quite a bit of work with composite materials, primarily metallic fibers impregnated with teflon, nylon, and other soft filler materials. I have noticed two time related relationships: the stress-strain relationship that exhibits a definite time dependency, and the rate of recovery.

Question: (contd)

This material impregnated with teflon, for example, does not appear to recover immediately, but after one or two hours or days, it will come back to the original dimensions. What is your rate of load application, and when do you measure the recovery?

Answer: Composites are much like a pure teflon gasket that will flow under stress. We have looked at composites of metallic systems, but in a metallic system, like a metal fabric, you obtain complete wetting and have no void content to act like a spring. The material can only flow, and of course, this is strictly time dependent. It is a function of the binder and the spring-like nature of the reinforcement that permits the gasket to flow back (partically at least) to where it was before the load was released. Our loading rate was about 100 psi per minute, possibly a little faster.

Question: Did you consider the permeability of your materials in getting the true results from your tests?

Answer: This is discussed in the following paper.

N67-86151

THE DEVELOPMENT OF A NEW CRYOGENIC GASKET FOR LIQUID OXYGEN SERVICE PART II

by

Frank M. Wilson
Jay W. Feldmann
Charles R. Thompson

NARMCO RESEARCH & DEVELOPMENT
A Division of Telecomputing Corporation

This program was sponsored by the George C. Marshall Space Flight Center, National Aeronautics and Space Administration.

THE DEVELOPMENT OF A NEW CRYOGENIC GASKET FOR LIQUID OXYGEN SERVICE

The dual requirements of cryogenic application and LOX compatibility reduced the field of possible gasket materials to one: fluorocarbon polymers. The material that has been most attractive and has been used most often in the program is DuPont Chemical's Teflon. However, this material undergoes creep (deflection with time under a load), which is undesirable for a gasket. This phenomenon has been best controlled by fabricating gaskets from laminates composed of alternate layers of resin and reinforcement material. The effectiveness of the reinforcement in restricting creep has been demonstrated by stress relaxation tests. These tests, performed at ambient temperature, measured the reduction in compressive load with time for the solid resin and for a glass reinforced laminate (see Figure 1). Figure 1 indicates that the reinforced laminate exhibited less relaxation. In addition, the small amount of relaxation it did experience occurred within the first 30 minutes, while the solid resin specimen was still relaxing when the test was terminated (after 2 hours). Creep rate is less at lowered temperatures but still is present (Reference 1, Figures 6 and 7, p. 9). The results of this investigation are that the laminate construction is preferred for the gasket application because it induces a lower amount of bolt load dropoff than the solid resin does. Reference 2 (p. 4) states that a laminated gasket design shows "promise" for cryogenic applications.

There are two types of Teflon resins: tetrafluoroethylene, commonly called TFE, and fluorinated ethylene-propylene, referred to as FEP. Besides the difference in appearance (TFE is opaque, while FEP is transparent), many of the properties of these materials are dissimilar. One of the most important properties for the gasket application is the modulus of elasticity, since good compressibility is quite desirable. (These are inversely related; i.e., the higher the modulus, the lower the compressibility.) FEP possesses a higher modulus than TFE (Reference 1, Figures 1, 2, and 3, pp. 6 and 7), making it less desirable from a compressibility standpoint. The compressive moduli of both greatly increases with decreasing temperatures, as shown in Figure 2 (Reference 3, Figure 82, p. 145).

Another important difference between TFE and FEP greatly affects fabrication of laminates. FEP is a true thermoplastic and melts. This results in relatively easy lamination of FEP and the substrate (the reinforcement material). As FEP

Preceding page blank

melts, it wets the glass fiber to form a relatively strong bond, whereas the TFE forms only a mechanical interlock. Optimum lamination conditions with FEP have been experimentally determined to be 525°F, 100 psi, and 15 minutes. TFE, however, does not melt: at 621°F, it undergoes transition into a gel state, but will never melt regardless of temperature or pressure. Therefore, the lamination technique that has been developed involves a relatively high lamination pressure, which serves to drive the substrate into the soft resin. The optimum lamination values for TFE have been found to be 800°F, 500 psi, and 30 minutes. The mechanical bond thus obtained is quite strong, although not as good as that obtainable with the FEP laminates.

Figures 3 and 4 (microphotographs of TFE and FEP laminates) show that the FEP has melted and has been absorbed in part by the glass substrate, while this has not occurred with TFE. Besides the superior compressibility of TFE resin, TFE glass laminates are also more compressible than FEP laminates because the TFE does not melt and the glass substrate remains completely dry. Therefore, more of the mechanical compressibility of the glass fabric is retained. One of the major advantages of the glass reinforced laminate design is that the mechanical compressibility of the glass fabric is relatively unaffected by temperature. Hence, these laminates have performed very well at the cryogenic condition.

Laminates must be cooled under pressure to 400°F to prevent warping. At 400°F, they are quick-quenched in water. In addition to speeding up the fabrication time, this rapid cooling of TFE laminates has the advantage of resulting in a lower percentage of crystallinity in the TFE. The lower the crystallinity, the lower will be the modulus and the higher the compressibility. In addition, the percent recovery and flex life are higher with lowered crystallinity (Reference 1).

Various candidate constructions were compared on the basis of compressibility and compression set. The test devised for these comparisons (called the load vs. deflection test) consists of preloading a specimen to 1500-psi flange pressure at room temperature, cooling to 76°K with liquid nitrogen, then varying the flange pressure from 0 to 3000 psi for 10 cycles. An extensometer measures the gasket deflection. An x-y plotter records on tape the load vs. deflection data (see Figure 5 for a typical set of curves).

Since the load can easily be converted to stress and the deflection to strain, the load vs. deflection curves also represent stress-strain curves. As such, the slope of the curve should be the compressive modulus. However, due to the nonlinearity of the curves, there is no single slope for a particular cycle. This did not allow the modulus determination in this classic manner. Nevertheless, it was reasoned that the area under the curves, representing the amount of energy absorbed, could be just as useful a standard of comparison. Therefore, these areas were measured and energy absorption figures calculated for the first, second, and tenth cycles to determine the effects of short- and long-time cycling. Candidates showing higher energy absorption values with minimum fall-off with cycling were judged superior in compressibility.

Different substrates have been considered for reinforcement in the laminate: glass fabrics, knit glass, a few metals in various shapes, and spirally wound glass. Because it has performed so well, most of the investigation has been with glass fabrics.

Various weaves of fabric were considered and tested. Although the fabric weave does not appear to greatly influence the characteristics of the laminate, the weave called crowfoot satin has yielded the most compressible laminates; consequently, its use was indicated. As mentioned earlier, the lower modulus of TFE made it preferred to FEP as the resin. Testing was performed to determine the optimum thicknesses of the resin and glass plies; a resin thickness of about 0.005-in. TFE film and about 0.010-in. thick crowfoot satin glass fabric have been determined to be the best combination. The fabrication technique involves the rotation of successive layers of fabric, producing a multiaxial laminate (see Figure 6). Such rotation, in addition to strengthening the laminate, also improves the compressibility properties. The compressibilities of the optimum construction and of a less than optimum glass reinforced laminate are shown in Figure 7, where the energy absorption, which is a measure of compressibility, is plotted for one, two, and ten load cycles.

The knit glass performed poorly because it lost most of its mechanical compressibility in the lamination process. Therefore, the glass fabric is preferred.

Because of the mechanical compressibility of the glass fabric, a gasket design has been conceived that has completely encapsulated layers of glass fabric only (i.e., with no internal resin). This design, called the envelope approach, has also been investigated. Compressibility curves for this design compared to the optimum laminate design are given in Figure 8. Note that this design does exhibit superior compressibility as expected, which would make it preferred. However, it has the disadvantage of being weaker than the laminate design because the structure consists of individual plies of glass that are unattached. The strength requirements of a particular gasket application must influence the choice of gasket material.

Metal substrates that were considered and tested as reinforcement for the laminate included perforated corrogated aluminum, stainless steel screening of several meshes, and knit stainless steel. All of these proved to be inferior to the optimum glass reinforced laminate (see Figure 9 for energy absorption curves, comparing the best glass reinforced laminate with the best metal reinforced laminate).

Glass spirally wound gaskets were fabricated and tested. FEP was used for the resin, because a wetting of the glass fibers was required to provide structural integrity. The energy absorption curves for a spirally wound gasket and the optimum glass reinforced laminate are given in Figure 10. Since the resin used for the spirally wound gasket is less compressible than that used in the laminate, and the glass roving does not have the built-in spring of the woven glass cloth, it is not surprising that the spirally wound design is less compressible. However, it does offer a distinct advantage over the glass fabric laminate for small cross-section gasket applications (for example, in large diameter and small flange dimensions, where hoop strength becomes important).

The material currently being used for LOX service is a styrene-butadiene copolymer reinforced with asbestos fiber. This material is not LOX-compatible and must be impregnated with fluorolube, a tedious process requiring batch-to-batch LOX-compatibility testing. The performance of this material, compared with the optimum glass reinforced laminate, is shown in Figure 11. Note the superior compressibility characteristics of the newly developed material.

When specimens were cut from a glass reinforced TFE laminate, the inner and outer circumference surfaces exposed glass fibers. Since the resin has not melted, the glass is still dry. This would allow the contained gas or liquid to soak through the gasket radially. To prevent this type of leakage, encapsulation of the inside circumference surface was desired. The easier fabrication of FEP meant that it was preferred for encapsulation. Moisture and contamination still had access to the gasket, however, through the outside circumference surface. Tests confirmed the hypothesis that moisture would reduce the compressibility at cryogenic conditions. Therefore, encapsulation of both circumferential surfaces, locking out all moisture and contamination, was adopted. Laminates are fabricated with glass fabric plies on the outer layers. Specimens are then cut from the laminates and all exposed surfaces are covered with FEP resin. Totally encapsulated gaskets have thus been developed. Figure 12 is a photograph of an encapsulated gasket and Figure 13 is a photograph of an enlarged crosssection of a gasket, showing the TFE and glass plies totally encapsulated with FEP resin.

The leak-sealing ability of the various candidate constructions was measured at room temperature by inserting the test specimen between flanges and increasing the load to 3000 psi. The gasket was then internally pressurized to 200 psi with gaseous nitrogen, the pressure source locked off, and the flange load dropped until a leak occurred. The flange pressure at initial leak divided by the internal pressure gave the gasket "m" factor. It is thought that "m" factors smaller than one can only be attained by pressure-energized or bonded gaskets, neither of which was considered during this program. The leak-sealing ability of the gaskets was measured at cryogenic temperatures in the same fashion, except that after loading the gasket to 3000 psi at room temperature, the gasket and fixture were cooled to 76°K with liquid nitrogen. The remaining procedure was unchanged. With these tests, "m" factors as low as 1.31 at room temperature and as low as 1.56 at 76°K have been obtained from Teflon-glass gaskets. The gasket material currently being used, an asbestos-reinforced rubber treated with a fluorocarbon oil, yielded an "m" factor of 1.30 at room temperature. At 76°K, no seal was obtained at a flange pressure of 3000 psi.

In each of these tests, a drop of 5 psi in internal pressure was considered the leak point; however, since the pressurized volume of the gasket, tubing, and valves was only 0.4 cu in., the actual gaseous leakage was quite small.

Since both leak tests were concerned only with gross leakage, and since normally a gasket with repeatable high energy absorption characteristics exhibited the best leak-sealing ability, the energy absorption test was given added weight for the purpose of selecting the optimum combination of materials.

Since the ASME "m" factor is the ratio of flange pressure at the point of leak to the internal pressure, it cannot be used to predict a gasketing material's leak-sealing ability. An approach was desired which would take into consideration the size of the gasket, the pressure to be sealed, and the physical properties of the material under consideration.

Using the following nomenclature for Figure 14, this development is summarized.

Nomenclature (see Figure 14)

a = gasket inside radius
b = gasket outside radius
g = gasket thickness (uncompressed)
p_i = inside pressure
p_o = outside pressure
p_f = flange pressure
E = modulus of elasticity
δ = compressed gasket thickness
ϵ = strain
μ = Poisson's ratio
σ = normal stress

The approach taken concerns the gasket only, ignoring for the moment the flange pressure and considering the pressure differential between the inside and outside conditions as the only loading. This allows the determination of the normal stresses developed transverse to the gasket. This represents the minimum value of flange pressure required to contain the internal pressure. (See Figure 15.)

Using the Cylindrical Coordinates r, θ, z:

$$\sigma_r = \frac{a^2 b^2 (p_o - p_i)}{b^2 - a^2} \cdot \frac{1}{r^2} + \frac{p_i a^2 - p_o b^2}{b^2 - a^2} \tag{1}$$

$$\sigma_\theta = -\frac{a^2 b^2 (p_o - p_i)}{b^2 - a^2} \cdot \frac{1}{r^2} + \frac{p_i a^2 - p_o b^2}{b^2 - a^2} \tag{2}$$

(Solution from Lamé; see Reference 4)

For the launch vehicle application, p_o will be zero psig at launch and zero psia in space. At all times, $p_i \gg p_o$ so that p_o may be taken as zero at all times. Equations (1) and (2) then simplify to

$$\sigma_r = \frac{a^2 p_i}{b^2 - a^2} \left(1 - \frac{b^2}{r^2}\right) \tag{3}$$

$$\sigma_\theta = \frac{a^2 p_i}{b^2 - a^2} \left(1 + \frac{b^2}{r^2}\right) \tag{4}$$

Inserting equations (3) and (4) into Hooke's Law:

$$\epsilon_z = \frac{1}{E}\left[\sigma_z - \mu(\sigma_r + \sigma_\theta)\right] \tag{5}$$

yields

$$\epsilon_z = \frac{1}{E}\left[\sigma_z - \frac{\mu a^2 p_i}{b^2 - a^2}\left(1 - \frac{b^2}{r^2} + 1 + \frac{b^2}{r^2}\right)\right]$$

$$= \frac{1}{E}\left[\sigma_z - \frac{2\mu a^2 p_i}{b^2 - a^2}\right]$$

or

$$\sigma_z = E\,\epsilon_z + \frac{2\mu a^2 p_i}{b^2 - a^2} \tag{6}$$

Now impose the condition that the strain be equal to the change in gasket thickness divided by the original thickness:

$$\epsilon_z = \frac{\delta - g}{g} \tag{7}$$

Substituting (7) into (6):

$$\sigma_z = E\,\frac{\delta - g}{g} + \frac{2\mu a^2 p_i}{b^2 - a^2} \tag{8}$$

The flange pressure must at least equal this normal stress to maintain a seal.

$$p_f \geq \sigma_z \tag{9}$$

From equations (8) and (9), therefore, the required flange pressure is a function of the gasket dimensions (a, b, g), the gasket properties (E, δ, μ), and the loading (p_i).

This derivation has been based on the theory of elasticity, which requires materials that are elastic, isotropic, and homogeneous. However, Goodman (Reference 5) states that "substantial plastic flow of at least one of the materials at the seal interface is necessary for zero leakage." It is therefore desirable that the gasket be loaded beyond its yield point. This would mean that the theory of plasticity, rather than elasticity, would apply. However, opinion is that using the inequality sign in equation (9) would place the gasket in the plastic range. Therefore, disregarding the equality sign in the equation should overcome this difficulty.

Most gasket materials, including those developed by Narmco Research & Development, are neither isotropic nor homogeneous. Nevertheless, the belief is that effective E's and μ's can be determined in the appropriate directions so that equation (8) may still be applied.

In addition to the small gasket used to evaluate candidate constructions (see Figure 16 for gasket being placed in encapsulation fixture), the program has recently included gaskets of larger dimensions. Figure 17 shows a set of these three gaskets being removed from the encapsulation fixture. The construction of these gaskets is the optimum glass reinforced laminate design.

The testing of these three sizes of gaskets, in addition to providing data for comparison with the gasket material currently being used, will be used to provide experimental verification of equation (8) derived above. See Figure 18 for the assembly of the test fixture for the smallest of the three gaskets; Figure 19 for the bolting down of the joint (note leads from load indicating bolts), and Figure 20 for actual test.

The optimum gasket designs developed for LOX service will be investigated for possible liquid hydrogen application. It is expected that this more severe environment will further reduce the compressibility of the gasket materials. However, the glass-Teflon gaskets will probably maintain an adequate seal.

The knowledge gained from this program has already found application to another problem — the sealing of LOX valves. Although the application is quite different, the glass reinforced Teflon design appears to be a good solution. Whittaker Controls and Guidance Company, a sister division of Narmco Research & Development in Telecomputing Corporation, is developing a series of valves for LOX service. Narmco has designed a Teflon-glass laminate seal for a 17-in. valve (see Figures 21 and 22) and has fabricated seals for 4-in. and 10-in. valves (see Figures 23 through 28). The compressibility of the Teflon-glass laminate at the cryogenic condition greatly improves sealing because it allows more deflection of critical parts, such as the vizor, while still maintaining a seal.

Preliminary testing of the 4-in. and 10-in. valves which utilize the glass-Teflon seal design indicates that leakage rates approaching zero can be obtained.

REFERENCES

(1) E. I. du Pont de Nemours and Company, "New Design Data for Teflon," by L. H. Gillespie et al. (Machine Design reprint), 21 Jan 1960 and 18 Feb 1960

(2) National Bureau of Standards, Elastomeric Seals and Materials at Cryogenic Temperatures: Quarterly Report 7918, by R. F. Robbins et al., 15 July 1963

(3) Rocketdyne Division of North American Aviation, Inc., Program of Testing Nonmetallic Materials at Cryogenic Temperatures: Final Report, by R. E. Mowers et al., 30 Dec 1962

(4) Timoshenko and Goodier, Theory of Elasticity, second edition, Engineering Society Monographs, McGraw-Hill Book Co., New York, 1957

(5) Advanced Technology Laboratories, Design Criteria for Zero-Leakage Connectors for Launch Vehicles, by T. P. Goodman et al., Schenectady, New York, 1963

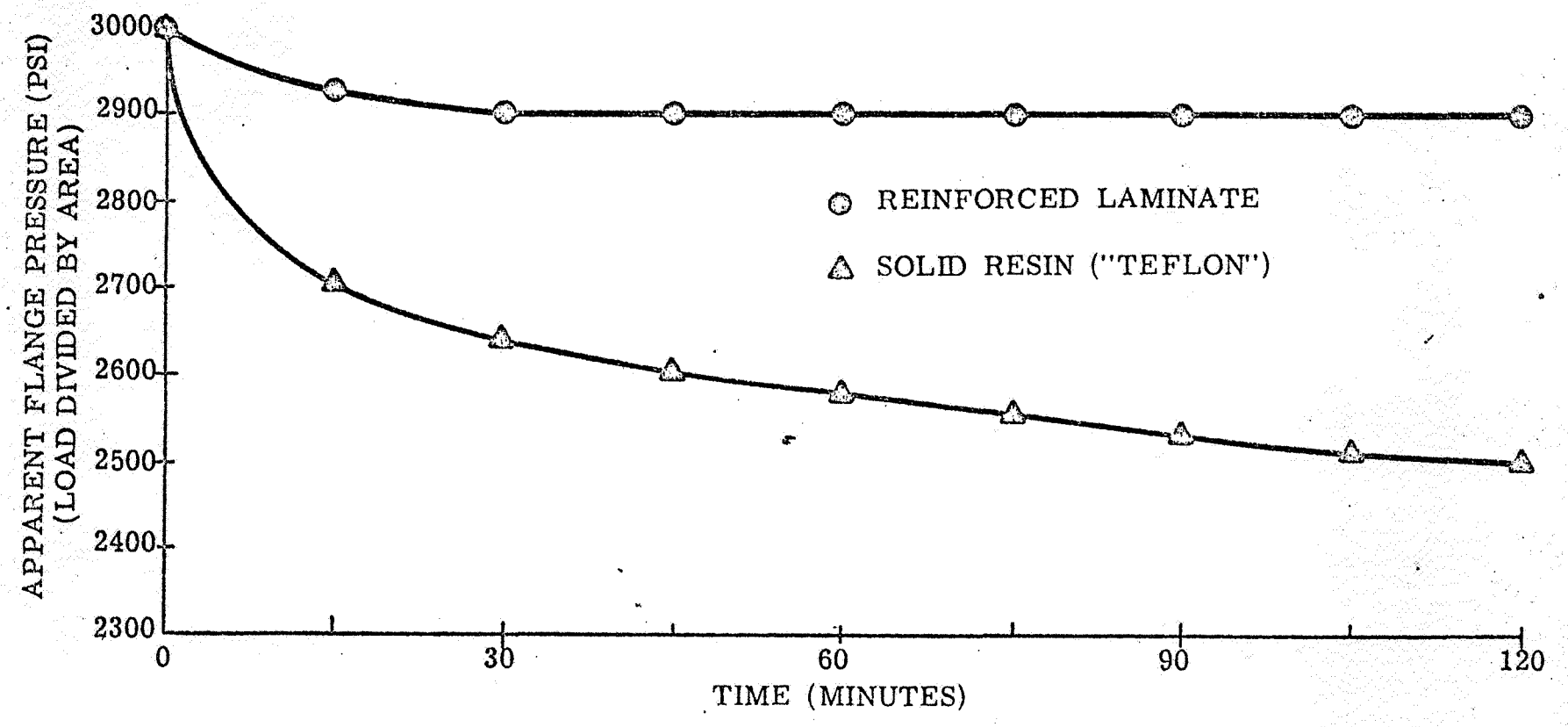

FIGURE 1. STRESS RELAXATION

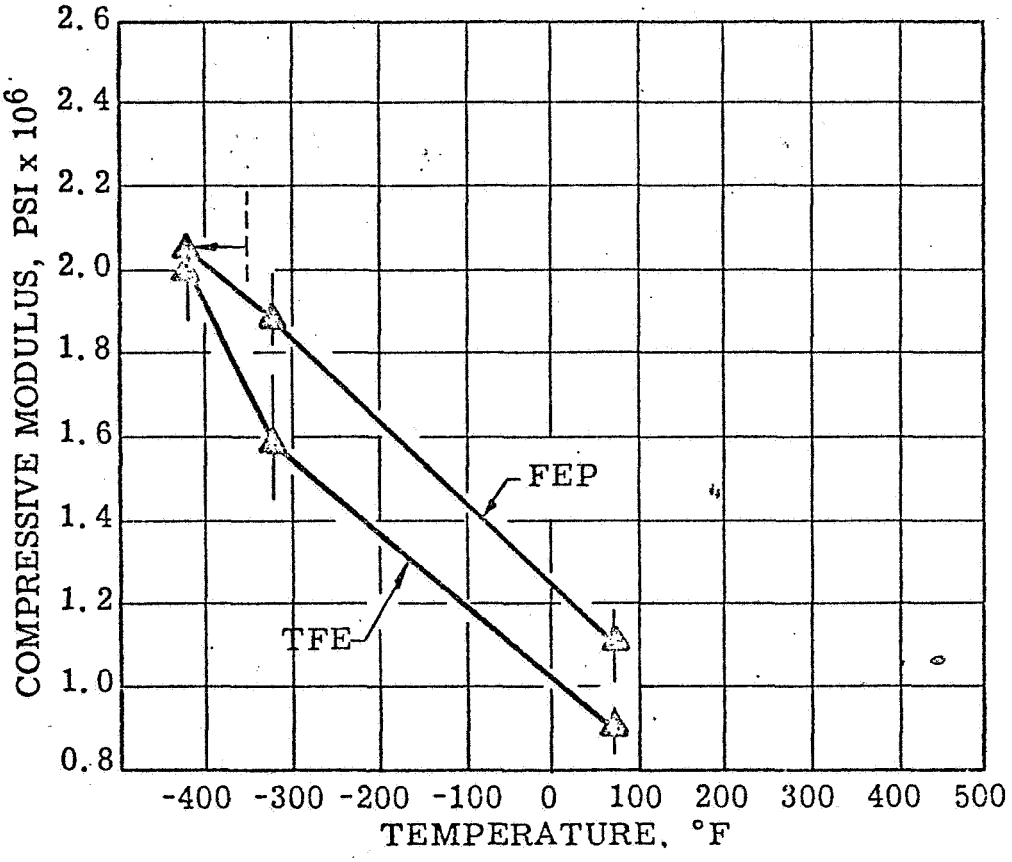

FIGURE 2. EFFECT OF TEMPERATURE ON THE COMPRESSIVE MODULUS OF GLASS FABRIC REINFORCED TEFLONS

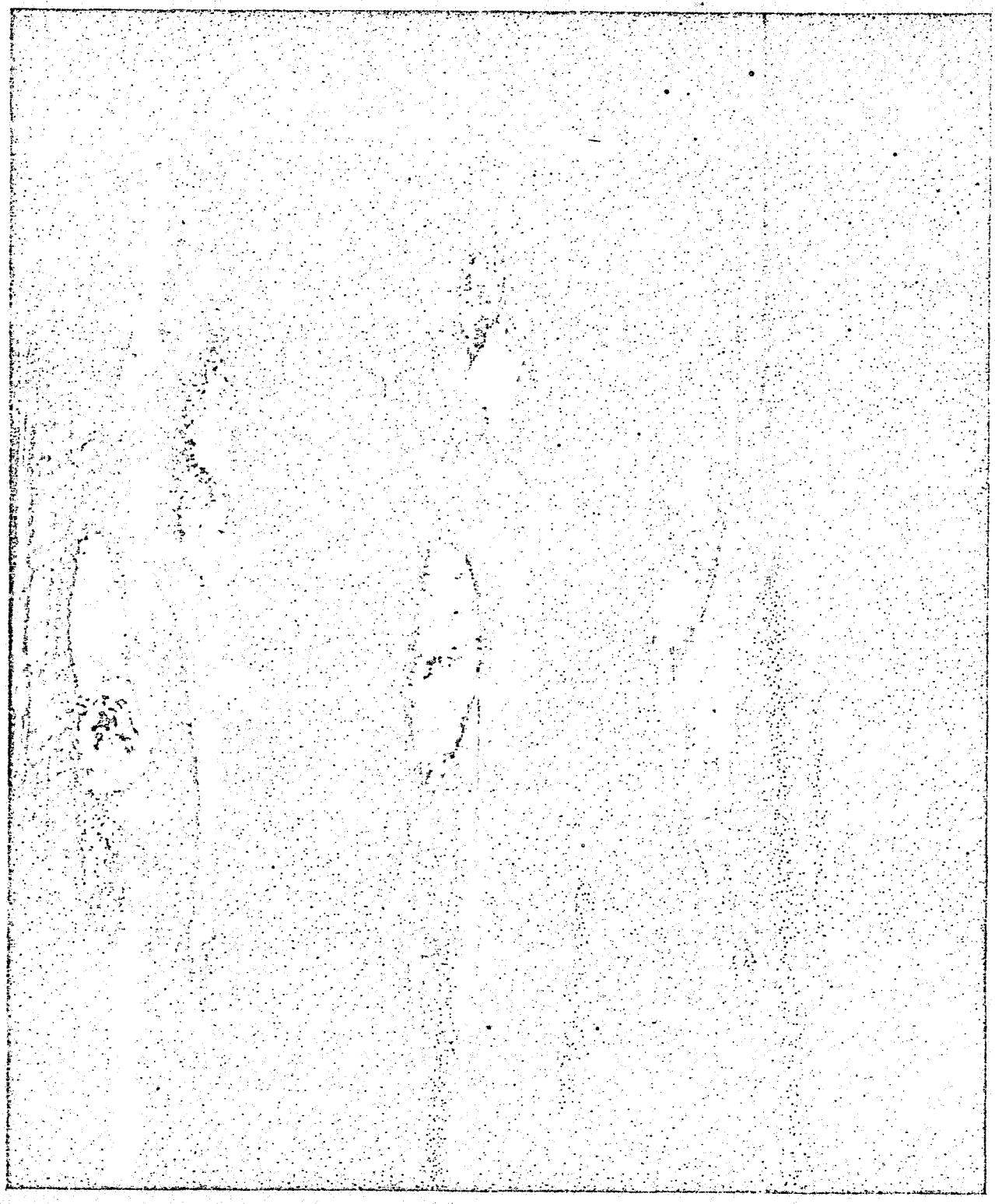

FIGURE 3

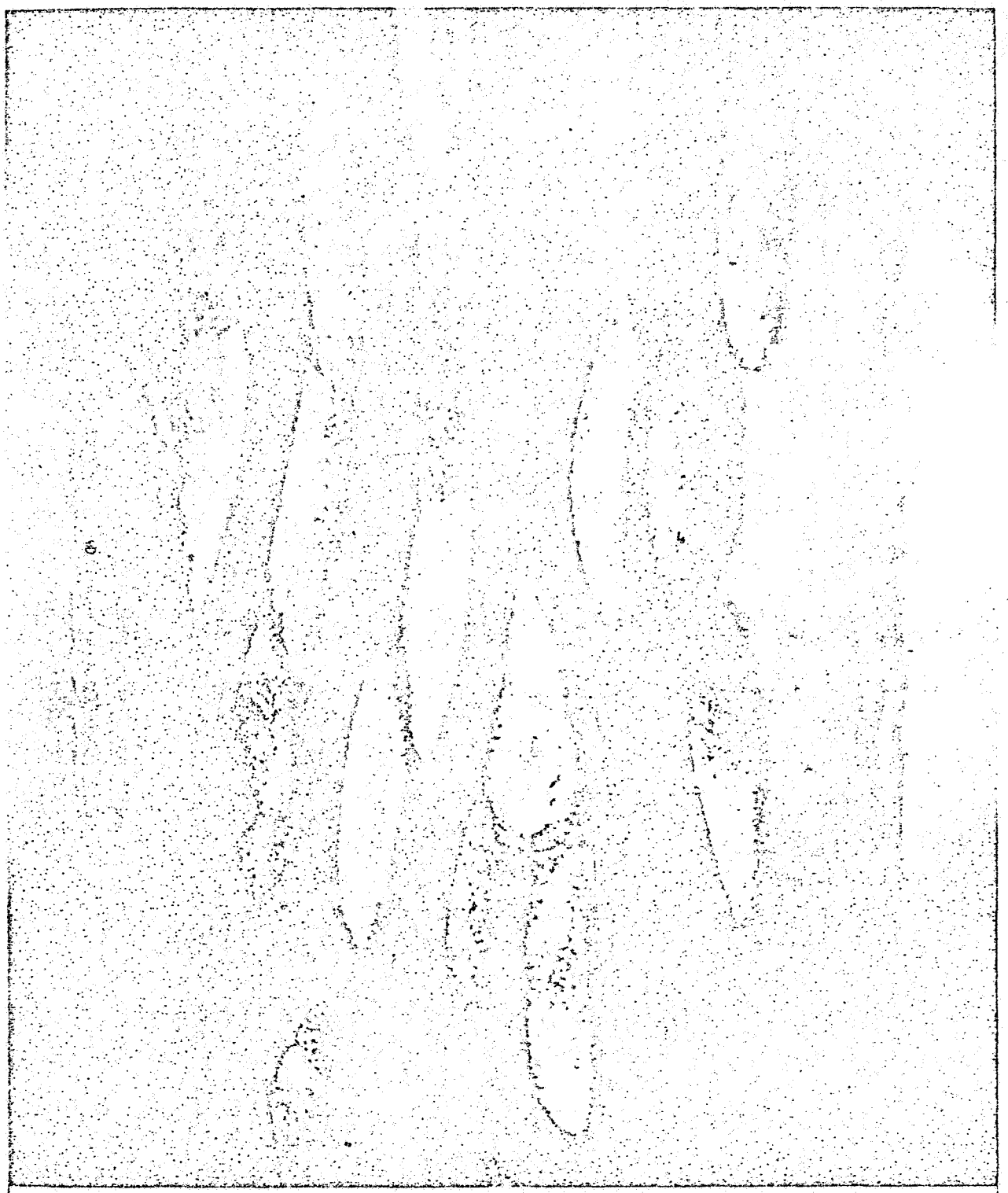

FIGURE 4

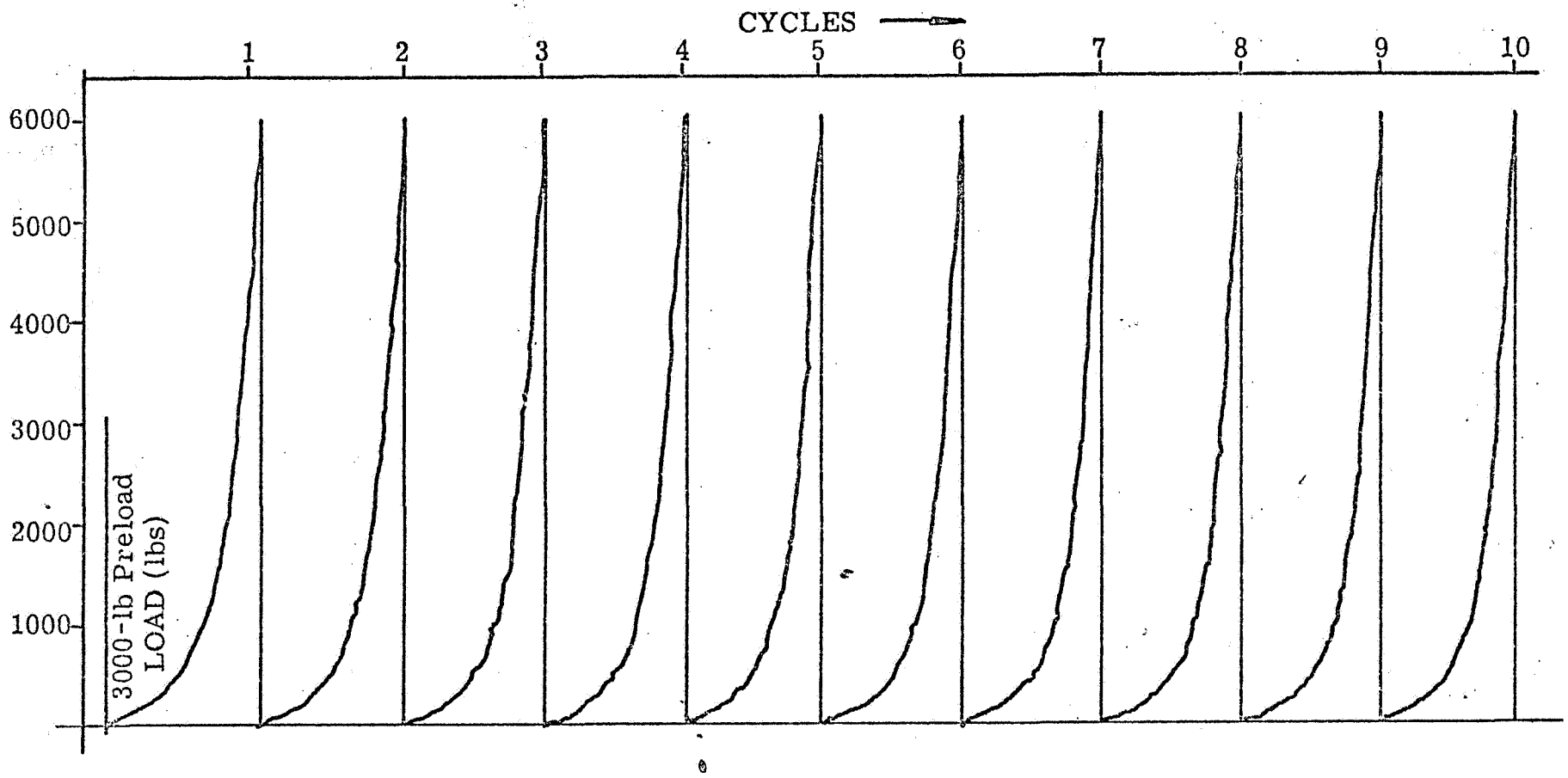

FIGURE 5. TYPICAL CYCLE OF ENERGY ABSORPTION CURVES

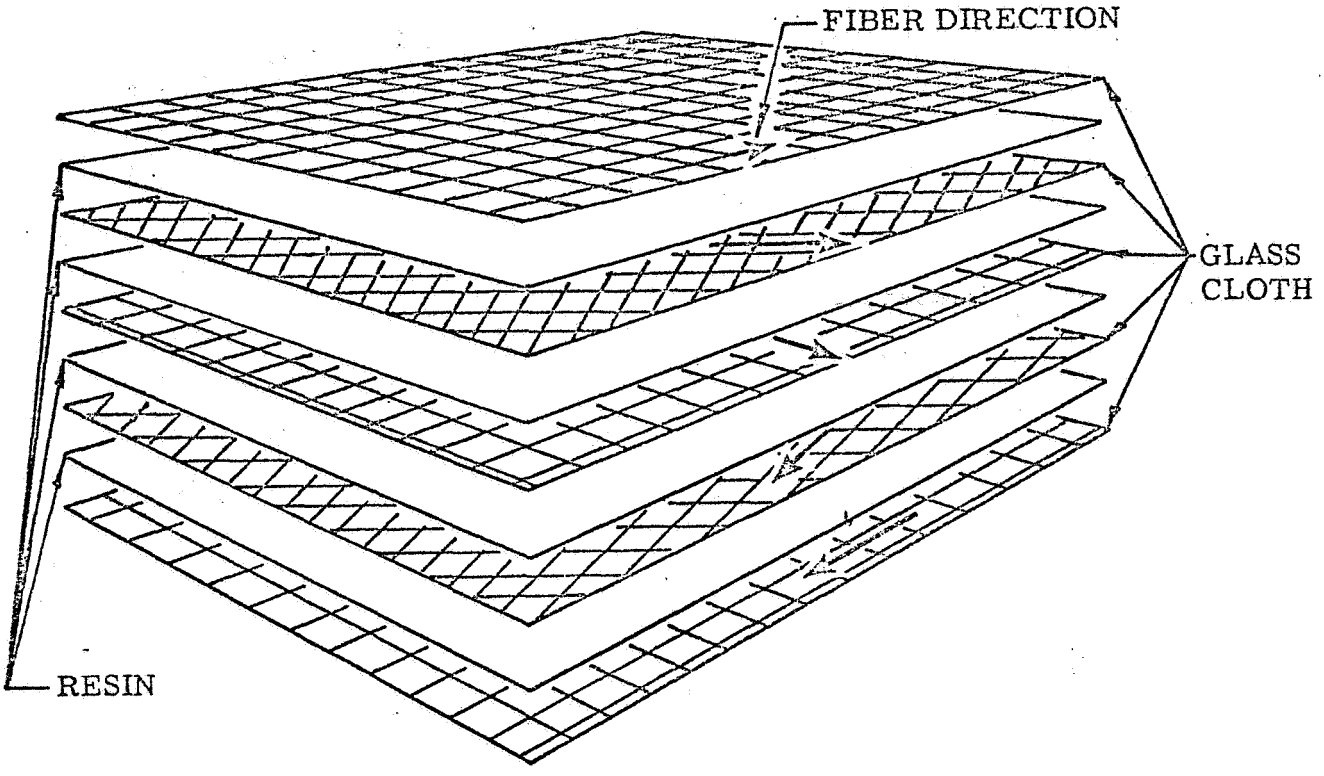

FIGURE 6. LAMINATE LAYUP

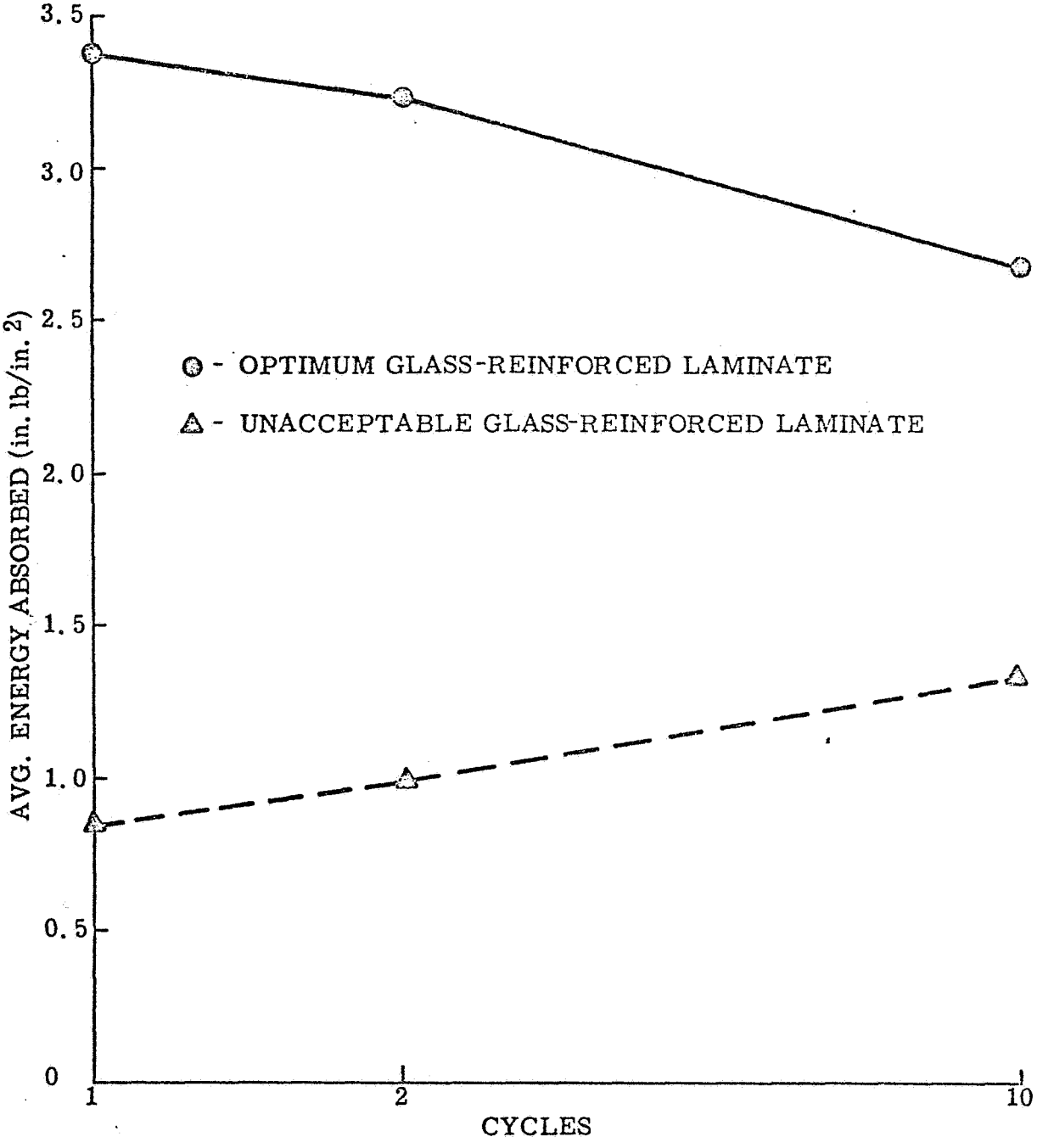

FIGURE 7. ENERGY ABSORPTION OF GLASS-REINFORCED LAMINATES

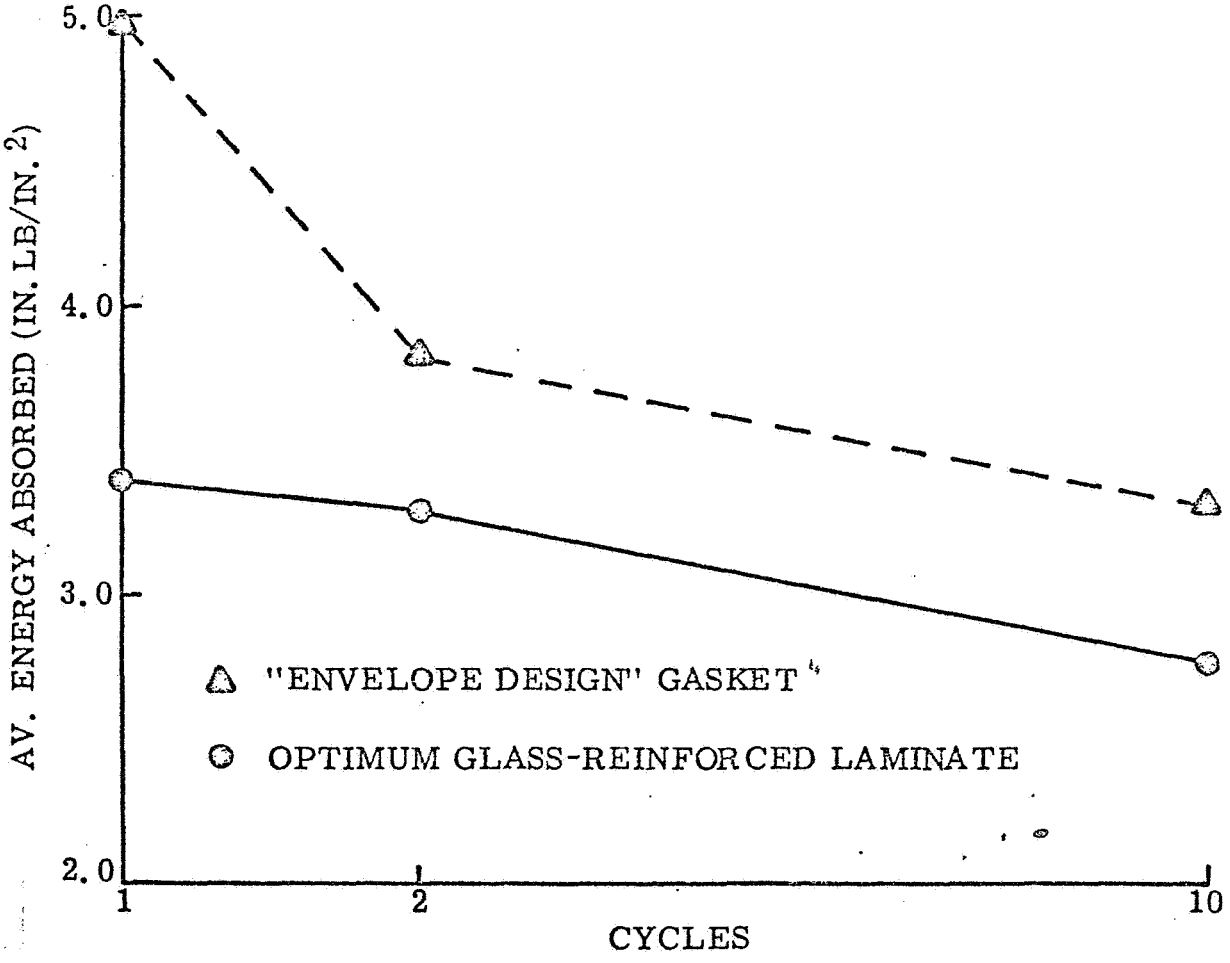

FIGURE 8. ENERGY ABSORPTION OF GLASS-REINFORCED LAMINATE AND "ENVELOPE DESIGN" GASKET

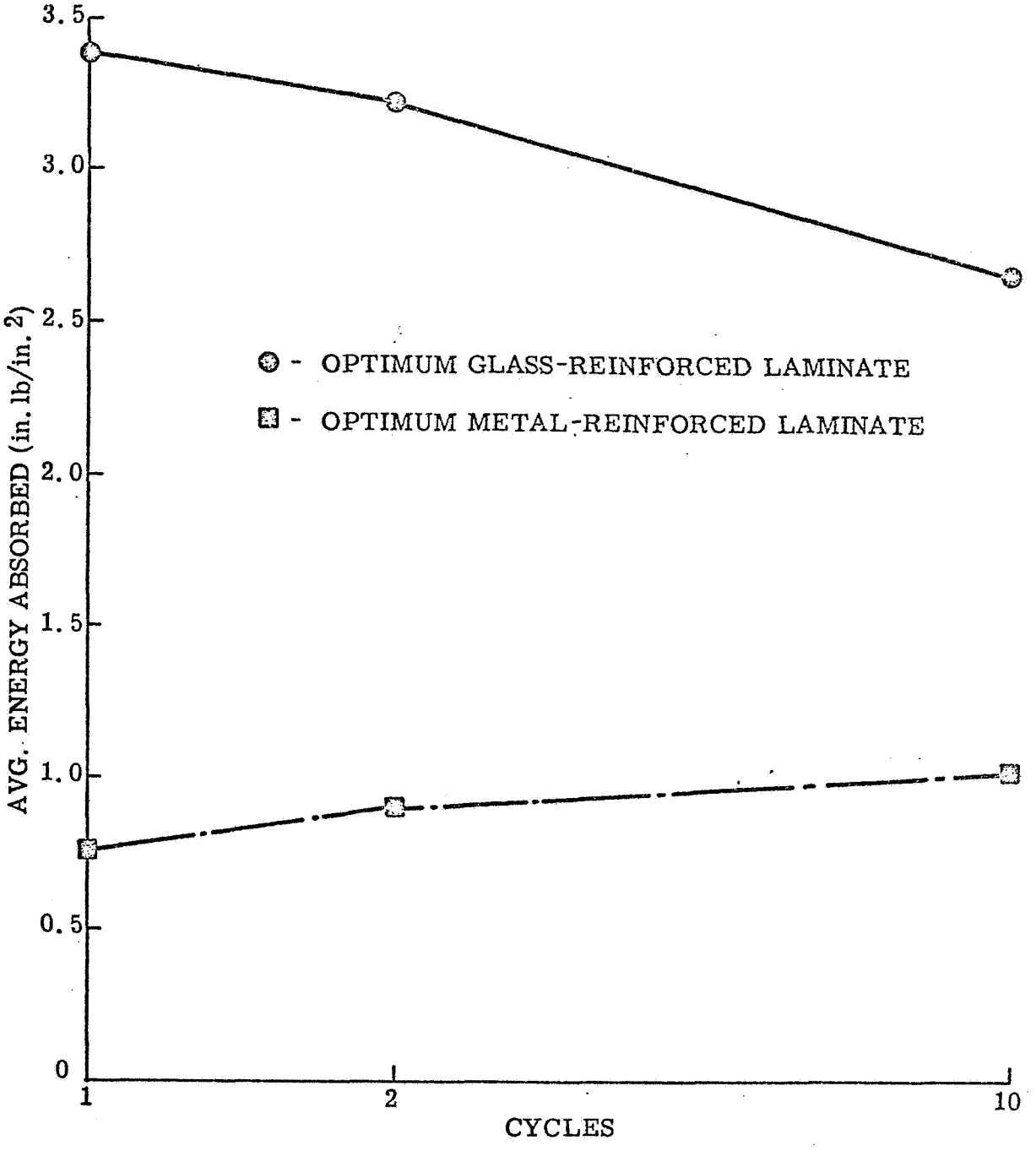

FIGURE 9. ENERGY ABSORPTION OF GLASS-REINFORCED AND METAL-REINFORCED LAMINATES

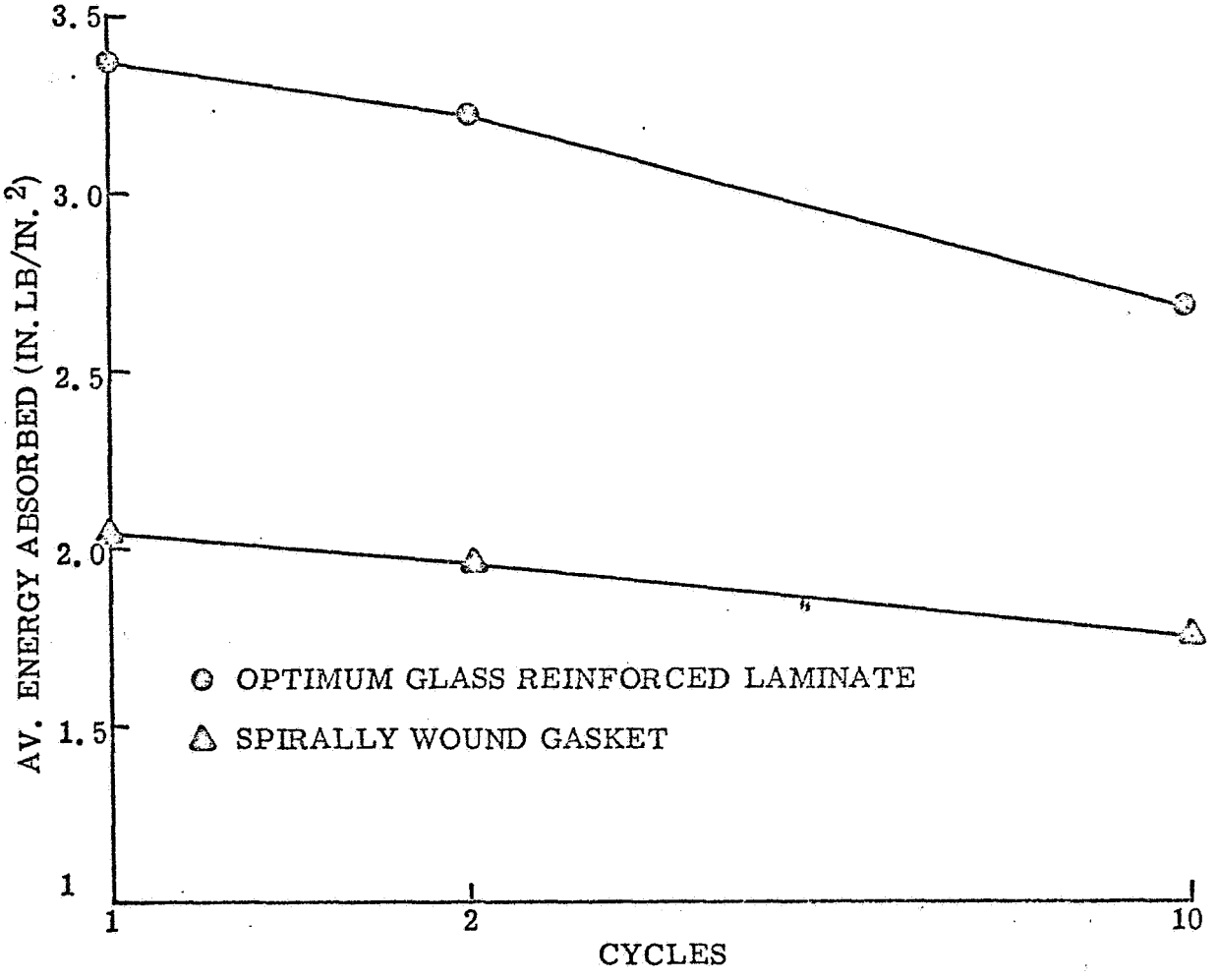

FIGURE 10. ENERGY ABSORPTION OF GLASS-REINFORCED LAMINATE AND SPIRALLY WOUND GASKET

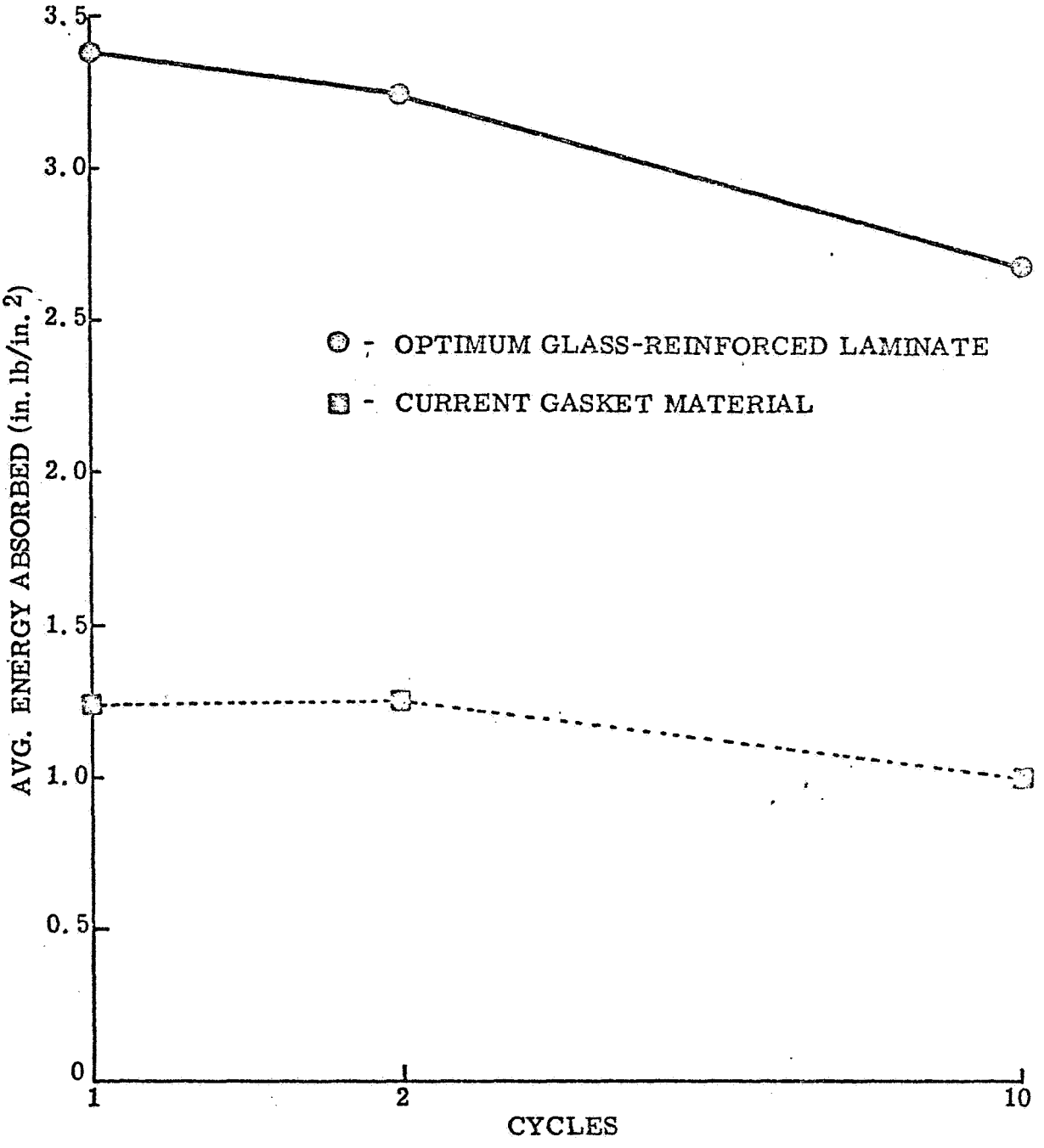

FIGURE 11. ENERGY ABSORPTION OF GLASS-REINFORCED LAMINATE AND CURRENT GASKET MATERIAL

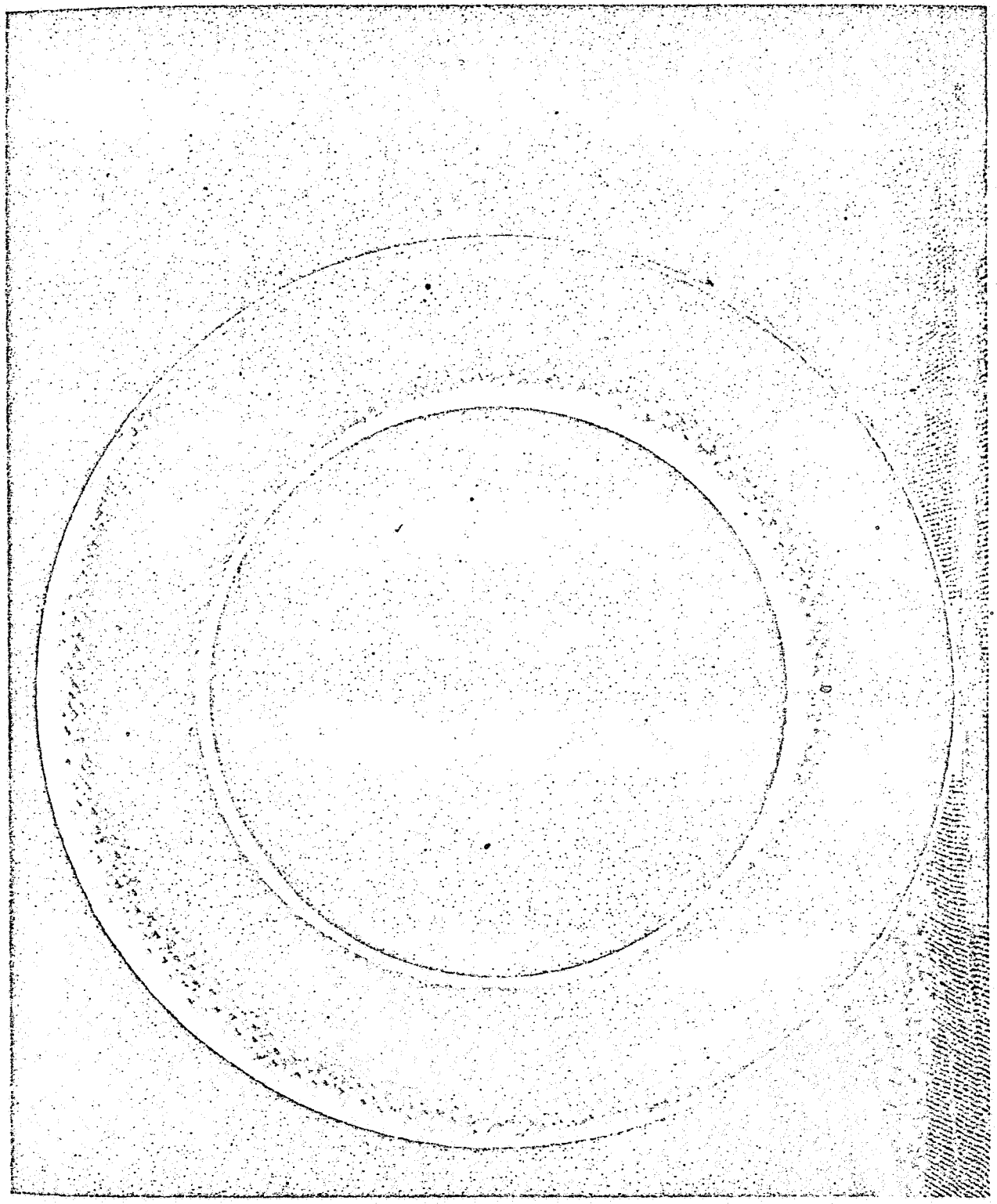

FIGURE 12

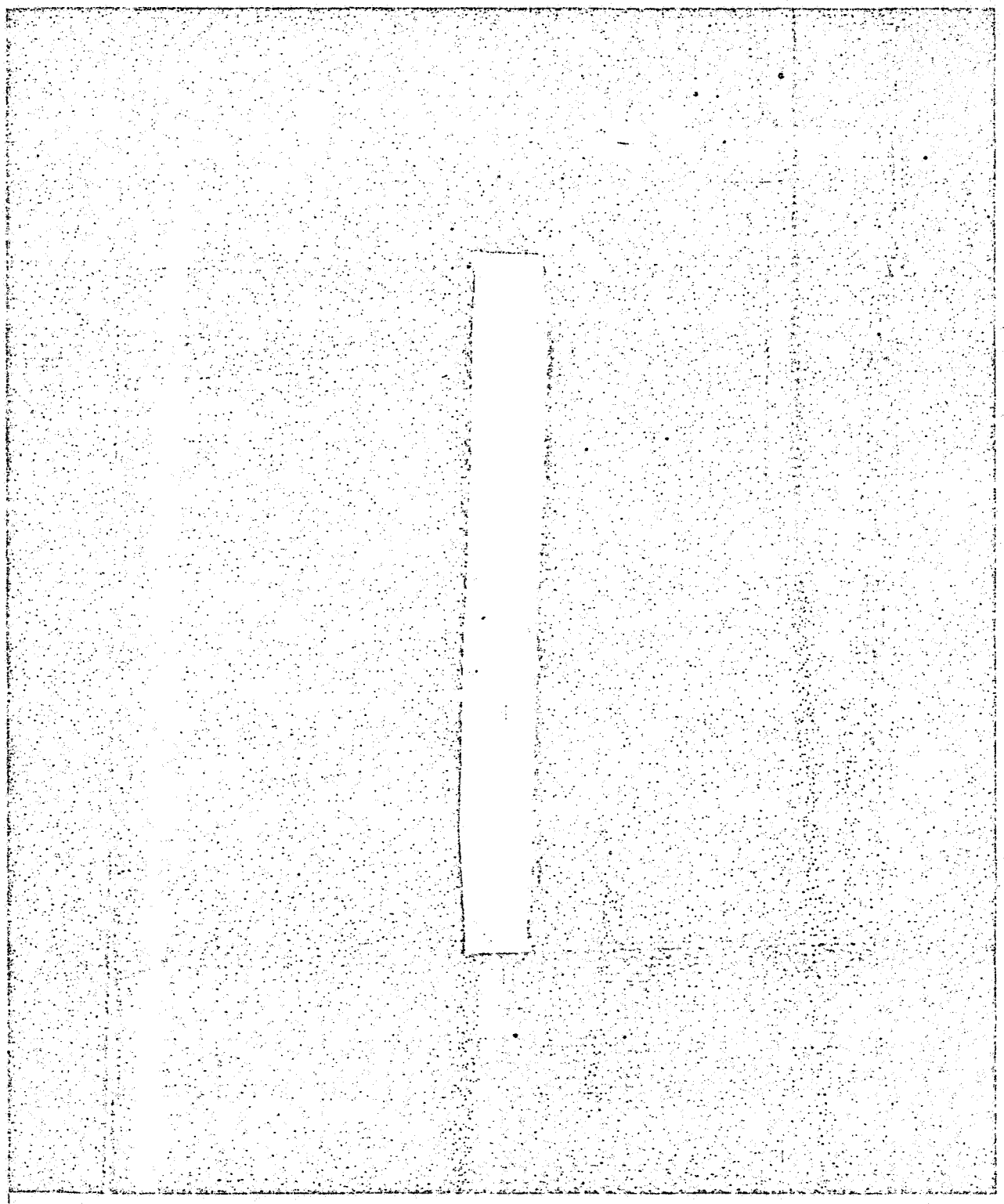

FIGURE 13

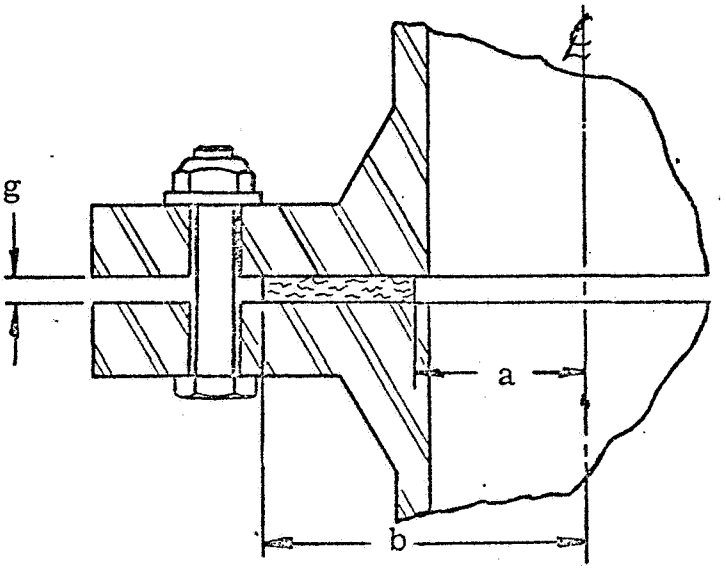

FIGURE 14. TYPICAL JOINT SECTION

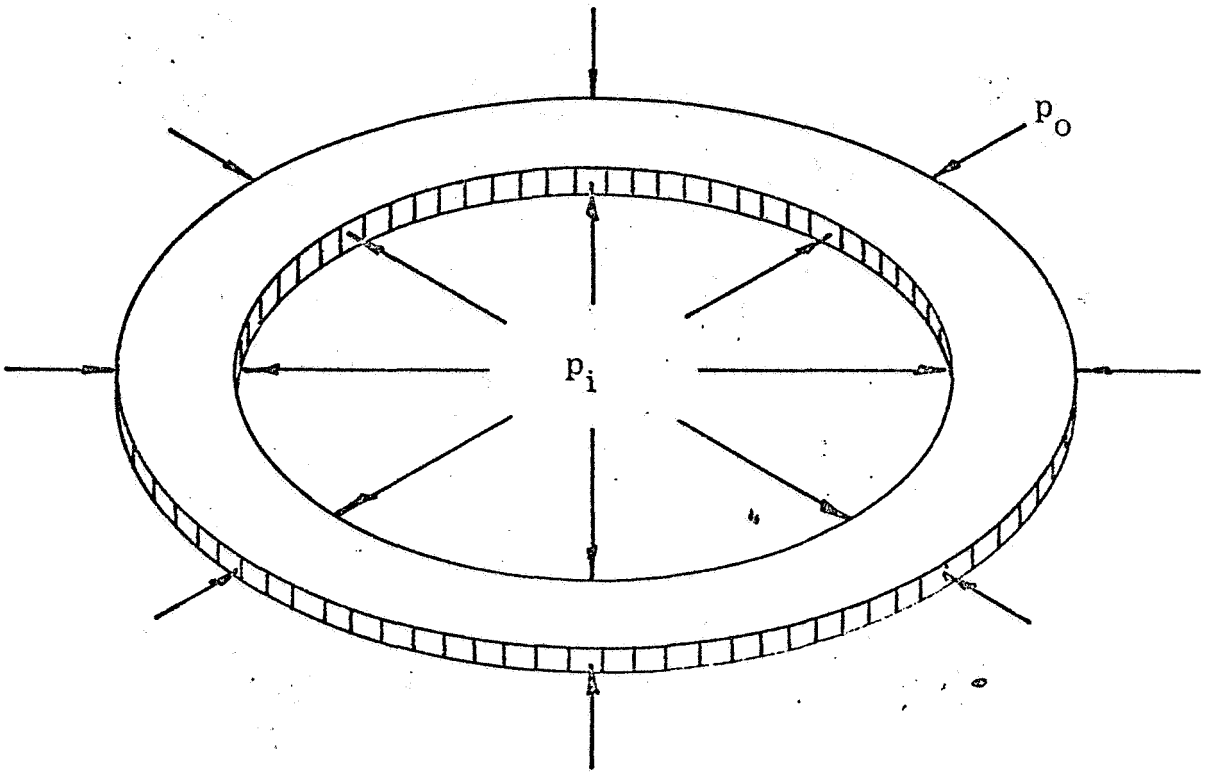

FIGURE 15. GASKET LOADING LESS FLANGE PRESSURE

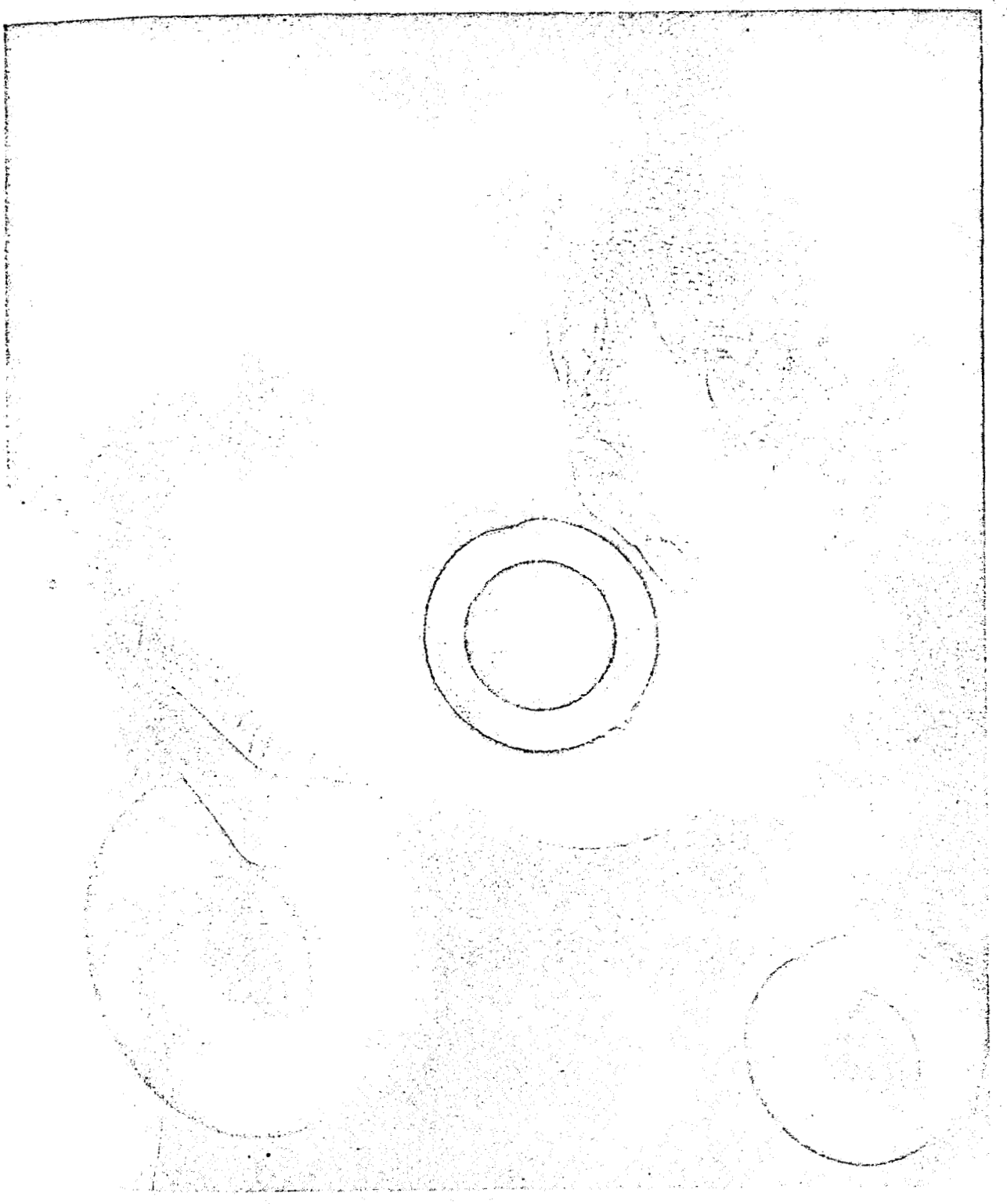

FIGURE 16

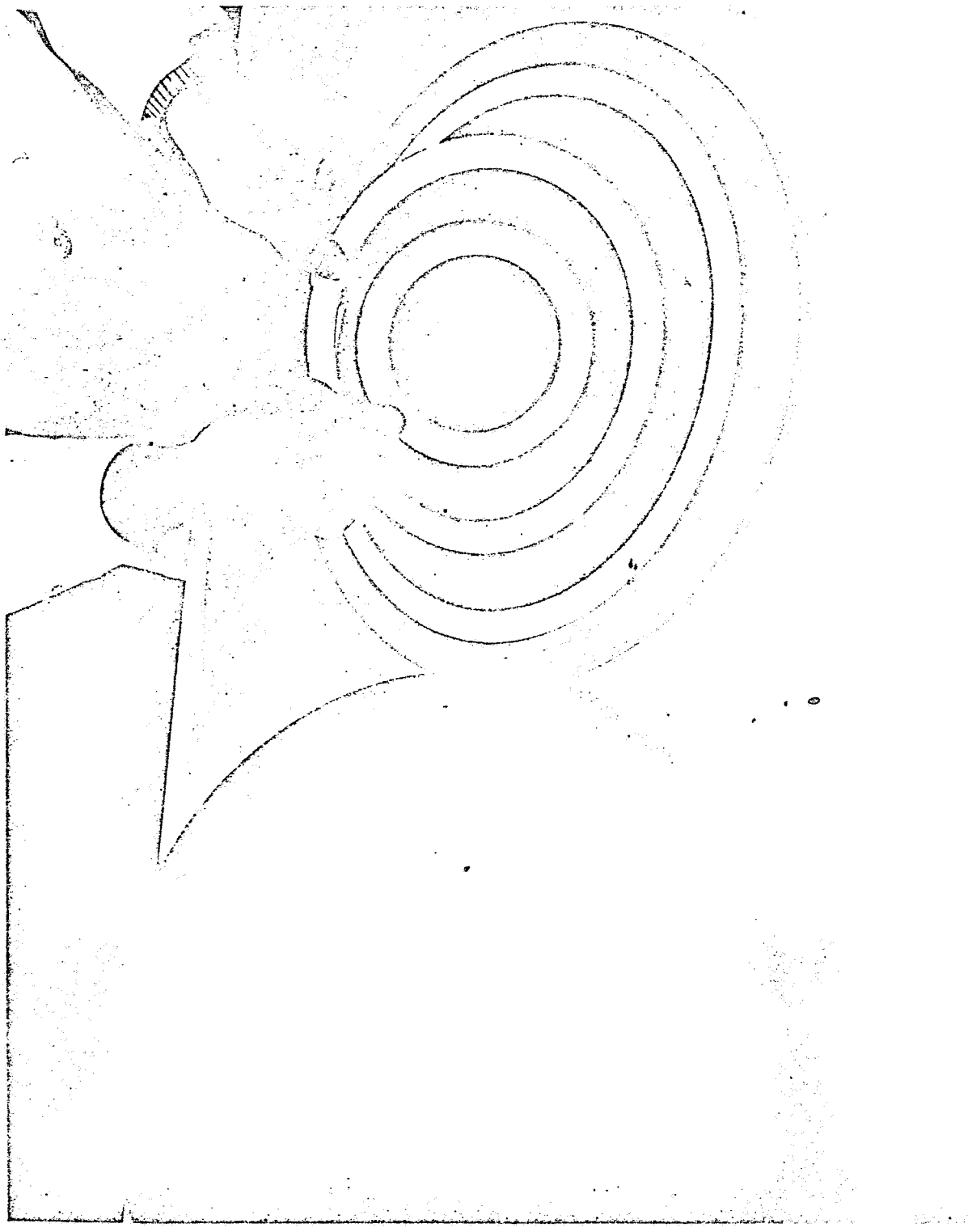

FIGURE 17

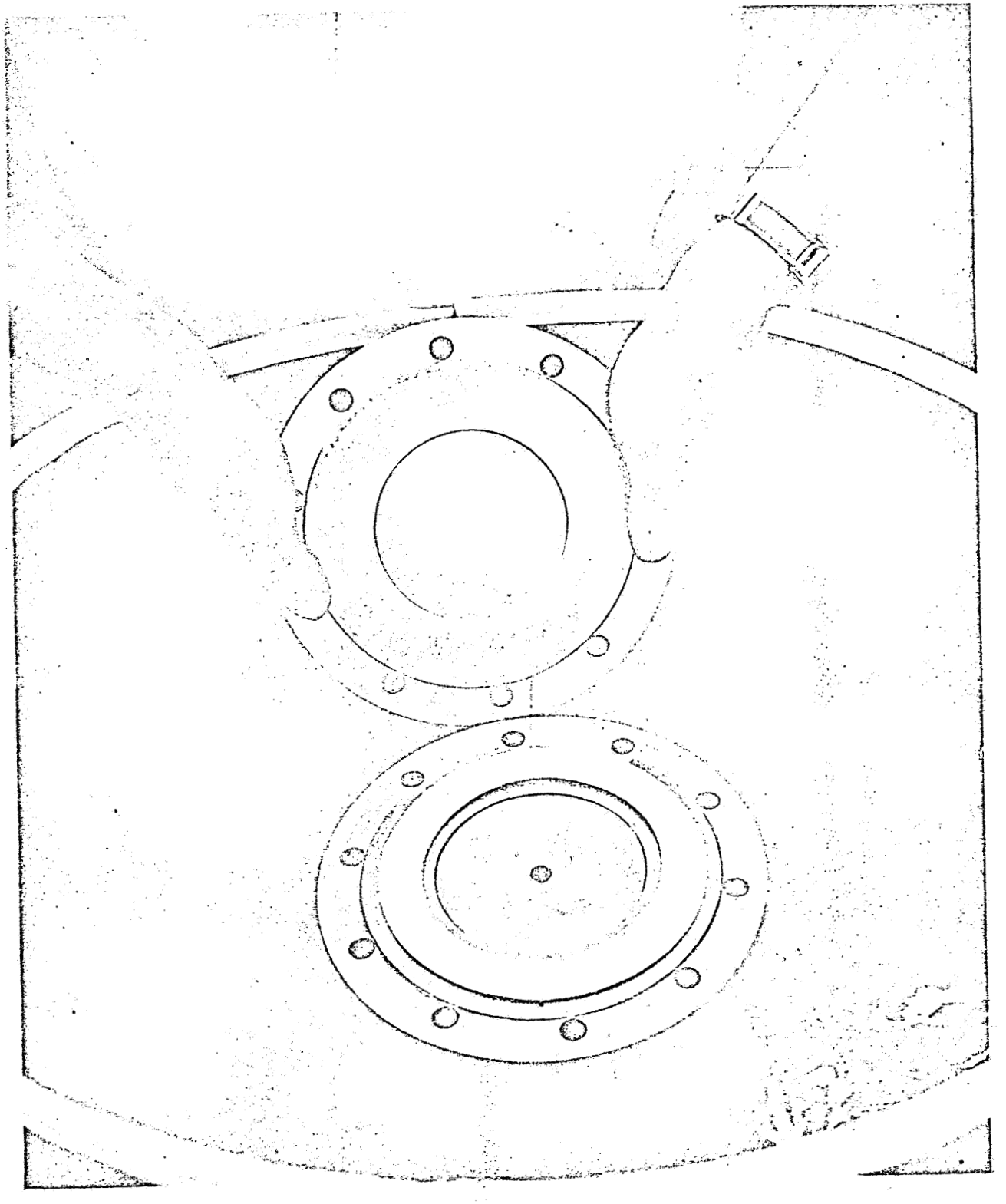

FIGURE 18

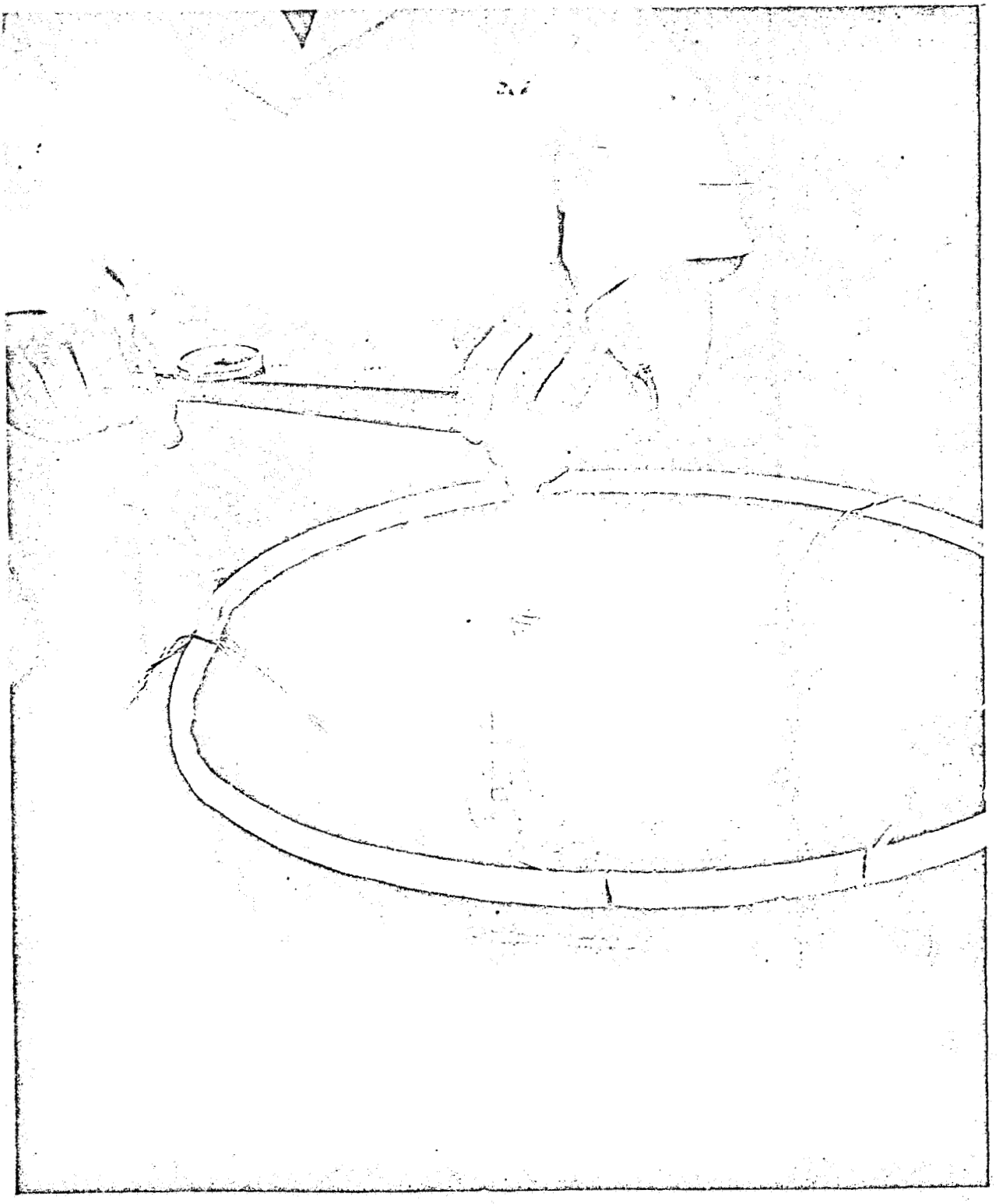

FIGURE 19

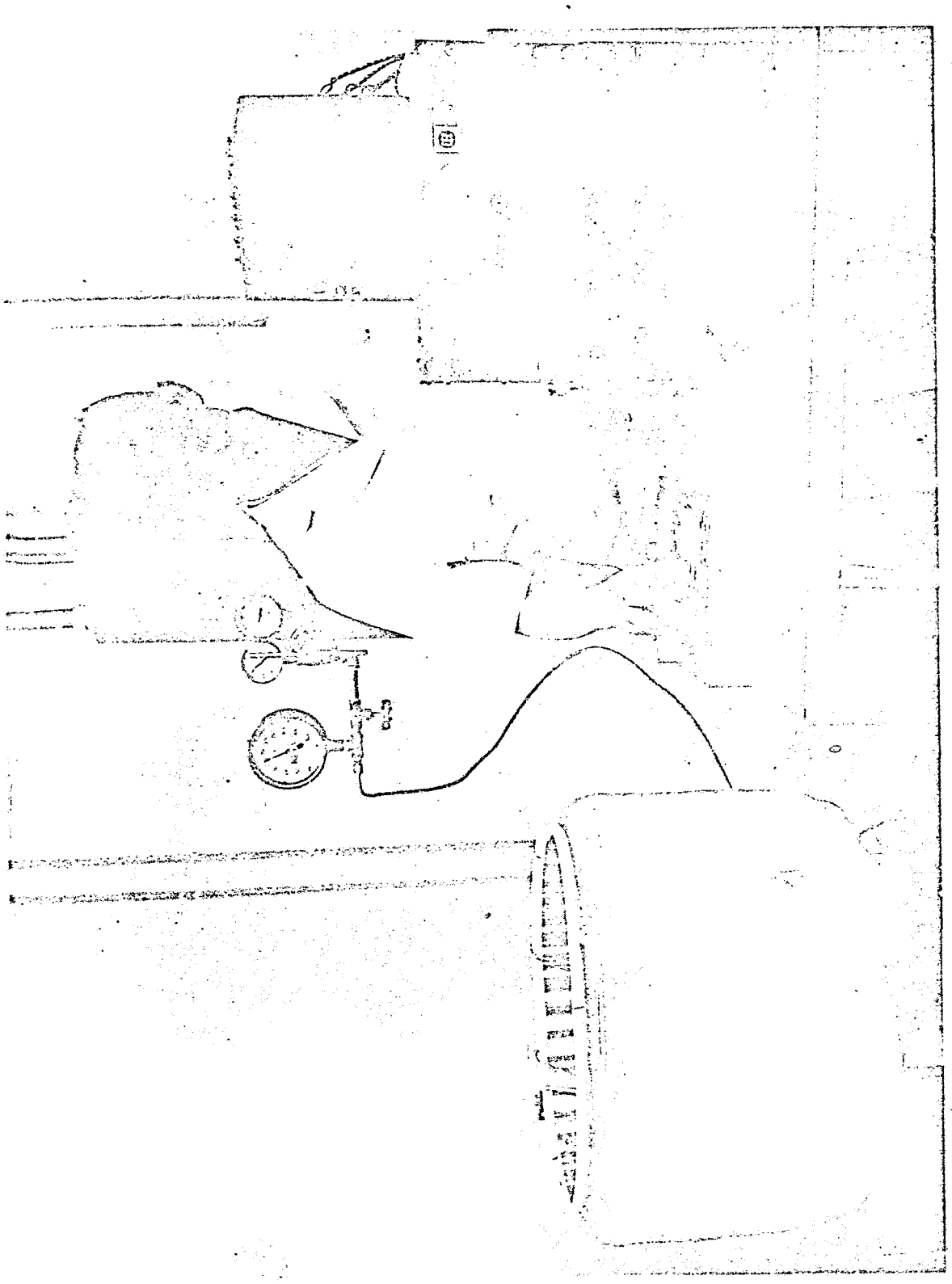

FIGURE 20

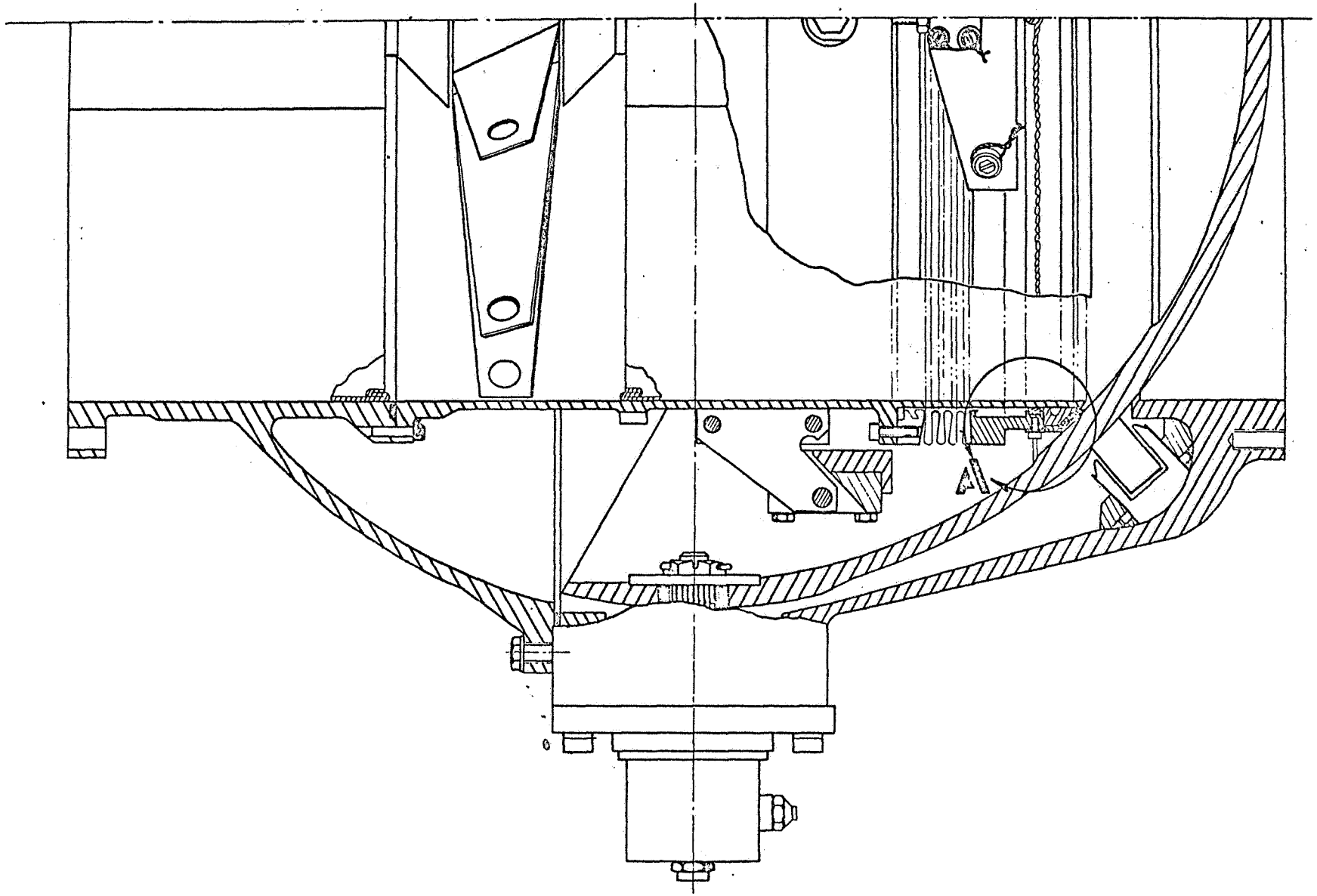

FIGURE 21. 17-IN. LOX VALVE

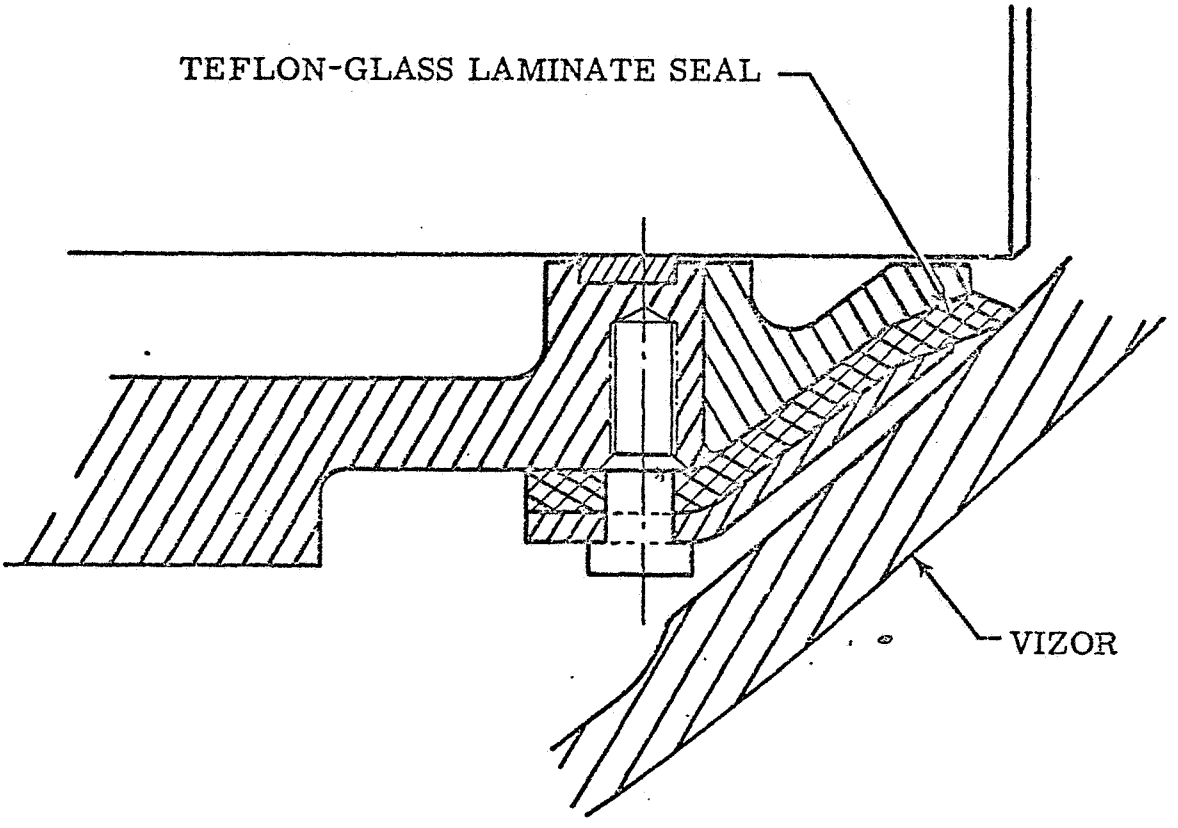

FIGURE 22. SECTION "A" WIPER SEAL

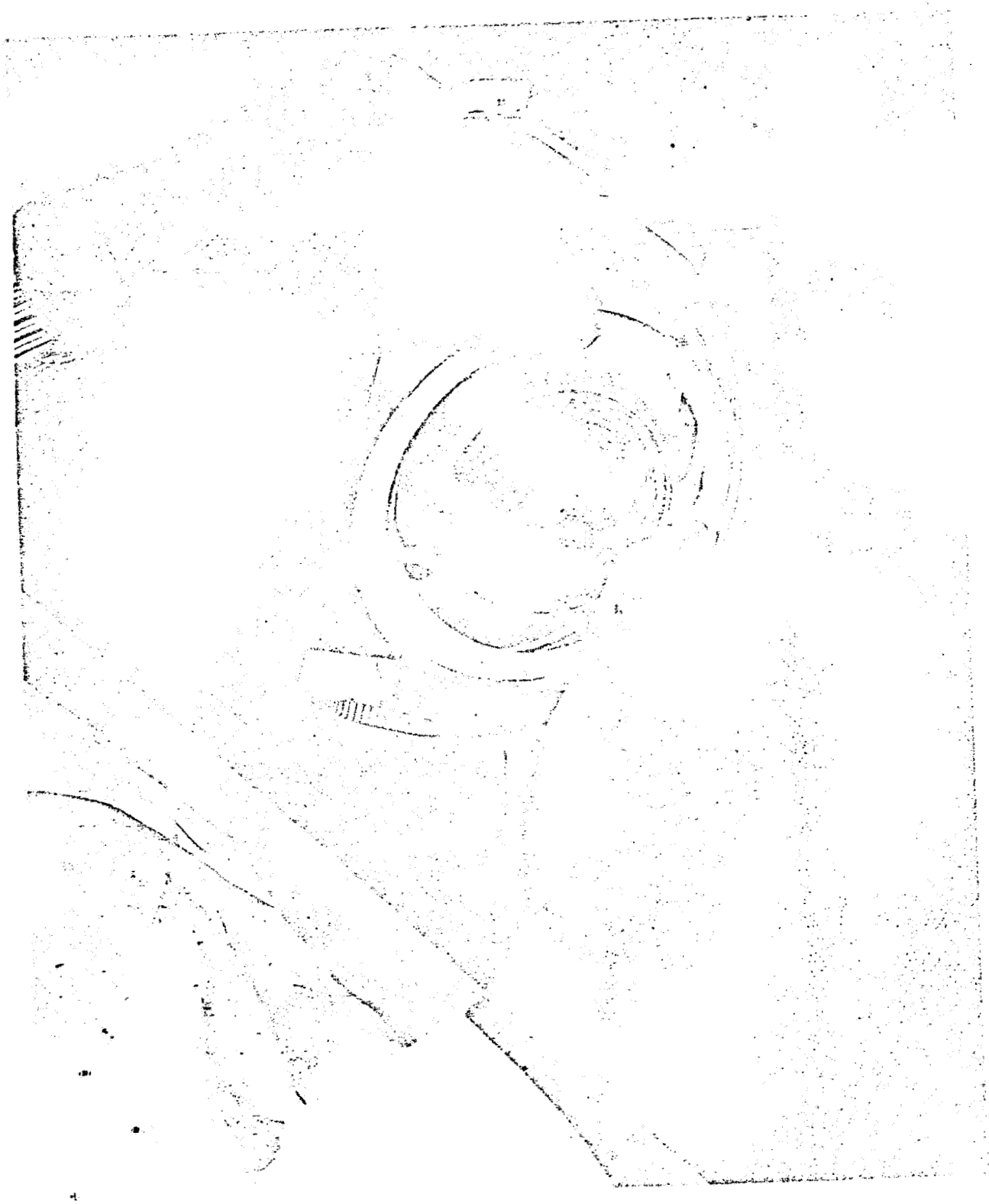

FIGURE 23

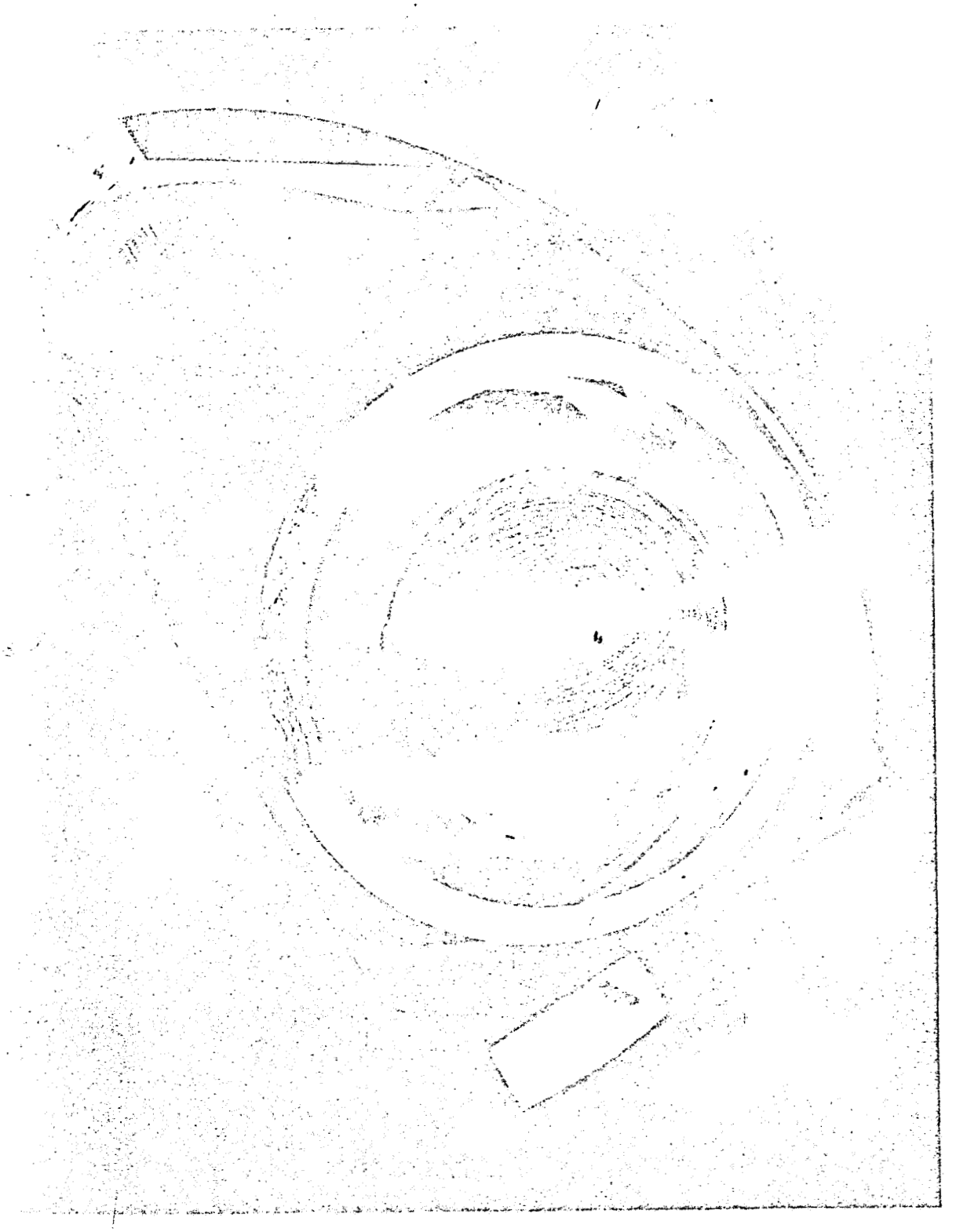

FIGURE 24

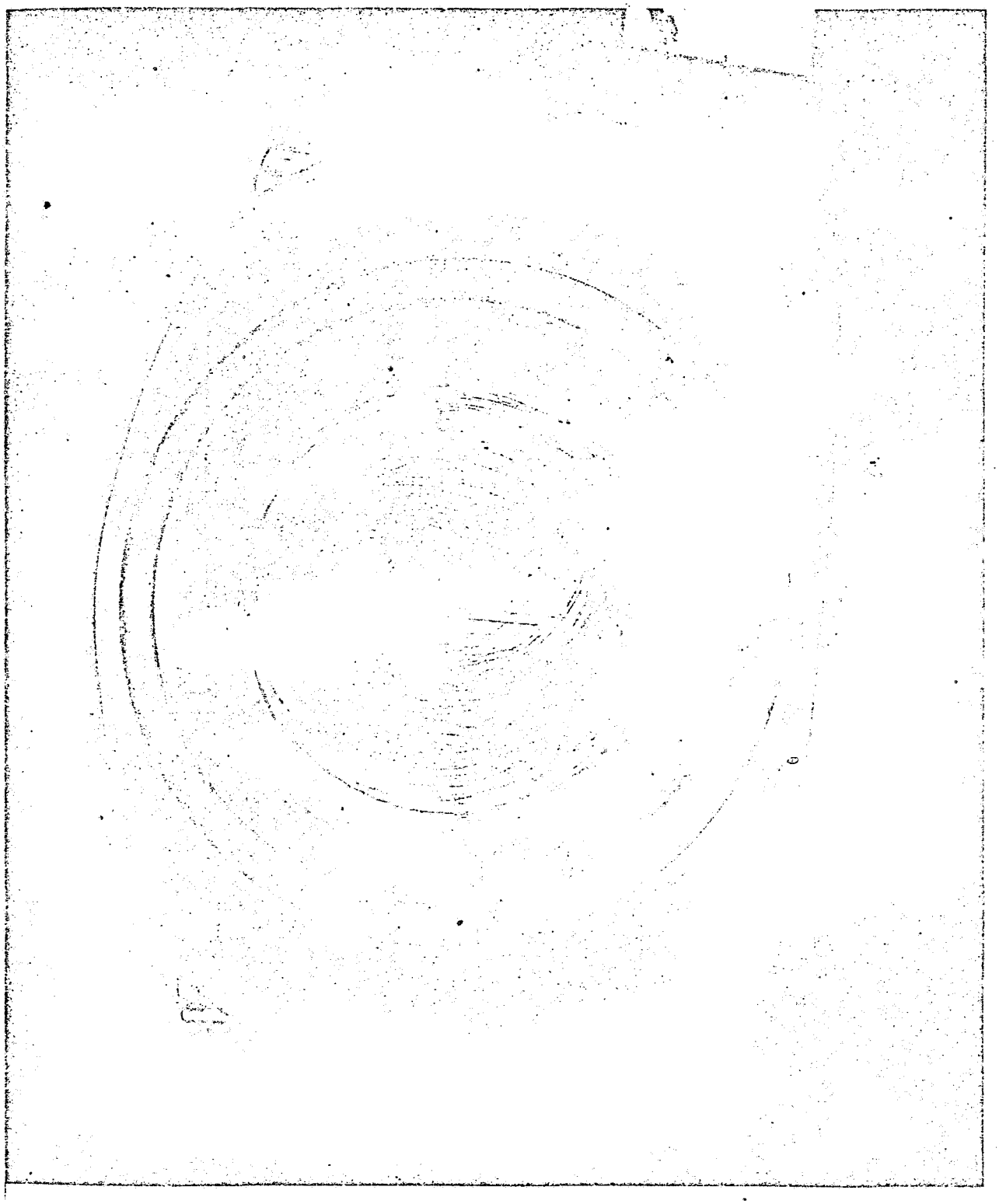

FIGURE 25

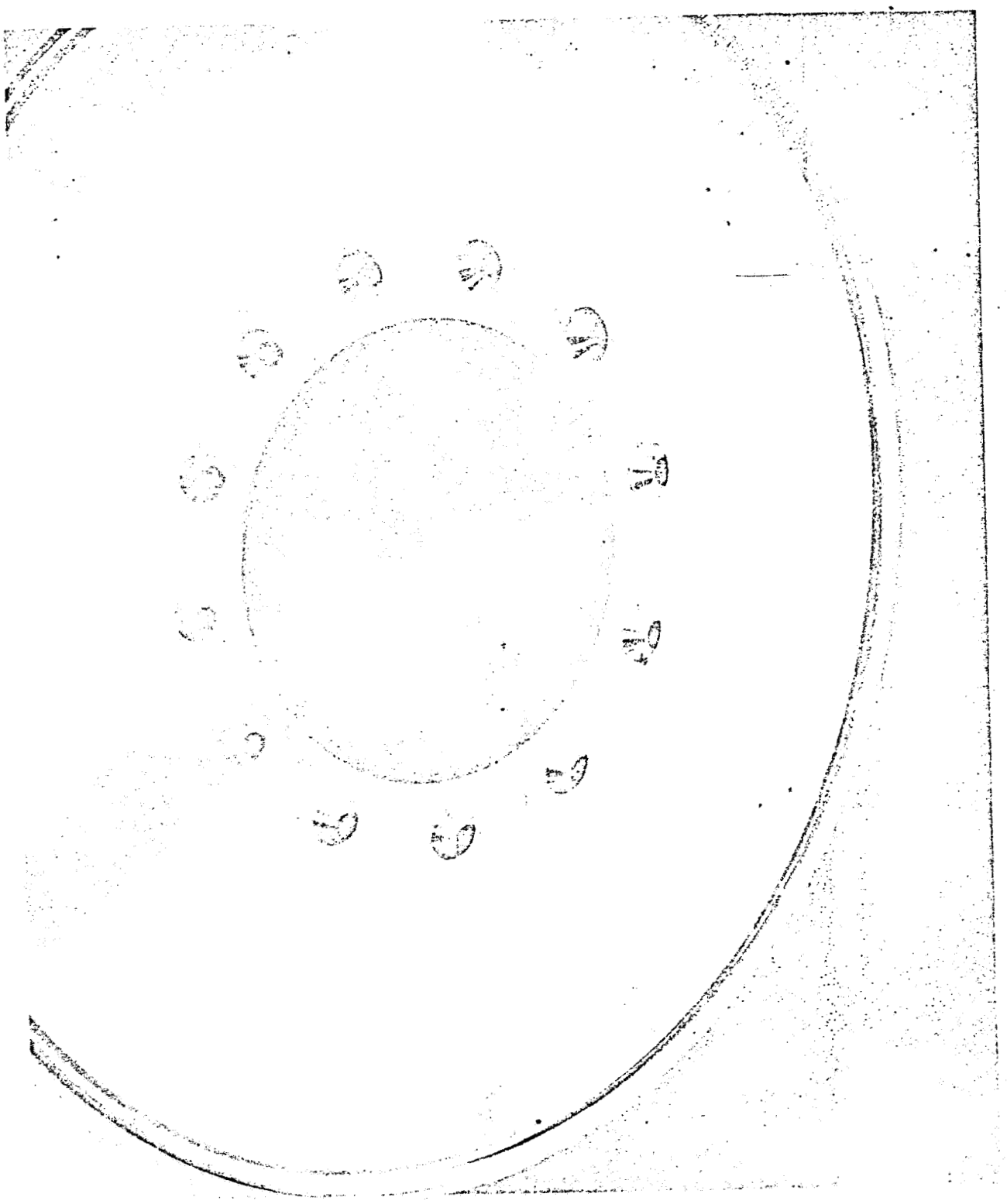

FIGURE 26

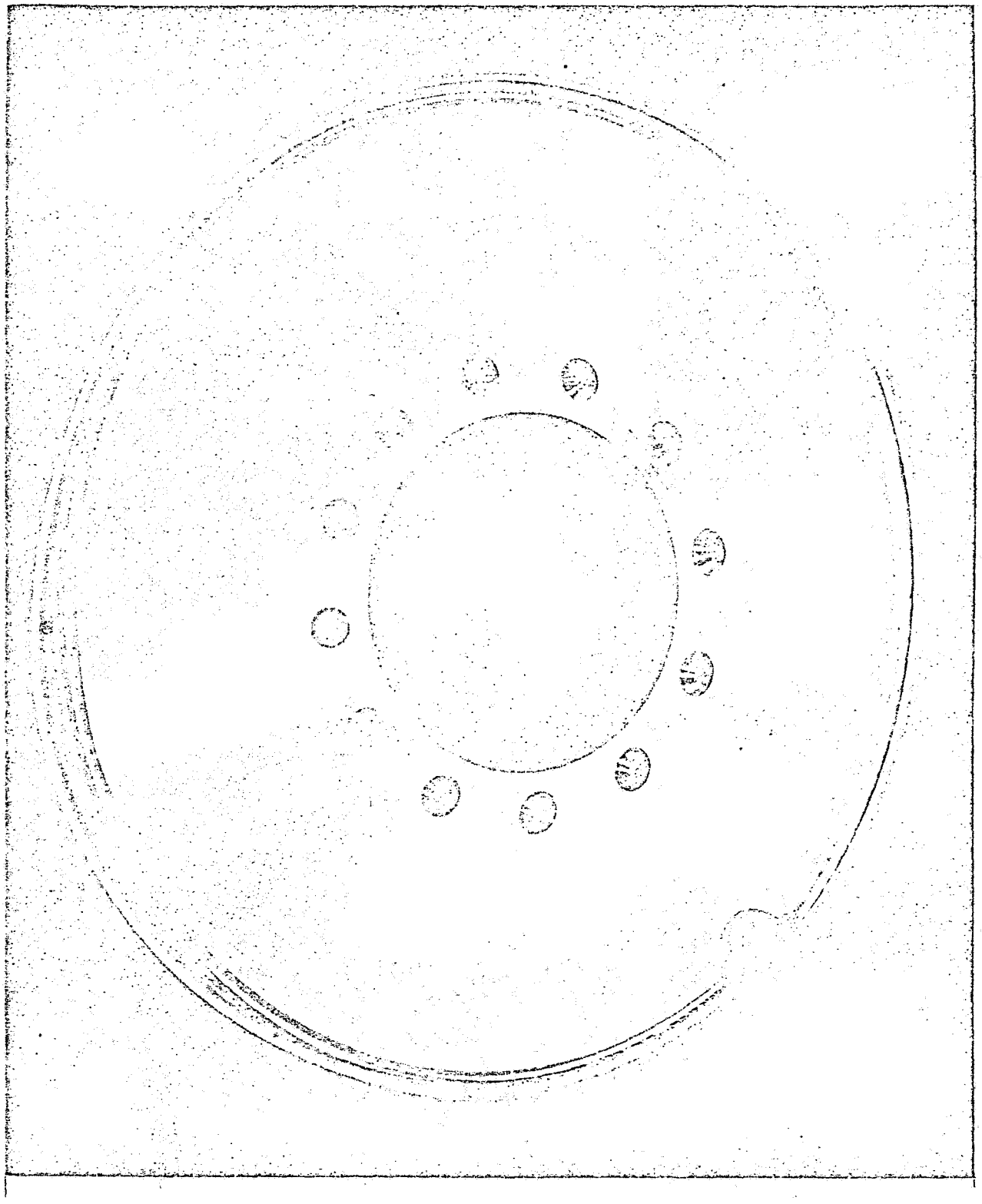

FIGURE 27

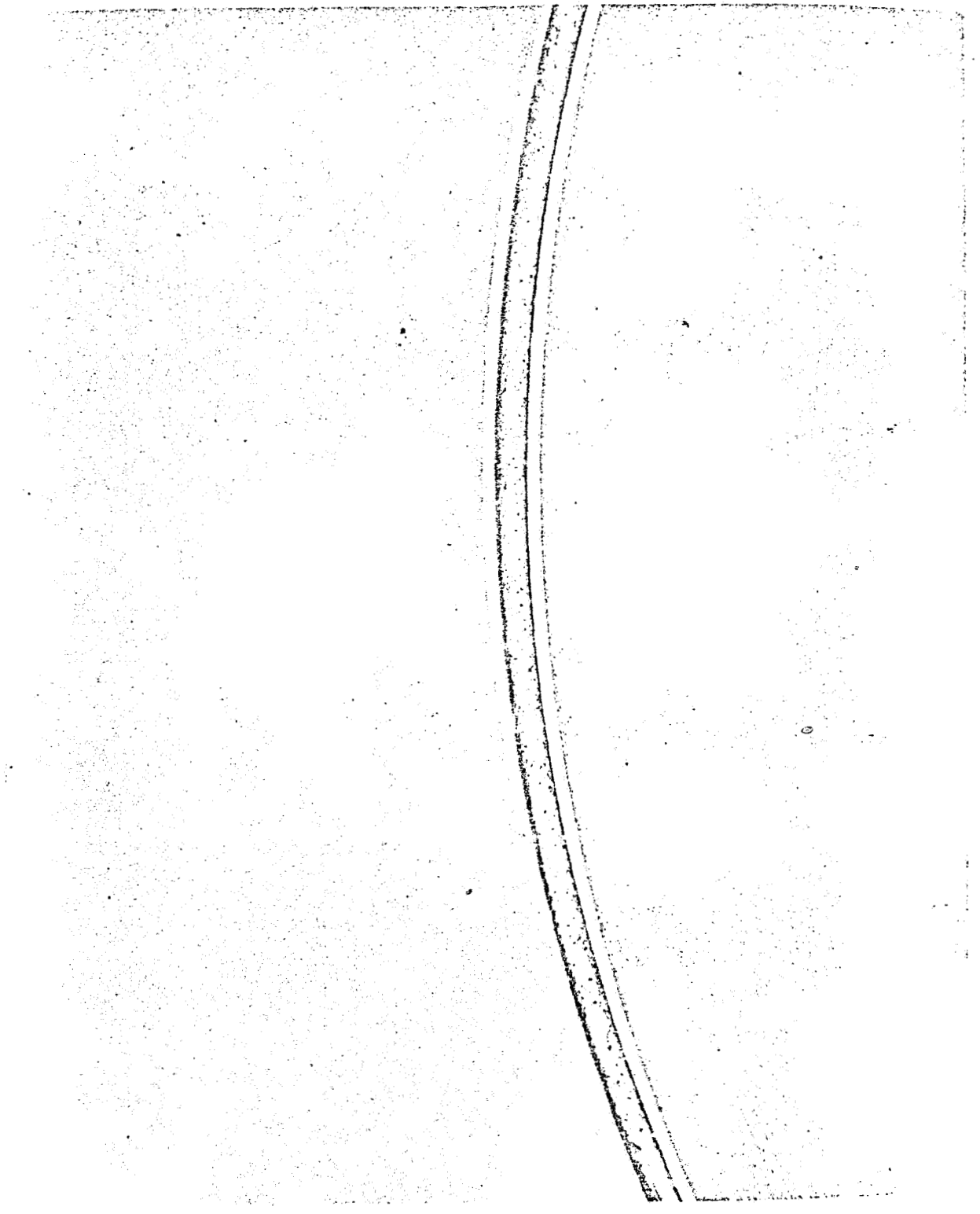

FIGURE 28

N67-86152

EXPERIMENTAL LEAKAGE RATE EXPERIMENTS

BY

F. O. RATHBUN, JR., MECHANICAL ENGINEER
ADVANCED TECHNOLOGY LABORATORIES
GENERAL ELECTRIC COMPANY
SCHENECTADY, NEW YORK

This program was sponsored by George C. Marshall Space Flight Center, National Aeronautics and Space Administration.

1. Introduction

If the fluid connector problem is viewed as involving three areas of study, (1) the leakage of a fluid through passages at the interface between two sealing surfaces, (2) the design response of the supporting structure which positions the sealing surfaces, and (3) the environmental conditions which the system will encounter, it is seen that the basic leakage phenomenon is that of area (1). It is also noted that this area of study has received in the past less analytical and experimental consideration than the others. While some flange geometries and a few mechanical devices have been determined which will cause a gasket-flange system to respond in a certain manner under various environmental conditions, our knowledge to date of the interface phenomenon has been extremely limited. Hence the investigation described herein has been undertaken - that of experimentally describing the leakage phenomenon in terms of a limited number of meaningful parameters.

Parameters which naturally suggest themselves are the gas (or liquid) pressure differential Δp existing across the seal, the stress applied to the gasket, and the rate of leakage through the connector. In this paper, the leakage L is measured as a volumetric rate - atmosphere cubic centimeters per second. The stress referred to as a parameter is applied normally to the surface of a flat annular gasket and is an average value over the surface; hence, a nominal normal stress σ is used.

The above three parameters are, of course, inadequate to completely describe the phenomenon. Some quantitative parameters must be used to describe the gasket and the "flanges". Rather than the consideration of "compatible" materials and the resultant conclusions for certain materials, it appears more basic to consider material properties as parameters rather than the sealing characteristics of particular materials. Thus, two material properties - yield strength and the strain hardening property - are referenced. Each material can be described in terms of these; whatever conclusions can be drawn for a material with a given combination of yield strength and strain hardenability, it is hoped can be drawn for other materials with similar properties. The strain hardenability can be written in terms of a Meyer strain hardening number n, and the yield strength may be called Y. Aside from internal pressure, stress applied to the gasket, the leakage, and the gasket and "flange" material properties, consideration of the leakage phenomenon requires a knowledge of surface finish of the mating surfaces. Hence, the last parameter to be included will be the surface finish, S.F.

Thus, the desired result would be a relationship such as,

$$L = f\,(Y, n, \sigma, \Delta p, S.F.) \qquad (1)$$

The main effort in the experimental program has been to measure accurately, for a given combination of gasket material properties and sealing surface finish, the relationship between leakage through such a sealing system as functions of gasket load and internal pressure. Such an experiment has been conceived to promote a greater understanding of the leakage phenomenon itself. Since analyses have shown that the fundamental leakage phenomenon can be studied

Preceding page blank

in terms of a limited number of parameters which do not include the response of the supporting structure, the experimental apparatus used to study the leakage problem has been designed to exclude the problems of flange deformation, bolt load non-uniformity and relaxation. The concept of the experimental work has been to isolate the leakage phenomenon in terms of those parameters, mentioned above, which are absolutely needed to evaluate the problem, namely, sealing surface finish, material properties, gasket stress, and internal pressure. Hence, the task assigned to such an experimental apparatus is to:

(a) Support two sealing surfaces in such a manner that the inherent flexibility of the sealing surface material will be present, but such that no geometric flexibilities are present. The surfaces should be parallel, one above the other, such that a flat annular gasket can be compressed between them.

(b) Provide a means of compressing the annular gasket uniformly between the sealing surfaces. Means should be available to monitor the magnitude and uniformity of gasket compression. The compressive load should be applied under control at known levels.

(c) Provide a means of internally pressurizing the sealing system with helium. It should be possible to vary the pressure through a given range, and also to maintain such a pressure over finite time intervals.

(d) Provide a means to measure quantitatively the leakage of helium through the gasket system.

In line with the above objectives, an experimental apparatus was designed and is described in the following section. The experimental procedure is outlined in Section 3.

2. Experimental Apparatus

The entire leak test apparatus is shown in Figure 1 and the ensuing photographs.

Components (3) and (4) (the head and body) have machined or ground onto them the prescribed test surface finishes, locations (12) and (13). Item (11) is a locator pin to insure that the head and body seat concentrically. Two safety devices are incorporated, an internal safety ring (2) to protect the vacuum bellows (6) and an external safety ring (7) to protect the experimenters in case of a catastrophic gasket failure at high pressure.

The testing machine used for the applications of load was a Baldwin Southwark load-regulated testing machine with a 60,000-pound capacity. The machine has been equipped with a load maintaining device to allow testing of gaskets at given load over long time periods.

Figure 2 shows the test body surmounted by the test gasket in the correct test position. Two locating pins are placed in drilled holes to properly locate the mating head. Three linear differential transformers are shown in position to monitor gasket deflection. Shown to the left of the photo is the

vacuum line which draws all helium leaked through the seal to a mass spectrometer. The electrical leads shown are for the differential transformers.

Figure 3 shows the internal test facility ready for operation. Affixed to the head are three linear differential transformer cores which ride freely in the transformers themselves. The safety ring is shown in position in the gasket region between head and body. The rectangular grooves in the head (and body) are for positioning the pieces exactly on the "Talysurf" profile recording device. The internal helium pressurizing system is partially shown. The valve and tube in the upper right-hand corner of the photo are the purge line and outlet valve. Shown on the face of the sealing surface are the two passages for helium flow - inward and outward. The tube in the lower left-hand corner is the inlet tube, which has an inlet valve. A helicoid pressure gage, a dry gas filter and a pressure regulator mounted on a 2000 psi helium tank complete the pressurizing system. The dry gas filter used will prevent passage of 98% of all particles 0.4 microns in diameter and 100% of all one-micron-diameter particles. The helium line is also passed through a liquid nitrogen trap to insure that the gas is dry when it reaches the pressure chamber.

The final photograph, Figure 4 shows the entire testing facility, including the testing machine, linear differential transformer instrumentation, General Electric mass spectrometer leak detector (supplemented by a Kiethley 410 micro-microammeter), and the apparatus already described.

In order to measure accurately the leakage from the gasket system, a vacuum is drawn between the outside of the seal and the flexible bellows. A constant pumping action draws the helium molecules escaping from the seal into the leak detector. A vacuum of approximately 4 microns of mercury can be attained within the bellows after the system has been made leaktight itself. The leak detector ideally produces a current proportional to the number of helium molecules passing through it. However, the sensitivity of the system varies from day to day slightly, and the absolute ratio factor between leakage and current is not initially known. Thus, a daily calibration was made on the leak measuring equipment.

Six constant-value leaks have been manufactured. Each day, prior to and after leakage measurements on the test facility, each leak was placed in the leak detector system, and a value of current associated with that leak was recorded.

A separate endeavor was made to evaluate the size of the six leaks by other means. By the method of causing a one-atmosphere pressure differential across the leak, helium was made to flow through the leak. The volume from which the helium flows is maintained constant by allowing a slug of liquid to flow through an affixed capillary tube toward the leak to make up the volume lost by flow through the leak. By monitoring the rate of motion of the capillary slug, the leakage flow rate was ascertained.

This study was successful in evaluating standard leaks through a range of four decades. A constant ratio was found to exist between leakage and current. Hence, a calibration curve for each day was determined. Extrapolation of the linear curve was necessary in the 10^{-8} cc/sec leak range. A

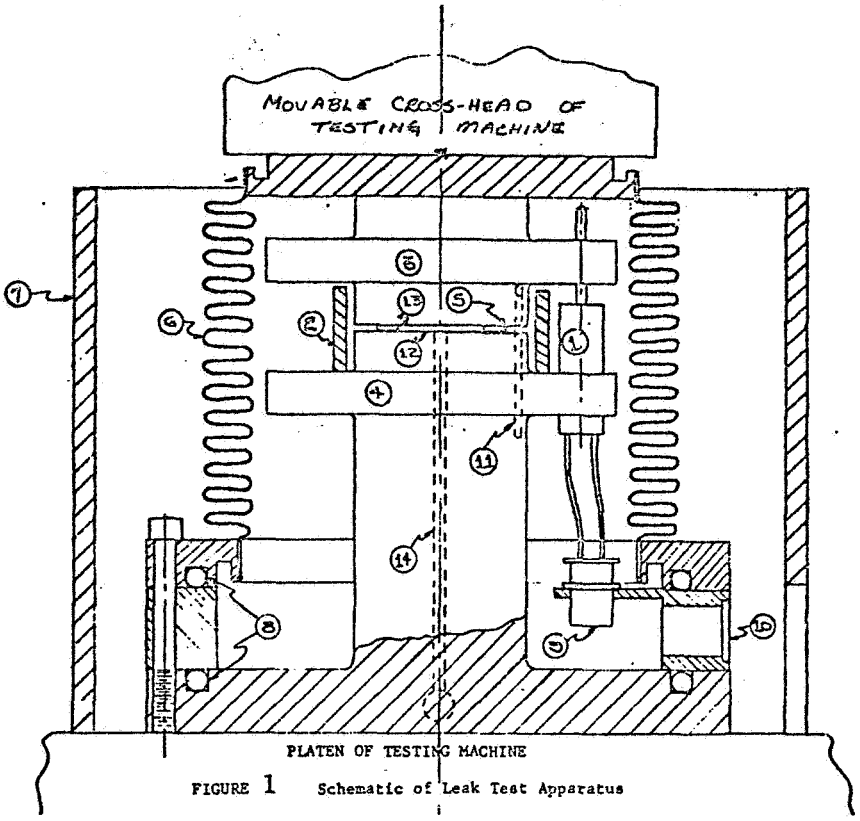

FIGURE 1 Schematic of Leak Test Apparatus

NOTES ON LEAK TEST APPARATUS

(1) Three standard Schaevitz variable differential transformers, model 100-MS-L, located 120° apart - to measure uniformity and magnitude of gasket compression.

(2) Safety cylinder - placed outside gasket-sealing surface system to prevent damage to apparatus by a sudden gasket blowout.

(3) Head of sealing surface fixture - has circumferential lip to support Schaevitz transformer cores.

(4) Body of sealing surface fixture - has lip to support Schaevitz transformers.

(5) Gasket to be tested.

(6) Vacuum system - a U.S. Flexible Bellows (stainless steel), welded to a cover plate and base ring.

(7) Metal cylinder placed around system as a safety precaution in the event of gasket blowout.

(8) Precision #430 O-Rings - for sealing vacuum system.

(9) Three AMPHENOL miniature socket and plug No. 78 S-6-S and 71-S, with retainer rings - to receive leads from Schaevitz transformers.

(10) Instrumentation rings - has three STUPAKOFF multiterminal glass headers, CAT. No. 971606, to receive leads from Schaevitz transformers; has orifice for vacuum pump.

(11) Two holes drilled in fixture body and head, outside gasket live - to receive pins to locate head and body positively.

(12) Sealing surface of fixture body - can be refinished several times to desired roughness.

(13) Sealing surface of fixture head - can be refinished several times to desired roughness.

(14) Two holes drilled axially in fixture body, each to an orifice in the body base - one for pressuring system with helium and one for purging air from system.

X on movable crosshead of testing machine denotes point through which load passes (ball and socket fixture).

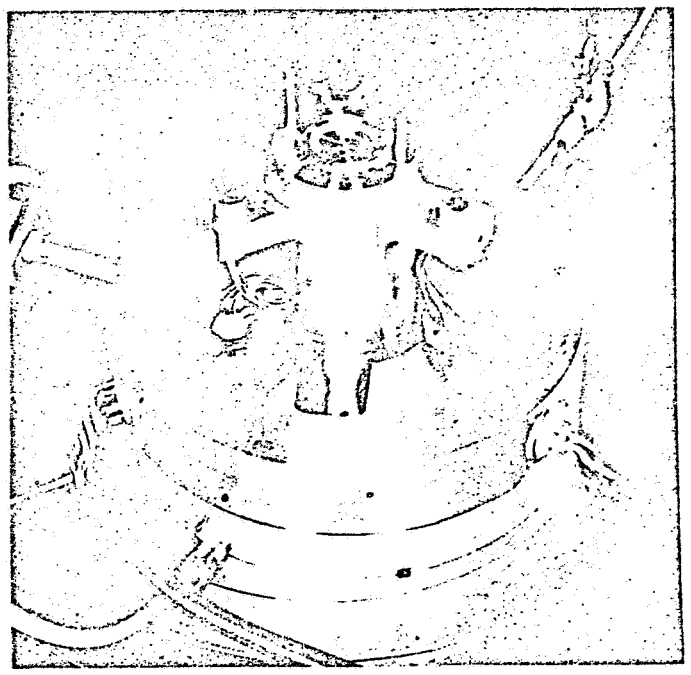

FIGURE 2 Body of leakage testing apparatus showing linear differential transformers in place, gasket resting on body sealing surface, and head locating pins.

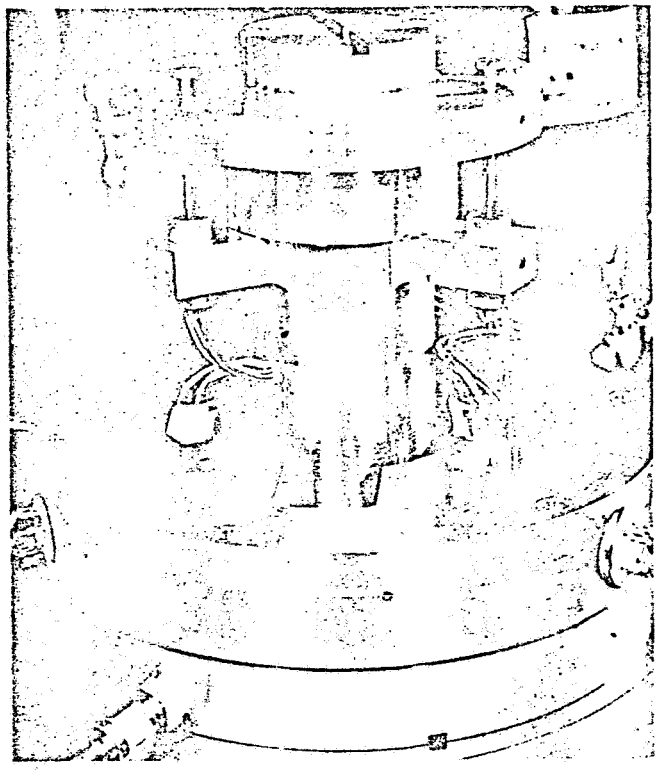

FIGURE 3 Leakage testing apparatus (without vacuum container), showing linear differential transformers connected to head and body. Safety cylinder surrounds gasket region.

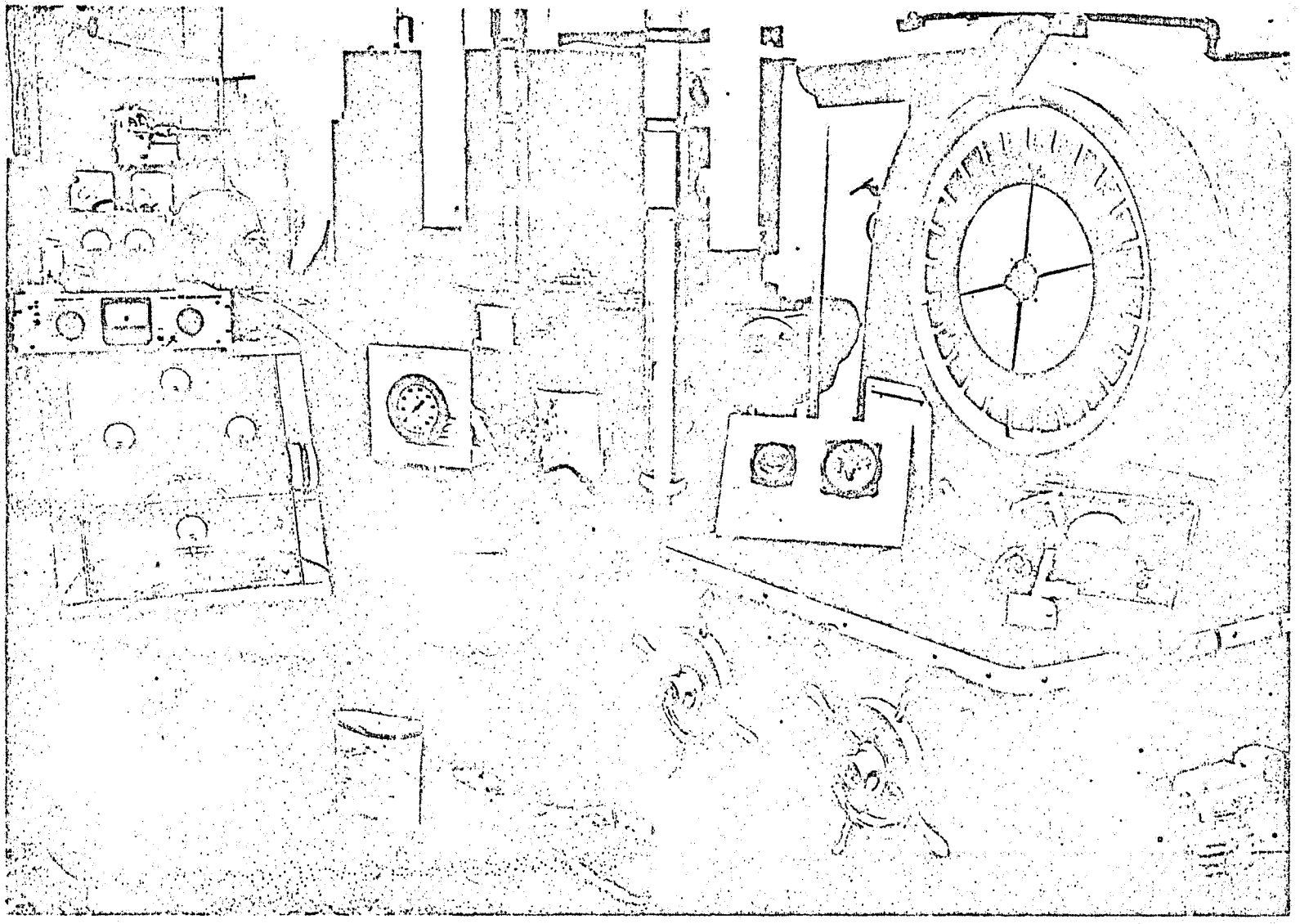

FIGURE 4 Entire leakage testing facility, showing General Electric mass spectrometer, testing machine, linear differential transformer instrumentation, and leakage testing apparatus covered by external safety cylinder.

FIGURE 5 TYPICAL CALIBRATION FOR LEAK DETECTOR

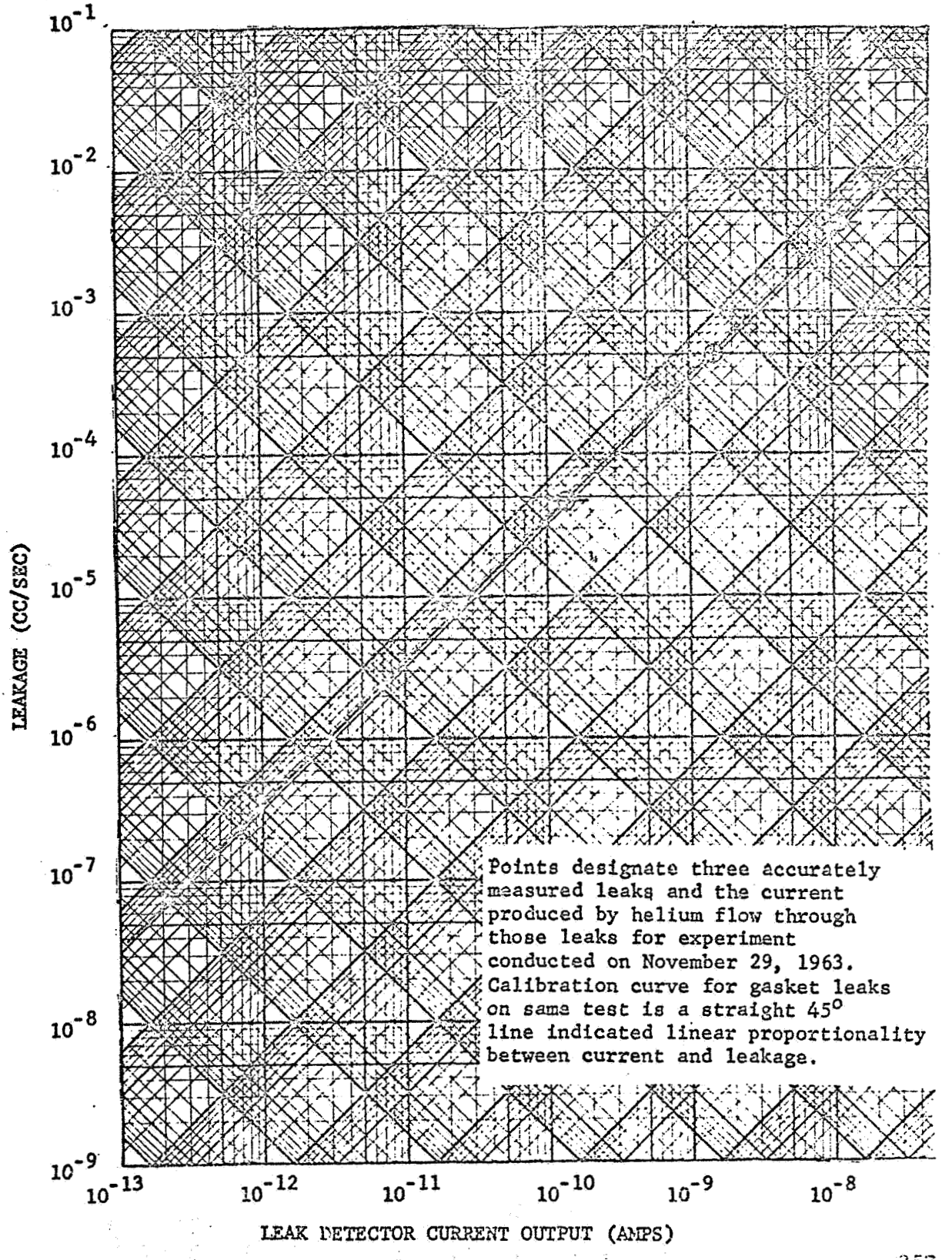

typical resulting calibration curve is shown in Figure 5.

3. Test Procedure

For any given experiment, the sealing surface material, gasket material and surface finish were fixed. The variables of each test then became the normal load P applied to the system and the internal pressure p_i (helium) within the system. The data gained from the experiment is the leakage for various combinations of P and p_i.

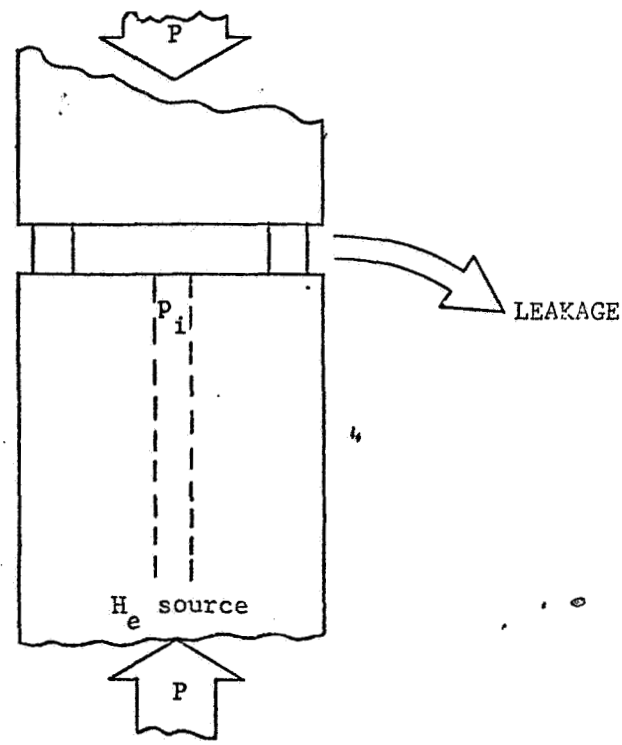

FIG. 6

A LEAKAGE FLOW PATH (schematic)

The chronological order with which load and internal pressure are applied becomes important in the evaluation of the data.

In each experiment three phenomena, referenced phase I, II and III, which could occur in a bolted connector were reproduced in the test.

Phase I

A vacuum is drawn around the outside of the connector system. A helium flush is maintained within the system; hence, a one atmosphere pressure differential exists across the potential leak. The sealing load P is then applied in increments as the reduction of leakage at each increment is recorded. Since the response time of the leakage measurements is in the order of several

seconds, and the load-deflection response of the gasket is not always immediate (particularly in the case of lead and indium, which creep at room temperatures), the leakage is recorded after all transients die out. The time at which the leakage is recorded and the load increment applied is recorded. Increments of loads are applied until the leakage is reduced to the 10^{-7} cc/sec range (or below). The object of this test is to gain information as to the mating of the surfaces and its effect on leakage.

Phase II

At the conclusion of Phase I, the leakage is very low; however, it is caused by a pressure differential of one atmosphere only. As the internal pressure is increased, more leakage is expected. If the gasket system has attained a low leakage by good mating of the interfaces, then the increase in leakage with increasing pressure should flow a smooth curve. If the low leakage is attained by a foreign particle in a potential leak path or by a thin mating barrier, then it is possible for the leakage to increase drastically with pressure. To insure that the low leakage is due to proper mating and to gain a leakage-pressure relationship for a given applied normal stress, Phase II is included in the test. Pressure p_i is increased in increments up to 1150 psi. The leakage-internal pressure relation also shows whether the leakage flow is in the viscous or molecular range. (Viscous flow exhibits a leakage~pressure squared relationship while molecular flow shows a linear leakage-pressure relation).

It can be adjudged from the Phase II test how good a seal exists under the terminal mating and peak stress for a practical internal pressure. Under certain conditions these data can be extrapolated to show leakage for even higher internal pressures.

It must be noted that the nominal normal gasket stress is not kept truly constant during the test; however, it does not vary by more than about 10%. As the internal pressure is increased, the resultant downward force for a given testing machine load decreases by the (pressure X area) vertical load. However, to show the phenomenon, the normal stress can be assumed constant.

Phase III

In a conventional flat gasket connector, a common occurence is that the normal load on a gasket decreases with time. Such can occur due to creep of the bolt, creep of the gasket, external forces being applied, changes in temperature, changes in internal pressure, and a host of other phenomena.

Hence, for a given plastic deformation of a gasket (which has deformed to attain a low leakage rate of the joint), it is of interest to discern the sensitivity of the joint to removal of load. Thus, Phase III consists of removal of normal load in increments while recording the leakage at each stage. To reduce the possibility of a "catastrophic tragedy" should the seal blow out, the internal pressure is reduced to 500 psi (or lower in some tests). Hence, at a constant pressure, load is removed down to approximately twice the internal-pressure vertical load (for safety reasons).

FIG. 7

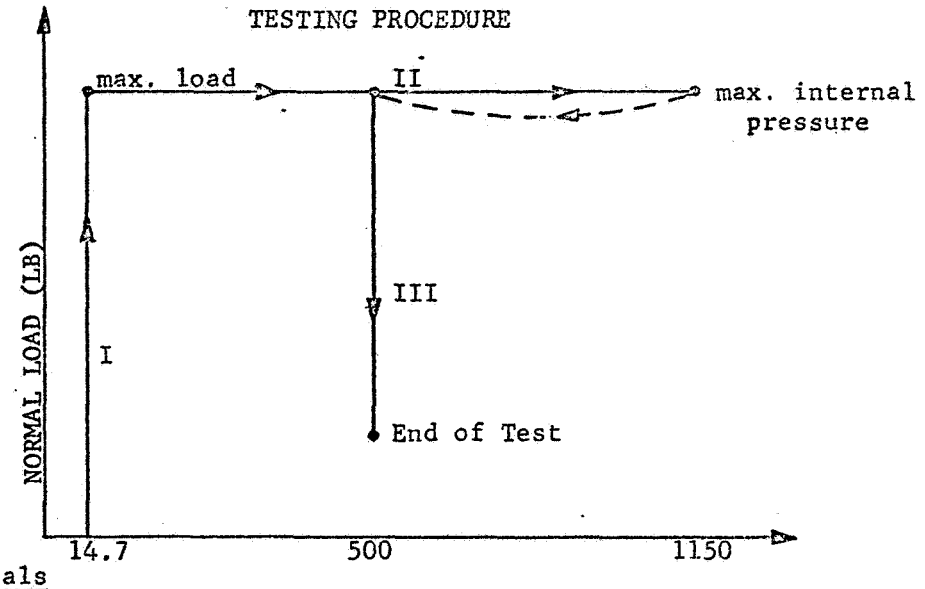

4. Test Materials

4.1 Sealing-Surface Materials

Two materials were selected for use as sealing surfaces (flange materials). Both are currently in use in connector test facilities at the G. C. Marshall Space Flight Center. They are:

(1) 347 stainless steel

(2) 2024(24S)T4 aluminum

The steel used is a tough, difficult-to-machine material with an ASTM listed yield strength of from 35,000 to 40,000 psi. The aluminum has an ASTM listed yield strength of 47,000 psi. To insure a precise knowledge of the actual yield strength of the specimens used in leakage tests, room-temperature tensile tests were accomplished on one-half-inch-diameter specimens of each material. Normal room-temperature ASTM testing procedure was utilized. Two standard yield strengths were evaluated for each material - the 0.2% yield strength and the 0.02% yield strength. The tensile strength was also evaluated in the same experiment. Table I lists the resultant strength properties.

TABLE I SEALING SURFACE MATERIALS

Material	0.02% Yield Strength	0.2% Yield Strength	Tensile Strength
347 S.S.	30,750 psi	39,125 psi	85,000 psi
2024(24S)T4 aluminum	50,000 psi	51,750 psi	69,000 psi

4.2 Metal Gaskets

All gasket metals utilized were much weaker than the materials used for sealing surfaces. Five metals have been used:

1.	Indium	99.97% pure
2.	Lead	99.90+% pure, ASTM B29.55
3.	Aluminum	99.6+% pure, 1060-0 Temper. ASTM209-61
4.	Copper	99.9+% pure, federal specification QQ-C-576
5.	Nickel	99.4% pure, ASTM B160-58T

Material for gaskets was procured in flat stock. Hence, yield strength data for these metals have been gained from specimens cut from flat stock. Since the gaskets cut from the stock are loaded normal to the plane of the stock, the possibility of the yield strength being different for the application and the test exists. Anisotropy of strength of flat rolled stock is possible.

However, tensile test data are indicative of relative strength. Experimental results of tensile data are shown in Table II.

TABLE II GASKET METAL STRENGTHS

Metal	0.02% Yield Stress	0.2% Yield Stress	Tensile Strength
Indium	41 psi	82 psi	202 psi
Lead	1040 psi	1425 psi	2000 psi
Aluminum	3388 psi	4400 psi	10000 psi
Copper	6140 psi	7770 psi	29100 psi
Nickel	10200 psi	13230 psi	45300 psi

The tensile tests for indium and lead were done as prescribed in ASTM Standard 1961, Part 3, ASTM Designation E21-58T (tensile tests for metals at high temperatures). Since at room temperature, indium and lead creep, a prescribed rate of strain was employed consistent with rates for other metals tested within their creep ranges.

The approximate yield strengths of the actual gasket materials used can be obtained also by inspection of the load-deflection curve associated with the leakage experiment. Since three linear differential transformers were used around the periphery of the gasket to monitor the uniformity of gasket compression, it is possible to ascertain the location of the yield point of the gasket material loaded normal to the plane of the gasket. Hence, any effects of anisotropy of the gasket material will not be seen. Since the tensile tests conducted on specimens cut in the plane of the gasket give the yield stress in that direction, but offer no guarantee that the characteristics are the same for the material used as a gasket, the evaluation of a yield strength during the actual leakage test provides a check on the tensile test value and becomes a more meaningful parameter for study.

Because of the gasket height-to-area ratio, the specimen shape is not ideal for compression testing. Friction plays an unusually high role in the compression phenomenon. Also, the compression of a flat annular gasket

approximates the plane strain problem; i.e., the material flow will be radial only (no tangential displacement). Hence, the yield strength noted from load-deflection data associated with the actual leak test will be approximately 1.1 times the yield strength as measured in a normal tensile test. Of course, it is assumed that the yield strength does not vary from the tensile to the compression case.

Also, any data gained from the leak test load deflection curve can be used only to evaluate strength properties independent on magnitude of strain (such as a yield strength evidenced by a distinct change in slope of the load deflection curve). Due to the flexibility of the supporting structure and the local deformation of surface asperities, the relationship between stress and strain will not resemble the true case; e.g. Young's modulus could not be attained. However, the phenomenon does not detract from the yield-strength evaluation as long as the parameter is evaluated consistently for each test.

For the metal-gasket leak tests, data have been accumulated concerning the load-deflection relationship; load-deflection curves have been plotted for each of the three linear differential transformer readings for every test. The indium tests produced no significant data since the yielding occurred before enough data points could be accumulated.

The tests utilizing lead as a gasket material produced a mean yield strength of 2300 psi. The 2300 psi value is that gained directly from the test and hence is approximately 1.1 times the desired yield strength. Thus, by the leak-test evaluation, the yield strength of lead is approximately 2090 psi. Also, it must be stated that the selection of a yield strength by these means is not as refined as the selection of an 0.02% or an 0.2% yield strength. The method used is that of selecting the intersection of the extensions of two straight lines coincident with the elastic line and the yielded load-deflection curve. The resultant load is then divided by the instantaneous area, thus giving a yield-strength value.

Comparing this point geometrically to a similar procedure used on the tensile-test data, it can be seen that the method gives approximately the same results as the 0.2% yield-strength criterion.

Hence, for the case of lead, it can be seen that anisotropy or the effect of friction was a factor. The 0.2% yield strength of the lead in the direction normal to the gasket would be approximately 2090 psi. Extrapolation of these data to an 0.02% yield strength gives a 1525 psi magnitude.

Similar evaluations have been made for copper, aluminum, and nickel. The results of each are listed in Table III.

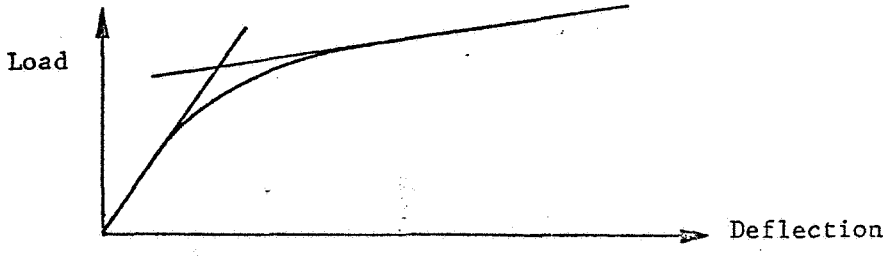

FIGURE 8 DETERMINATION OF YIELD POINT FROM GASKET COMPRESSION TESTS

TABLE III YIELD STRENGTHS OF GASKET MATERIALS

Material	Tensile Test Data			Leak Test Data			
	0.02% Y.S	0.2% Y.S	Y*	1.1 Y*	Y*	0.02% Y.S.^{x}	0.2% Y.S^{x}
Lead	1040	1425	1518	2300	2090	1433	1960
Aluminum	3388	4400	3930	5700	5350	4620	6000
Copper	6140	7770	7200	14000	12700	10820	13600
Nickel	10200	13230	12530	32000	29100	23700	30800

Y* gained directly from load-deflection curves: intersection of extensions of elastic and plastic portions of the curves.

x same ratio of 0.02% Y.S. to Y* as in tensile test data.

It is to be noted that the data gained from the leak tests concerning yield point are averaged in the above table. The dispersion of data was such from test to test to allow such an averaging technique in the case of metals. Since each gasket was cut from the same piece of material, it is reasonable to assume that variances are due to non-uniformity of loading, and that a single value of yield strength is to be expected. It is noted in all cases that the yield strength evidenced in leak tests is much larger than that evidenced in a tensile test. For lead and aluminum, the increase is approximately 37%; for copper, 77%; and for nickel, 137%. Obviously, both the geometry and large friction between surfaces plays a large role; also, anisotropy affects each case differently.

Whatever the reasons, the leak test results are more indicative of the phenomenon of yielding during the actual test; hence, these results are more meaningful as standards of comparison.

Reliable strain hardening characteristics for the metals used both as sealing surfaces and gaskets was not attained.

5. Experimental Results

5.1 List of Experiments

For each metal gasket material utilized, four different sealing surfaces were employed. Both 347 stainless steel and 2024(24S)T4 aluminum base material were employed for sealing surfaces. The yield strengths of each being much higher than the gasket yield strengths, random combinations of sealing-surface specimens and gasket materials were made. No attempt was made to match a particular gasket material to a particular sealing-surface material.

Efforts were made, however, to insure that the surface finishes used for each gasket were nearly identical (for a given type finish). Whenever the sealing surface was damaged in the gasket compression process, a new

surface finish was placed on the sealing surface. Profilometer traces were made of each surface used to insure its adequacy and similarity with previous surfaces of that type. The four surfaces employed in the metal gasket tests were:

(a) Diamond burnished surfaces (DB) with approximately a 4 micro-inch rms surface finish, diamond burnishing accomplished circumferentially. A typical radial profile of such a surface is shown in Figure 9.

(b) Radially ground surface (RG), with approximately a 55 micro-inch rms finish. Grind marks run in 2-inch-diameter arcs from the center of the test apparatus to the edge, resulting in approximately straight radial asperities across the gasket width. A typical circumferential profile of such a surface is shown in Figure 10.

(c) Fine circumferentially machined surface (FM); purely concentric profile, no lead used in the machining process, pitch equal to 0.002 inch, nearly a wedge-shaped profile with a 100 micro-inch rms finish. A typical radial profile is shown in Figure 11.

(d) Coarse circumferentially machined surface (CM) purely concentric profile, no lead used in the machining process, pitch equal to 0.003 inch, nearly a wedge-shaped profile with a 300 micro-inch rms finish. A typical radial profile is shown in Figure 12.

The surface profile on the annular gaskets was recorded only in the case of aluminum, copper, and nickel (the three with the highest yield strengths). For these gaskets, the profile was a normally machined circumferential profile, roughly wedge-shaped, with approximately a 33 micro-inch rms finish. The machining was done with a normally applied lead of 0.001 inch. Such a typical profile is shown in Figure 13. No surface machining was attempted on the lead and indium gaskets due to the softness of the material and the ready deformation of the surface under compression.

The initial gasket geometry was the same in all cases:

inside diameter	0.937 ± 0.0005 in.
outside diameter	1.187 ± 0.0005 in.
thickness	0.060 ± 0.001 in.

The combinations of metal gaskets and surfaces tested, and producing useful data, are listed in Table IV. Early tests with indium were helpful in establishing experimental procedure. The Roman numerals listed are the test numbers.

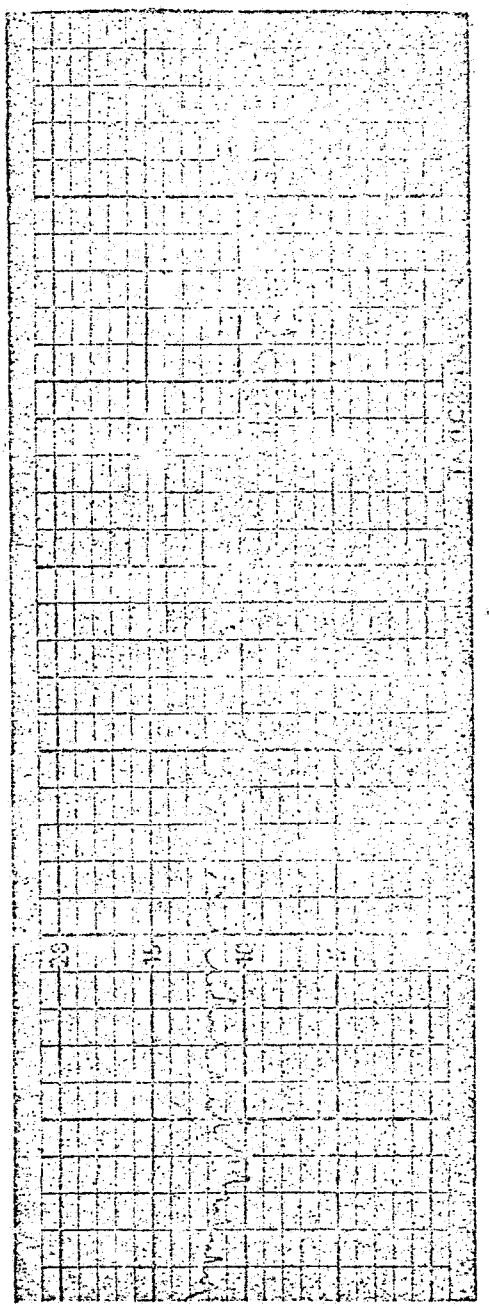

FIGURE 9

Typical radial profile of diamond burnished sealing surface.

Vertical Scale: 10 micro-inches between light lines.

Horizontal scale: 0.01 inch between heavy lines.

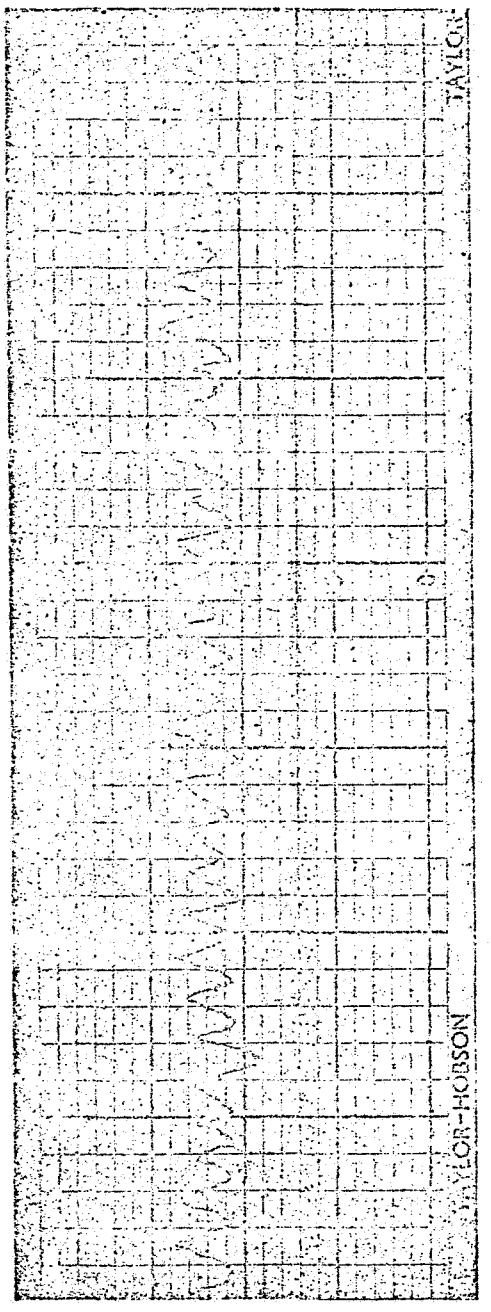

FIGURE 10

Typical circumferential profile of radially ground sealing surfa

Vertical Scale: 50 micro-inches between light lines.

Horizontal Scale: 0.01 inch between heavy lines.

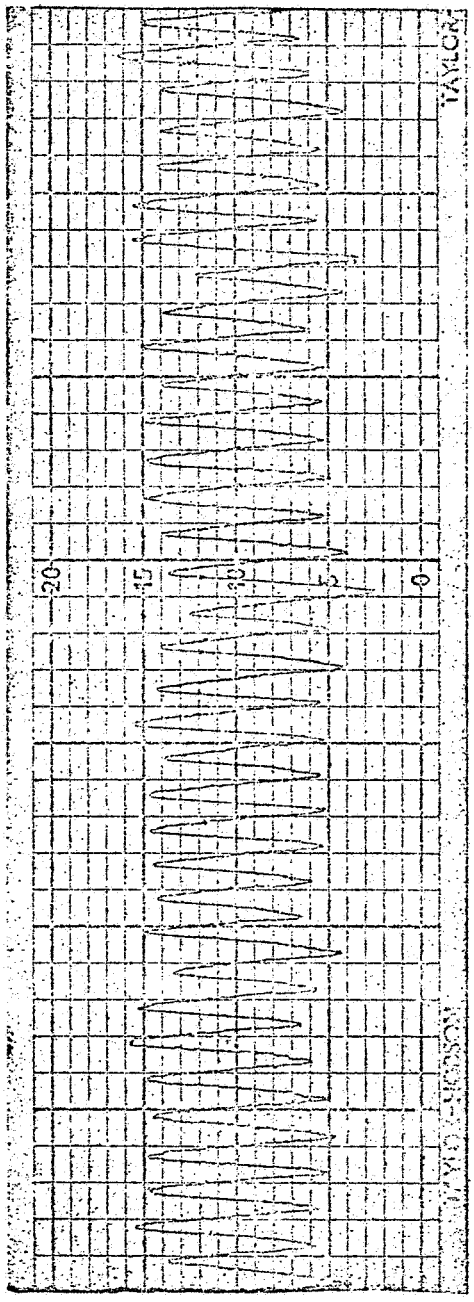

FIGURE 11

Typical radial profile of fine machined sealing surface.

Vertical Scale: 50 micro-inches between light lines.

Horizontal Scale: 0.01 inch between heavy lines.

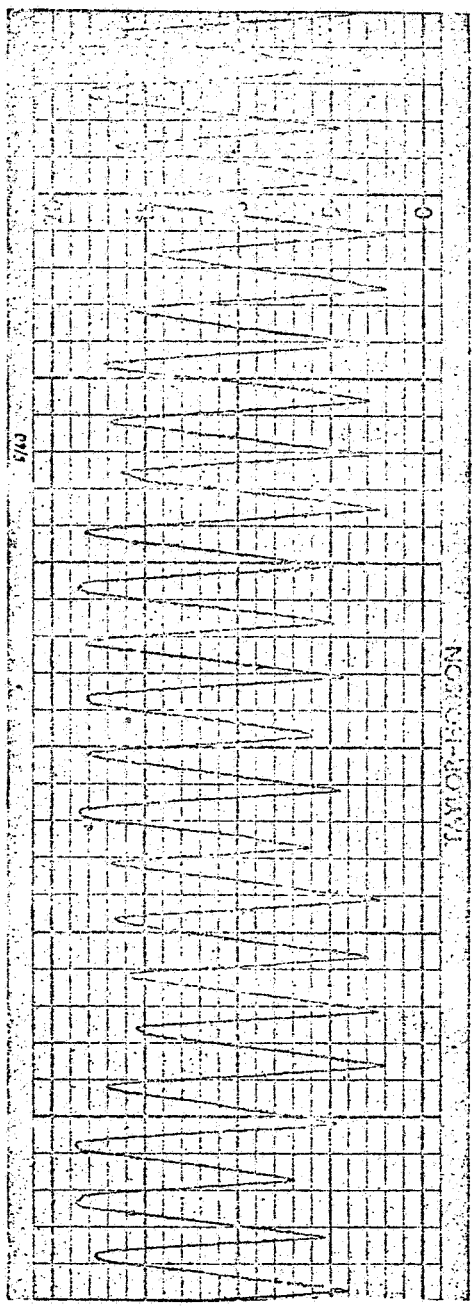

FIGURE 12

Typical radial profile of coarse machined sealing surface.

Vertical Scale: 100 micro-inches between light lines.

Horizontal Scale: 0.01 inch between heavy lines.

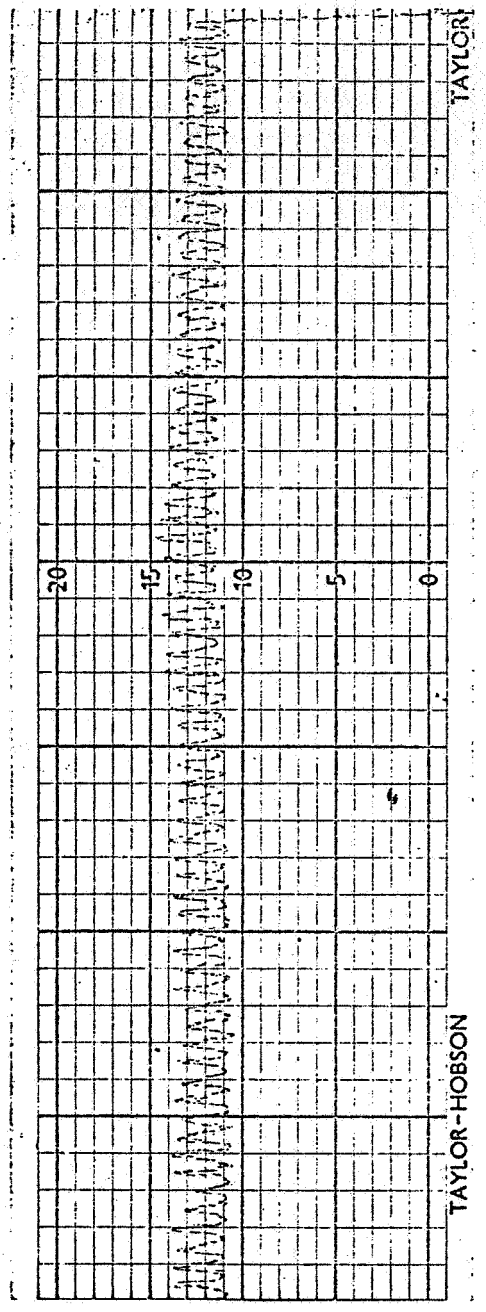

FIGURE 13

Typical radial profile of Al, Cu and Ni gaskets.

Vertical Scale: 50 micro-inches between light lines.

Horizontal Scale: 0.01 inch between heavy lines.

TABLE IV MATERIAL-SURFACE FINISH COMBINATIONS

Sealing Surface Material	347 S.S. Surface Finish				2024(24S)T4 Al Surface Finish			
Gasket Material	D.B.	R.G.	F.M.	C.M.	D.B.	R.G.	F.M.	C.M.
Lead	IX				XI VI	III VII, VIII		
Aluminum		XVI			XIII		XX	XVII
Copper		XIV		XVIII	XV		XXI	
Nickel	X	XII		XIX			XXII	

5.2 Experimental Leakage Rates

During Phase I, leakage rate varies as a function of the increasing nominal gasket stress. Since the quantity to be viewed as a possible meaningful parameter is the yield strength of the gasket material, the stress has been normalized by division of each stress by the yield strength of the gasket material under test. During each test, two parameters have, by necessity, been constant: surface finish of the sealing surfaces and gasket material. Hence, it is of interest to observe the effect of each of these when making comparisons. As is described in Section 4.2 the stress at which yielding occurred during the tests varied as compared with the yield strength as determined by tensile tests. Thus, for Phase I data, the compressive yield stress as determined during the tests was used as a normalizing factor. The Phase I results are plotted in Figs. 14 through 17. Were the same data to be plotted with the results of a given gasket material grouped on a sheet (thus, encompassing several surface finishes), the curves would not appear similar in shape; nor would they group roughly together.

During Phase II, the leakage rate varied as a function of the internal pressure. In each case, the internal pressure at the start of Phase II was 14.7 psi. In all cases, 1150 psi was a goal for the ultimate pressure. However, in some cases, such a peak could not be attained due to extremely high leakage rates at lower pressures. Also, in some cases, no increase in leakage was evidenced until the internal pressure exceeded 14.7 psi by a large amount. In still other cases, leakage dropped off at high pressures due to the closing off of some passages.

For Phase III, in which the sensitivity of the seal to decreasing normal load is explored, the leakage rate is measured as a function of normal gasket load. During this phase, the internal pressure was maintained at an arbitrary value of 500 psi. The data are grouped by sealing-surface finish. In this case, the stress has been normalized by the tensile-test yield strengths. It must be noted that, chronologically, the events graphed read from right to left, i.e., from high stress toward low stress. The results of Phase III are plotted in Figs. 18 through 21.

FIGURE 14 LEAKAGE RESULTS - PHASE I, DIAMOND BURNISHED SURFACE FINISH

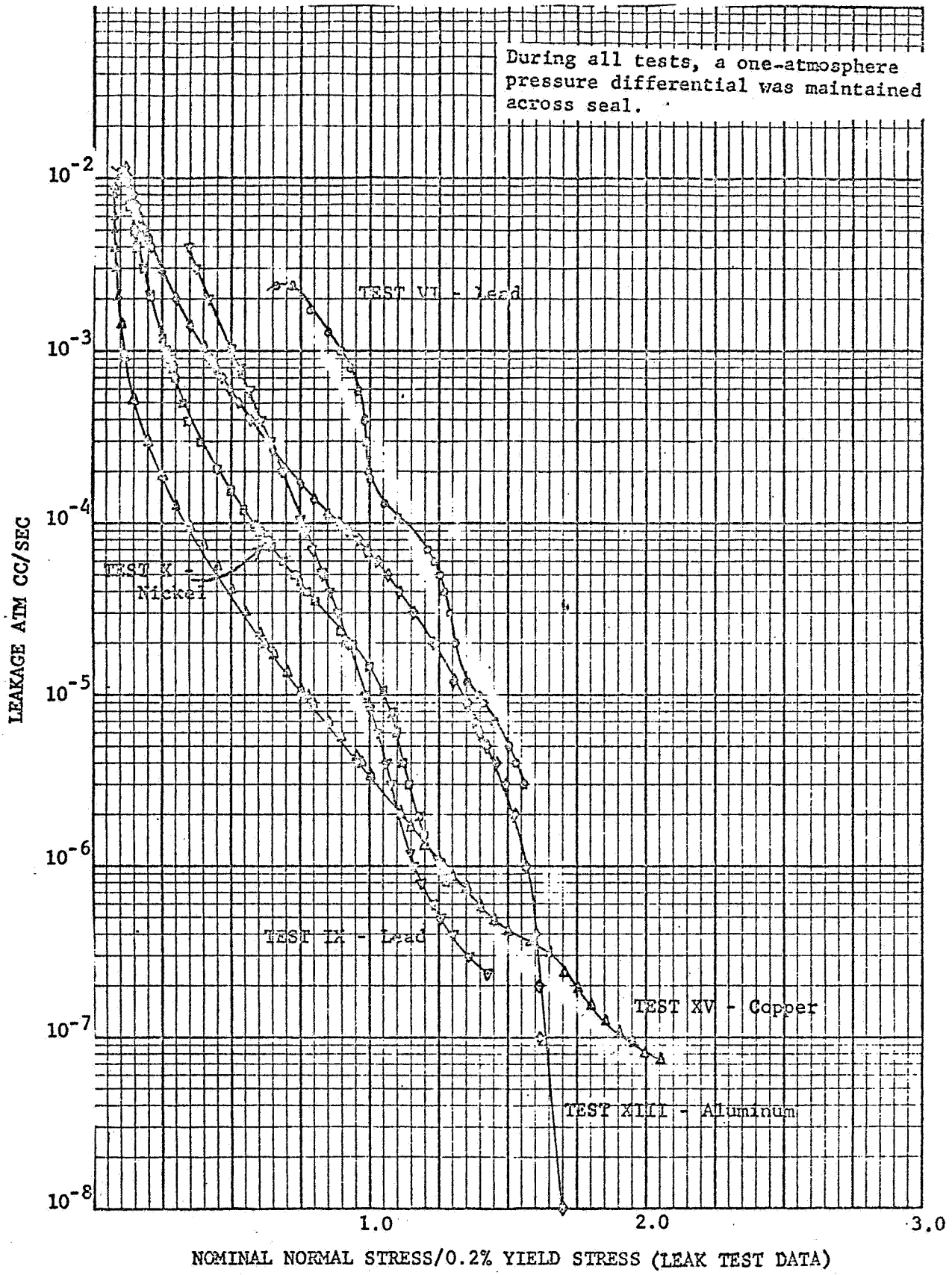

FIGURE 15 LEAKAGE RESULTS - PHASE I, RADIALLY GROUND SURFACE FINISH

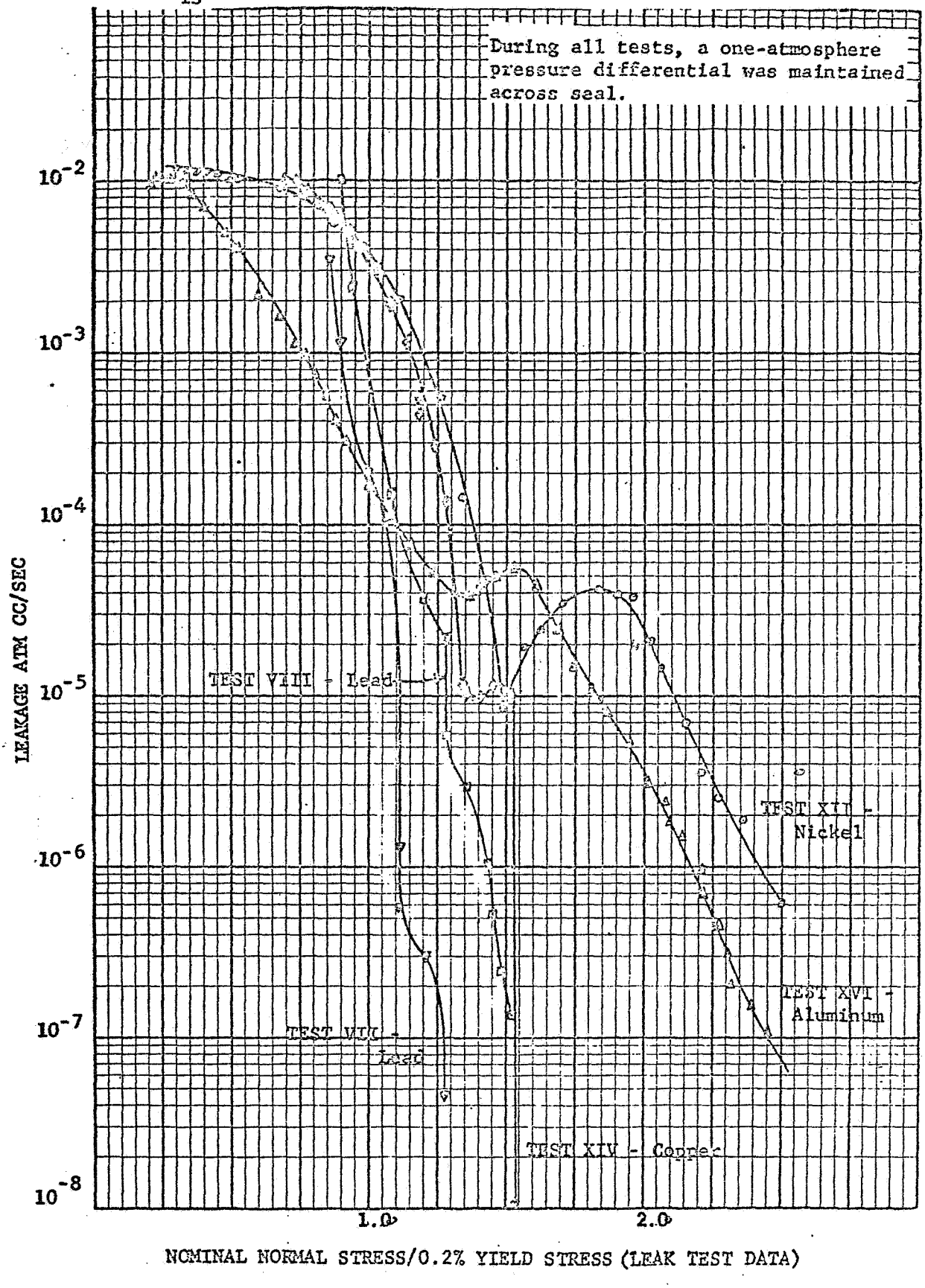

FIGURE 15 LEAKAGE RESULTS - PHASE I, FINE MACHINED SURFACE FINISH

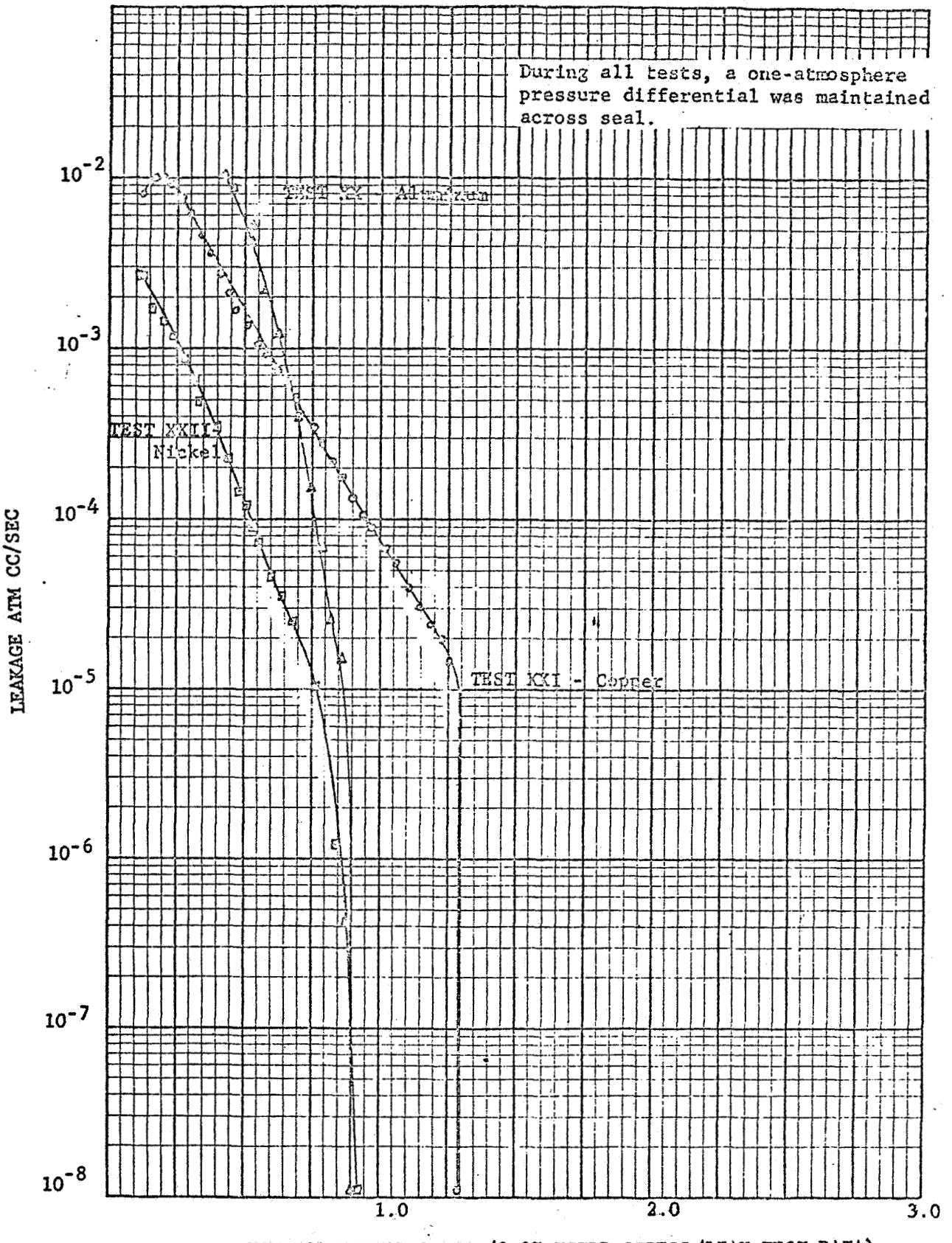

FIGURE 17 LEAKAGE RESULTS - PHASE I, COARSE MACHINED SURFACE FINISH

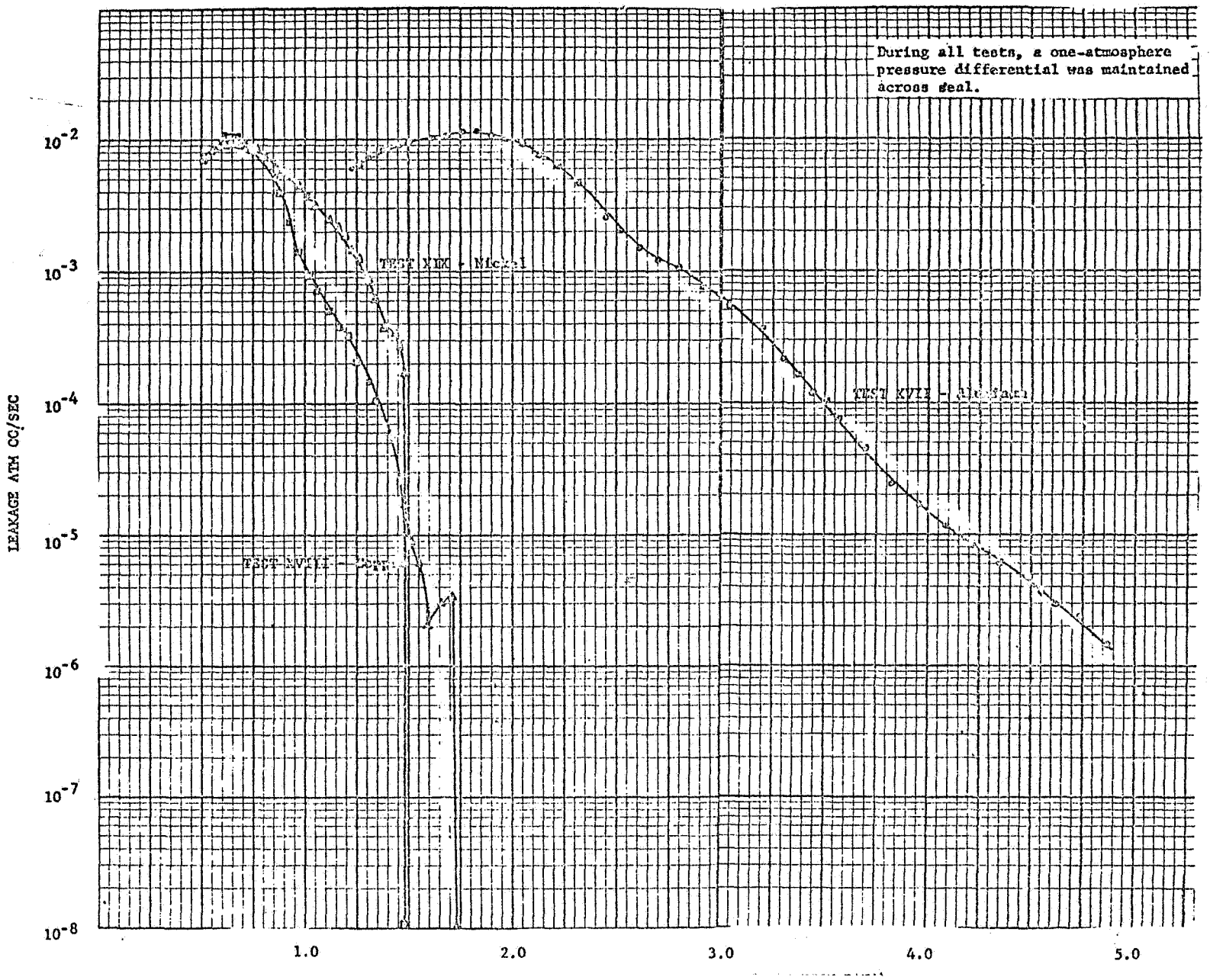

FIGURE 18 LEAKAGE RESULTS - PHASE III, DIAMOND BURNISHED SURFACE FINISH

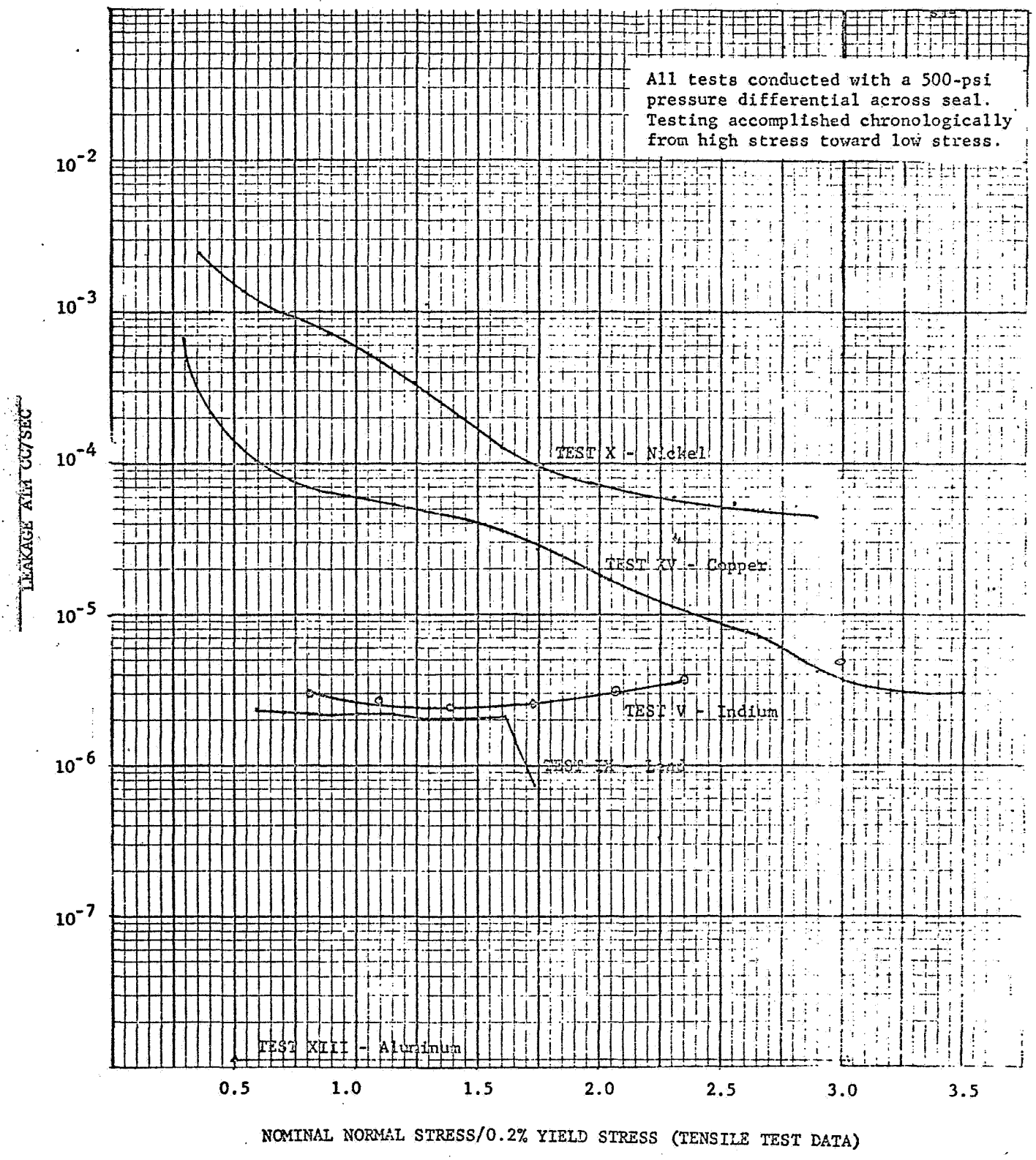

FIGURE 19 LEAKAGE RESULTS - PHASE III, RADIALLY GROUND SURFACE FINISH

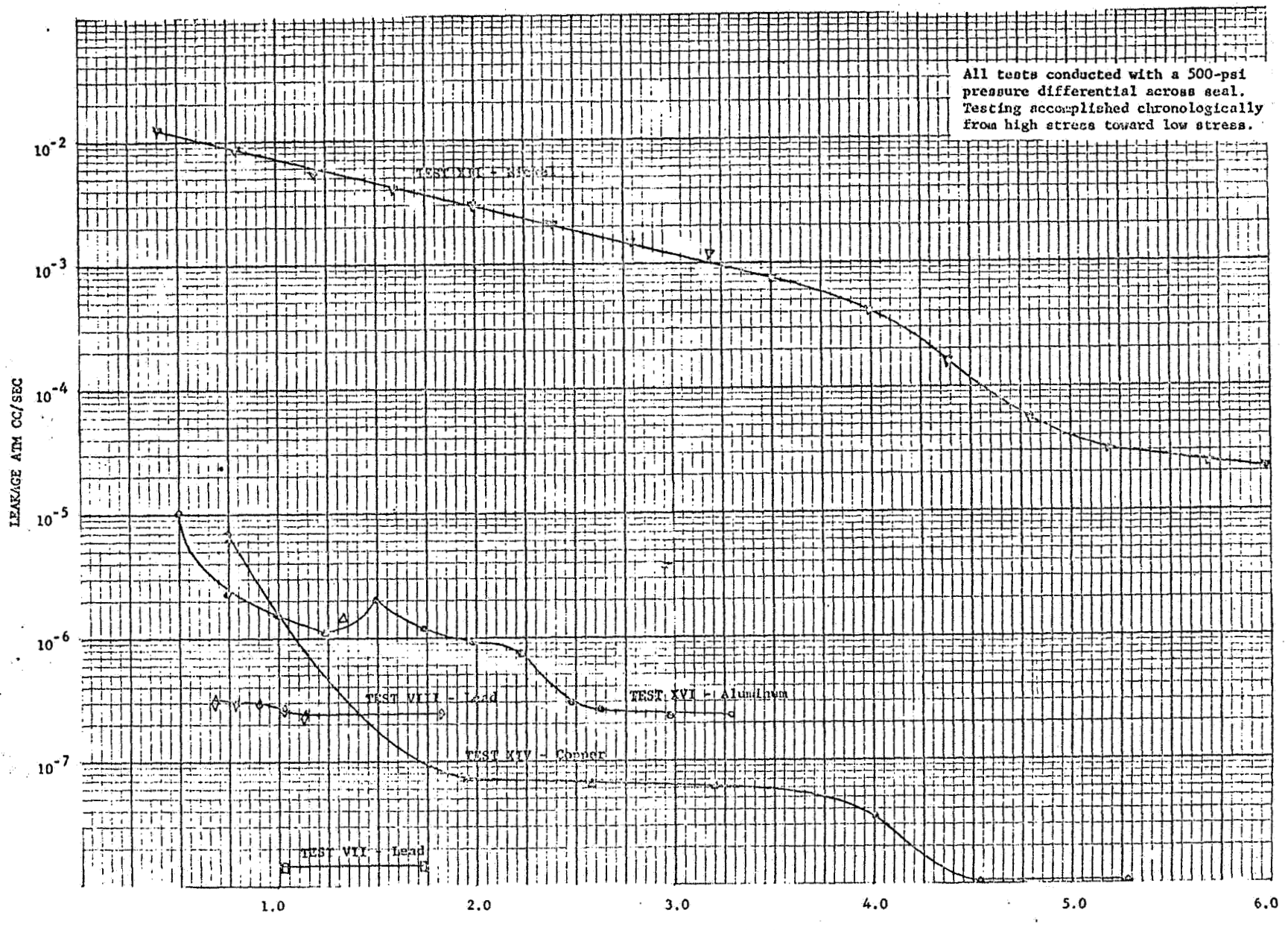

FIGURE 20 LEAKAGE RESULTS - PHASE III,
FINE CIRCUMFERENTIAL MACHINED SURFACE FINISH

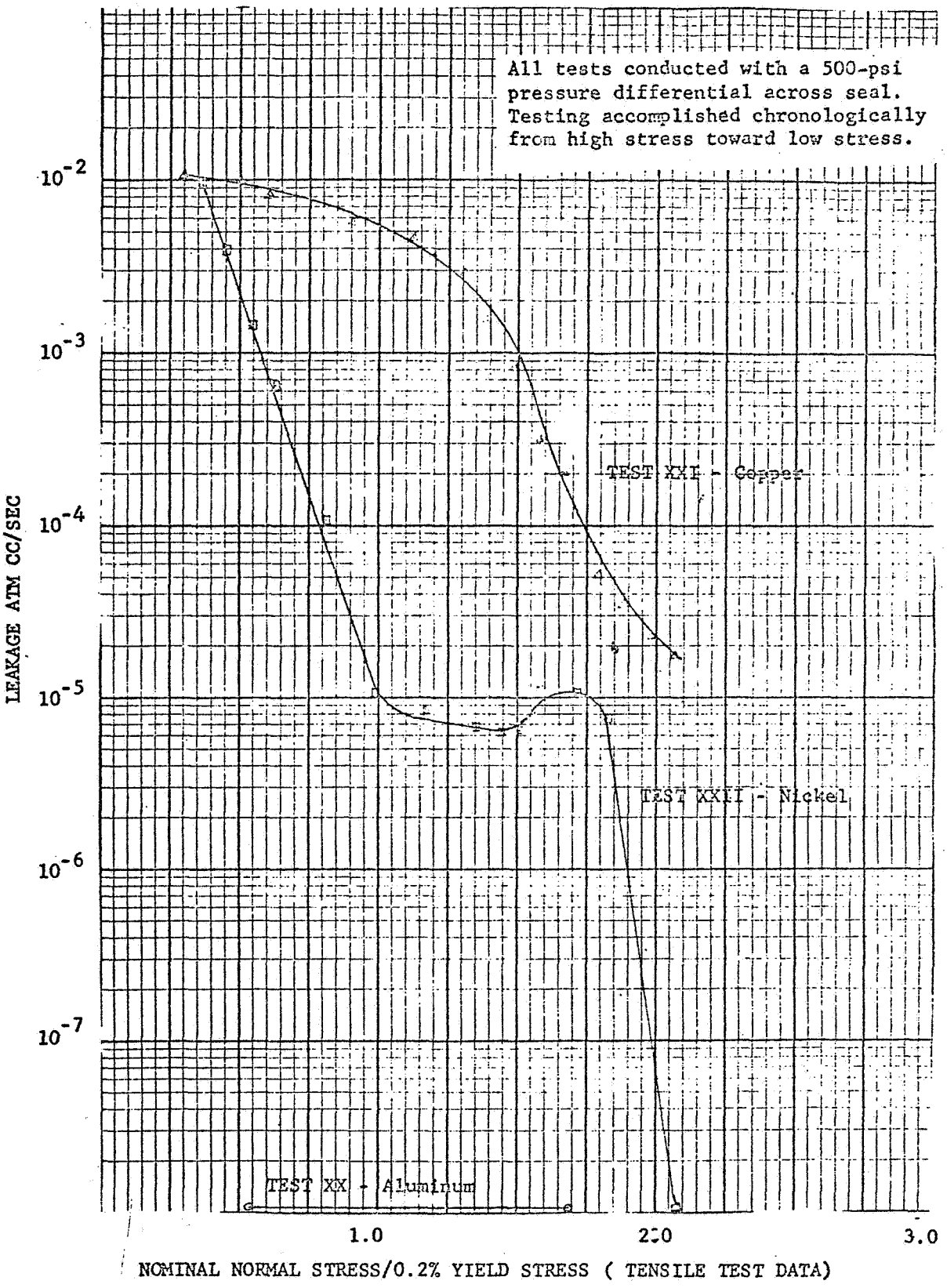

FIGURE 21 LEAKAGE RESULTS - PHASE III, COARSE CIRCUMFERENTIAL MACHINED SURFACE FINISH

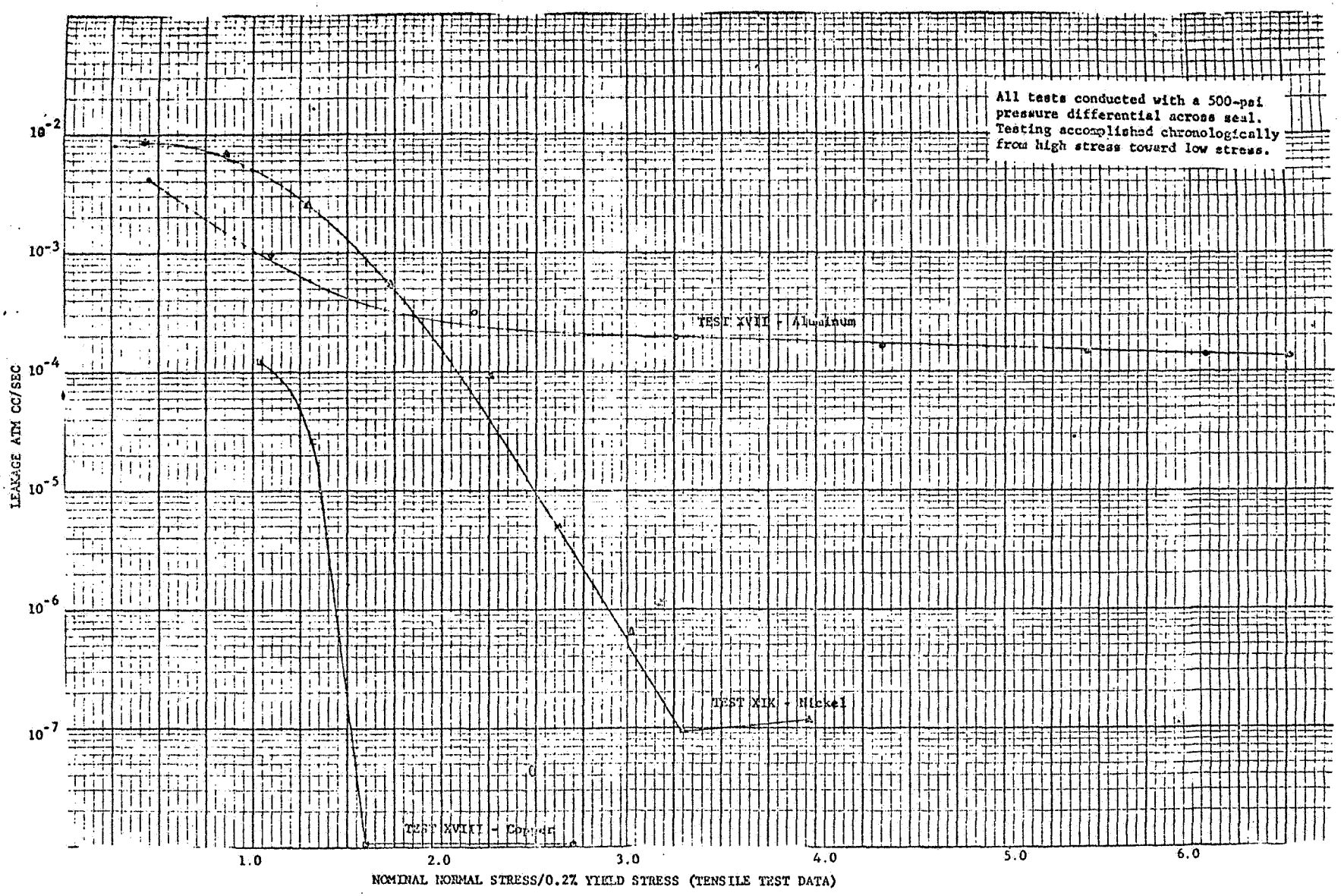

5.3 Visual Inspection of Mated Surfaces

Each sealing surface, regardless of surface finish, was marked with a stylus in four locations prior to the leakage experiment. The marks were positioned, one in each quadrant, such that they lay either near the center of the gasket area or at a point near a gasket edge. In all cases, the mark was very small compared with the gasket width, thus precluding a potential continuous leakage path across the seal.

During the gasket compression, the entire sealing surface was impressed onto the gaskets to a certain degree. The stylus mark also became a feature on the gasket. Hence, upon completion of the leakage experiment, inspection and comparison of both the gasket surface and the sealing surface could be made at four points of mating. In areas near the stylus mark, the actual mating of the surfaces could be examined. Such was done in all cases; high-magnification photographs were taken of both sealing surfaces and both sides of the gasket. Where possible, interference photos were taken (not possible when the sealing surface was extremely rough). All of the photographs yielded information concerning the degree of mating attained in the experiments. In this paper, however, only those photographs are presented which illustrate the lack of uniformity of mating across the interface.

Figures 22 through 25 show an aluminum gasket after a leakage test with a radially ground stainless-steel sealing surface. Two locations are shown, one near the center of the gasket area, and one near the edge. A comparison can be made as to the variation in mating at the two locations. Three different magnifications are shown to illustrate the phenomenon.

6. Experimental Observations

6.1 Experimental Gasket Deformations

Post-leak-test measurements of the nominal dimensions of the gaskets show that the material deforms inwardly and outwardly to about the same extent. The radial deformations inward and outward were identical in all cases involving the stronger gasket materials (aluminum, copper, nickel); in these cases, the deformation was slight, however.

In the case of indium and lead where the deformations were great, the changes in inside and outside radii were not identical but quite close. The change in outside radius was slightly larger than the change in inside radius. In these cases the ratio between normal gasket stress and internal pressure was not as great as in the former cases. Hence, the internal pressure had some effect on the gasket deformation.

It can be concluded, however, that in the metal gasket tests the deformation was nearly a plane-strain phenomenon (as far as gross deformation are concerned), and that curvature and internal pressure played very small roles in determining the geometry of gasket deformation.

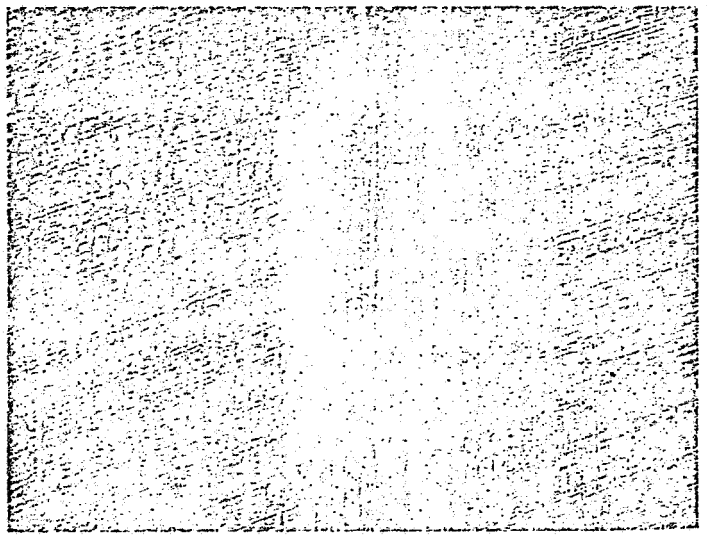

FIGURE 22 Photomicrograph of aluminum gasket after leakage test with radially ground 347 stainless steel sealing surface; - Test XVI. Photo near center of gasket width.
Magnification: 0.0125 inch between scale marks
Maximum nominal normal gasket stress - 2.52 x 0.2% YIELD STRENGTH (LEAK TEST DATA)

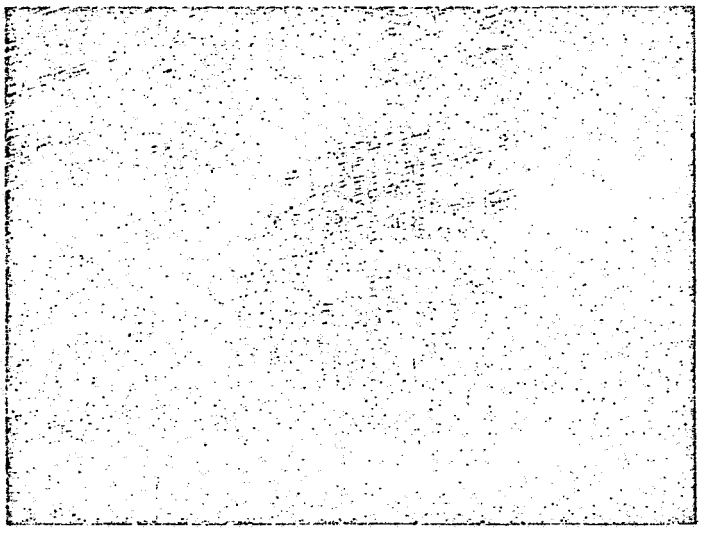

FIGURE 23 Photomicrograph of aluminum gasket after leakage test with radially ground 347 stainless steel sealing surface; - Test XVI. Photo near edge of gasket.
Magnification: 0.0125 inch between scale marks.
Maximum nominal normal gasket stress - 2.52 x 0.2% YIELD STRENGTH (LEAK TEST DATA)

FIGURE 24 Interference photomicrograph of aluminum gasket after leakage test with radially ground 347 stainless steel sealing surface; - Test XVI. Photo near center of gasket width. Magnification: 0.00192 inch between scale marks. Interference lines 11.8 microinches apart. Maximum nominal normal gasket stress - 2.52 x 0.2% YIELD STRENGTH (LEAK TEST DATA)

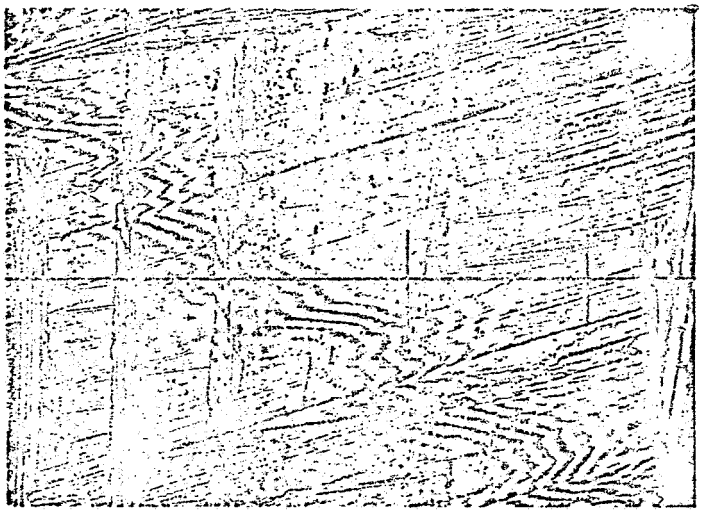

FIGURE 25 Interference photomicrograph of aluminum gasket after leakage test with radially ground 347 stainless steel sealing surface; - Test XVI. Photo near edge of gasket. Magnification: 0.00192 inch between scale marks. Interference lines 11.8 microinches apart. Maximum normal nominal gasket stress - 2.52 x 0.2% YIELD STRENGTH (LEAK TEST DATA)

6.2 Gasket Material Flow Along Interfaces

Tests with gasket materials which underwent large plastic deformations (indium, lead) show that the surfaces initially in contact tend to remain in contact and that the material flow radially tends to emanate from the internal portion of the gasket. This tendency was noted visually in early tests where the gasket surfaces were not thoroughly cleaned. The final area of contact showed the original "dirty" inner region and a bright outer ring. It can be seen then that the bulk flow occurred as shown in Figure 26.

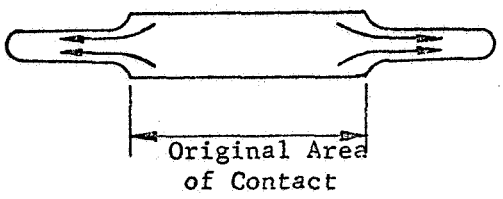

FIGURE 26

DESCRIPTION OF LARGE BULK GASKET FLOW
(FOR NORMAL STRESS YIELD STRESS)

From this observation, it is concluded that the friction along the interface between gasket and sealing surface plays a major role in the actual mode of deformation of the gasket. The problem of the gasket bulk flow then becomes very similar to the Prandtl problem bulk flow of a purely plastic material between two rigid flat plates. The analogy is quite good in the case of the soft metals and generally descriptive in any case where the gasket yield strength is much lower that the sealing surface material yield strength.

Thus, the phenomenon of sealing - the closing of the space between the two surfaces - becomes affected by the friction, at least that portion of the mating accomplished during gross gasket deformation.

6.3 Variation in Plastic Deformation Across Gasket Width

If the gasket - sealing surface compression phenomenon is nearly the same as the Prandtl problem phenomenon, then the normal stress distribution on the gasket surfaces will be of the form shown in Figure 27.

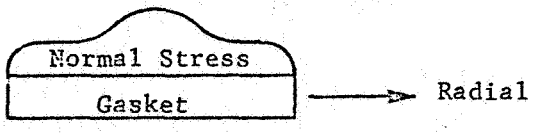

FIGURE 27

NORMAL STRESS DISTRIBUTION ON GASKET

The nominal normal stress is, of course, the average value of such a distribution, and is known from the applied load. The distribution shown is predicated on the gasket being purely plastic, the sealing surface being rigid, and the ends of the gasket being unrestrained.

No controlled measurements on the normal stress distribution were made during the investigation. However, some observations show that the distribution is probably correct. During one test, where a nickel gasket was used in conjunction with a radially ground sealing surface, great difficulty was experienced in attaining a low leakage rate. Thus the gasket stress was increased to a maximum value of 79,150 psi, which is 2.02 times the 0.2% yield strength of the stainless steel. Hence, gross plastic deformation occurred in the head and body of the apparatus. An annular shaped depression was formed under the gasket. Its profile was as shown in Figure 28.

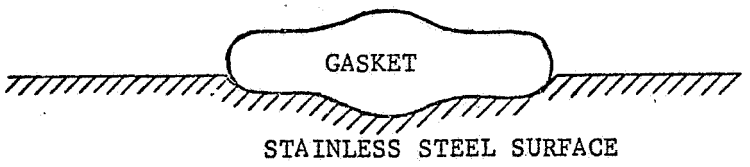

FIGURE 28

DEFORMATION OF STAINLESS STEEL SEALING SURFACE

The similarity between the depression profile and the probable stress distribution on the gasket surface (and therefore the steel) can be noted. Thus, even in the case of nickel, the strongest of the gasket materials used, the stress distribution shown in Figure 27 seems descriptive.

Concomitant with the depression in the stainless steel in test XII, a retention of the original surface finish was noted. While the stainless steel had deformed grossly, the surface geometry (asperity distribution) had not. Pre-test and post-test profilometer traces showed that the surface had changed very slightly. Only the tips of the asperities had been rounded somewhat. The rms and CLA values of the surface had not changed appreciably.

Such a phenomenon can be predicted from previous experimental and analytical work on rigid dies and plastic half spaces. Slip line theory predicts that the plastic flow will initially occur at a distance beneath the area of contact and to the sides as shown in Fig. 29.

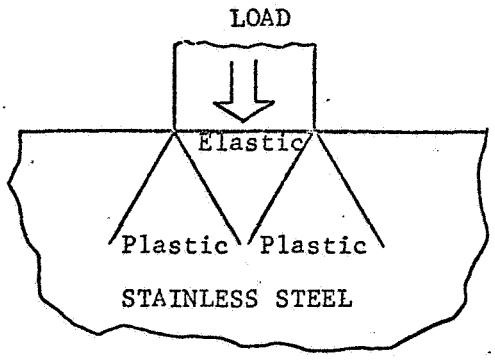

FIGURE 29

PROBABLE PLASTIC - ELASTIC REGIONS IN STAINLESS STEEL

Such a phenomenon has some practical ramifications regarding the fluid-connector problem. First, the stronger of the two metals will retain to a great extent its surface profile. Since the weaker material (usually the gasket) will deform plastically and fill the spaces between asperities on the stronger material, those asperities are "protected" during further deformation of the system. Re-use of the sealing surface (the stronger material) is thus possible, even in cases where the applied stress has exceeded its yield stress. (In cases where the substructure has been grossly deformed, this is certainly not true).

Secondly, it is illustrated that no matter how high the normal stress, the surface deformation is not severe on the stronger material. Hence, it must be concluded that the sealing must be completely accomplished by deformation of the weaker material. It can be shown that even with higher normal stresses, further deformation will occur at other than the area of contact (beneath the surface of the stronger material).

The important question arising from the above observation is, "What effect does increasing normal stress have on the weaker material?" That is, can the weaker material completely mate across the area of contact?

Results of several tests show that the degree of mating, even under extremely high stress, is not uniform. Figures 22 through 25 illustrate clearly the non-uniformity of mating. The test results shown apply to an aluminum gasket and a radially ground stainless-steel sealing-surface material. The phenomenon was not limited to this particular test; however, this test illustrates both the non-uniformity (and distribution) of mating and other important phenomena occurring. In Figures 22 through 25, the asperities running roughly horizontally constitute the pattern of asperities on the stainless steel. These asperities were not originally on the aluminum shown. The vertical lines are the asperities machined onto the gasket, and constituted the original gasket profile. The gouge marks shown in the photos are the stylus marks originally made on the stainless steel and not originally appearing on the gasket material. The original directions of asperities are as shown in Figure 30.

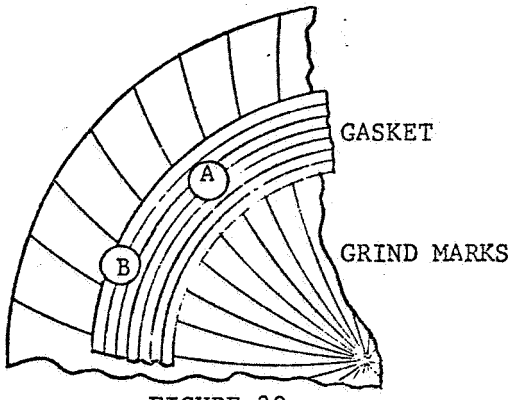

FIGURE 30

SURFACE PROFILE DIRECTIONS, TEST XII

Upon completion of the leakage test, the gasket was removed from the fixture and the photos taken at locations A and B (Figure 30).

In Figure 22, the central area A is shown; and it is obvious that the degree of mating is very poor. The vertical lines dominate. Figure 23 shows location B; and it can be seen here that the horizontal lines not only dominate, but are the only pattern visible at the edge. It can be estimated that, at the center, mating occurred over about 40% of the area and near the edge, from about 65% up to 100% at the very edge. The interference lines in Figures 24 and 25 show that where mating did occur, at the edge or near the center, the mating was the same. (The variation in interference lines is the same magnitude). Inspection of the stainless steel surface at the same points showed identical features. Two important phenomena are seen here - each very important in connector design.

First, it can be seen that the best mating (sealing) does not occur at the point of maximum normal stress; it occurs at the edge, where normal stress was minimal. It does occur where the greatest amount of gross gasket translation took place. It can be seen that, no matter how hard the gasket is pushed vertically onto the sealing surface, if the gasket material is contained (as it is at the center) the gross deformation is not large. This, theoretically, is due to a large hydrostatic condition of stress, but a small stress deviator, (the plastic deformation being proportional to the stress deviator). At the edge, where no constraint is available, the deformation is large, and the mating better. Here the stress levels are less; however, the stress deviator is large, and the hydrostatic stress is small.

The phenomenon can also be explained by viewing the mating as a function of shear deformation. Where no shear deformation at surface was allowed, the mating was poor. Where the surfaces "slid", one with respect to the other the mating was good.

Hence, we conclude that mating of surfaces is best performed not by brute-force compression, but by the shear deformation of the softer material. Hence, geometrical configurations which utilize shear deformation as the means of sealing (such as knife-edge seals) have excellent prospects of success.

Secondly, this test (along with other tests) illustrates that, even though the stronger material in a flat annular gasket geometry connector has asperities running in the direction of potential leakage flow, the prospects of obtaining a successful seal are good. In this test (and others) very low leakages were attained. This is true because the "hills and valleys" of the stronger material not only are paths for fluid flow, but are excellent paths for plastic flow of the gasket material. As the gasket flows outward, little geometric resistance to plastic flow at the interface exists. Hence, the mating is quite good. An important corollary of this is that surface-finish requirements on flanges need not be so severe in certain cases if the phenomenon occuring is understood and offers the type of mating described above.

6.4 Evaluation of Phase I Leakage

During Phase I, the two parameters varied from test to test were surface finish and gasket material. In order that a comparison of materials could be made, the stress level at each stage was divided by the yield strength of the gasket material. Two such yield strengths were used; the first is that measured from a tensile test (and would constitute a pure material property known by the test), and the second is the stress level at which gross yielding occurred during the leakage experiment. This, of course, is also a function not only of the material properties but also of the geometry of the gasket and the friction at the interface between gasket and sealing surface.

Comparing curve shapes for all tests conducted, it becomes apparent that surface finish has a larger role than the deformation properties of the materials. It can be said, in general, that traces for a given surface finish are similar in shape regardless of the gasket material used.

When the yield-strength data from tensile tests were used as a normalizing factor, the spread in curves for a given surface finish was great. However, when the compressive yield stress as determined during the leak tests was used, the curves become much closer in all cases, and the following statements can be made:

(1) For the diamond burnished surface tests the leakage rate reached 10^{-6} atm cc/sec by the time 1.6 times the yield stress was reached for all cases. The steepest slope of the leakage stress curve occurred at stress levels of about .25 times the yield stress.

(2) For the radially ground case, the sudden increase in leakage rate occurred between 1.25 and 1.5 times the yield strength. Sealing to the degree of 10^{-6} atm cc/sec was attained in all cases by a stress level of 2.1 times the yield strength.

(3) For the fine machined surface, the sealing occurred at about the yield stress in two cases, and at 1.30 times the yield stress in another.

(4) Again, the coarse machining surface tests yielded wide scatter, two tests sealing at about 1.7 times the yield stress and one at about 5 times the yield stress.

Thus, in all cases except for one coarse machined surface case, sealing to 10^{-6} atm cc/sec was attained by the time the stress level was equal to 2.1 times the yield stress. Thus twice the yield stress (where the yield stress is identified as the point of initiation of bulk yielding of the gasket) appears to be a reasonable minimum value of stress for general flat annular gasket use (across a one atmosphere pressure differential).

6.5 Evaluation of Phase II Leakage

The meaningful information found in Phase II is the sensitivity of the leakage to internal pressure. Can data gained at a one-atmosphere pressure differential be used when the pressure is increased?

Results show that the lead and indium (soft metals) are very insensitive to pressure, regardless of surfaces used. The most sensitive is the radially ground surface. Whether the leak was molecular or viscous cannot be determined from the tests concluded. One important fact shown in Phase II is that the curves are generally smooth, indicating that a solid mating has been attained, and no "blowout" occurred during the test. The conclusion gained from this phase is that insensitivity to pressure can only be assured when very soft gaskets are utilized.

Loads found from Phase I for small leakages must be increased to insure sealing at higher internal pressures. However, it was noted on several tests that the increase of load at the close of Phase II to cause the leak to drop was not too great, never an increment more than 0.25 times the yield stress.

6.6 Evaluation of Phase III Leakage

A very important consideration in any connector is what happens when the initial sealing stress decreases. Will the seal open? Phase III results largely answer this question. From the graphs showing leakage as a result of decreasing load, it can be concluded that,

(1) If a very soft gasket is used, and mating is nearly completed over the apparent area (large plastic deformations), the connector will be almost completely insensitive to reduction of stress.

(2) As the gasket material becomes stronger, and the deformation is, to a great degree elastic, the seal will be very sensitive to loss of stress.

(3) The coarse surface finish tests, where sealing occurred only at points, show that the seal is extremely sensitive.

(4) For smooth surfaces, the sensitivity is less.

The most important factor is the amount of plastic flow in the system at the time. If the plastic flow is the factor governing leakage, then the seal will be generally insensitive. The plastic flow can be caused by the disparity in material strengths or by surface geometry.

7. Conclusions and Recommendations

The principal findings in the study of the seal interface are briefly summarized below.

7.1 Conclusions - General

1. The gross deformations of the flat annular gaskets obey plane strain criteria.

2. If the sealing of a gasket system is caused by plastic flow of the materials mated, then the seal is very insensitive to removal of the deformation-causing stress.

3. When gasket normal stresses are so severe as to cause gross sealing surface distortion, the surface asperities tend to be preserved.

4. The stress on the gasket is highest at the middle of the gasket width and becomes less at the edge.

5. Observations show that sealing of an annular gasket-sealing surface system is possible even when the asperities on the stronger material run in the direction of potential leakage flow.

7.2 Conclusions - Metal Gaskets

1. The best mating on the flat annular gasket-sealing surface system occurs at the gasket edge, the point of minimum normal stress.

2. The plastic flow of soft metal gaskets tends to start from regions internally within the gasket. The surface shear stress tends to control the mode of plastic flow.

3. Insensitivity of metal gasket seals to increases in pressure differential can be assured only if the gasket deformation producing the seal has been plastic in nature. Thus, from this standpoint, the soft gasket materials which experience gross plastic deformation at low stress levels appear to have better potential in static fluid connector design than harder metals.

4. Rough sealing surfaces cause sealing to be affected by elastic gasket deformation, and are quite unstable during removal of load.

5. Where metal gasket seals were found sensitive to internal pressure, it was possible to reduce the leakage rate by adding an increment of stress not more than 0.25 times the yield strength of the gasket material.

6. For all metal gaskets used, it has been possible to attain leaks as low as 10^{-6} atm cc/sec for nominal normal stresses on annular gaskets equal to twice the stress level causing initial bulk flow of the gasket material (at a pressure differential of one atmosphere).

7. At the center of the gasket width, mating between gasket and sealing surface can be effected only by applying normal stress many times the yield stress.

N67-86153

A BOLTED FLANGE JOINT INCORPORATING A SOFT ALUMINUM GASKET

BY

J. A. Zimmerman
Group Engineer
Titan II Propulsion
Martin Company

INTRODUCTION

During the basic design phase of the Titan II I.C.B.M. the need became evident to develop a sealing device which could contain propellants for periods up to one year without leakage. The propellants concerned are a 50% mixture of UDMH and Hydrazine in the fuel system and Nitrogen Tetroxide in the oxidizer system. The propellants are hypergolic, which in itself creates stringent requirements on leakage. Any leakage in the oxidizer system causes nitrogen tetroxide to combine with humidity producing nitric acid, which results in corrosive attacks to the aluminum components. Figure 1 reflects the Stage I, Titan II, propellant system and the location of the areas requiring a leak tight connection. The Stage I propellant lines are 10" diameter and 7" diameter in the oxidizer system and 6" diameter in the fuel system. The Stage II propellant system is similar; however, the propellant line sizes are 4" diameter in the fuel system and 6" diameter in the oxidizer system.

The bolted flange was investigated and selected for use because of its long established reliability. It can be designed to cover a wide range of environments by changing a few variables such as the material, strength, flange thickness, and the number and the size of bolts. It can be designed for any range of internal pressures, axial tension, compression, bending, torsional, or vibration loads. The flange is relatively easy to manufacture because it does not require extremely tight machining tolerances. Several types of bolted flanges where investigated and eliminated for various reasons such as material compatibility and/or inability of the design to meet the leakage criteria.

SINGLE SERRATED FLANGE

A. Design

To solve both the compatibility and the leakage problems, a soft flat aluminum gasket design was investigated. The investigation resulted in a design which incorporates a serration in each flange. The serrations, when the joint is assembled, embed into the soft aluminum gasket (1100-0 series aluminum) and provide a seal. Figure 2 shows the design. Both flange mating halves are identical in order to simplify machining and reduce cost. The gasket in combination with the flange groove is used to provide alignment during assembly. The flange bolt holes were bored 1/32" oversize in order to permit positive indexing of the gasket with groove and eliminate the need for matched and co-ordinated tooling. The serration was made a nominal .020 high and had an included angle of 60°. A .005 to .010 inch radius at the point of the serration was needed to help eliminate damage during handling. A RMS finish of 63 was chosen on the serration to help establish a good seal when the serration is embedded in the soft aluminum gasket. Figure 3 shows the assembled flange and the amount of gap allowed between the two flange halves after assembly. This gap condition verifies that the gasket has been installed correctly and has not been pinched between the flanges. It also indicates whether the serrations have fully embedded into the gasket. Uniform torque of the bolts is required and can best be achieved by using a crisscross pattern and stepping the torque values up in increments until the final torque is reached.

Helium gas was employed as a leak check medium, and a C.E.C. (Consolidated Ektric Corporation) helium leak detector was used to measure leakage rates. The machine sensitivity was established around 1.5×10^{-10} scc/sec, and any leakage rate above 3×10^{-6} scc/sec, as measured by the probe method, was reason for rejection.

B. Analysis

The design is such that the gasket is loaded to the bearing ultimate stress at the serration and then compresses the flat surfaces of the gasket to a point below the elastic limit. To assure complete penetration calculations were made indicating that 1100-0 aluminum with an ultimate bearing stress of 23000 psi requires a load of 780 lbs/in to embed the serration into the aluminum.

$$P_{(lb/in)} = \text{Stress} \times \text{Area/in}$$

$$P_{(lb/in)} = 23000 \text{ lbs/in}^2 \times .034 \text{ in}^2/\text{in} = 780 \text{ lb/in}$$

These calculations were based on maximum tolerance conditions of the serration. A test program was required to establish the torque value on the bolts necessary to provide the required load. The test program established the torque requirements for the various size flanges. With the proper torque full penetration of the serration into the gasket is achieved and material creep or loss of torque is avoided.

C. Environmental Testing

Several test units of the sizes being considered were designed and tested according to the individual load requirement and vibration environment required for their specific use on the missile. The following is a brief description of what the the test program involved:

1. Limit Load

Each unit was installed in a test fixture, stabilized at a specified temperature and internally pressurized to the specific design pressure. Maintaining internal pressure, the unit was then subjected to a specific axial tensile load followed by a specific applicable bending moment. A leak check was made of the joint after each load cycle, using a Consolidated Electric Corporation helium leak detector. Leakage rates above 3×10^{-6} scc/sec using the probe method constituted a failure.

2. Yield Load

The same procedure as that specified under limit load was followed except the internal pressure, the axial tensile load, and the bending moment were increased by 15%.

3. Ultimate Load

The same procedure as that specified under limit load was again followed except the internal pressure, the axial tensile load, and the bending moment were increased by 50% of the limit load.

4. Load Cycle

An electric timing device was connected to a solenoid valve and automatically programmed to apply the following load cycle for a total of 450 cycles on each unit.

a) Limit load internal pressure was applied and held.

b) Limit load axial load was applied and held.

c) Limit load bending moment was applied and held.

d) All pressures and loads were relieved.

5. Vibration

Each of the test units was mounted in a test fixture and stabilized at a given pressure and temperature. The vibration schedule was applied in two axes. Each unit was tested sinusoidally between 15 to 2000 CPS according to the environment required for their specific missile compartment use. The units were leak checked with the GEC helium leak detector after each vibration test.

6. Storage Test

One of each size unit was assembled with a shutoff valve on one end port and shutoff valve and pressure gauge on the other end port. The units were then filled with a 50/50 mixture of UDMH and Hydrazine or Nitrogen Tetroxide and pressurized with nitrogen gas at 45 psig after which the inlet valve was closed. The units were then placed in a stabilized temperature environment of 50 $\pm$ 10^{o}F and stored for six months and 1 year periods.

Test results indicated that all units except one 4" size completed testing without a recorded failure. The 4" test fixture but not the flange failed in the combined load test. An alternate fixture completed the test.

The test program revealed that the radius on the corners of the gasket had a tendancy to cause the gasket to slip out of the flange grooves during assembly making the assembly difficult and the gasket susceptible to being pinched between the two flanges. The single serration proved to be susceptible to damage and if damaged (severely scratched or gouged) leakage would occur. This was particularly a problem with the cast aluminum design.

DUAL SERRATED FLANGE

A. Design

The test program of the single serrated flange pointed out a need for redesign of the flange for actual missile use. In order to increase reliability in the case of damage during installation or parts storage, two serrations were provided. A lip was added to the inside of the gasket groove to aid in the prevention of damage to the serrations. The gaskets was revised to add sharp corners and thus provide more positive alignment during assembly. Figure 4 reflects the revised design. After assembly the gap requirement between the two mating flanges remains 0 - .020, the same as the single serrated flange. Figure 5 depicts the assembled connection.

Inspection procedures were established which insured gasket flatness to .020 and a surface finish equal to or better than R.M.S. 63 before assembly. Prior to assembly and after fabrication the gasket must be packaged in a rigid container to maintain flatness, roundness, and surface finish. Precautionary measures must also be taken to protect the flange, particularly the serrations, during missile fabrication.

The torque procedure, a crisscross torque pattern, is also required for the dual serrated flange; however, the final torque value is higher than the single serrated flange because of the additional load required to embed two serrations in the soft aluminum gasket.

More stringent leak check requirements were imposed on the flight configuration flange design. The allowable helium leakage rates were reduced from 3×10^{-6} scc/sec to 3×10^{-10} scc/sec as determined by the C.E.C. helium leak detector sniffing probe method.

B. Analysis

Analysis indicates that for the dual serrated flange a bearing load of 1600 lbs/in in required to embed the serrations into the soft aluminum gasket. This however does not include the force required to compress the air trapped between the serrations of the flanges. Tests have shown that a running load of 2000 lbs/in is necessary to prevent creep or bolt torque relaxation. A test program was initiated to determine torque values for the various size flanges. During the torque test, it was discovered that a large difference in the bolt tensile load for a given flange size can be obtained simply by varying the source of supply of nuts. Using lightly lubricated bolt threads, the average bolt load at 250 in-lbs torque on nuts from three different vendors

was respectively 800, 2500 and 5000 pounds per bolt. The reason for the variable bolt tensile load was determined to be the variable friction in the nut locking mechanism. The lower bolt load resulted in a gasket load which was not high enough to fully penetrate the serration into the gasket. The bearing stress on the gasket at the point of the serration was above the bearing yield stress and the gasket creeped thus relieving the bolt torque.

C. Testing

Since the only significant difference between the single and dual serrated flange design is the addition of the protective lip, no further environmental testing was performed. Flange thickness was increased where necessary to account for the increased requirements of gasket load. The dual serrated joint has been subjected to the R & D flight environment and has withstood extensive leak checks prior to flight.

STANDARD SERRATED FLANGE

From the knowledge gained during the development program on the single serrated flange and the dual serrated flange as used in the Titan II program, a review program was initiated to improve the dual serrated flange for future use. The primary problem with the design was the possibility of pinched gaskets during assembly. The connection was redesigned to provide a male and female flange. The tolerances on the inside diameter of the gasket and the lip on the male flange were made such that it is impossible to pinch the gasket during assembly. The lip on the male flange also acts as an alignment device. Figures

6 and 7 show the dual serrated flange as set up for a standard to be used on any future designs.

SUMMARY

In summary the dual serrated bolted flange connection is capable of preventing leakage in storable liquid propellant systems. It can be used with line sizes of 4" diameter and up and, because of the dual serrations, can provide reliability.

Figure 8 is a picture of the Booster Engine Compartment on Titan II. Three bolted flanges are shown in actual use in this photograph. The major problems with this type of connection are: 1) insuring proper bolt preload to prevent gasket creep, 2) providing bolt and nut hardware which will not allow a relaxation of torque, 3) protecting the gasket to insure roundness, flatness, and surface finish, and 4) protecting the serrations on the flanges against possible damage.

CONCLUSION

The major disadvantage of this type of connection is that it is bulky and is not readily adaptable to small line sizes because of its bulkiness. It also requires much time to assemble because of the necessary torquing procedure.

The major advantages of this joint are its complete compatibility with storable propellants, ease of manufacture, and it can be adapted to a wide range of loading conditions while still demonstrating a high degree of reliability. This flange design will also meet "zero" leakage requirements in storable liquid propellant systems.

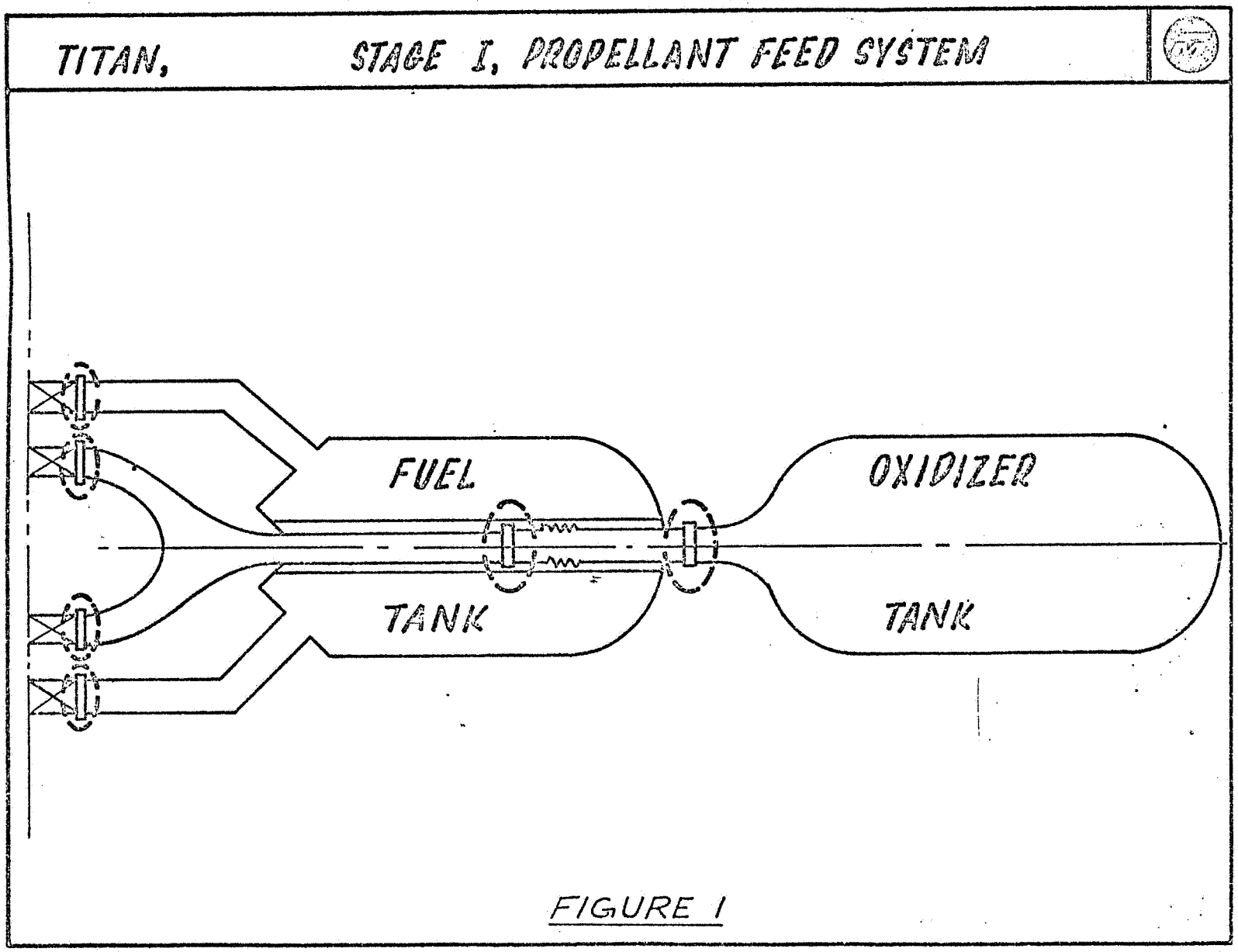
TITAN,
STAGE I, PROPELLANT FEED SYSTEM
FUEL
TANK
OXIDIZER
TANK

FIGURE 1

SINGLE SERRATED BOLTED FLANGE

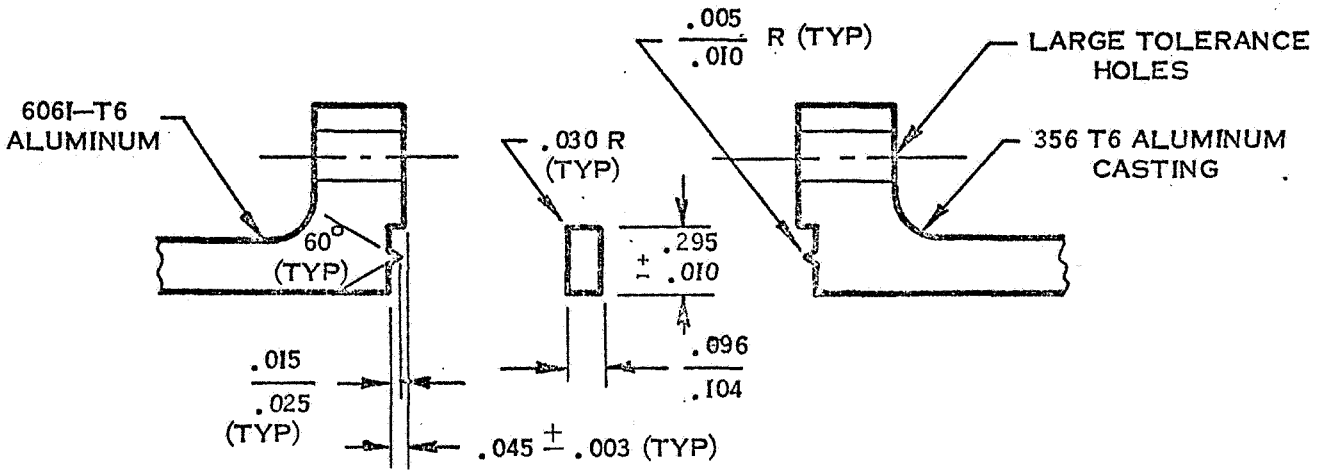

FIGURE 2

ASSEMBLED SINGLE SERRATED BOLTED FLANGE

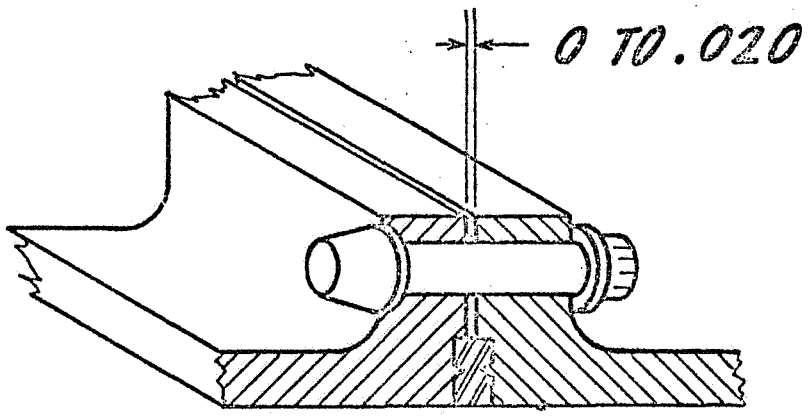

FIGURE 3

DUAL SERRATED FLANGE

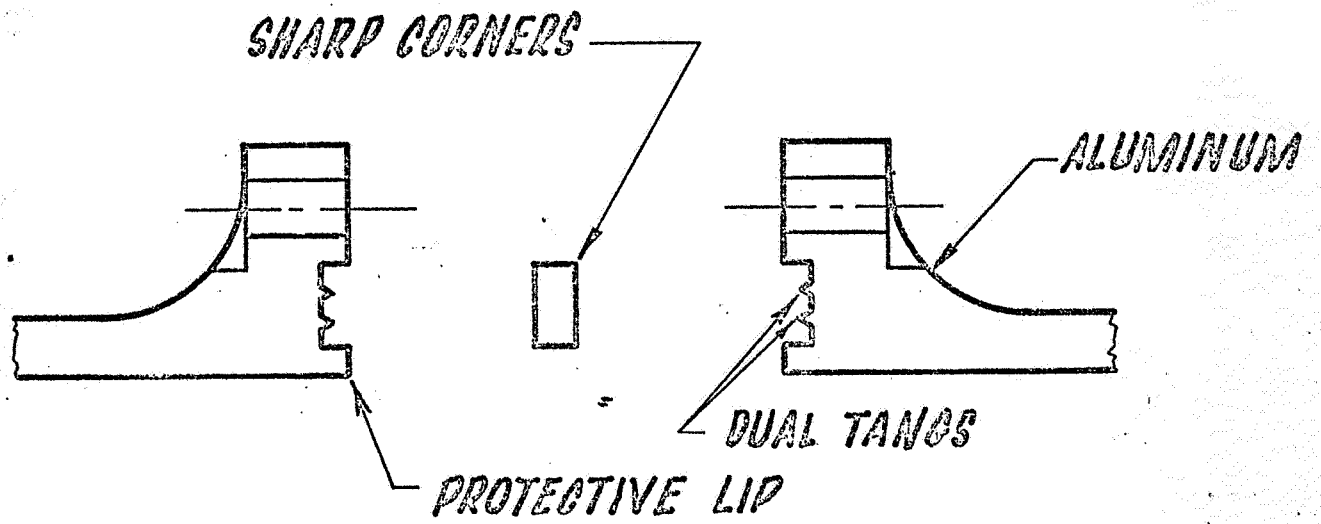

FIGURE 4

ASSEMBLED DUAL SERRATED FLANGE

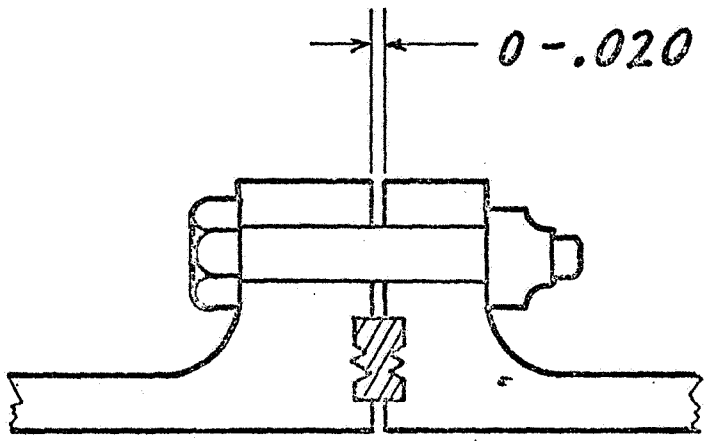

FIGURE 5

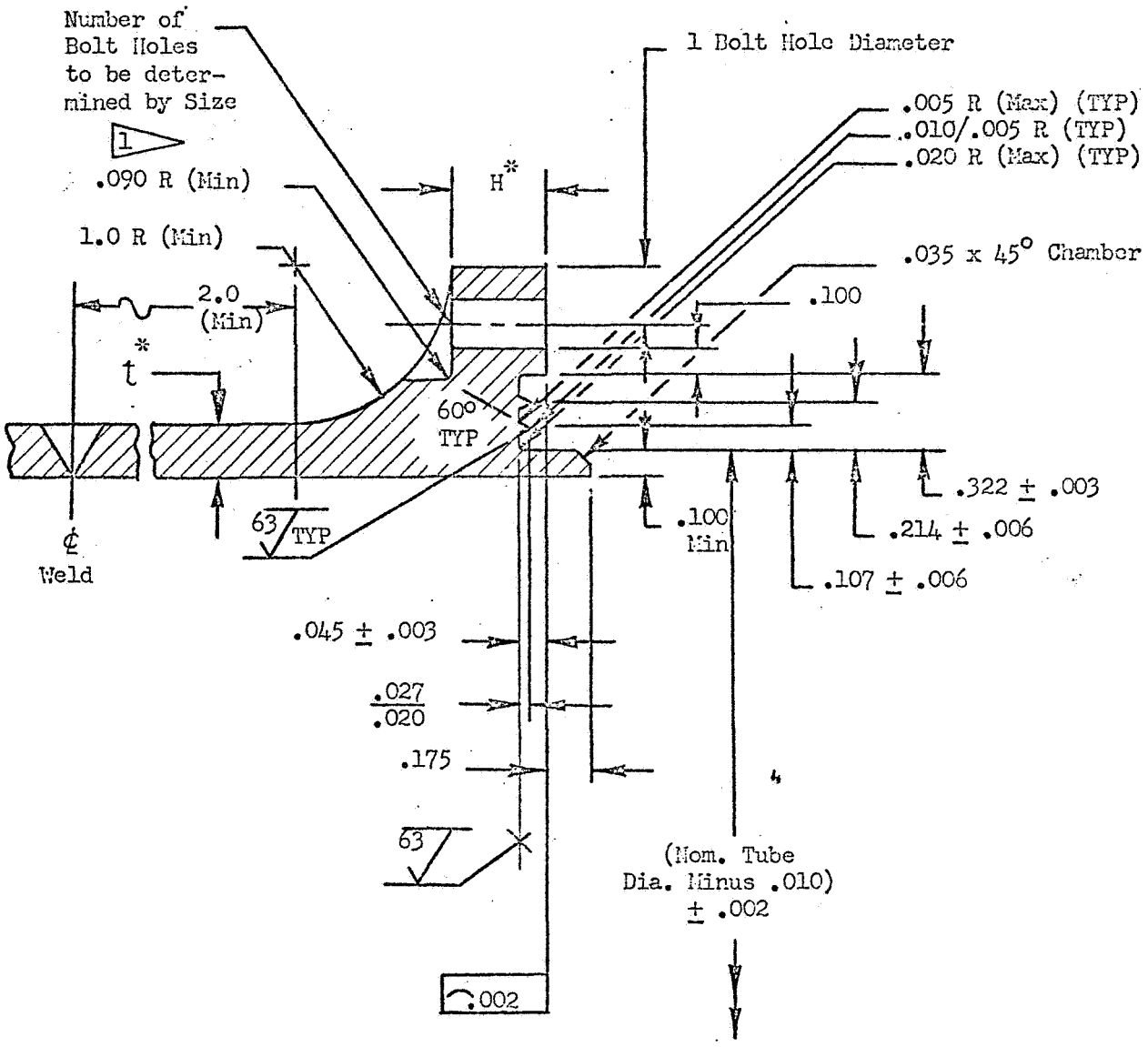

NOTES:

1. Decimal tolerance ± .010 unless otherwise noted.
2. Material*
3. All surfaces 125 except as noted.
4. Remove all burrs and break sharp edges .010 R (Max).
5. The flange, after fabrication, must be packaged in a rigid container to protect the serrations from damage.
1 6. A minimum gasket load of 2000 lb/in is required to maintain a seal using an 1100-0 aluminum gasket.

*To be determined by the specific environment in which the joint is to be used.

Figure 6

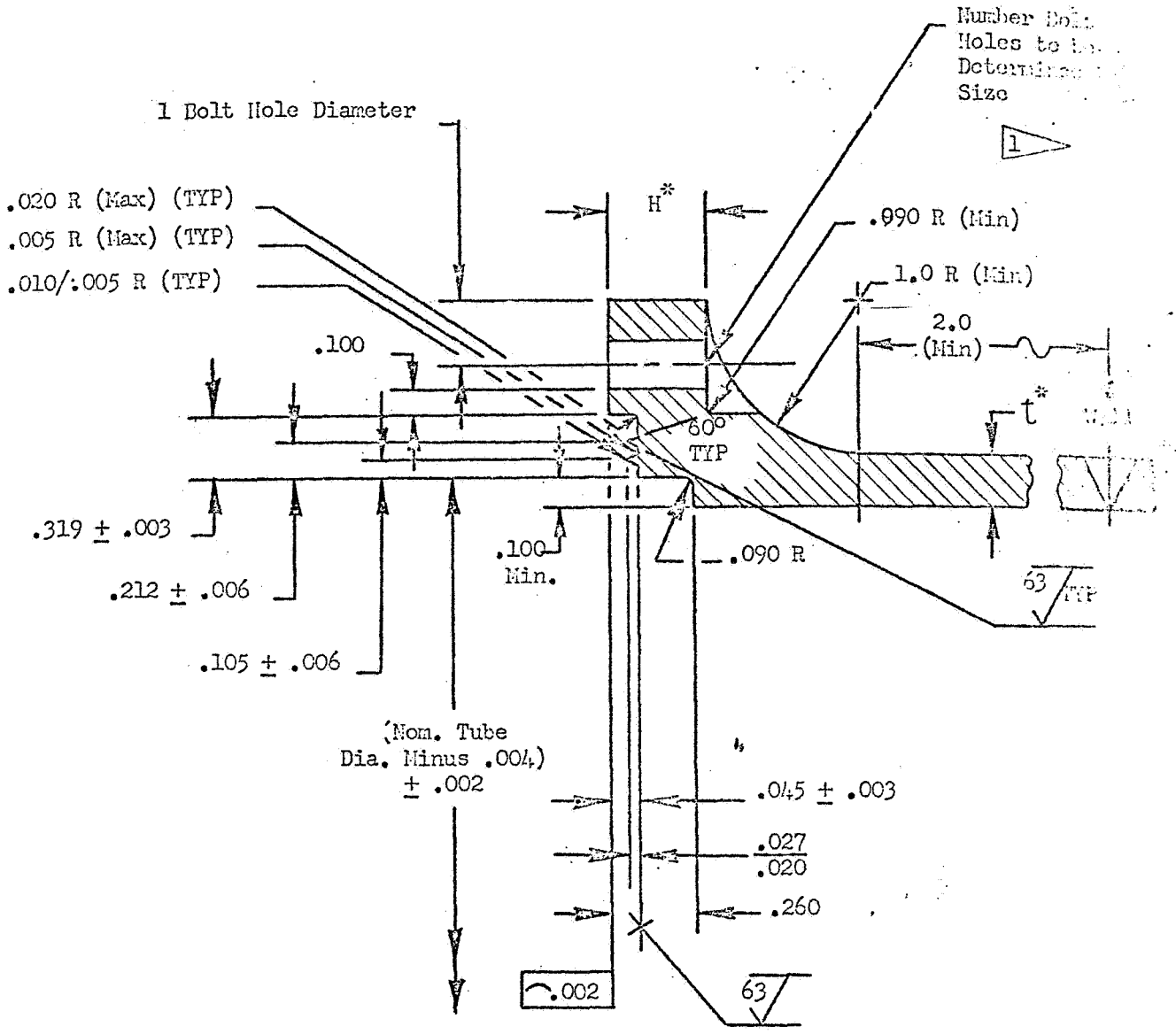

NOTES:

1. Decimal tolerance ± .010 unless otherwise noted.
2. Material*
3. All surfaces 125 except as noted..
4. Remove all burrs and break sharp edges .010 R (Max).
5. The flange, after fabrication, must be packaged in a rigid container to protect the serrations from damage.
1 6. A minimum gasket load of 2000 lb/in is required to maintain a seal using an 1100-0 aluminum gasket.

*To be determined by the specific environment in which the joint is to be used.

Figure 7

N67-86154

BIMETALLIC SEAL FOR ADVANCED AEROSPACE FLUID SYSTEMS

by
W. A. Prince
Senior Design Engineer
General Dynamics/Astronautics
San Diego, California

Preceding page blank

INTRODUCTION

The difficult task of sealing unusual media such as liquid nitrogen and oxygen and helium gas under extreme operating parameters and environments accompanied the early development of missiles a decade ago. During the transitional period from aircraft to aerospace production, it was readily recognized that the previously acceptable designs of connectors and joints were inadequate for the new set of service requirements. In re-evaluating these designs it became apparent that there were, in general, three constituent aspects that required appraisal: one was the method used to attach the fitting to the tube; the second was the sealing device; and the third was the inherent resiliency or spring action used for locking. Underlying these factors was the core of the problem, namely the stringent weight and space limitations, and thermal effects. This deduction lead to the conclusion that an optimum design could not be obtained without first resolving the sealing requirement. Since that time, progress in separable fluid connectors has been hampered partly because of the innumerable multiplications of the same sealing concept, and partly because the problem was not confined to its logical discipline. The purpose of this paper, therefore, is to contribute a seal technique for separable fluid connectors that is more appropriate to advanced aerospace systems than those underlying present designs. Although it may seem presumptuous to make this assertion in the wake of so many recent and voluminous expositions of seal and connector criteria, yet there are many fundamental and applied problems remaining to be solved.

Preceding page blank

BACKGROUND

In order to propose a seal concept for advanced systems, it is necessary to re-examine some fundamentals of sealing mechanisms. From an inspection of the evolution of the basic designs illustrated in Fig. 1, and the following discussion, it is not difficult to understand the subsequent developments.

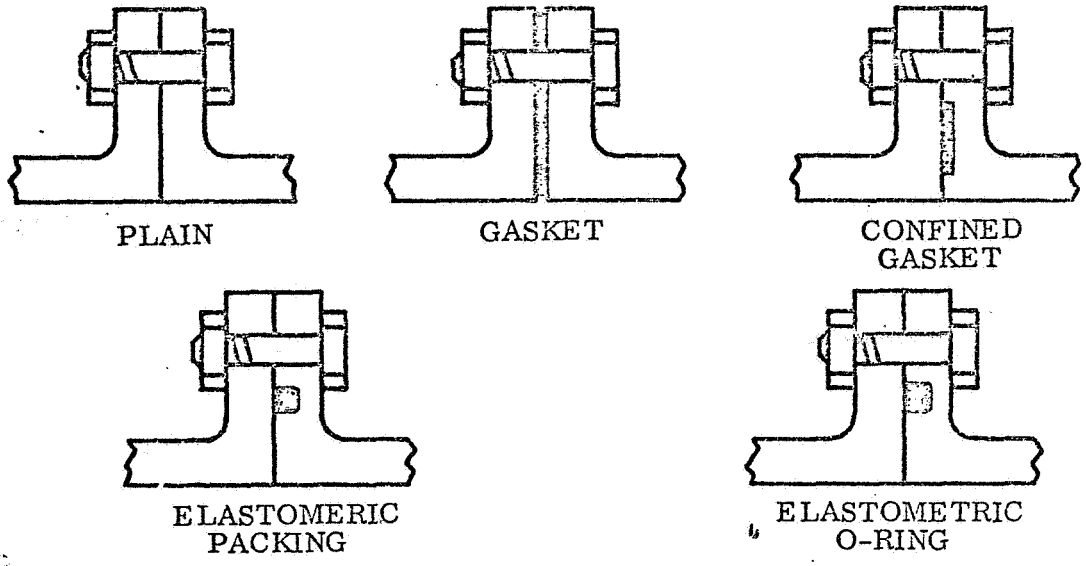

Fig. 1. Evolution of classic seals.

If, theoretically, the void between two mating surfaces of a joint could be entirely eliminated, there would be no leakage, and, aside from the compressive force necessary to maintain the joint against the internal pressure, no compressive pressure would be required for sealing. Such a condition would be ideal, and may be approached by polishing the mating surfaces to a mirror finish, but this method is not considered practical from an over-all point of view, because a single scratch could result in leakage. Therefore, the only known alternative of resolving this objective is to make the material of one of the surfaces softer than the other, and apply a compressive force to yield it into the asperities of the other.

In the most primitive type of seal, this operation is accomplished by introducing a "gasket" made from a resilient and compressible material, having an adequately low compression set, between the mating surfaces of the joint. Although there are many variations of this concept, the mechanics of the basic design are the same. High compressive loads are required for sealing, and the spring-back of the gasket is of a low

magnitude, which results in thick and heavy flanges for high pressure. On the other hand, the mass of the flanges must be compromised when further considering the effects of extreme temperatures. Hence, the application of gaskets in aerospace systems presents a complex problem.

Enclosing the seal in a cavity reveals another mode of operation. If the seal (packing) is made of a pliable elastomeric material and is slightly compressed in a cavity, it transmits pressure in much the same manner as a fluid. Consequently, the sealing pressure will always exceed the pressure of the internal fluid by the margin initially derived from the compression of "squeeze" [Ref. 1]. The limiting factor of this type is the extrusion of the packing through the clearances or irregularities of the mating surfaces. Here it will be noted, the seal is primarily loaded by the fluid pressure instead of the compressive or clamping force of the joint, as in the case of the flat gasket. Such an inversion of loading is commonly termed "pressure-sensitive" or "pressure-actuated". It results in a compact and light-weight seal, as exemplified by the widely used elastomeric O-ring. Although this long-standing and acceptable seal satisfied the needs of subsonic aircraft, its use in aerospace systems is restricted to applications which do not have the extreme temperature requirement. Efforts to select a compound for extreme temperatures or to replace the elastomeric compound with fluorinated polymers only gave more recognition to the problem.

The original Bridgman closure [Ref. 2] for superpressures, illustrated with its predecessor in Fig. 2, represents another variation of the pressure-actuated principle.

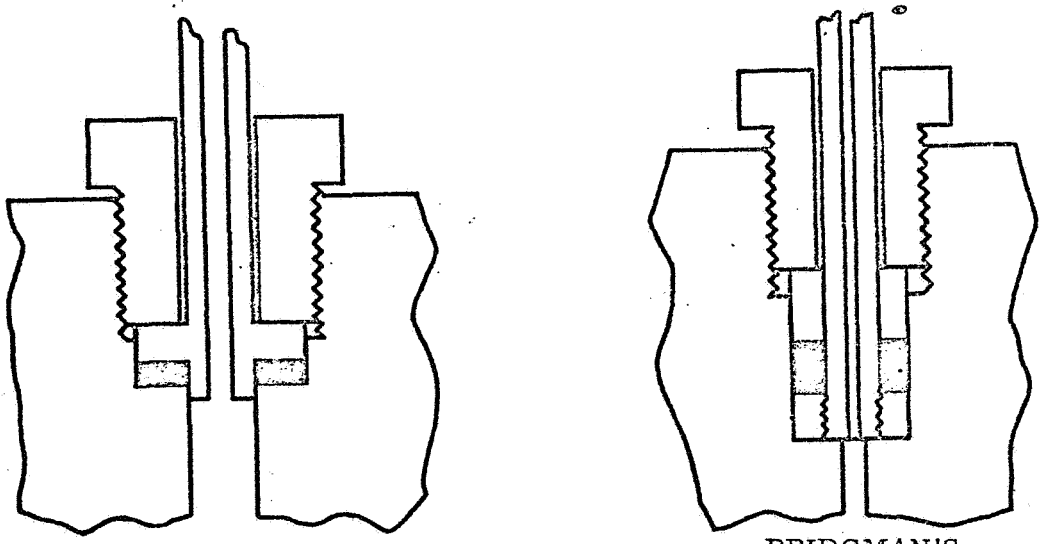

Fig. 2. Derivation of Bridgman's closure.

In this design the packing is loaded by the internal fluid pressure effecting a closure of the cavity. This is accomplished by the fluid pressure acting in an axial direction over a greater area of the closure housing the packing than that by which it is externally supported. Hence, the sealing pressure of the packing is always maintained at some fixed ratio above the fluid pressure. Experience with this method has shown that the packing is not prone to extrusion, and that the pressures attainable are only set by the strength of the metal parts. Although this concept is not used in aerospace systems, it was the forerunner to later developments.

Instead of axially compressing the cavity, a more practical method is to allow the internal fluid pressure to expand a metal ring radially against an outer surface which is not subject to pressure. Initial sealing is accomplished by compressing the joint to stretch or elastically deform the ring. This modification introduced the radial type metal seal. The solid O-ring, delta-ring, lens-ring, wave-ring, double-cone, etc. [Ref. 3 & 4] are representative of this type. Fig. 3 illustrates a few of these designs. They are extensively used by the chemical industry.

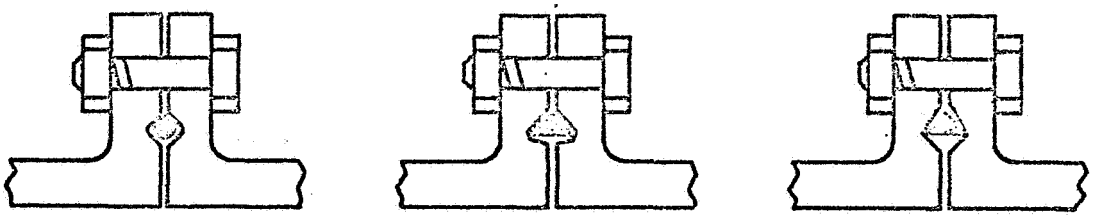

Fig. 3. Typical radial seals.

The new set of conditions for seals, imposed by the development of missiles, had created demands for which there were no precedents; the only obvious solution was to resort to metal seals. The metal types previously mentioned required high flange loads which increased the weight of joints, and they did not have sufficient spring-back to follow flange deflections. The designs therefore had to be re-evaluated and modified for aerospace joints.

Hollow metal O-rings, introduced in this country about the time that missiles were first being developed, received swift recognition as the likely modification, and were readily adopted. This design was soon followed by the introduction of many new designs such as the K-Seal, V-Seal, C-Seal, W-Seal, E-Seal, etc. Coatings, platings, and hoods of softer material were added to reduce clamping force and improve performance. Today, the problem appears to have become one of selection. Actually, all of these seals operate on the same principle and vary only in configuration and detail features. They are pressure-actuated seals which combine both spring and internal fluid pressure to produce the necessary sealing force. Although the pressure-actuated principle cannot be discounted in seal technology, it certainly cannot be considered as the only possible solution. Before presenting another concept, the principles of two other significant developments should be considered. These are:

1. Ring Spring. A ring spring is a rather unusual type of spring, that is used to absorb a large amount of energy in a relatively small space. Ordinarily, it is used as a shock absorber for cranes [Ref. 5], locomotives [Ref. 6], power hammers, and other such heavy equipment. Illustrated in Fig. 4, the ring spring consists of a series of inner and outer rings alternately arranged with mating conical surfaces to form a column. When an axial load is applied, the spring is compressed by radial expansion of the outer rings and compression of the inner rings.

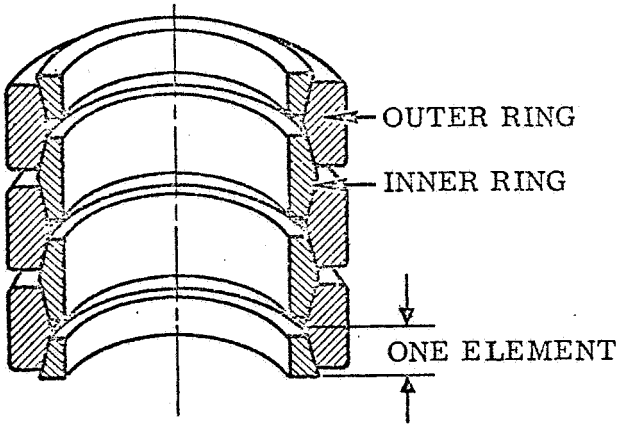

Fig. 4 Typical ring spring.

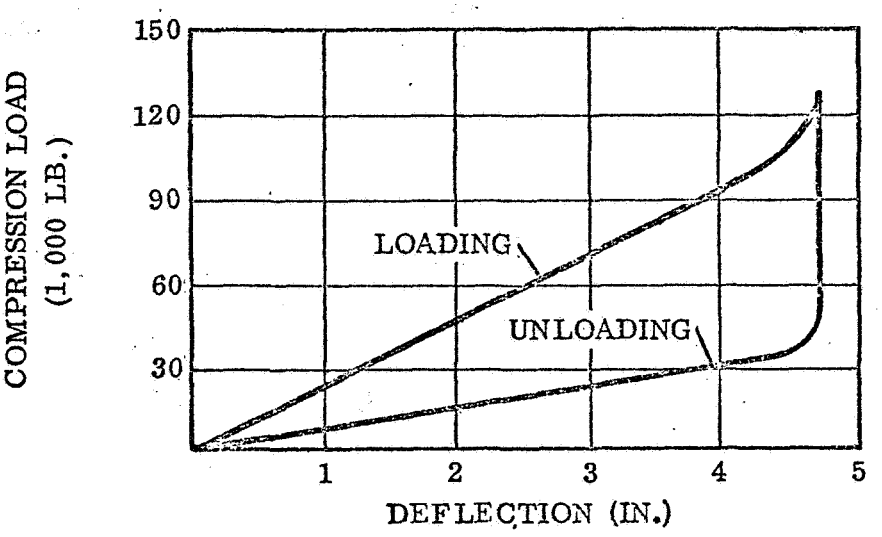

Fig. 5. Typical load-deflection of ring spring.

Fig. 5 shows a typical hysteresis loop for this type of spring. It will be noted in this curve that friction increases the compression loads and is released during the recoil stroke. Unlike the usual coil or leaf springs, which are unequally stressed in torsion or bending, the tensile or compressive stress distribution in a ring spring is very nearly uniform. For this reason it can absorb more energy per weight or volume of material than any other type of spring [Refs. 7 and 8]. Spring formulas and data for the stress analysis of these rings have been derived by Wahl [Ref. 8].

The ring spring design is presented, not only to point out its unusual characteristics as a true spring, but also to show how it has been adapted to a variety of applications. For example, when the rings are confined between a hub and shaft and axially compressed, the spring is converted into a unique clamping or fastening device. Such an arrangement has been used for locking marine propellers and pulleys to shafts [Ref. 9], because it eliminates the stress concentrations associated with splines, keyways, etc., and permits the transmission of high torques. It has also been used for fastening bolts in holes [Ref. 9], and for fastening and sealing high pressure tubing [Ref. 10]. The applications are extended to such divergent uses as piston rings [Refs. 11 and 12] and adjustable bushings [Ref. 13], usually with the rings

split, or radially cut. From these considerations it can be seen that a ring spring inherently provides a design which can be utilized as a sealing mechanism. Recently J. W. Hull [Refs. 14 and 15] investigated the feasibility of the design, and developed a seal of this type for high-temperature aircraft hydraulic systems. Fig. 6 shows Hull's basic configuration, which is actually one element of a ring spring. The rings are made from high-strength steels, hardenable by heat treatment, and the cross section is relatively small - 1/10-in. wide for a five-inch diameter seal. The particular advantage of this design, in contrast with the aforementioned metal seals is the relatively large axial spring-back. This maintains an effective seal and permits a greater freedom in flange deflections and separation. Moreover, it is reported that the compressive or clamping loads are equal to or less than the aforementioned types. The seal is also pressure-actuated, since the sealing force is boosted by the internal fluid pressure; however, its prime advantage is the spring-back factor.

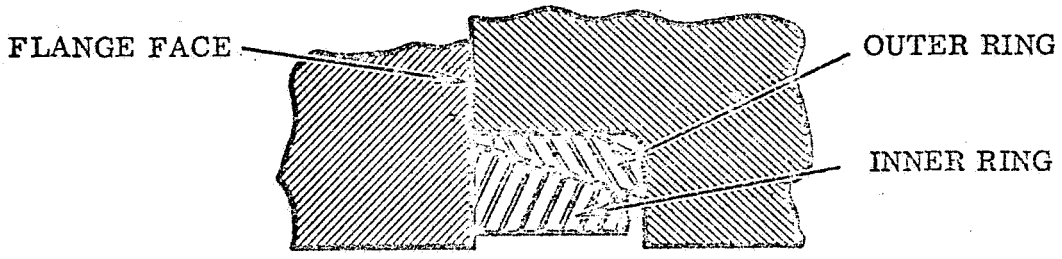

Fig. 6. Basic configuration of Hull's ring spring seal.

2. Temperature actuation. Just as pressure was considered a drawback in high-pressure joints until its energy was utilized, so is temperature considered a drawback in aerospace systems today. In fact, statistical investigations [Ref. 16] indicate that the most probable cause of leakage in these systems is thermal effects. Yet nearly a decade ago, Logan [Ref. 17] introduced a technique for sealing cryogenic fluids which clearly demonstrated how a drop in temperature could be utilized for maintaining a seal.

The basic configuration of Logan's design is described in Fig. 7. Here, an elastomeric material is confined in a cavity between an inner ring made from an alloy having a low thermal contraction rate, such as "Invar", and the flange which is made from a relatively high thermal contraction alloy, such as aluminum alloy. During cooling, the differential contraction effects a closure of the cavity which compensates for the high thermal contraction of the elastomeric material, and maintains the sealing pressure at temperatures below its glass state transition (-40°C). At temperatures above this, the seal functions similar to a pressure-actuated O-ring.

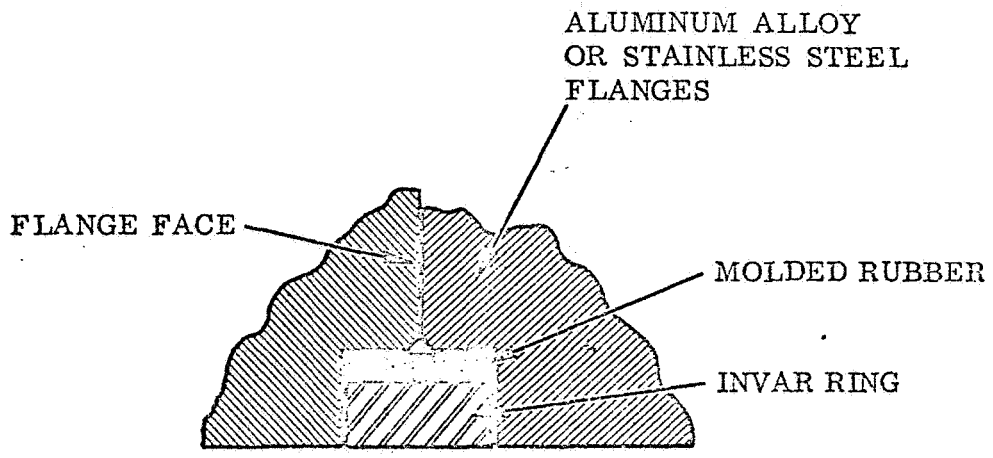

Fig. 7 Basic configuration of Logan's temperature-actuated seal.

Initial sealing is accomplished by a slight squeeze of the elastomeric material, so almost no compressive or clamping force is required. Since, the seal is primarily operated by the temperature ofthe internal fluid, in its critical range it is referred to as a "temperature-actuated" seal. Although this concept is basically excellent, the technique has not received appreciable acceptance in aerospace systems. This is apparently due to the unusual application of an elastomeric material in this temperature span, and the non-uniform characteristics of the coefficients of thermal contraction.

Attention has been directed to these two concepts, however acceptable, because they represent an evolution of sealing principles. It appears that the sealing mechanism is the essence of present problems, rather than the characteristics of the sealing surfaces, contact area, and other such peculiarities which are considered secondary. As suggested in this discussion, a trivial improvement in this domain creates a real extension of design philosophy.

BIMETALLIC SEAL

The bimetallic seal combines the fundamental principles of the ring spring and temperature actuation; it employs the configuration of the former to obtain a relatively large elastic restoring force and deflection for sealing at ambient temperatures, and the thermal compensating aspect of dissimilar materials of the latter for maintaining the sealing pressure through extreme temperatures. Fig. 8 illustrates an original version of the concept which was designed to fit an existing cavity of a liquid nitrogen coupling in service.

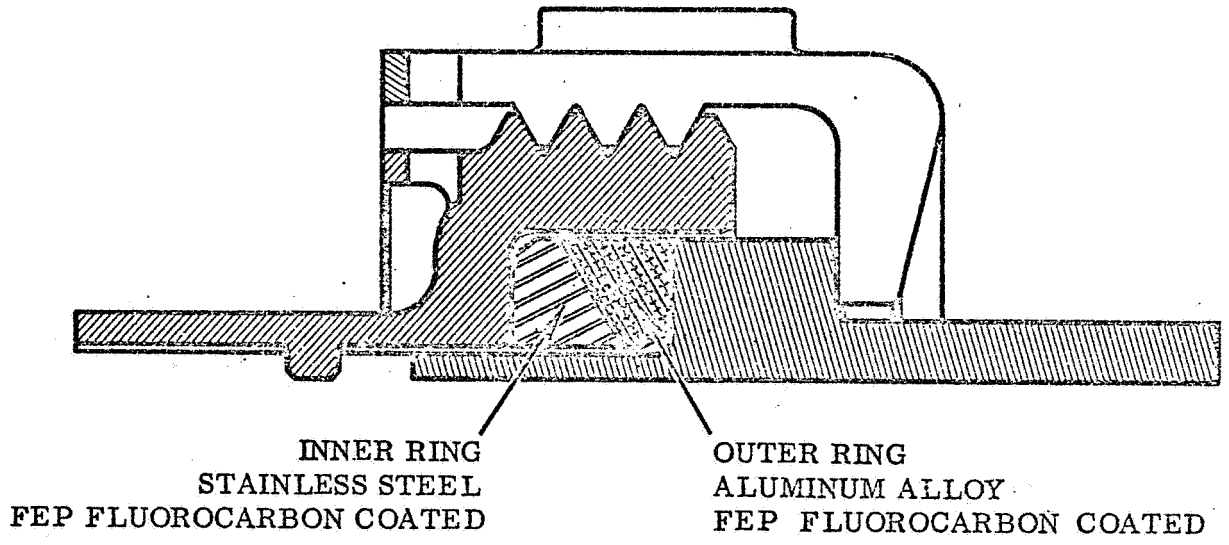

Fig. 8. Basic configuration of bimetallic seal retrofitted in shroud-to-bellows coupling.

Although this configuration does not represent an optimum design, since it was not integrally designed with the joint, it served as a test model for validating the concept. Also, the particular joint shown in the coupling in Fig. 9, served as a challenge to a very difficult seal problem, because it presented a unique set of adverse factors.

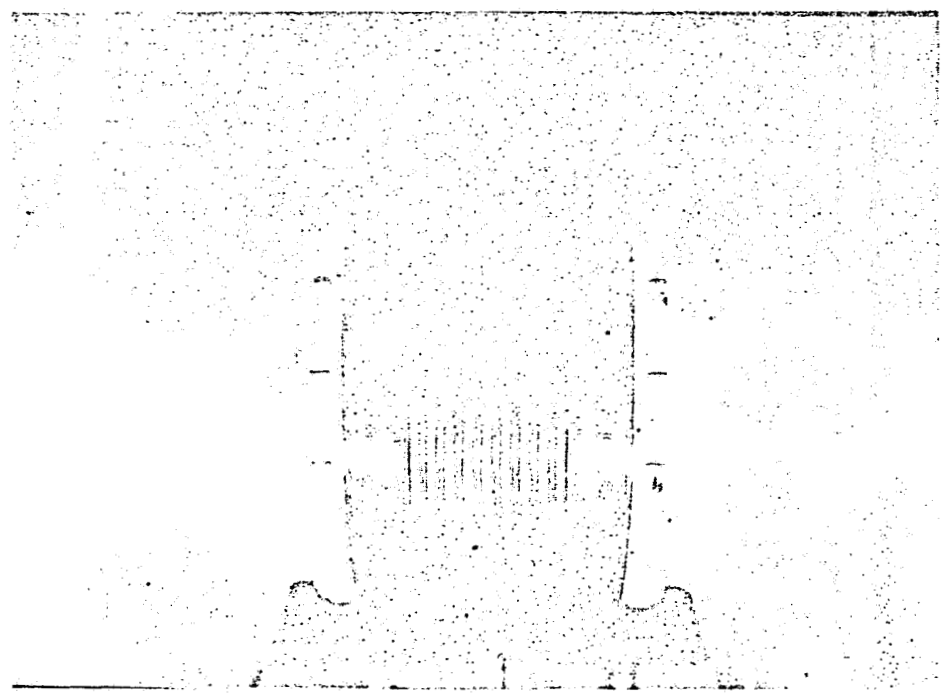

Fig. 9. Shroud-to-bellows coupling for liquid nitrogen.

First, the size of the cavity was relatively small compared with its 6.25-in. diameter, being only 1/10 in. between ID and OD and less than 2/10 in. wide. This was further restricted with 0.010/0.030 in. corner radii and unusually wide tolerances. In addition, the joint was fragile, which limited the tightening torque and consequently the axial clamping force to around 50 lb. per circumferential inch. A third factor was the dissimilar materials which formed the cavity. The outer gland was 321 stainless steel, and the inner sleeve was 6061-T6 aluminum alloy. At low temperatures the aluminum alloy contracted at a greater rate than the stainless steel causing an opening of the cavity. Aside from these adverse factors, the maximum pressure was 10 PSIG, the surface finish of the cavity was 32 microinches, and there was a possibility of slight misalignment on assembly.

The seal consists of two adjacent rings with a conical interface, essentially forming an element of a compression-type ring spring. The materials of the rings are dissimilar, the outer ring being made from 6061-T6 aluminum alloy which has a greater coefficient of thermal contraction than the inner ring made from 321 stainless steel. The coefficients of thermal contraction of these materials in this temperature range are somewhat uniform. When the joint is assembled, the rings are compressed together producing an axial spring force which closes the voids at the shoulders of the cavity as well as at the conical interface. This initial pressure seals the joint at ambient temperatures. Through low temperatures, the outer ring contracts at a greater rate than the inner ring maintaining the sealing pressure. A 45°taper was used for the conical surfaces, and the parts are stressed well within the allowable yield of the material. To reduce friction at the conical interface, and to reduce the sealing pressure, both rings are coated with fluorienated ethylene propylene (FEP) fluorocarbon resin, 2 to 4 mils thick.

To evaluate the performance, four seals were simultaneously tested in a series of connected joints subjected to installation and operating conditions. The temperature was cycled from ambient to liquid nitrogen temperatures through 100 cycles with a maximum operating pressure of 10 PSIG in the cryogenic range. Leakage was determined by visual observation, with a soap solution being applied to the joint at ambient temperatures. Aside from a sporadic leak from one seal on the 75th cycle at ambient temperature, no leakage was observed. The results [19] had shown that the seal provided a zero-leakage connection in this temperature range. Since the test, the seal has been successfully used in service for nearly a year.

The test set-up was also used to compare the performance of the bimetallic seal with some other types, both metallic and non-metallic. However, the number of metallic types was limited, because only a few could be designed to fit this particular small cavity. This comparison demonstrated a wide variance in performances. All the non-metallic seals leaked profusely at cryogenic temperatures, as expected, and the performance of the bimetallic seal was far superior to the other metal types.

Some very interesting experimental data was also obtained on the Instron Test Machine shown in Fig. 10. As illustrated, the spring characteristics of the seal were obtained by axially loading and unloading the seal between two platens. The platens had the same surface finish as the cavity of the liquid nitrogen coupling, and the compressive force was equivalent to the load sustained by the coupling torque. This load was

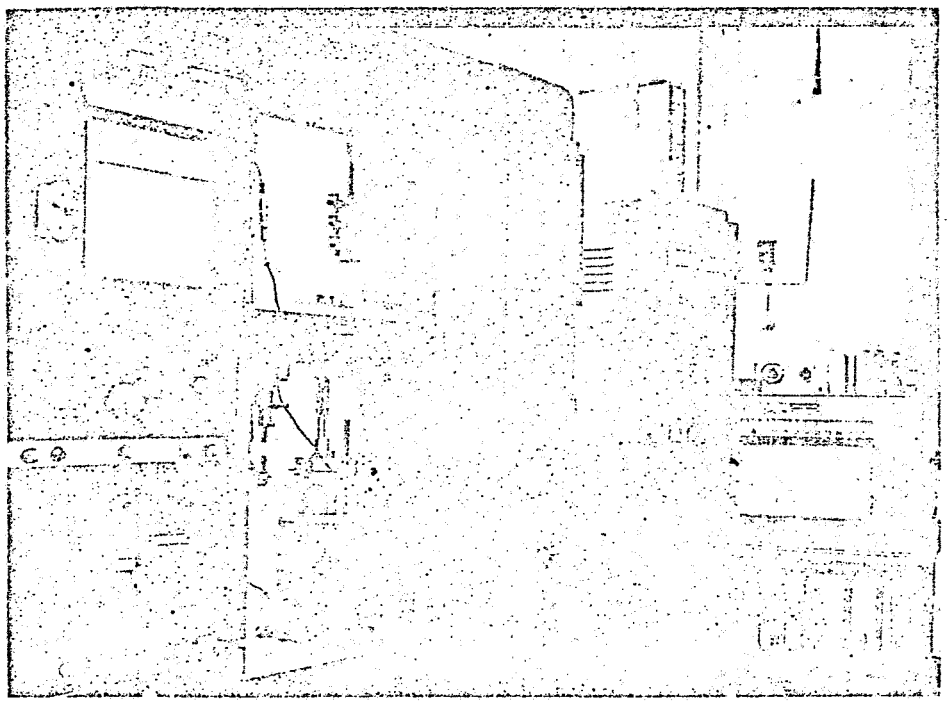

Fig. 10. Load-deflection test apparatus.

applied at a rate of 0.010 in/min., and the deflection was measured with a 2-inch Baldwin extensometer. Fig. 11 shows the actual curve (solid line) of the load-deflection hysteresis loop, demonstrating that the spring constant is higher on the compression stroke than on the return or recoil stroke.

This difference is due to the friction of the conical surfaces. As far as metal seals are concerned, the curve can be examined from another standpoint - the upper or loading portion of the curve represents the clamping force required to energize the spring features of the seal for initial sealing, and the lower or unloading portion represents the actual spring-back force that is considered with the contact area factor for establishing the sealing pressure. In other words, the upper curve is the tradeoff for the lower one.

The apparatus was not rigged to maintain the deflection during cooldown to the liquid nitrogen temperature. Therefore, to obtain the total axial force due to spring-back and the differential thermal contraction, the seal was submerged in liquid nitrogen and loaded and unloaded after temperature stabilization. Fig. 11 illustrates the load-deflection diagram of this simulated operation and shows that the spring-back characteristics are maintained at the low temperature extreme.

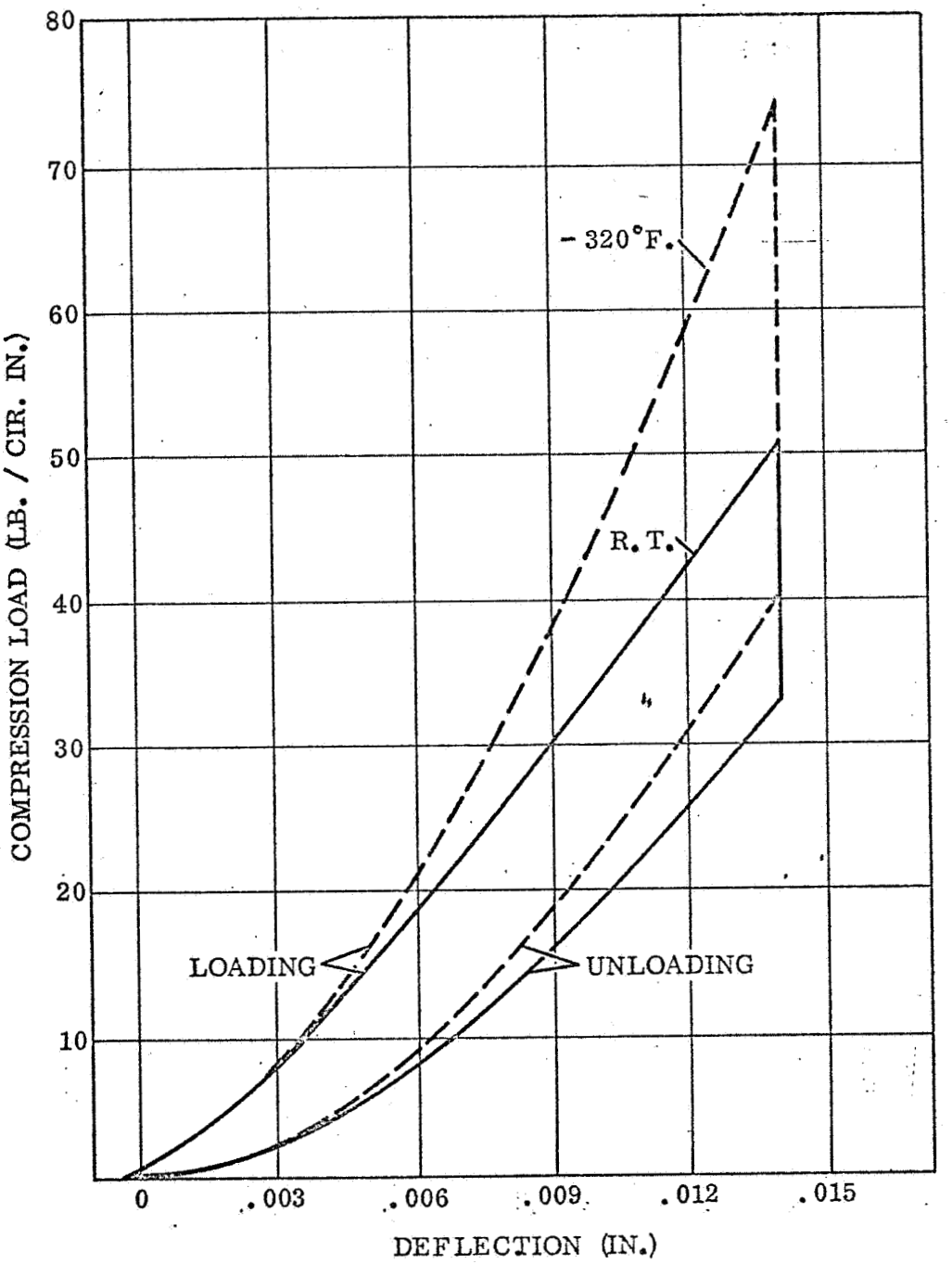

Fig. 11. Load-deflection for bimetallic seal showing hysteresis loop during loading and unloading at room temperature and at -320°F.

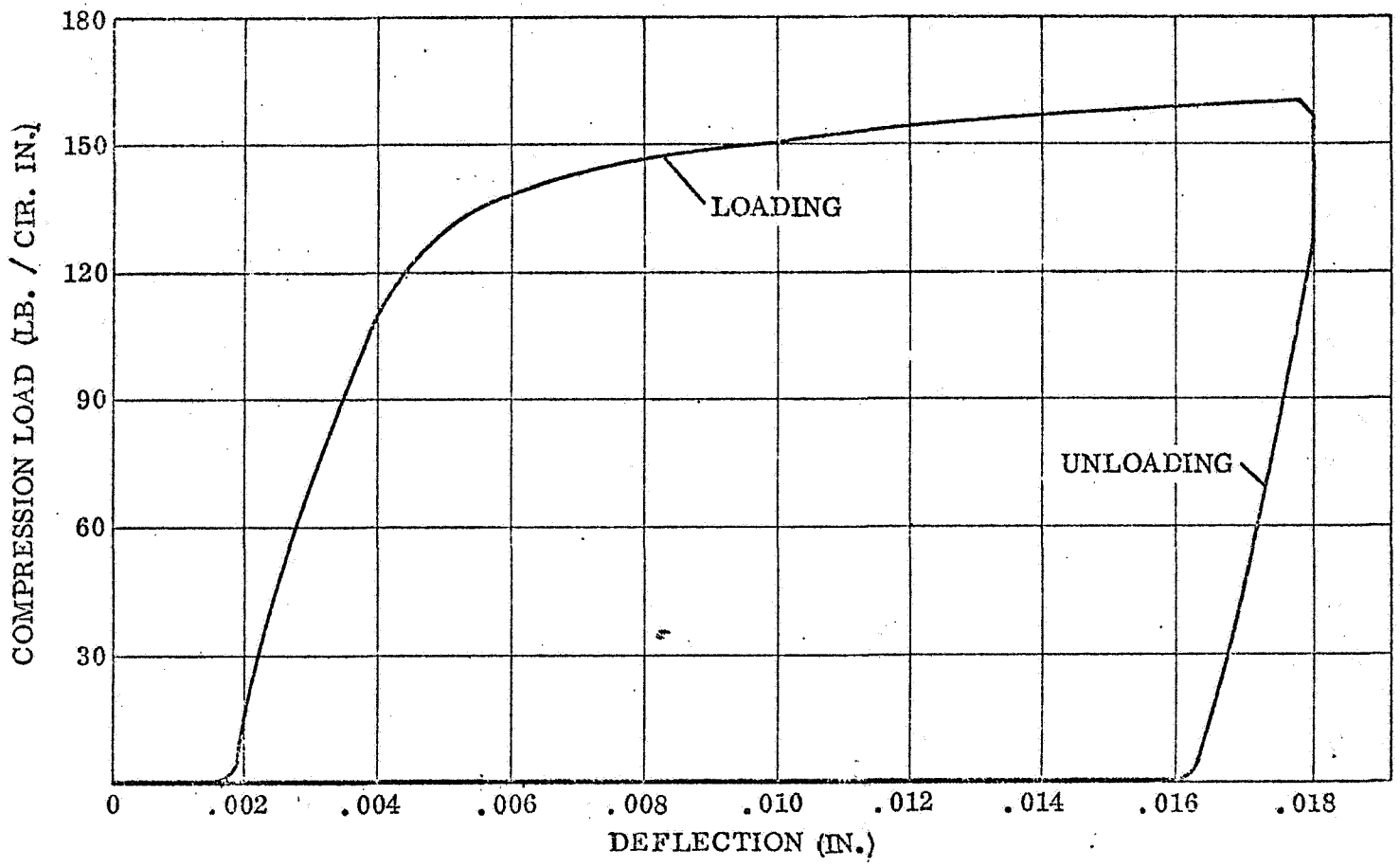

Fig. 12. Load-deflection for type 321 stainless steel O-ring, 1/8 in. tube size by 0.010 in. wall, compressed 0.018 in. Deflection limits are 0.013 to 0.023.

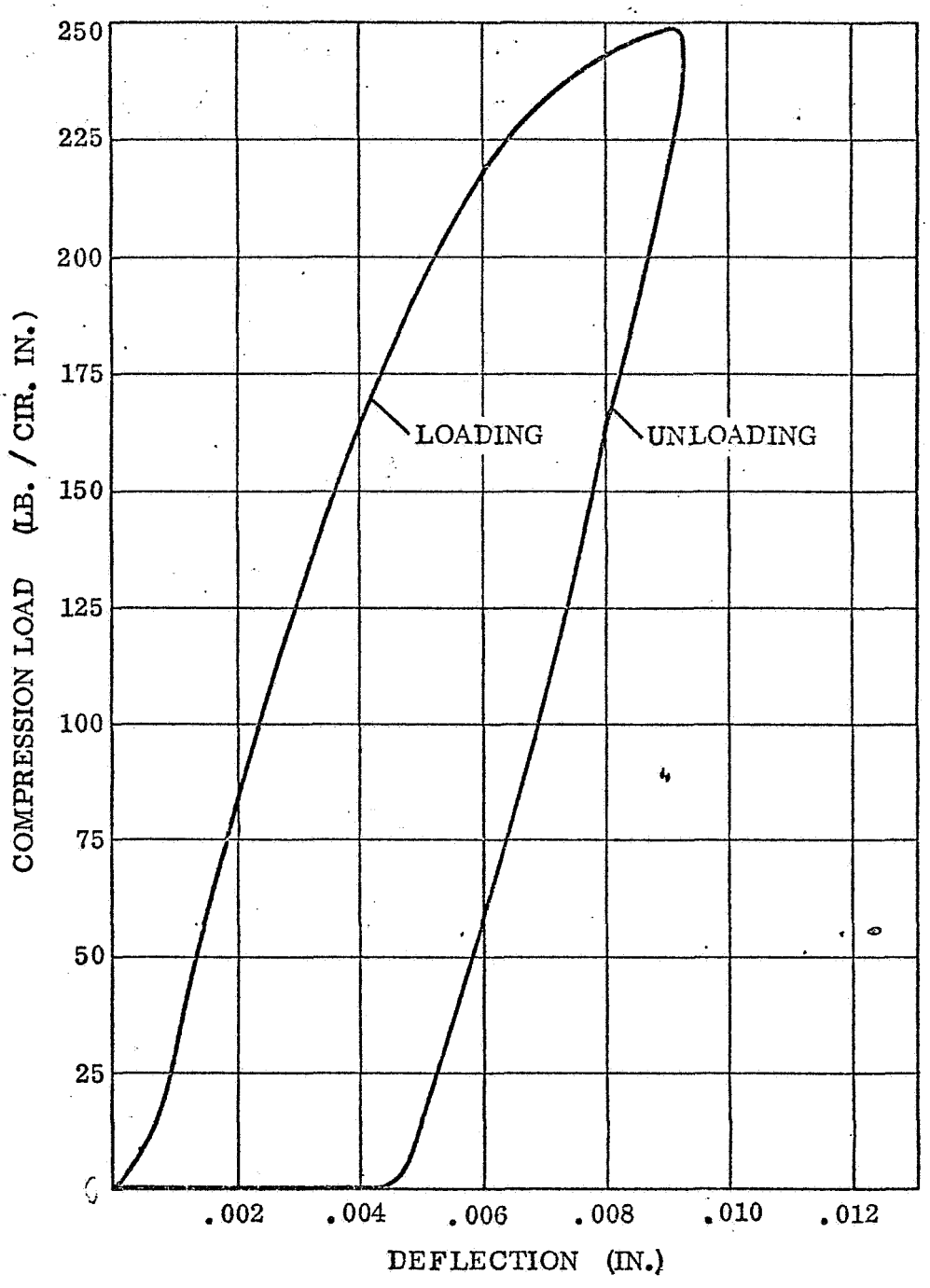

Fig. 13. Load-deflection for A-286 stainless steel K-seal .143 - .137 in. high by .180 in. wide, compressed .009 in. Deflection limits are .007 - .018 in..

The spring-back deflection is 0.014 in., and well within the elastic limit of the material. It is noteworthy that these curves agree reasonably well with calculations.

Similar tests were made with the hollow metal O-ring and K-seal to draw a general comparison of the spring-back characteristics at ambient temperature. Neither of these two seals could be effectively designed to fit the small cavity dimensions of the bimetallic seal; nevertheless they were selected because of their wide usage. The same apparatus and procedures were used, except that the seal was subjected to a predetermined deflection instead of a load. Deflection was oriented to a mid-point between the minimum and maximum squeeze values calculated from the tolerances of the seal and the recommended groove depth. Sizes were selected from available stock as close as possible to the bimetallic seal.

Fig. 12 shows the load-deflection diagram obtained for a Type 321 stainless steel O-ring, 1/8-in. tube size by 0.010 in. wall thickness by 5-1/4 in. outside diameter. The ring was compressed 0.018 in., which was mid-point between the installation deflection limits of 0.013 to 0.023 in. The loading portion of the curve shows that the ring is stressed behond its elastic limit, and the unloading portion shows a spring-back deflection of 0.002 in.

Fig. 13 shows the load-deflection diagram obtained for an A286 stainless steel K-seal, 0.137 to 0.143 in. high by 0.180 in. wide by 6-1/2 in. outside diameter. As shown, the ring was compressed between its deflection limits of 0.007 to 0.018 in. at a point slightly beyond the minimum value. Had the load scale of the machine been adjusted higher, as determined on a repeat run, the ring would have gradually yielded further. This would have given the curve an appearance somewhat similar to the O-ring with the exception of the spring-back. The spring-back deflection of this ring was slightly over 0.004 in.

This cursory comparison indicates that significantly higher spring-back deflection can be attained with the bimetallic design than with the other types. And unlike the other types, it can be produced to operate within its elastic limit. Ordinarily, the taper of the conical surfaces of the bimetallic seal would be lower, reflecting an even greater deflection. At the present time, no comment can be made about the compressive loads, because the test did not include leakage. It is noteworthy that the Instron machine made an excellent test apparatus. If equipped with a pressurization system and mass spectrometer, it would make a very effective unit for standardizing the method of evaluating seals.

The bimetallic concept appears to have all the qualities of a simple seal, and as such it is versatile and can be readily modified. Fig. 14 shows an O-ring configuration that was experimentally tested [Ref. 19] in the previously mentioned liquid nitrogen coupling.

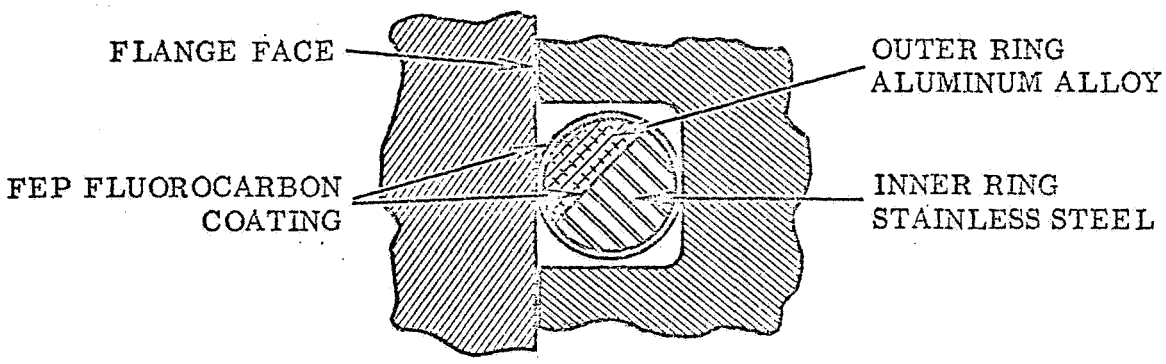

Fig. 14. Bimetallic seal with O-ring configuration.

In this design the contact pressure is intensified, and the leakage path through the conical interface is eliminated by a fluorinated ethylene, propylene (FEP) fluorocarbon coating. The coating also reduces the sealing pressure, acts as a lubricant, and provides a means for retaining the parts as an integral unit. The particular rings used for test were machined from bar stock; however, wire formed into a circle, butt-welded and conically ground, would probably represent a less costly method of production. Although the test evidenced some leakage at ambient temperatures, indicating insufficient spring-back in the design, it nevertheless demonstrated the feasibility of the configuration. This version can also be made hollow with the dissimilar materials welded together, but this would reduce the action to that of distortion.

Fig. 15 shows another configuration that was conceived to show how the concept could be made pressure-actuated. In this design the axial deflection is also increased because of the double-cone arrangement.

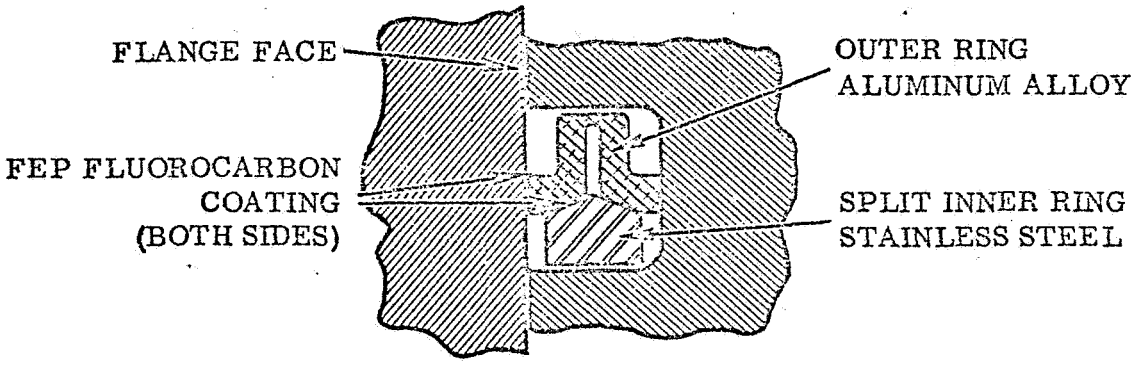

Fig. 15. Bimetallic seal with pressure-actuated configuration and double cone for increased deflection.

In addition to these examples, the cavity could be designed to form one of the conical surfaces, or it could be eliminated, by designing a self-contained unit which could be installed between the flat surfaces of a joint. Moreover, the concept could be embodied as a conical bimetallic washer for installation in a conical cavity. In this case, slightly different tapers would be employed for effecting the axial sealing pressure.

From these cryogenic examples it is apparent that for high temperature applications, or for both high and low temperatures, the geometry can be inverted or compounded. In addition, the concept can also be utilized to exclude pressure, and for combined services such as cryogenic-vacuum, etc.

It is believed that if the three basic rules for evaluating a connector, given in the Introduction, are correlated with the bimetallic concept, a more complementary combination of design elements would be available for the conception of a universal "aerospace" connector. Such a connector should be capable of connecting tubes to components as well as to each other. The bimetallic seal, similar to the widely used elastomeric O-ring, can be used under a connector fitting for the component connection. It further provides the feature of a spring lock. To this can be added another advantage - that the pretensioning of a threaded connection can be measured accurately by the diametrical expansion of the ring spring element, rather than inaccurately by torque.

CONCLUSIONS

Although no effort has been made to evaluate all of the parameters involved in creating an optimum bimetallic seal design, or connector, the results of this limited investigation show that the concept has merit and should be further explored and its applications extended. Experience gained so far in testing the seal indicates that sealing either high or low temperature aerospace fluids presents less of a problem than sealing at room temperature.

ACKNOWLEDGEMENTS

The author wishes to express his deep appreciation to J. R. Gooch, formerly with General Dynamics/Astronautics, for jointly conceiving and developing the bimetallic seal, and to H. W. Schneider of NASA for inspiring him in this technology.

REFERENCES

1. Morrison, J. B., O-Rings and Interference Seals for Static Applications, Machine Design, February 1957, pp. 91-94.
2. Bridgman, P. W., The Physics of High Pressure, G. Bell and Sons, Ltd., 1952, pp. 30-40.
3. Niemeier, B. A., Seals to Minimize Leakage at Higher Pressure, Transactions of the ASME, April 1953, pp. 369 - 379.
4. Freeman, A. R., Gaskets for High-Pressure Vessels, Mechanical Engineering, December 1952, pp. 969 - 972.
5. Engineering Report No. 595, The Application of Edgewater Ring Springs to Crane Bumpers, Edgewater Steel Co.
6. Engineering Report No. 601, Typical Applications of Edgewater Ring Springs, Edgewater Steel Co.
7. Wikander, O. R., The Ring Spring, Mechanical Engineering, February 1926, pp. 139 - 143.
8. Wahl, A. M., Mechanical Spring 2nd Ed., McGraw-Hill Book Company, 1963, pp. 204 - 210 (also published in Machine Design, August 1943, pp. 124 - 127.
9. Tutt, F. J. H., Ring Spring Clamping, The Marine Engineer and Naval Architect, March 1955, pp. 95 - 97.
10. Kreissig, E., Schmidt, O., The Use of "Ring Springs" as Fastening Elements and in Other Applications, The Engineers' Digest, October 1957, pp. 433 - 435, 441.
11. Norwood, J. E. Patent No. 1,462,043, United States Patent Office, July 17, 1923.
12. Church, H. D., Patent No. 1,528,814, United States Patent Office, March 10, 1925.
13. Design Information, Adjustable Wall-Thickness Bushings, Adjustable Bushing Co.
14. Hull, J. W., Ring-Spring Design for High Performance Metal Static Seals, Hydraulics & Pneumatics, September 1960, pp. 122 - 126.
15. Hull, J. W., Status Report, Metallic Seal Development, Contract AF 33 (600) - 39506, SAE Committee A6 Meeting, April 17-21, 1961.

16. Schneider, H. W., Consideration of Reasons for the Mechanical Failure of Separable Missile Duct and Tubing Joints, NASA In-House Report M-S&M-PL, December 1960.

17. Logan, S. E., Static Seal for Low-Temperature Fluids, Jet Propulsion, (J. Am. Rocket Soc.) July 1955, pp. 334 - 340.

18. Logan, S. E., Temperature-energized Static Seal, Advances in Cryogenic Engineering, Vol. 7, Plenum Press, 1962, pp. 556 - 561.

19. Christensen, A. H., Evaluation Test Report No. 27A 1939, Liquid Nitrogen Seals for Helium Shroud Bottle Application, General Dynamics/Astronautics July 10, 1963.

Report No. 10074

N67-86155

DESIGN AND TEST OF MARMAN "CONOSEAL" JOINT

By

Hub Dykstra

Aeroquip Corporation/Marman Division
Los Angeles, California

Preceding page blank

PATENT NOTICE

CONOSEAL is patented under Patent Number 2, 992, 840 granted to Aeroquip Corporation.

ACKNOWLEDGMENT

To Mr. Gerald Forrest, Manager, NASA Projects, Aeroquip Corporation/Marman Division, for assistance in furnishing information and photographs on CONOSEAL applications.

Preceding page blank

I. INTRODUCTION

In the March 1964 issue of NATIONAL GEOGRAPHIC, there appeared an article entitled, "Footprints on the Moon" by Hugh L. Dryden, Ph. D., Deputy Administrator, NASA. In this article, Dr. Dryden sets forth the standard of performance required for the lunar mission. The mission must have a 99.9 per cent probability for safety of the astronauts. It is difficult to imagine the reliability required of the myriad of components in such a complex vehicle.

One of these components is a separable fluid connector. Just what are the requirements for this connector?

It must be simple, yet reliable.

It must withstand extremes of temperature, along with higher pressures and vacuum in outer space.

It must contain new and exotic propellants.

It must endure tremendous G-loads and vibrations.

And it must remain leak-tight--less than 1×10^{-9} cc/sec (equivalent to 3 cc of helium in 100 years).

All this is required--and then some.

This presentation, then, attempts to portray by design and by test a sealing concept to satisfy the aforementioned requirements.

II. DESIGN

A. Sealing Concept

The CONOSEAL sealing concept uses a frusto-conical-shaped gasket similar to a Belleville washer, with a cross-sectional height greater than the radial difference between the mating flange sealing diameters. In Figure 1a the CONOSEAL Gasket is shown between the flanges when seating load is first applied. Stress concentration in the gasket is clearly shown by the photo-elastic method. As the flanges are brought together, the gasket is fully compressed (Figure 1b), a plastic flow (as noted by maximum stress in gasket extremities) is induced in the gasket sealing corners by the columnar loading. The inclined flange faces limit gasket buckling.

Although the mechanics of the actual bond between the gasket and flange are not clearly understood, it is apparent that a plastic flow of the gasket material is required to obtain the intimate contact necessary to contain a medium such as helium or hydrogen gas.

Figure 2a is a 50X enlargement of a typical gasket-to-flange sealing relationship. The gasket sealing corner has plastically yielded following the contour of the flange sealing area.

Figure 2b is a 200X photo-micrograph of the bond obtained along the gasket-to-flange interface.

Prints of Figures 1a and 1b unavailable

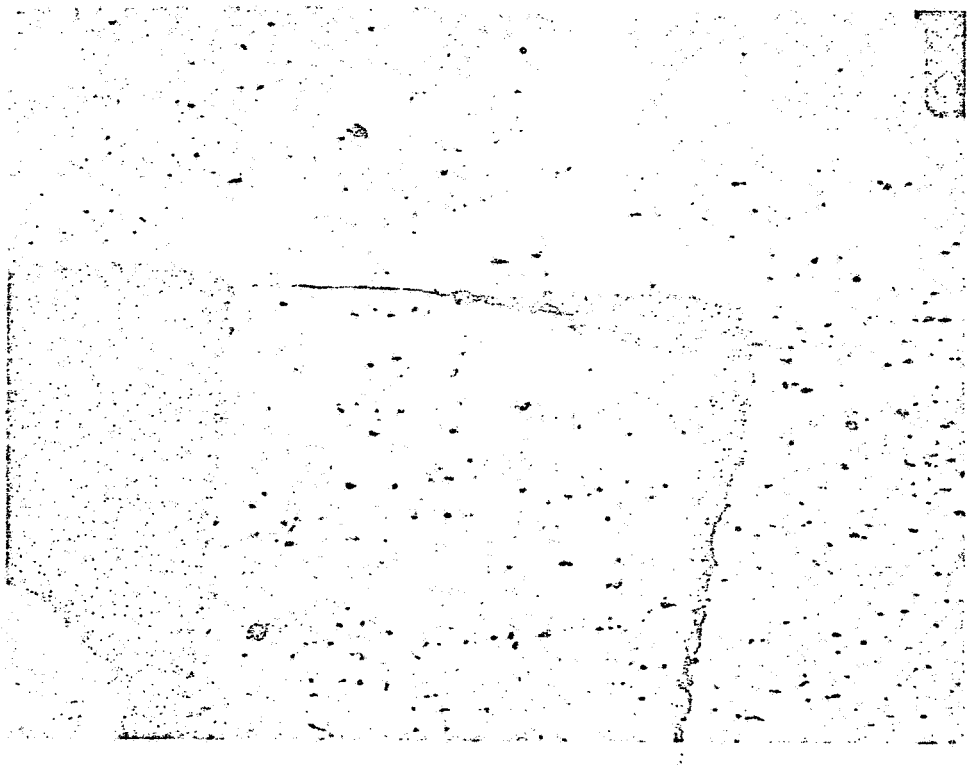

a
Sealing Corner 50X

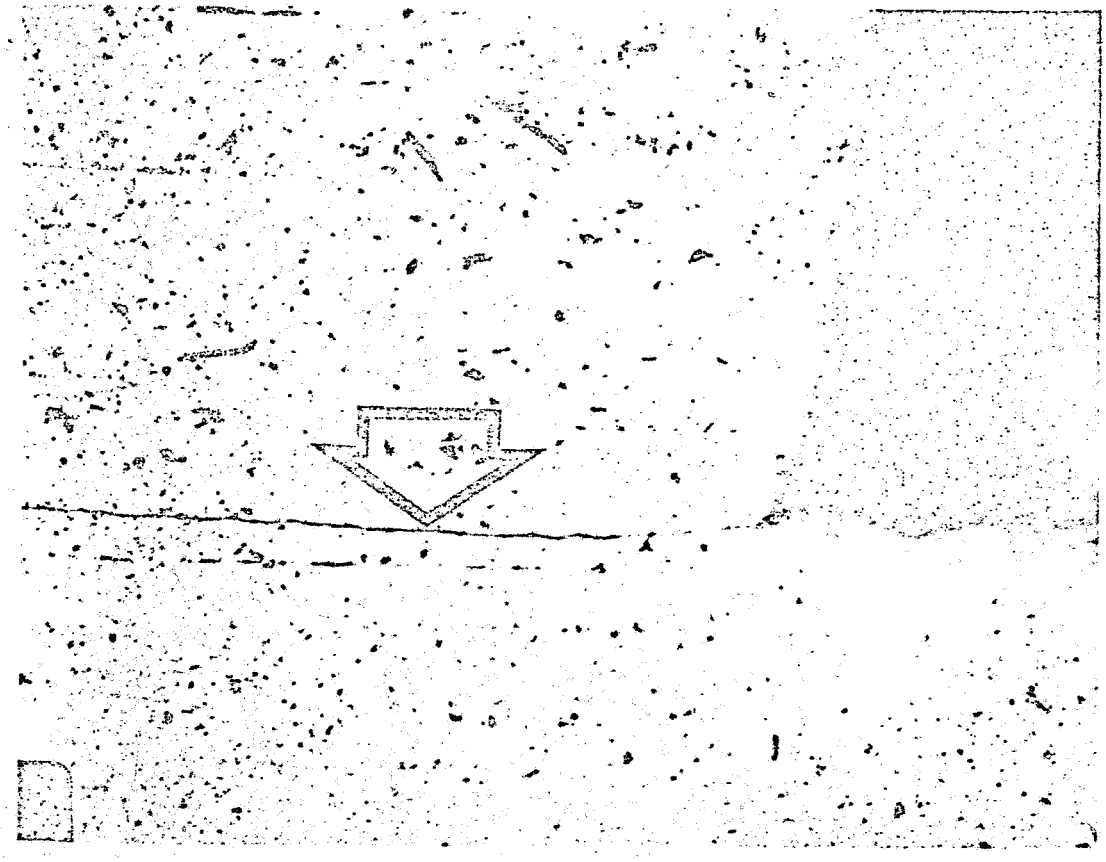

b
Inner Diameter Sealing Interface 200X
Figure 2
Photomicrographs: Gasket to Flange Seating Relationships

B: Analysis

1. Gasket Seating Load

The stress pattern so clearly shown by the photo elastic method (Figures 1a and 1b) is resolved in a force diagram of the CONOSEAL Gasket seating action as shown in Figures 3a and 3b. The load required to seat the CONOSEAL Gasket can be calculated from the formula:

$$F_a = k\,S\,t\,\pi\,D_m \sin\alpha$$

Where F_a = Axial force in pounds

k = Coefficient (correction for hoop tension forces)

(1 for sizes 1 inch and over)

(3.5 for sizes below 1 inch; .020 x .125 gasket)

S = Gasket seating stress, psi

t = Gasket thickness, inches

D_m = Gasket mean diameter, inches

α = Angle of gasket at maximum load, degrees

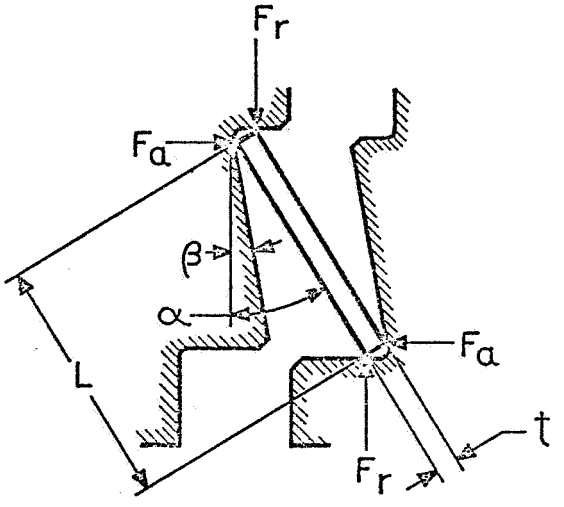

FIGURE 3a BEFORE ASSEMBLY

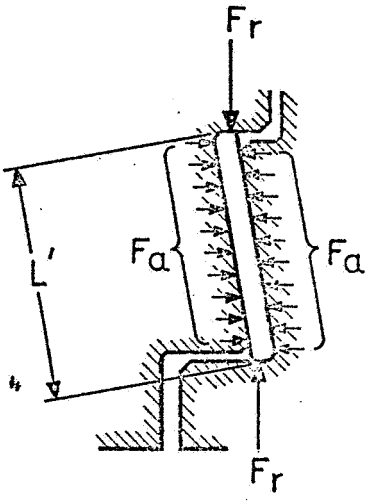

FIGURE 3b ASSEMBLED

FIGURE 3 SEATING ACTION OF "CONOSEAL" GASKET

Figure 4 is a graph of axial load required to seat CONOSEAL Gasket for various gasket thicknesses based on a seating stress of 10,000 psi. The dotted lines represent a more ideal curve, accounting for effects of hoop on smaller sizes. Seating stresses for common gasket materials are shown in Table I. The seating stresses are in excess of the compressive yield strength of the gasket material in order to achieve a plastic deformation of the gasket.

TABLE I

Gasket Seating Stresses for Common Materials

Gasket Material	Seating Stress, psi
321 CRES	50,000
6061-0 Aluminum Alloy	15,000
Copper, Annealed	25,000

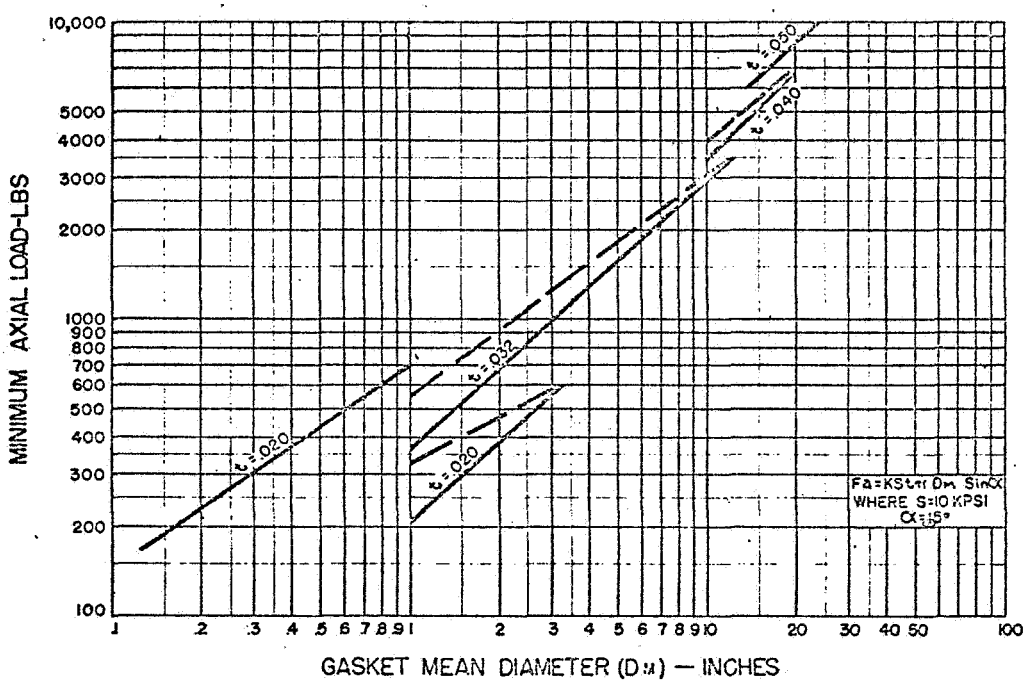

FIGURE 4 MINIMUM AXIAL LOAD REQUIRED TO SEAT "CONOSEAL" GASKET

2. Flange Analysis

A shearing force is exerted on flanges by the gasket (as shown in Figure 3b). The thickness of the flange lip is determined as a result of the shearing force. The radial force, F_r, exerted against the inner lip and outer lip results in hoop loads in these members. The deflection of these members within elastic limits actually aids in maintaining a reaction force against gasket along with residual strain in gasket.

The method used in claculations for flange design is based upon Section VIII of the ASME Boiler & Pressure Vessel Code, Appendix II, "Rules for Bolted Flange Connections." The ASME design method is modified for use on flanges where V-band coupling or threaded nut is employed. The method used for flanges with V-band couplings is included in Appendix I. A method for analysis of threaded fittings is covered adequately elsewhere [1].

Determination of stresses induced in flanges as a result of gasket seating depends upon the following factors:

a. Gasket cross section

b. Amount of gasket compression

c. Gasket material

d. Connector size

e. Flange design

For lightweight connectors, the effects of gasket seating stresses could affect the design significantly and must be compensated for in design. On pipe joints and joints utilizing ASME Code allowable stresses, gasket stresses have been found to have an insignificant effect upon joint performance under operating condition.[2]

3. Preload

The torque required to assemble a fitting is based on the higher of two axial loads as follows:

a. The gasket seating load

b. Load due to internal pressure and/or other external operational loads

Any additional axial load imposed by internal pressure over initial preload decreases with increasing preload. A method for calculating additional load based on spring constants is graphically demonstrated in a report referenced elsewhere.[1]

The torque calculations for various configurations are shown in Table II.

TABLE II
Assembly Torque Calculations

	Bolted Flange Connection	V-band Coupling Connection	Threaded Connector
Torque lb in.	$\frac{.2\ D_t\ F_a}{\text{No. of Bolts}}$	$.064\ D_t\ F_a \tan\frac{\alpha}{2}$	$.2\ D_t\ F_a$

Where D_t = Thread diameter, inches

α = V-band Coupling included angle, degrees

C. Materials and Surface Coatings

1. Flange and Gasket Materials

The use of materials in the CONOSEAL connector is limited only by the selection of a gasket material that will not Brinell the flange sealing area while maintaining structural rigidity. Generally, the gasket material has lower mechanical properties than the flange material, but there are notable exceptions such as a 300-series stainless gasket used with identical flange material. No Brinelling of the flanges has occurred even under extreme temperature conditions. This can readily be explained as follows:

a. A maximum hardness on gasket raw material is specified.

b. Gasket and flange geometry and contact surface relationship benefit gasket coining without flange Brinelling.

The problem of mating flanges employing materials with markedly different thermal expansion properties has been overcome, within limits, by taking advantage of gasket residual strain and initial flange deflection.

Flange and appropriate gasket materials are summarized in Table III.

TABLE III

Flange and Gasket Materials

Flange Material	Gasket Material	Operational Limitations		Remarks
		Temperature, °F	Service*	
300-Series Stainless Steel	300-Series Stainless Steel	-423 to +1500	Propellant Pneumatic Hot Gas	Easily machined and welded. Excellent resistance to most corrosive media.
19-9DL	321 CRES	-423 to +1500 **	Propellant Pneumatic Hot Gas	Higher mechanical properties than 300-series stainless steel.
6061-T6 Aluminum Alloy	6061-0	-423 to +400	Propellant	Most weldable high-strength aluminum alloy
Inconel X or Inconel 718	Inconel or 321 CRES	-423 to +1300	Propellant	High strength-to-weight ratio
Hastelloy-X and Haynes 25	321 CRES	-320 to +1500	Hot Gas	High strength-to-weight ratio
Zircalloy 2 to 300-Series Stainless Steel	321 CRES	~ 900 max	Reactor Systems	Limited to ~5-inch diameter.
Aluminum to CRES	6061-0	Within aluminum alloy temperature limits	Propellant	

* The use of CONOSEAL is limited to compatibility of materials with propellant.

** Charpy V-notch test value less than 15 ft lb at -423°F

2. Flange and Gasket Surface Coatings

Extensive tests have been conducted on the effects of anodic and chemical coatings of aluminum flanges.[3] Increasing leakage rates can be expected dependent upon the initial surface finish and degree of etching caused by cleaning agent concentration and type of coating used. Lower leakage rates have been obtained with chemical coatings than with anodic coatings.

Coating the gasket with Teflon has proved successful in overcoming minor scratches in flange sealing surface and for use with anodized flanges. In certain cases where stainless and aluminum flanges are employed, a Teflon-coated aluminum gasket with the addition of a color pigment can be used to identify gasket material. This would avoid improper use of a stainless gasket with aluminum flanges.

Other coatings in use are summarized in Table IV.

TABLE IV
Flange and Gasket Surface Coatings

Coating	Component	Remarks
Silver Plating	Gasket	Improved sealing on carbon steel components and other special applications.
Cadmium Plating	Gasket	Improved sealing on carbon steel components.
Nickel Plating	Flanges and Gaskets	For corrosive media.

D. Flange and Gasket Geometrical Relationship[4]

To achieve optimum sealing, geometric similarity of gaskets and sealing cavities should be approximated throughout the entire size range of gaskets and flanges.

The gasket compression curve shown in Figure 5 defines the radial compression required to maintain geometrical similarity of the gasket cross-sections. An increase in gasket cross-section is necessary to allow for increasing flange seal diameter tolerance on larger diameters. Gasket No. 3A, being below the line, indicates the reason for the addition of Gaskets No. 3B and No. 3C to obtain a more desirable geometrical relationship. Testing has substantiated the improvement in reliability of the increased width or thickness.

The flange diametral tolerance curve indicates the acceptable tolerance. The deviation from the curve of Gaskets 1 and 2 is compensated for by increasing gasket compression.

The range of flange diameter versus gasket cross-section is shown in Figure 6. This graph is self-explanatory, but several other reasons exist for increasing gasket cross-section with increasing diameter in addition to machining difficulties.

They are as follows:

Handling difficulties associated with large diameters of gaskets with light cross-sections.

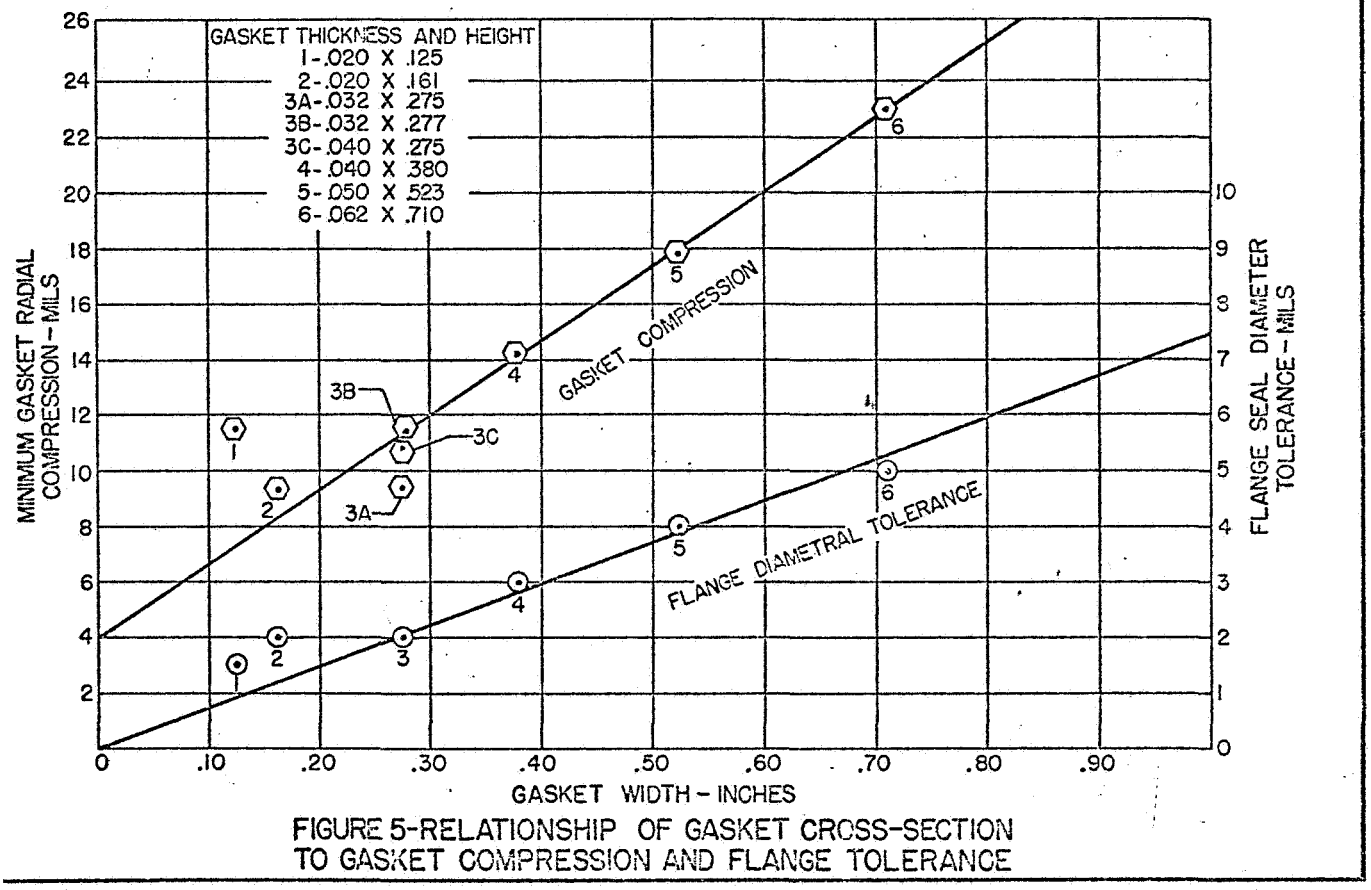

FIGURE 5-RELATIONSHIP OF GASKET CROSS-SECTION TO GASKET COMPRESSION AND FLANGE TOLERANCE

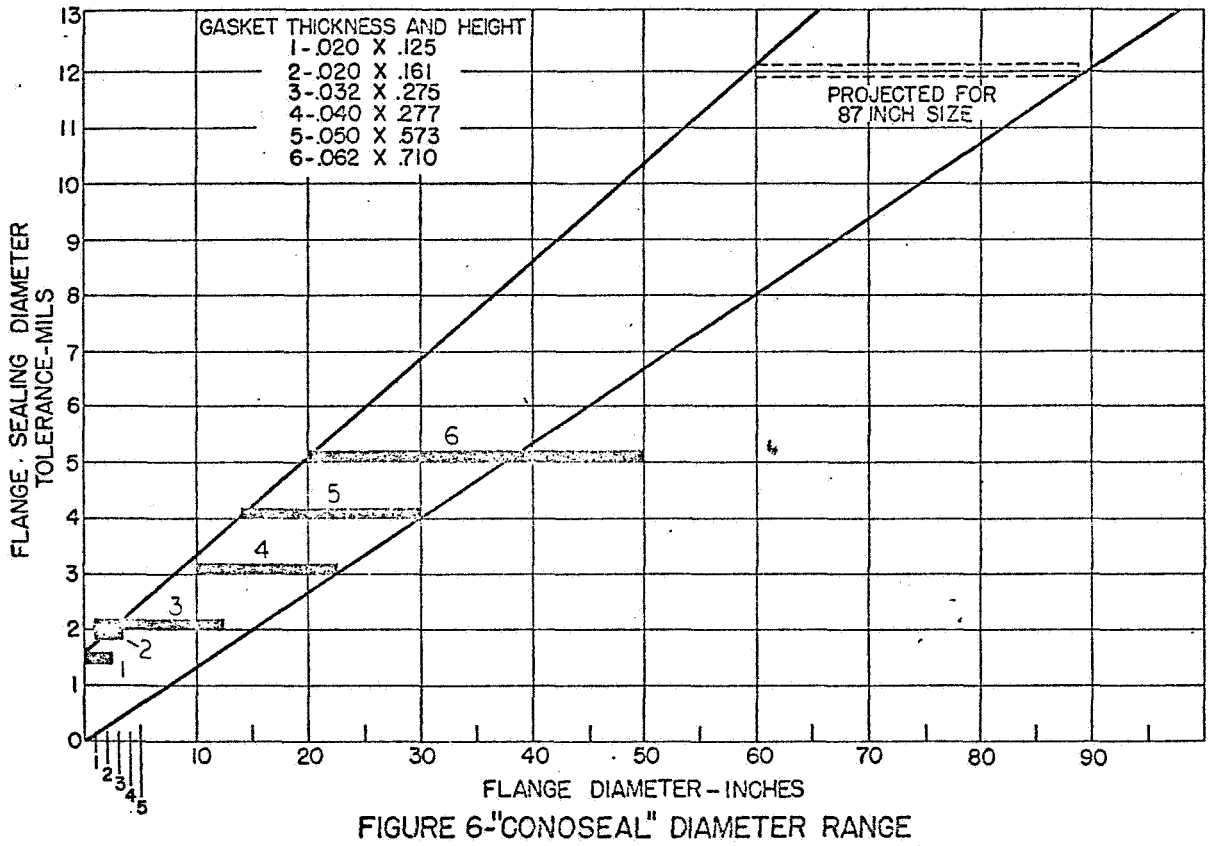

FIGURE 6-"CONOSEAL" DIAMETER RANGE

Increased flange warpage encountered on large diameters, not only in welding but also as a result of stress relaxation. Flange ovality from .005 to .010 inch on a 10-inch size to .060 inch on a 42-inch size has been found on flanges after machining.

E. Design Refinements and Applications

The CONOSEAL Sealing Concept has been incorporated into a number of challenging problem areas in the missile and nuclear fields. A few of the notable applications are listed below.

A 36-inch remotely operating CONOSEAL Joint used on Tory II nuclear propulsion ram jet engine. Gases reach a temperature of 1050°F with a pressure head equivalent to 650 psi. Figure 7 is a photograph depicting the CONOSEAL Joints employed in the engine while Figure 8 shows the complete test vehicle.

A remote-operating Double-seal CONOSEAL is shown in Figure 9. The inner and outer seals are separated by a buffer zone used to monitor any possible leakage past the primary seal. This type of joint was intially developed for use on reactors and at present is being employed in the M-I engine and the NERVA project. Sizes from 1/8 inch to 45 inches have been produced. Variations of the double seal using an organic secondary seal are being utilized by Douglas Aircraft on the Saturn DSV-IV stage.

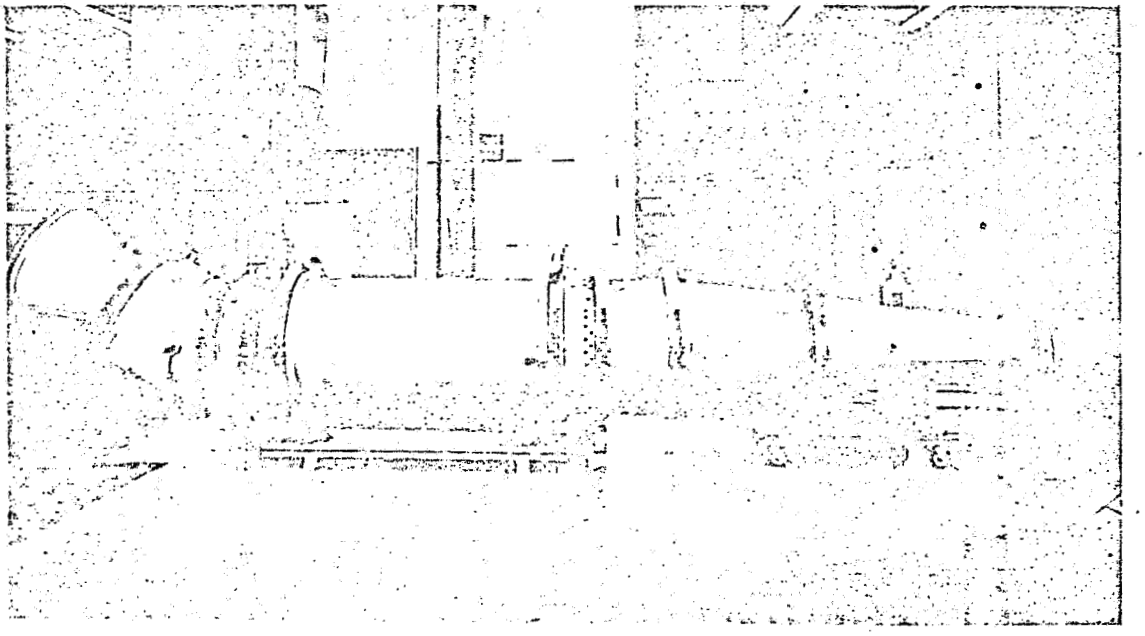

Figure 7
Remotely Operated CONOSEAL Joints - Tory 2A

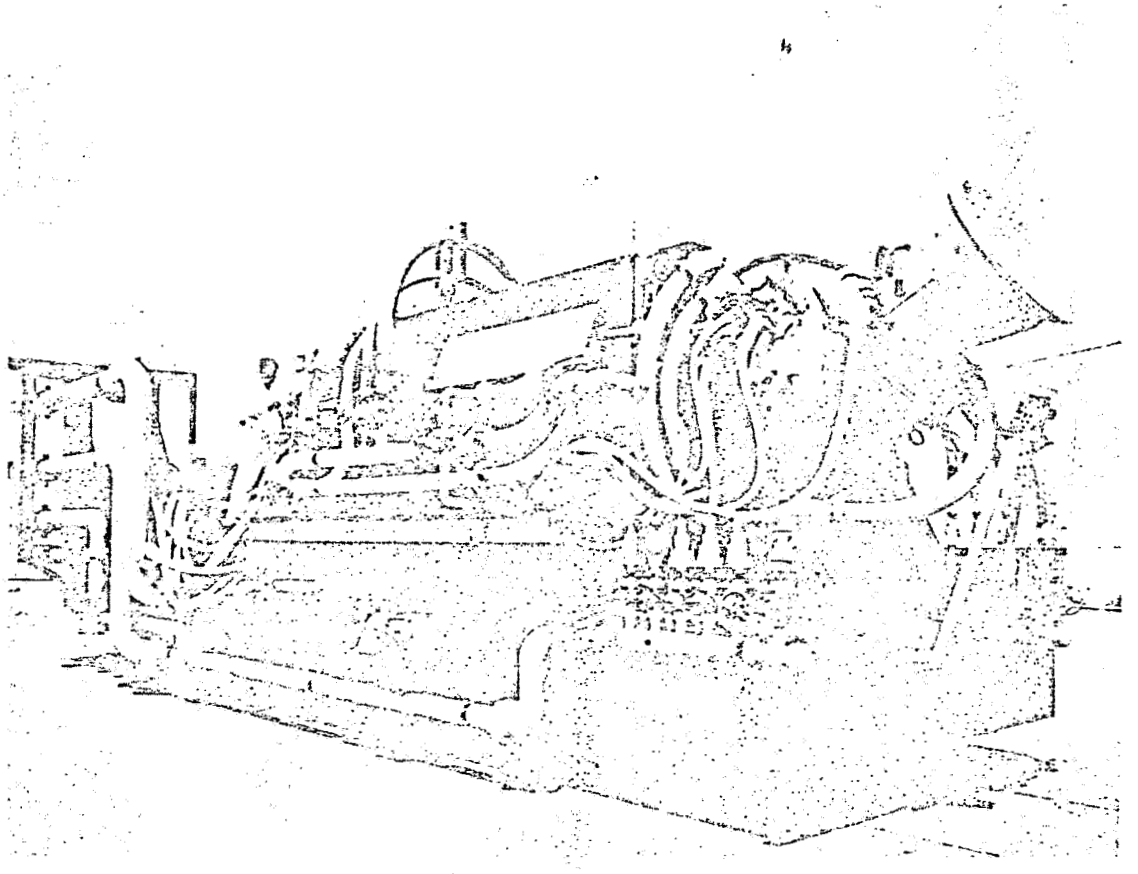

Figure 8
Tory 2A Test Vehicle

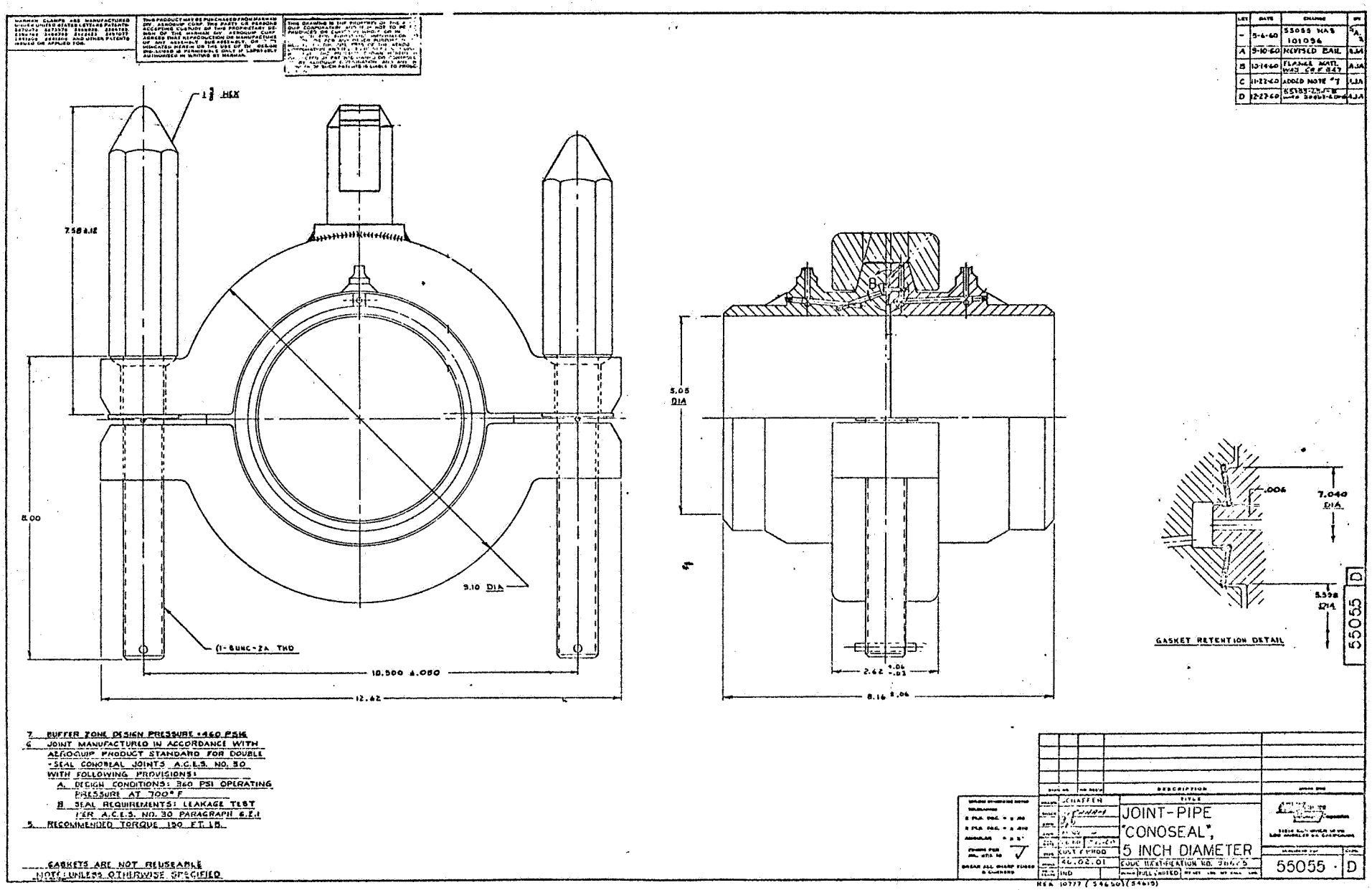

Figure 9
Double Seal CONOSEAL Joint

Figure 10 illustrates a CONOSEAL with a back-up weld-lip seal for the liquid metal system on SNAP-8. This design provides for frequent disassembly during ground testing, with permanent weld added just prior to flight time. CONOSEAL Joints have been used in liquid metal systems at temperatures up to 1350°F.

Vacuum-jacketed lines for cryogenic applications have employed CONOSEALS (Figure 11) to contain fluid and to maintain vacuum between inner and outer ducts.

Figure 12 depicts a Zircalloy-to-stainless steel permanent-type fitting as used in the CVTR reactor[5].

Other areas of incorporation include the use of a CONOSEAL in a bakeable valve[6].

Figure 13 depicts an 87-inch diameter remotely operated coupling to be actuated by four actuators simultaneously. This coupling design has been incorporated into various-size CONOSEAL duct systems and is proposed for use in the EST-1 NES duct facility for testing the NERVA engine. A subscale seal test program has been conducted on a Double-seal CONOSEAL with remote coupling[7].

PART NUMBER	PIPE SIZE	B REF	C DIA	D	E REF	F DIA	G ± .12	COUPLING HALF PART NUMBER	MALE FLANGE PART NUMBER	FEMALE FLANGE PART NUMBER	GASKET PART NUMBER	BOLT PART NUMBER	BOLT LENGTH	QUANTITY OF BOLTS REQUIRED	QUANTITY OF NUTS REQUIRED
54054-1-4	1	1.900	3.50	3.50	6.12	2.81	2.87	58852-1	58856-1	58854-1	52899-1-6	58882-400	4.00	4	4
54054-2-4	2	2.875	4.88	4.50	7.50	4.00	3.72	58852-2	58858-2	58854-2	52899-2-6	58882-500	5.00	8	8

SYM	CLASS	DESCRIPTION	DATE	APPD
C	2	WAS C SIZE PROPOSAL - LAST REV B	1-15-62	
D	2	ADDED NOTE NO. 4	2-21-62	
E	2	(1) REVISED "G" DIM: 1½ SIZE WAS 2.81, 2½ SIZE WAS 3.69	9-19-62	
F	2	(1) BOLT MATERIAL WAS A286	11-5-62	
G	2	(1) ADDED NOTE: VIEW OF -1½ SIZE SHOWN	9-6-63	

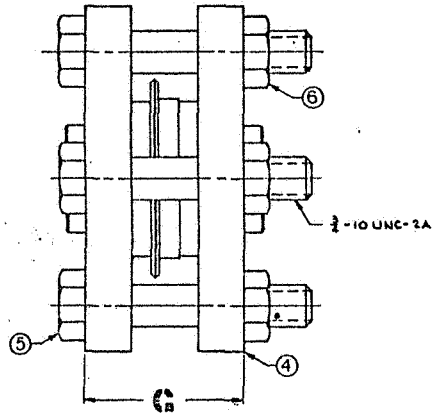

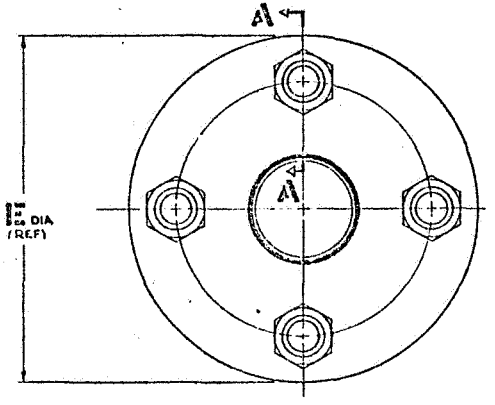

(6) VIEW OF -1½ SIZE SHOWN

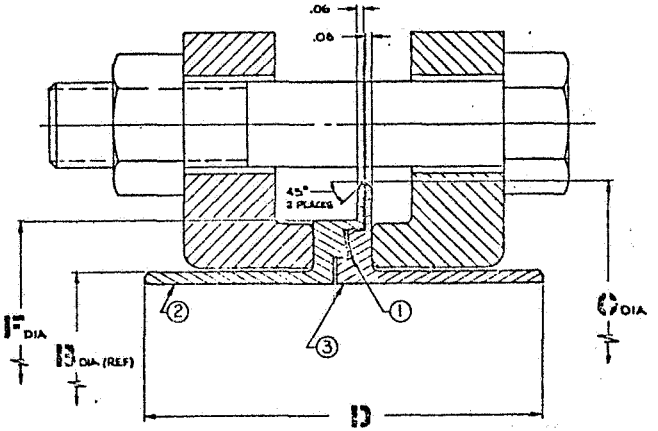

SECTION A-A
SCALE: 2/1

4. MARK TORQUE 250 LB IN. PER ACES 20 P 20
5. NUT SILVER PLATED PER AMS 2410
2. DESIGN CONDITIONS
   - OPERATING PRESSURE 15 PSIG
   - PROOF PRESSURE 100 PSIG
   - OPERATING TEMP 1200°F
   - MAX TEMP 1450°F
1. GASKET NOT REUSABLE

NOTE: UNLESS OTHERWISE SPECIFIED

ITEM	QTY REQ	PART NUMBER	NAME	MATERIAL	MATL SPEC	CODE IDENT
6	TAB	54054-6-4	NUT		ASTM A194 GRADE 8C (347)	
5	TAB	TABULATED	BOLT		AMS 5648 (316)	
4	2	TABULATED	COUPLING HALF		AISI 316	
3	1	TABULATED	FEMALE FLANGE		QQ-S-763 (316)	
2	1	TABULATED	MALE FLANGE		QQ-S-763 (316)	
1	1	TABULATED	GASKET		MIL-R-5059 COMP 316	

SUB ASSEMBLY AND MTL REQ

LIST OF MATERIAL

UNLESS OTHERWISE SPECIFIED DIMENSIONS ARE IN INCHES; TOLERANCES ON XX ± .03, X ± .010, ANGLES ± 30'
WELD SYMBOLS PER MIL-STD-15 WELD PER MIL-W-6858 AND/OR MIL-W-8611
ENVIRONMENT AND TOLERANCE PER MIL-STD-8
FINISH PER MIL-STD-10
DO NOT SCALE

TYPE C 2 P

NEXT ASSEMBLY

INDEX 46.02.01

DRAWN AJA 10-15-62
CHECKED 10-19-62
APPROVED 10-19-62
APPROVED 10-19-62
RELEASE 10-24-62
PROJECT NO. 6856
DESIGN APPROVED
APPROVED

Aeroquip AEROQUIP CORPORATION MARMAN DIVISION Los Angeles, California, U.S.A.

DRAWING TITLE
JOINT - "CONOSEAL" SCH 10 IPS

CODE IDENT NO. 80625 | SIZE D | DRAWING NUMBER 58476

SCALE NONE | WEIGHT | SHEET

58476

Figure 10
CONOSEAL Incorporated Back-Up Seal Weld Lip
SNAP 8 Program

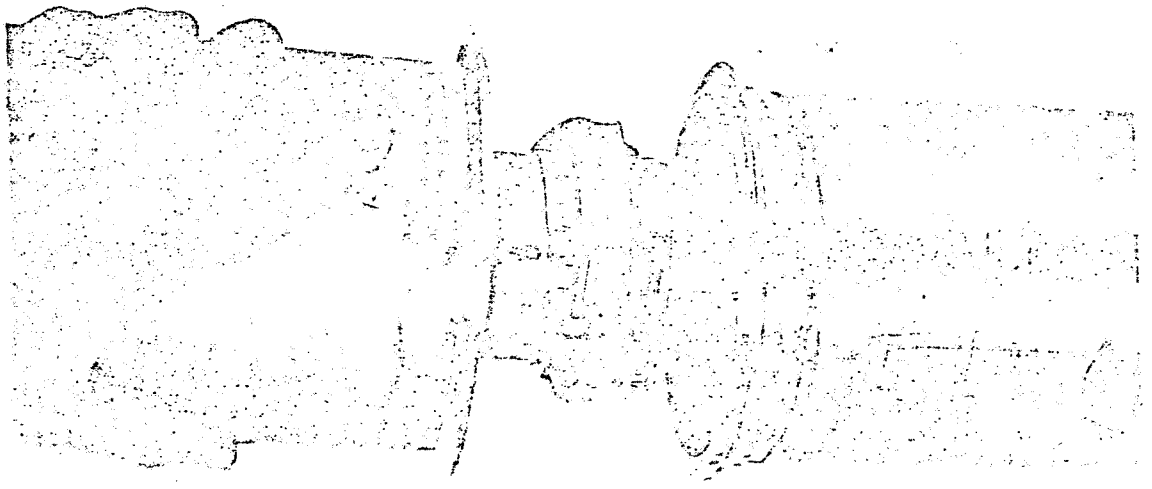

Figure 11
Joint for Vacuum Jacketed Line

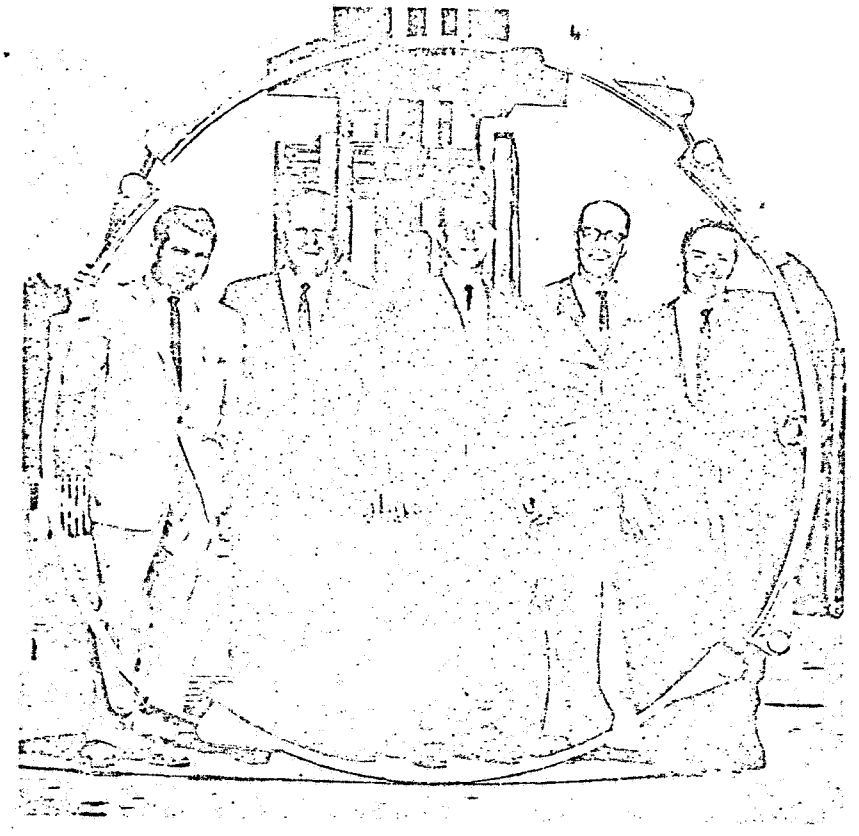

Figure 13
87-Inch Remotely Operated Coupling

PART NO.	NOM. PIPE SIZE	A DIA	B DIA	C DIA	D DIA	E	F	G	AXIAL LOAD REQD TO SEAT GASKET	MAX AXIAL PRELOAD JOINT WILL WITHSTAND
-100	1	1.315	1.049	2.36	2.11	4.12	.78	7.46	2000 LB	24000 LB
-150	1½	1.900	1.610	3.15	2.67	4.12	.78	7.46	2750 LB	29300 LB
-200	2	2.375	2.067	3.62	3.13	4.12	.78	7.46	3500 LB	33200 LB
-250	2½	2.875	2.469	4.12	3.53	4.12	.78	7.46	4150 LB	37500 LB
-300	3	3.500	3.068	5.28	4.13	6.00	1.34	10.68	4800 LB	47500 LB
-400	4	4.500	4.026	6.28	5.08	6.00	1.34	10.68	6000 LB	54000 LB
-600	6	6.625	6.065	8.40	7.13	6.00	1.34	10.68	8300 LB	66000 LB

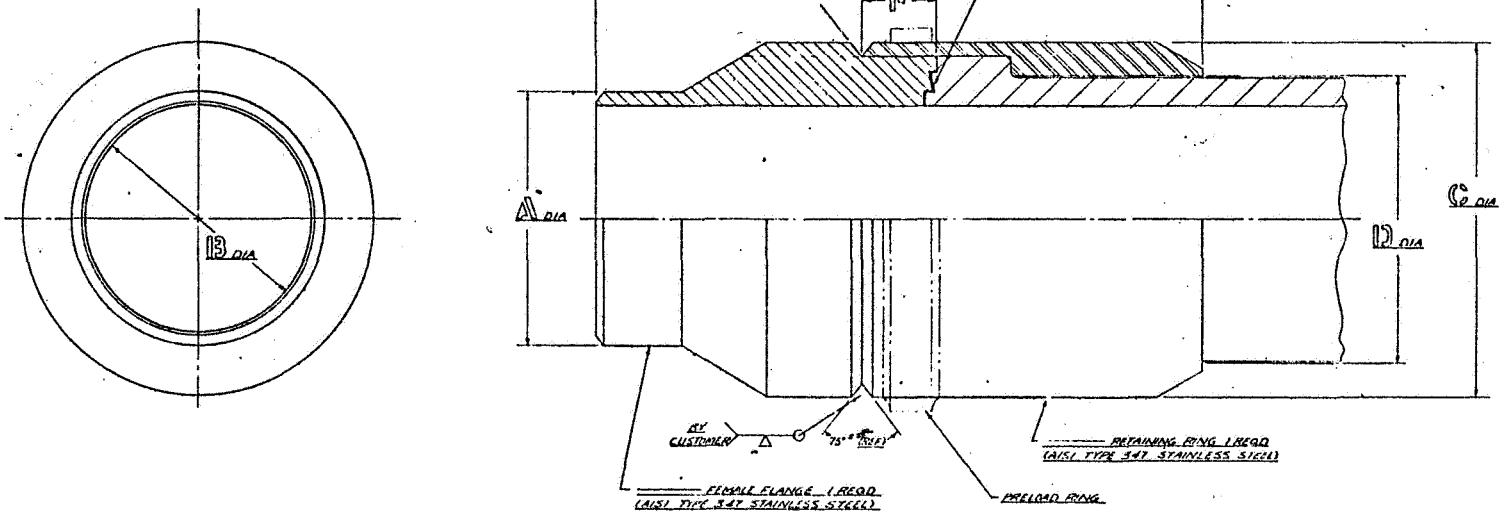

2. DESIGN CONDITIONS @ 900°F
OPERATING PRESSURE = 600 PSI
SAFETY FACTOR 3:1 FOR ZIRCALOY-2 FLANGE
SAFETY FACTOR 4:1 FOR AISI 321 SST
1. GASKETS ARE NOT REUSEABLE

JOINT ASSEMBLY "CONOSEAL", CODED

100962 -

Figure 12
Permanent Type Transition Joint

III. PERFORMANCE DATA

Evaluation of the CONOSEAL to general and specific operating parameters, various configurations and materials, over a broad range of sizes has been conducted. To attempt to present all these data here is impossible. Performance data presented will be limited to a summary of evaluation testing to general requirements, pressure and temperature limitations, effects of surface asperities, flange distortion, and installation and welding problems.

A. Surface Asperities

1. Flange Finish Requirements

Flanges with finishes to 63 RMS have been successfully tested with helium mass spectrometer. Scratches in flange sealing area, running in an axial direction are generally detrimental when they can be seen with the naked eye.

One of the most troublesome areas in the past has been the flange sealing corner. Incorrect radius, projections in flange inclined face, and tool chattering all affect sealing performance. Improved manufacturing techniques, using tracers for flange face geometry and specially ground throw-away-type tool inserts, along with more stringent quality control measures, have all but eliminated this problem area.

2. Gasket Finish Requirements

CONOSEAL Gaskets are manufactured from standard sheet or coil stock. Raw material is carefully controlled during manufacturing stages to prevent scratches on flat surfaces which are not machined. Scratches are allowed on flat surfaces within specified limits.

Gaskets are stacked for finish machining OD and ID to eliminate burrs and to maintain closer tolerances on inner and outer sealing diameters, along with finer finishes. A 32 RMS finish is specified.* A 100% visual inspection of sealing diameters is made under magnification just prior to packaging to insure that gaskets are free of nicks, burrs, and scratches.

On low-pressure applications, maximum depth of scratches has been determined by test to be 1 mil for aluminum and 0.5 mil for stainless in order to obtain a fluid-tight connection.[8]

CONOSEAL Gaskets in size range from 1/8 inch through 1 inch were originally punched with no additional machining steps. Because of the unpredictable leakage behavior of the gasket caused by scoring of the gasket during manufacture, a manufacturing process change was made to machine gasket sealing diameters.

*Gaskets have been manufactured with 16 RMS finish for ultra-high vacuum systems $< 1 \times 10^{-9}$ Torr

Improved reassembly reliability with reduced leakage rates resulted.

B. Welding

One of the most neglected or abused areas, but one that has a pronounced effect upon the sealing reliability of the CONOSEAL, is the welding of flanges to ducting. Poor welding has resulted in excessive flange warpage, flange growth, annealing of hardened flanges, along with premature weld failures.

Recommendations for welding CONOSEAL Flanges are contained in Appendix II.

C. Flange Warpage

As connector size increases, flange warpage is unavoidable. Warpage may be caused by a relaxation of stresses as a result of machining and by welding. The CONOSEAL design permits a relatively large degree of flange face out-of-flatness due to the radial-sealing concept of achieving a seal independent of flange-face alignment. Ovality in flanges is overcome within flange-to-flange and flange-to-gasket assembly clearances by the force generated by gasket during assembly.

Table V gives results of testing on a 3-inch and an 8-inch joint with flange warpage.

TABLE V

Results of Testing Sealing Capability of CONOSEAL with Flange Warpage (900 psi Joint, V-band Coupling Type)[9]

Size (inches)	Flange	Ovality After Weld (inches)	Ovality After Test (inches)	Helium Leak Rate at 1800 psi Proof Pressure
3	Male Female	.006 .007	Not recorded	4.96×10^{-9} cc/sec
8	Male Female	.008 .008	.002 .002	$< 5.9 \times 10^{-11}$ cc/sec

Flange warpage, causing a change in average sealing diameter will affect sealing reliability. For maximum performance, flange face separation as a result of warpage should be limited to one half the gasket thickness, and ovality for each flange should be limited to 0.5 mil per inch of diameter plus flange seal diameter tolerance (Reference Figure 5).

D. Installation

The installation of gasket between flanges is the same regardless of connector type. The following ground rules should be observed:

Flange faces, and especially the sealing corners, must be free of all contaminants. A lintless cloth with acetone is recommended for cleaning both flanges and gasket, unless other cleaning methods are specified for critical systems.

Gaskets should be handled carefully to prevent damage to seal corner. The gasket may be installed in either flange. The technician should be apprised of proper direction to place the gasket. Gaskets should be replaced each time a joint is assembled.

To prevent unequal loading of the gasket which may produce seating on one side first, there should not be over .020 inch variation in gap between flanges around the periphery. Alignment of the joint for installation of a V-band coupling should never require more than hand pressure. On bolted flanges, bolts opposite each other should be torqued, moving in a clockwise direction. They should not be torqued more than one half turn at a time except to make sure bolt is finger-tight prior to torquing.

There has been some concern regarding the effects of misalignment on sealing capability because of the following reasons:

Mating flange faces are not always parallel.

Mating tube sections' axes do not coincide.

Limited accessibility.

Misalignment caused by duct system supports.

Test results indicate that leakage rate will increase with increasing angular misalignment[10].

Although the CONOSEAL Configuration allows some degree of flexibility under various misalignment conditions, the maximum misalignment allowed is dependent largely upon the system design, i. e., use of bellows. Research into this region has been conducted, with the conclusion that greater reliability can be achieved by closer control in duct system manufacture and by provision of a longer flange index, along with a reduction in clearance between indexing diameters of the mating flanges.

E. Performance Evaluation

Considerable testing has been compiled on CONOSEAL Joints. Testing conformed to general and specific customer requirements for nuclear, aircraft, and missile applications. Representative test results, enveloping general design and operational parameters are delineated in Table VI.

There are many additional test reports, covering specific customer requirements, which are not included. Areas of interest, however, relating to CONOSEAL reliability are summarized below.

TABLE VI
Summary of Representative Test Reports on CONOSEAL

Size Range	Connector Type	Test Description	Report No.	Performance Tests Conducted
1/8 inch through 1 inch	Union (Threaded Fitting)	Summary of qualification & development testing of Marman P/N 54857 (stn stl) & 55800 (alum alloy) Union CONOSEAL Joints	Aeroquip Report No. 1476	Leakage, proof, installation misalignment, bending moment, thermal cycling, vibration, pressure impulse, cryogenic, reassembly. See summary page from Report 1476 in Appendix III.
1 inch through 4 inch	V-band Coupling (Lightweight)	Qualification test report of Marman Part No. 51393	Aeroquip Report No. 1360	Leakage, proof, deflection Vs. pressure, pressure drop, installation misalignment, pressure cycling, thermal cycling, bending moment, cyclic bending moment, cryogenic. See performance ratings in Appendix III.
1 inch through 12 inch	V-band Coupling (Medium weight)	Test summary of Marman CONOSEAL Tubing Joints	Aeroquip Report No. 1311	Bending moment, cyclic bending, maximum pressure, misalignment, vibration, impact, cryogenic. See performance ratings in Appendix III.
1-1/2 inch through 10 inch	V-band Coupling (Medium weight)	Evaluation test report for CONOSEAL Joint.	Beech Aircraft Report 10564-"A"	Leakage, proof, installation misalignment, load cycle, vibration, torsional load, storage (one year).
1 inch through 12 inch	Pipe Joint	Resume of CONOSEAL testing for nuclear applications	Aeroquip Report No. EDR 2127	Leakage, proof, thermal cycling, bending moment. See pipe joint performance ratings in Appendix III.

1. Allowable Leakage

The CONOSEAL Joint has repeatedly met leakage requirements of less than $1x10^{-9}$ cc/sec as measured by helium mass spectrometer under operating conditions.

2. Torque Relaxation

When recommended torques are followed, there is generally a relaxation of torque after initial load and/or thermal cycle. This is of particular importance on V-band Coupling applications where torque relaxation on the order of 25% is not uncommon. On V-band Couplings, torque drop is a result of a more even distribution of stresses around coupling periphery after joint is placed in use. Therefore, it is not required to increase torque to its original value. In fact, on high-temperature applications, it is recommended that a rigging torque be applied and then reduced to a lower value to compensate for thermal expansion differentials.

3. Reusability

Testing requirements to date have been limited to 10 to 20 reassemblies, using a new gasket each time. The results indicate that the flanges are reusable without loss of sealing capability, so long as a seal is obtained initially.

If a seal is not obtained during initial assembly, the reason generally can be traced to flange damage or other factors requiring corrective action.

To maintain the degree of reliability required, it is recommended that the flange sealing surfaces be cleaned or polished after six to ten assemblies.

IV. CONCLUSION

The need for a reliable connector is not limited to space programs. Wherever and whenever a connection is required, the demand is for increasing reliability for higher pressure and extremes of temperature, along with leakage capabilities consistent with advanced system requirements.

A continuing program of improvement to simplify and to provide a connector of unquestionable reliability is not just a requirement at Aeroquip/Marman. It is a necessity.

APPENDIX I

Calculation Methods for Stresses in CONOSEAL Joints Using V-band Couplings

Preceding page blank

INTRODUCTION

The CONOSEAL Flange design follows the rules for bolted flange connections as shown in Appendix II of Unfired Pressure Vessel Code Section VIII. The values for factors shown in Figures UA 51.1 to 51.6 for integral-type flanges have previously been used with success on a 12-inch CONOSEAL Joint subjected to the strain measurement test per paragraph UG 101 in the Unfired Pressure Vessel Code.

The CONOSEAL Coupling design is based on Aeroquip/Marman's experience on V-band Retainers, which is also substantiated by the aforementioned strain measurement test.

The required bolt load per ASME Code does not apply due to the radial seal concept. The bolt load requirement is based on the load required to seat the gasket or on the load due to internal pressure, whichever is greater.

NOMENCLATURE

Symbol	Units	Description
A	in.	Flange OD
AB	$in.^2$	Bolt Root Area
A_L	$in.^2$	Area of Coupling Leg
a	in.	Coupling Apex Thickness
B	in.	Flange ID
b	in.	Coupling Width
C	in.	Flange Hub OD
c	in.	Factor = $(a^2/a+4Q) + (A_L n/2QD)$
D	in.	Pitch Diameter
d	in.	Coupling Lug Depth
E	in.	Coupling Apex Diameter
F		Factor from fig. UA-51.2 Unfired Pressure Vessel Code Section VIII (Design Sheet II)
f		Factor from fig. UA-51.6 Unfired Pressure Vessel Code Section VIII (Design Sheet III)
G	in.	Sealing Diameter
g_1	in.	Thickness of flange Hub
g_o	in.	Thickness of flange Skirt
H	lb	Total Hydrostatic End Force
H_D	lb	Hydrostatic End Force on Area Inside of Flange
H_M	lb	End Force due to Externally Applied Bending Moment

NOMENCLATURE -- continued

Symbol	Units	Description
H_N	lb	$H + H_M$
H_T	lb	Difference between Total End Force, H, and End Force on area inside Flange, H_D
h	in.	Hub Length
h_D	in.	Moment Arm from D to circle on which H_D acts
h_M	in.	Moment Arm from D to circle on which H_M acts
h_o	in.	Factor $= \sqrt{B g_o}$
h_T	in.	Moment Arm from D to circle on which H_T acts
J	in.	Coupling OD
K	-	Ratio of Flange OD to Flange ID = A/B
L	in.	Moment Arm from Coupling Shoulder to $\mathcal{C}_L$ of Bolt
M	in.	Bolt Radius
M_D	in. lb	Component of Moment due to H_D
M_M	in. lb	Component of Moment due to H_M
M_T	in. lb	Component of Moment due to H_T
M_o	in. lb	Total Moment Acting on Flange
m	in. lb	Externally applied Bending Moment
N_O	lb/in.	End Force Per Inch of Circumference Acting on Coupling due to Operating Load
N_R	lb/in.	End Force Per Inch of Circumference Acting on Coupling due to Bolt Load
n	in.	Lever Arm on Coupling Leg

NOMENCLATURE -- continued

Symbol	Units	Description
p	psi	Operating Pressure
Q	in.	Moment Arm from D to Center of Coupling Ape:
R	in.	Radial Distance from D to Hub Diameter
r	in.	Depth of Coupling Leg
S_{AF}	psi	Coupling Apex Stress
S_{AT}	psi	Coupling Tangential Stress
S_B	psi	Maximum Allowable Design Stress for Bolt Material
S_c	psi	Maximum Allowable Design Stress for Coupling Material
S_f	psi	Maximum Allowable Design Stress for Flange Material
S_H	psi	Longitudinal Hub Stress
S_L	psi	Coupling Lug Stress
S_R	psi	Radial Flange Stress
S_T	psi	Tangential Flange Stress
T, U, Y, Z		Factor Involving K from fig. UA-51.1 Unfired Pressure Vessel Code Section VIII (Design Sheet I)
t	in.	Flange Thickness
u	in.	Coupling Leg Thickness
V		Factor from fig. UA-51.3 Unfired Pressure Vessel Code Section VIII (Design Sheet II)

NOMENCLATURE -- continued

Symbol	Units	Description
W_O	lb	Bolt Load due to Operating Loads
W_R	lb	Initial Bolt Load due to Torque
ϕ	Degree	The Angle of Inside of Coupling Leg in Contact with Flange
Θ	Degree	Friction Angle

"CONOSEAL" FLANGE DESIGN

DESIGN CONDITIONS				CALCULATIONS	
Operating Pressure, p			psi	$H = .785\ G^2p$	lb
Bending Moment, m			in. lb	$D = .5\ (E + C)$	in.
Operating Temperature			°F	$R = .5\ (D - C)$	in.
Atmospheric Temperature			°F	$h_T = .25\ (2D - B - G)$	in.
Flange Material					
Allowable Flange Stress	Oper. Temp.	S_{fo}	psi		
	Atm. Temp.	S_{fa}	psi		

FLANGE LOADS (pounds)	MOMENT ARM (inch)	FLANGE MOMENTS
$H_D = .785\ B^2p =$	$h_D = R + .5g_1 =$	$M_D = H_D \times h_D =$ in. lb
$H_T = H - H_D =$	$h_T =$	$M_T = H_T \times h_T =$ in. lb
$H_M = 1.57\ m/D =$	$h_M = h_D =$	$M_M = H_M \times h_M =$ in. lb
		$M_o = M_D + M_T + M_M =$ in. lb

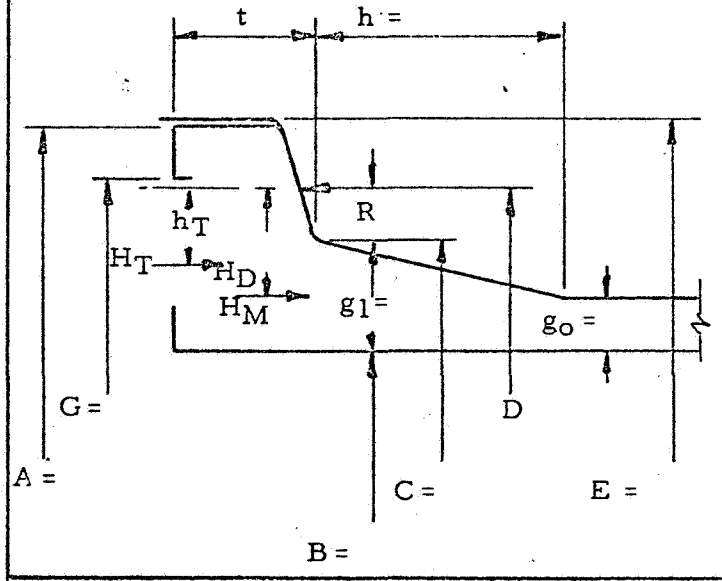

SHAPE CONSTANTS

$K = A/B =$		$h_o = \sqrt{Bg_o} =$	
$g_1/g_o =$		$h/h_o =$	
Fig. I	T =	Fig. II	F =
	U =		V =
	Y =	Fig. III	f =
	Z =		
$\rho = \frac{U}{V} h_o g_o^2 =$		$e = F/h_o =$	

FLANGE	MALE	FEMALE
t		
$\alpha = te + 1$		
$\beta = \frac{4}{3}\ te + 1$		
$\gamma = \alpha / T$		
$\delta = t^3/\rho$		
$\lambda = \gamma + \delta$		

ALLOWABLE	STRESS CALCULATION	MALE	FEMALE
$1.5\ S_{fo} =$ psi	Longitudinal Hub Stress, $S_H = fM_o/\lambda g_1^2 B$	psi	psi
$S_{fo} =$ psi	Radial Flange Stress, $S_R = \beta M_o/\lambda t^2 B$	psi	psi
$S_{fo} =$ psi	Tangential Flange Stress, $S_T = M_o Y/t^2 B - ZS_R$	psi	psi
$S_{fo} =$ psi	Greater of $.5\ (S_H + S_R)$ or $.5\ (S_H + S_T)$	psi	psi

Date _____ Project _____

Computed _____

Checked _____ Part No. _____

"CONOSEAL" COUPLING DESIGN

DESIGN CONDITIONS

Operating Pressure, p			psi
Bending Moment, m			in. lb
Operating Temperature			°F
Atmospheric Temperature			°F
Coupling Material			
Bolt Material			
Allowable Coupling Stress	Oper. Temp.	S_{co}	psi
	Atm. Temp.	S_{ca}	psi
Allowable Bolt Stress	Oper. Temp.	S_{bo}	psi
	Atm. Temp.	S_{ba}	psi

LOADS

$N_o = H_N / \pi D$	lb/in.
$N_R = W_R / D \tan (\phi + \Theta)$	lb/in.
$W_o = N_o D \tan (\phi - \Theta)$	lb
$W_R =$	lb

CALCULATIONS

$H_N = H + H_M =$	lb
$\Theta =$	°(friction angle)
$Q = .5(E-D+a) =$	in.
$n = .5(u + r \tan \phi) =$	in.
$A_L = ur =$	$in.^2$
$L = M - \sqrt{(.5J)^2 - d^2} =$	in.
$c = \frac{a^2}{a+4Q} + \frac{A_L n}{2QD} =$	

BOLT CALCULATIONS

Bolt Size	
A_B	$in.^2$
Torque	

BOLT STRESS

$S_{BR} = W_R / A_B$	psi
$S_{Bo} = W_o / A_B$	psi

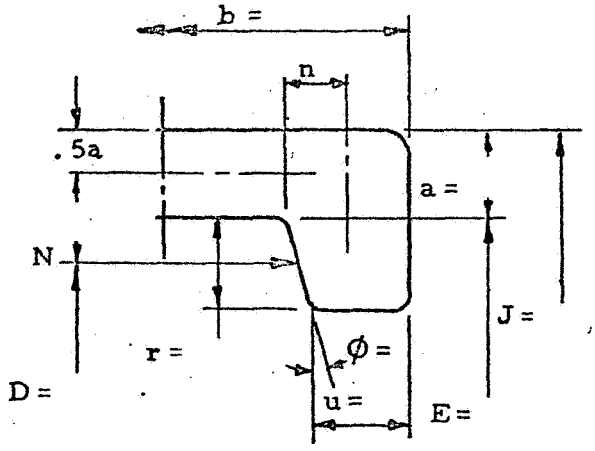

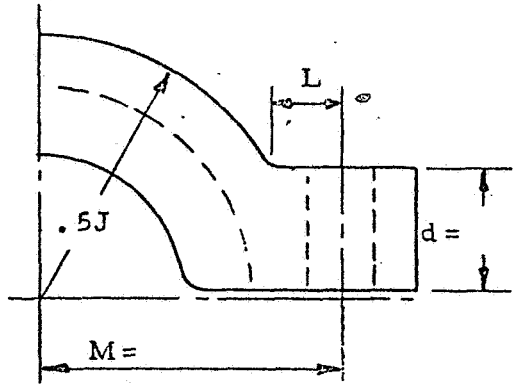

ALLOWABLE

$S_c =$ psi

STRESS CALCULATION

Apex Stress, $S_{AF} = \frac{\text{Greater Of } N_o \text{ Or } N_R}{.85\,c}$	psi
Lug Stress, $S_L = \frac{6 L W_R}{b d^2}$	psi
Tangential Stress, $S_{AT} = \frac{W_R}{2A_L + ab}$	psi

Date _____ Project _____

Computed _____

Checked _____ Part No. _____

FLANGE DESIGN

VALUES OF T, Z, Y & U (TERMS INVOLVING "K")

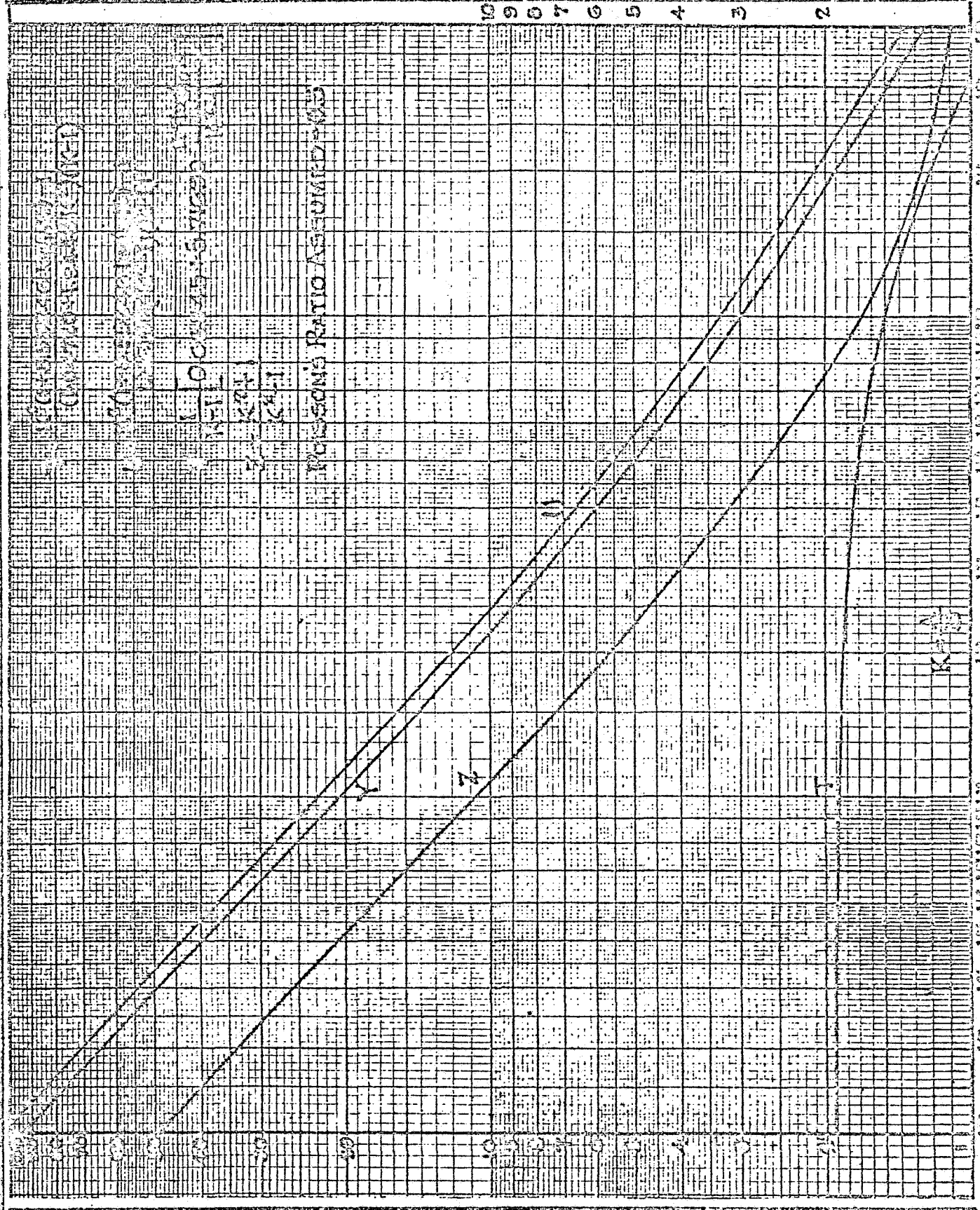

FIG. I

FLANGE DESIGN

VALUES OF F & V (INTEGRAL FLANGE FACTORS)

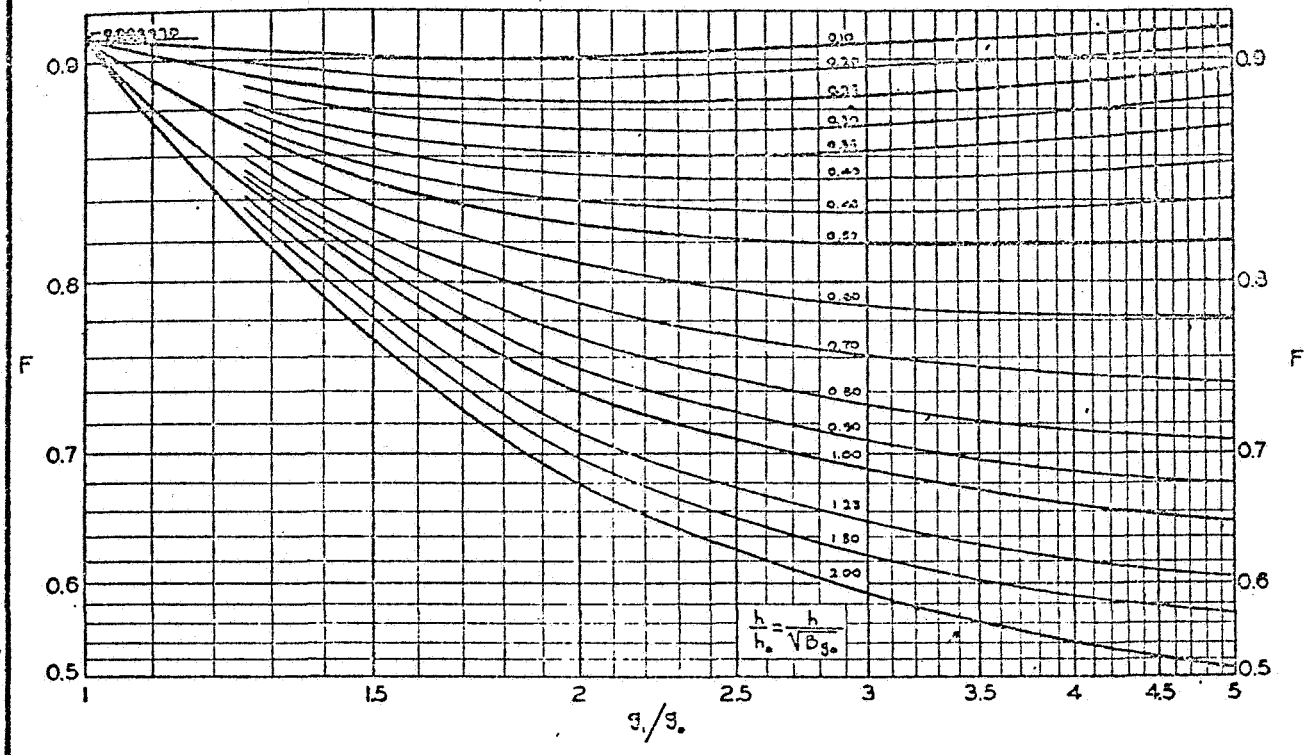

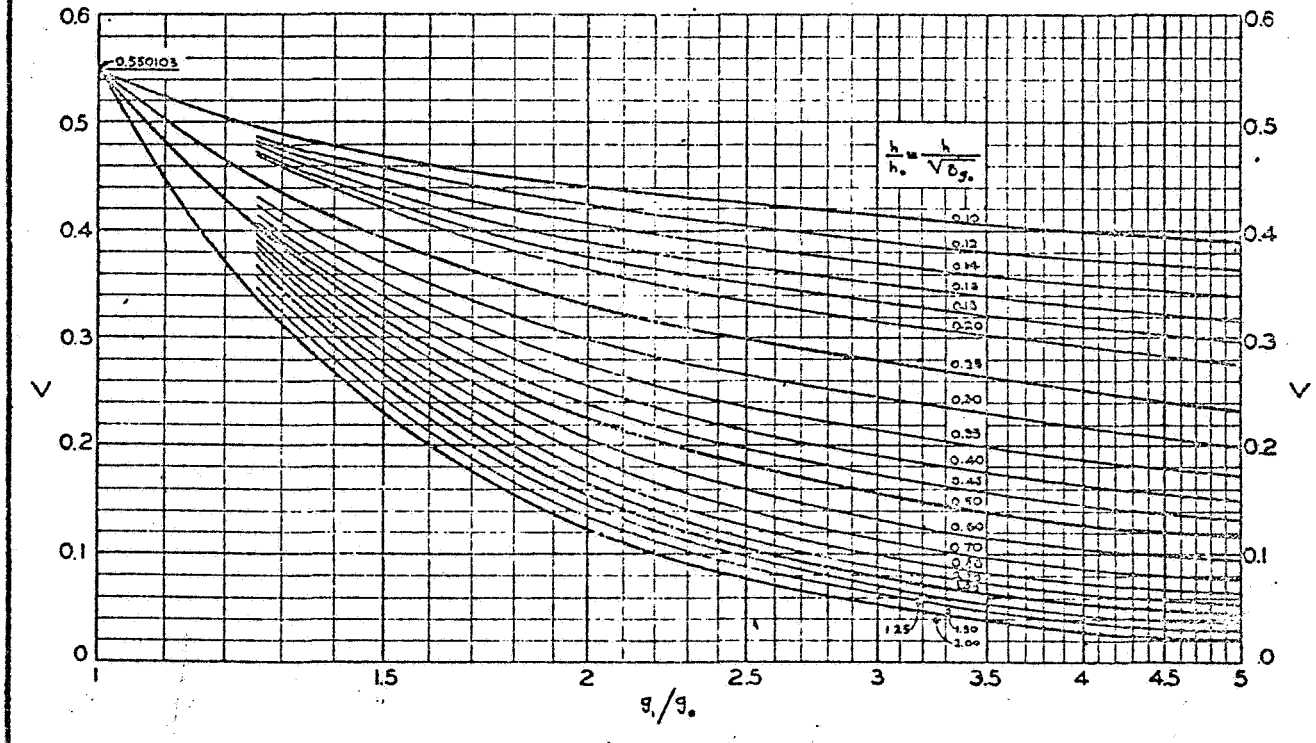

FIG. II

FLANGE DESIGN

VALUES OF "f" (HUB STRESS CORRECTION FACTOR)

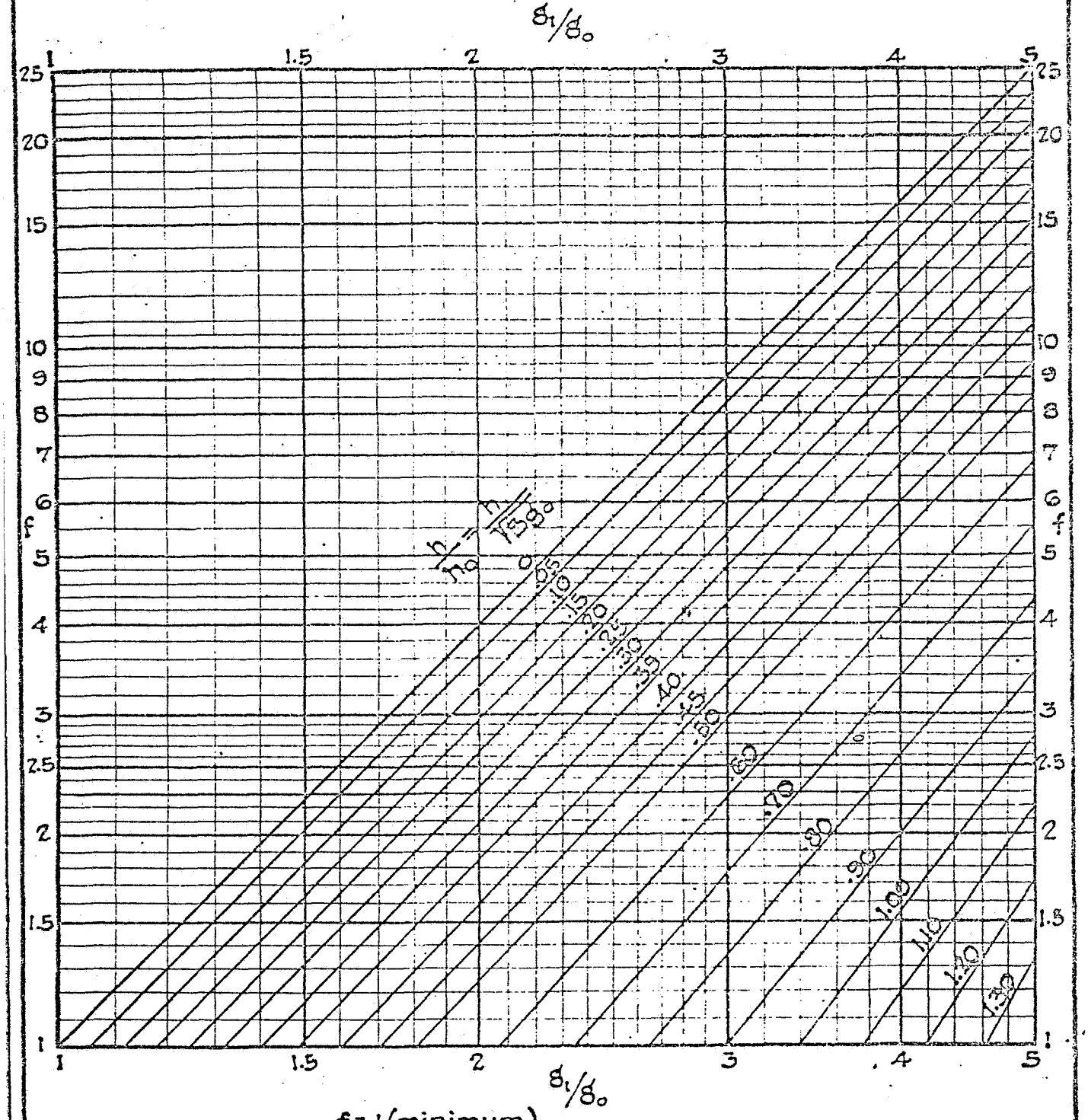

f = 1 (minimum)

f = 1 for hubs of uniform thickness ($g_1/g_0 = 1$)

f = 1 for loose hubbed flanges

FIG. III

APPENDIX II

Recommended Welding Procedures for Flange to Tubing.

Preceding page blank

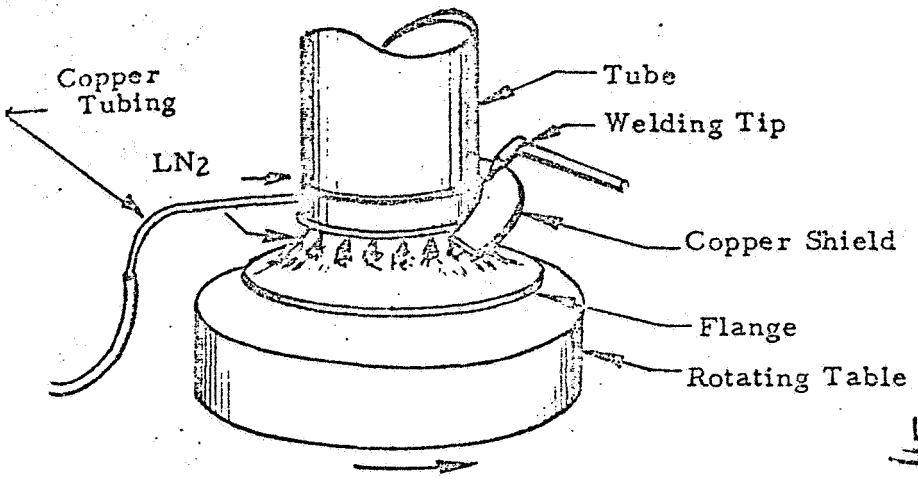

FIGURE 1

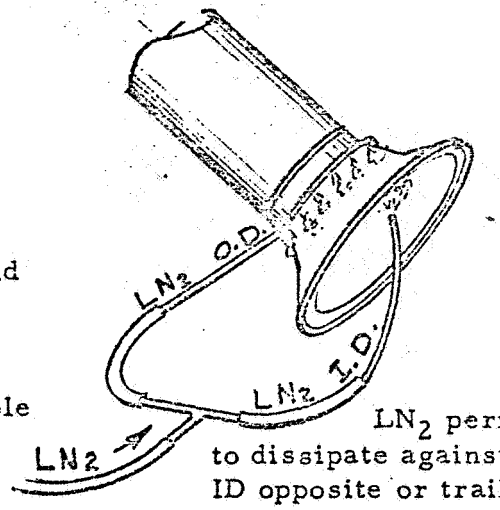

LN_2 perm
to dissipate against
ID opposite or trailir
weld being applied.

FIGURE 2

"Chill Ring" referenced herein is a device for chilling the flange using liquid nitrogen. Liquid nitrogen is circulated through a 1/4-inch copper tube (completely encircling the flange skirt) and permitted to dissipate against the flange through small (.062) holes drilled through one wall of the tubing.

These holes are angled to direct the LN_2 away from the welding operation.

The use of a copper shield is recommended to prevent escaping LN_2 from interfering with welding operation. (See Figure 1.)

"Chill Ring" should be in fixed position but permit flange to rotate inside at welding speed desired.

It is not deemed necessary to allow a period of "cool down" before welding.

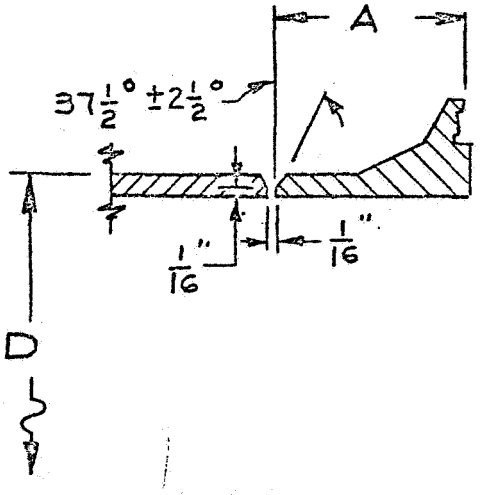

FIGURE 3

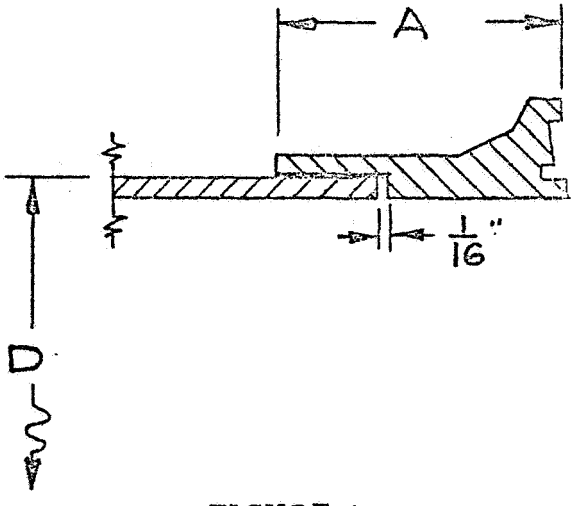

FIGURE 4

INSTALLATION OF FLANGES TO TUBE OR SHELL

1. Cut tubing off at a 90° angle with its axis and remove all burrs and sharp corners from tubing.

2. Keep flange sealing edges and surfaces protected at all times. Do not remove protective covers except when necessary.

3. Always size the tubing to the flange. This operation is of the utmost importance in controlling flatness and squareness of the flange face. The tubing-to-flange diametral clearance should not exceed .005 inch.

4. Acceptable methods of joining are: silver brazing, seamwelding, and gas or arc welding.

5. Chill rings serve to dissipate heat and reduce distortion of the flange sealing areas.

6. The use of a chill ring is recommended on all aluminum flange welding.

7. Prior to welding, the flanges should be spotwelded or tackwelded to the tubing four to ten places (depending on diameter), alternately around the tube (second weld 180° from first weld; fourth weld 180° from third weld, etc.).

8. When a method other than seamwelding is used, a 1/16-inch gap should be left between (a) end of tubing and flange skirt, Figure 3; or (b) end of tubing and socket terminus in flange skirt, Figure 4, to allow for thermal expansion and contraction.

9. When socket welding is used, Figure 4, the class of filler material should be compatible with the base metals in order to maintain the mechanical properties and corrosion resistance of the base metals.

10. A second or internal back-up chilling operation should be used on all aluminum socket-weld applications. (See Figure 2.)

11. Joint may be assembled minus gaskets to act as holding fixture for in-line assembly. This procedure is recommended for butt joint only and is not to be used for those applications where internal chill ring is recommended.

(continued)

INSTALLATION OF FLANGES TO TUBE OR SHELL

12. The use of a chill ring on metals other than aluminum alloys may be discontinued in applications of extreme diameters (over 20 inches) where flange mass is adequate to dissipate heat (where "A" dimension of either Figure 3 or Figure 4 exceeds 5 inches).

These recommendations are intended as a guide. The finished result can be only as good as the skill of the welder performing the operation.

This Welding Procedure, as applied to CONOSEAL Flanges, is intended as a supplement to Aeroquip/Marman Catalog 819 and is to be used in conjunction with Marman Drawing 52774, as well as Catalog 819.

Prepared By James A. Marks
James A. Marks
Design Engineer

APPENDIX III

Performance Ratings

SUMMARY

1. Qualification Testing. -

Test	Part No.	Specimen No.	Pressure psig	Temp °F	Leakage	Remarks
Leakage Check	54857-2 54857-8 54857-16	2A 8A 16A	4,000 4,000 4,000	Room Room Room	$<4.6 \times 10^{-11}$ cc/sec $<4.6 \times 10^{-11}$ cc/sec 5.5×10^{-10} cc/sec	Leakage checked with mass spectrometer helium leak detector.
Proof Pressure	54857-2 54857-8 54857-16	2B 8B 16B	8,000 8,000 8,000	Room Room Room	0 0 0	No visible leakage. Pressure held 5 minutes and repeated 15 times.
Installation Angular Misalignment	54857-8	8B	4,000	Room	0	Joint assembled with flanges misaligned 0°20' to 3°20' in 20' increments. Test stopped at 3°20'. Tube failure. No visible leakage.
Maximum Bending Moment	54857-2 54857-16	2B 16B	4,000 4,000	Room Room	0 0	Tube failed at maximum bending load. Tube failed at 4,515 lb in.
Thermal Cycling	54857-2 54857-8 54857-16	2B 8B 16B	2,000 2,000 2,000	1,000 1,000 1,000	0 0 0	After 100 thermal cycles, leakage was checked by decay method. No leakage was indicated.
Elevated Temperature	54857-8	8C	4,000	1,500	$<4.6 \times 10^{-11}$ cc/sec	After test, leakage was checked at room temperature with a mass spectrometer helium leak detector.
Vibration and Pressure Impulse	54857-2 54857-16	2A 16A	6,000 6,000	Room Room	* **	Conducted life cycle test per MIL-F-18280, para. 4.3.3.3. *Tube-to-flange weld failure at 280,000 bending cycles. **Tube-to-flange weld failure at 962,050 cycles.
Pressure Impulse	54857-8	8C	6,000	Room	0	100,000 pressure cycles were conducted. There was no visible leakage.
Burst Pressure	54857-2 54857-8 54857-16	2A 8A 16A	16,000 16,000 16,000	Room Room Room	0 0 0	No visible leakage or deformation with pressure held for 5 minutes.

2. Supplementary Testing. -

Low Temperature	54857-8 54857-12		4,000 4,000	-320 -320	3.6×10^{-9} cc/sec $<1.5 \times 10^{-10}$ cc/sec	Test cell was stabilized at -320°F and checked for leakage with a mass spectrometer helium leak detector.
Assembly Cycles	54857-8		0	Room		Joint assembled and torqued to 600 lb in. 15 times. Slight galling on flange-to-nut bearing surface.
Elevated Temperature	54857-8		300	1,000	0	Test cell temperature held at 1,000°F for four hours. No visible leakage.
Burst Pressure (Aluminum Joint)	55800-2 55800-8 55800-16		4,000 4,000 4,000	Room Room Room	0 0 0	No visible leakage. A mass spectrometer leakage check performed at 1,800 psi produced leakage rates $< 4.9 \times 10^{-11}$ cc/sec.
Burst	54857-6		28,500	Room	0	No visible leakage or deformation.

SINGLE SEAL PIPE JOINTS—PERFORMANCE RATINGS AND WEIGHTS

	Pipe Schedule	Pressure-Temperature Ratings: Recommended Operating Pressure (PSI)* Room Temp.	500°F.	750°F.	1000°F.	1250°F.	1500°F.	Burst Pressure at Room Temp.	Weight (Lbs.)** (Average Wt.) One Flange Stainless	Gasket Stainless	Coupling
1	Std or 40	3050	2470	2390	2130	610	165	12,200	.67	.02	2.7
	X or 80	4100	3320	3210	2870	820	225	16,400	.75		
	160	5700	4620	4470	4000	1140	310	22,800	.97		
	XX	8200	6650	6300	5740	1640	450	32,800	1.31		
1¼	Std or 40	2530	2050	1980	1770	500	140	10,120	.85	.02	3.1
	X or 80	3450	2800	2700	2400	560	190	13,800	.96		
	160	4500	3640	3530	3150	900	250	18,000	1.23		
	XX	6900	5600	5400	4830	1380	380	27,600	1.70		
1½	Std or 40	2300	1860	1800	1600	460	125	9,200	.97	.02	4.4
	X or 80	3150	2550	2470	2200	630	170	12,600	1.11		
	160	4400	3560	3450	3080	880	240	17,600	1.91		
	XX	6320	5120	4950	4420	1260	350	25,280	2.21		
2	Std or 40	1950	1580	1530	1360	390	105	7,800	1.38	.03	5.2
	X or 80	2750	2230	2160	1930	550	150	11,000	1.65		
	160	4340	3500	3400	3040	865	240	17,360	2.73		
	XX	5500	4450	4320	3850	1100	300	22,000	3.56		
2½	Std or 40	1900	1540	1490	1330	380	105	7,600	3.12	.05	13.2
	X or 80	2700	2200	2120	1890	540	150	10,800	3.42		
	160	3900	3160	3080	2730	630	215	15,600	4.96		
	XX	5300	4300	4160	3700	1060	290	21,200	7.19		
3	Std or 40	1850	1500	1450	1295	370	100	7,400	3.82	.06	14.1
	X or 80	2570	2080	2040	1800	415	140	10,280	4.69		
	160	3750	3040	2940	2620	750	206	15,000	6.78		
	XX	5000	4050	3930	3500	1000	275	20,000	10.29		
3½	Std or 40	1700	1375	1330	1190	340	95	6,800	4.78	.07	20
	X or 80	2380	1930	1870	1665	475	130	9,520	6.02		
	XX	4600	3730	3600	3220	920	250	18,400	11.39		
4	Std or 40	1580	1280	1240	1100	316	85	6,320	5.62	.08	24
	X or 80	2250	1825	1765	1575	450	125	9,000	6.94		
	160	3540	2860	2780	2480	710	195	14,160	11.88		
	XX	4200	3400	3300	2940	840	230	16,800	14.76		
5	Std or 40	1400	1130	1100	980	280	75	5,600	8.55	.10	33
	X or 80	2000	1620	1570	1400	400	110	8,000	11.71		
	160	3200	2590	2510	2240	640	175	12,800	19.58		
	XX	3800	3080	2980	2660	760	210	15,200	22.38		
6	Std or 40	1270	1030	1000	890	255	70	5,080	11.22	.11	38
	X or 80	1900	1540	1490	1330	380	105	7,600	15.02		
	160	3100	2500	2435	2170	620	170	12,400	27.45		
	XX	3600	2920	2825	2520	720	200	14,400	36.26		
8	Std or 40	1120	910	880	785	225	60	4,480	20.73	.21	57
	X or 80	1700	1375	1335	1190	340	95	6,800	31.55		
	160	2800	2270	2200	1960	560	155	11,200	53.32		

* ... pressure for flange material, other than type 347 stainless steel, may be found by ... pressure shown by factor indicated for material and temperature as shown in

... Material	Factor: Room Temp.	500° F.	750° F.	1000° F.	1250° F.	1500° F.
...	.80	.98	.88	—	—	—
...	.94	1.10	1.00	.50	—	—
...	1.00	1.00	1.00	.93	.90	.75
...	1.00	1.10	1.00	1.00	1.25	1.25
...	1.00	1.10	1.00	1.00	1.25	.77
...	.50	.25 ❶	—	—	—	—

... stress values of type 347 stainless steel for forging material ... United Pressure Vessel Code Section VIII.
... operating temperature is 450°F.

If the ambient temperature is the same as internal temperature, it is recommended that -HT coupling be used in 900-1000°F. range with a subsequent decrease in pressure. (Multiply allowable pressure at 1000°F. by .85.)

The CONOSEAL Pipe Joint will withstand working pressure, bending and temperatures simultaneously, within the limits of the accumulative loads and temperature specifications. Safety factor = 4:1.

**To determine weights of flanges and gasket made with aluminum material, multiply the above weights by .35.

Use the following formula to determine bending moment:

$$M = \frac{(P_1 - P_2)\,\pi\, D^3}{16}$$

Where M = Allowable bending moment, lb. in.
P_1 = Allowable pressure, psig, from table above.
P_2 = Operating pressure, psig.
D = Pipe O.D., inches.

PERFORMANCE RATINGS

Use Medium Weight Joint performance ratings for Bolted Joints shown in this catalog section.

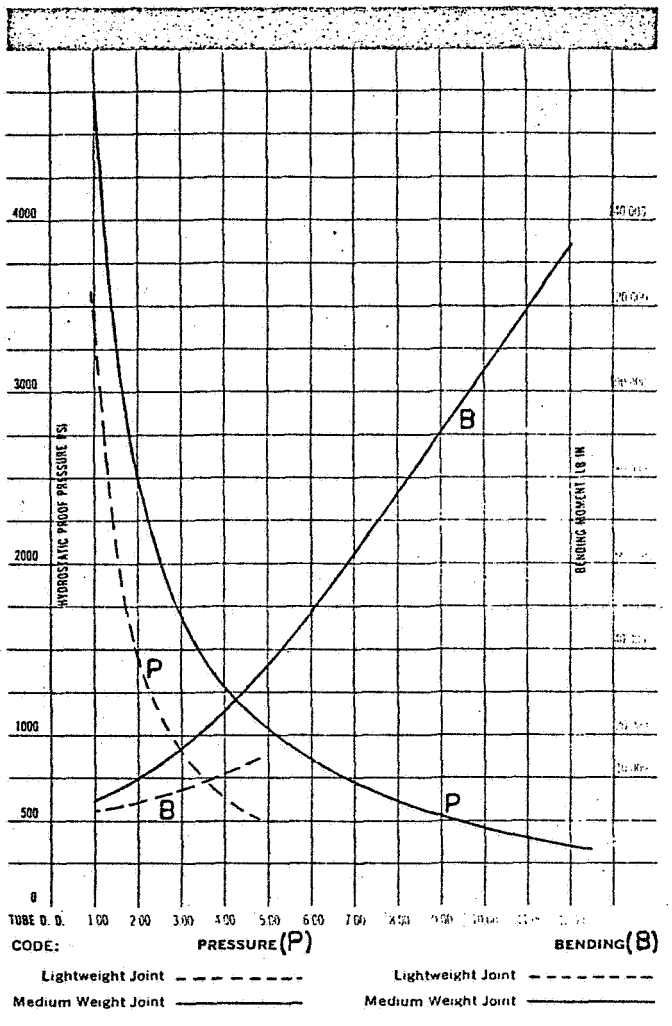

The graph indicates the bending moment and hydrostatic PROOF PRESSURE load capabilities of the Lightweight and Medium Weight CONOSEAL Tube Joints.

Operating pressure can be obtained by dividing the desired safety factor into the proof pressure rating. Burst pressure is 1½ times the proof pressure rating.

Proof pressure and maximum bending moment are based on the allowable stress value of 19-9DL at room temperature. If the joint is to be used at elevated temperatures, or if aluminum or stainless steel flanges are required, multiply the graph ratings by the values listed in the following table:

TEMPERATURE

Material	Room Temp.	400°F.	500 F.	750 F.	1000°F.	1250°F.	1500°F.
19-9DL Stainless Steel	1.00	—	.77	.68	.60	.53	.27
347 Stainless Steel	.60	—	.54	.45	.39	.35	—
Aluminum	.45	.22	—	—	—	—	—

If the joint will be subjected to combined loading (pressure and bending), divide the corrected load rating into the actual load conditions for each type of loading and express the answer as a percent. Divide this total percentage into 100% to determine the safety factor.

EXAMPLE:

A CONOSEAL Joint is required for the following conditions:

Tubing – 3.00 diameter, stainless steel

Proof Pressure – 600 psi

Bending Moment – 3000 lb. in.

Temperature – 500°F.

$$\frac{\text{Proof pressure (applied)}}{\text{Proof pressure (allowable) x temperature factor}} \quad \frac{600}{1700 \times .77} = 46\%$$

$$\frac{\text{Bending moment (applied)}}{\text{Bending moment (allowable) x temperature factor}} \quad \frac{3000}{16{,}000 \times .77} = 24\%$$

$$\frac{\text{Allowable \%}}{\text{Applied \%}} \quad \frac{100}{70} = 1.43 \text{ safety factor}$$

For applications requiring zero leakage when tested by a mass spectrometer leak detector, operating pressures should be no greater than 50% of proof pressures shown in graph above.

APPENDIX IV

Bibliography

BIBLIOGRAPHY

(1) Rodabaugh, E. C., Adam, J. W., Goobich, B., and Trainer, T. M., "Development of Mechanical Fittings--Phase 1", Technical Documentary Report No. RTD-TDR-63-14, February 1963.

(2) Floreen, E. D., "Analysis and Testing 12-inch CONOSEAL, Part Number 36444-12-347", Aeroquip Corporation/Marman Division, Report No. 1423, January 1960.

(3) Dykstra, H., "The Effects of Surface Treatment on Sealing Capability of CONOSEAL Flanges and Investigation of Various Protective Finishes", Aeroquip Corporation/Marman Division, Report No. P92084-4, January 1963.

(4) Ervin, G., "Geometrical Similarity of CONOSEAL Gaskets", Aeroquip Corporation/Marman Division Report No. EDR 2455, May 1963.

(5) Reavis, J., "CVTR Pressure Tube Fittings", Westinghouse Atomic Power Division Report No. CVNA-116.

(6) Ullman, J. R., "Commercial Seals as Seats in a Bakeable Valve", University of California, Lawrence Radiation Laboratory, Report UCRL-656-T, July 1961.

(7) Stennett, W. D., "ETS-1 NES Duct Facility Subscale Seal Test Program", Aerojet General Corporation, Report No. 2700, October 1963.

(8) Graves, R. W., "Production CONOSEAL Gasket Nick and Burr Evaluation Leakage Test", Aeroquip Corporation/Marman Division, Report No. P91471-1, January 1960.

(9) Robinson, D. S., "CONOSEAL Testing", Aeroquip Corporation/Marman Division, Report No. P91999-3, March 1962.

(10) Ohashi, C. N., "Allowable Angular Misalignment During Installation", Aeroquip Corporation/Marman Division, Report P92414-1 and -2, January 1964.

LIST OF INDUSTRY AND AGENCY ATTENDEES

GOVERNMENT AGENCIES

AIR FORCE ROCKET PROPULSION LABORATORY
Research and Technology Division
Air Force Systems Command
Edwards Air Force Base California 93523
AAMODT, GEORGE W.
FELDMAN, LT. JOHN L.
LAWRENCE, JAMES R.

LOS ALAMOS SCIENTIFIC LABORATORY
P.O. Box 1663
Los Alamos New Mexico
BRONSON, JOHN
LANDAHL, CHARLES
MELTON, BEN J. K-Division
ROGERS, JOHN

NATIONAL BUREAU OF STANDARDS
Boulder Laboratories Cryogenic Engineering Division
Boulder Colorado 80301
ROBBINS, R.F.
WEITZEL, D. H.

U. S. NAVAL ORDNANCE TEST STATION
Michelson Laboratory Metal Physics Branch Code 5012
China Lake California
LANGENECKER, DR. B.

NATIONAL AERONAUTICS AND SPACE ADMINISTRATION
Headquarters
Washington, D. C.
COMPITELLO, FRANK CODE RP
KAFKA, EGON CODE MAP

Western Operations Office
Santa Monica, California
WILSON, R. E.

Kennedy Space Center
Cocoa Beach, Florida

BALDWIN, JAMES	K-VE4
GRUMBLATT, L. J.	K-VM2
JACKSON, J. L.	K-VM4
LOTSPEICH, R. S.	K-VE23
MACKALL, RL. L.	K-VE23
MARSH, T.	K-VM42
MERSEREAU, E. F.	K-VE24
ROBINSON, J. F.	
RUSSELL, J. B.	K-VM3
SANFORD, R. J.	K-VM2

Lewis Research Center
2100 Brook Park Road
Cleveland, Ohio
BEYER, JOHN A.
LADD, JOSEPH M.
WILLOW, ROSS G.

Manned Spacecraft Center
Houston, Texas
EICHLEMAN, W. F.
THOMPSON, CLIFFORD D.

Manned Spacecraft Center
Office of NASA Resident Manager
St. Louis, Missouri 63166
DOUGLAS, W. HARRY
HOBOKAN, ANDREW
WARDELL, ANTHONY

INDUSTRIES

A.C.F. INDUSTRIES, INC.
Box. 1666
Albuquerque, New Mexico
LOGAN, S.E.

AEROJET-GENERAL CORP. (LRP)
Dept. 9725, Bldg. 2025
Box 1947
Sacremento, Cal
HENSON, F. M.

AEROQUIP CORPORATION/MARMAN DIVISION
11214 Exposition Boulevard
Los Angeles 64, Calif
BARNARD, GEORGE
DYKSTRA, H. A.
FORREST, GERALD
GRAVES, ROBERT W.
WINFIELD, ED C.

4315 Lakeview Drive
Huntsville, Alabama
MCMANUS, DEAN

AFCO LINAIR
701 N. Federal Highway
Dania, Florida 33004
MCGILL, J. H.
PETERJOHN, R. F.

AIR PRODUCTS AND CHEMICALS, INC.
Box 1687
Huntsville, Alabama
SNYDER, C. W.

ARO, INC.
Arnold Air Force Station
Tullahoma, Tennessee
BILLINGS, R. B.
BOURDET, E.
FANN, JOE D.
GUSTAFSON, P.
HART, S. W.
MATT, H. K.
MAYFIELD, R. C.
MCILLWAIN, J. T.
MILLER, L. W.
MOORE, H. D.

MULLICAN, T.
STERKEN, A.
SYKES, JIM
TRIPLETT, M. J.

BATTELLE MEMORIAL INSTITUTE
505 King Avenue
Columbus, Ohio 43201
ADAM, JAMES W.
CUNNINGHAM, G.W.
GOOBICH, BERNARD
RODABAUGH, E. C.

BELL AEROSYSTEMS
Buffalo, New York
TURANSKY, C. J.

THE BOEING COMPANY
P. O. Box 1680
Huntsville, Alabama 35801
CHAVEZ, LEO
FINDLEY, JAMES H.
KOEHLER, M. L.
STAAB, HAROLD

MICHOUD OPERATIONS
P. O. Box 26088
New Orleans, Louisiana
BENSUSSEN, ISAAC
GLEEN, DON Dept. 5-2316
GOODENOUGH, WILLIAM
OLSON, GEORGE
WELLS, TOM

P. O. Box 3707
Seattle, Washington
BARNES, TOM MS 14-30
BENJAMIN, D.E. MS 45-72
MCGILL, ANDREW

BROWN ENGINEERING COMPANY, INC.
300 Sparkman Drive, N.W.
Huntsville, Alabama
HAYES, ROBERT
KAYLOR, CHARLES
VAN EYSENBERGEN, D.

CHRISTENSEN, D. L. (Consultant)
P. O. Box 3180
Huntsville, Alabama

THE CHRYSLER CORPORATION-SPACE DIVISION
P. O. Box 857
Huntsville, Alabama 35801
HARRIS, CLYDE
HENDRIX, HOWARD

P. O. Box 26018
New Orleans 26, Louisiana
BLAKELY, RICHARD
LOOMIS, RALPH
NIELSON, CHARLES
POTRAFKE, W.

8880 Astronauts Boulevard
Cape Canaveral City, Florida
NOTARY, AL
WALL, JIM

CURTIS WRIGHT CORPORATION
Woodridge, New Jersey
MILLER, G. P.

D.S.D. MANUFACTURING COMPANY
2964 Whitney Avenue
Hamden, Connecticut
EMMERSON, JOHN O. 290 Hartland Rd, West Granby, Connecticut
SMITH, DOUGLAS

DEUTSCH HYDRAULIC COMPONENTS DIVISION
7001 West Imperial Highway
Box 90920
Los Angeles, California 90009
KELLER, GEORGE
SCHWANK, H.E.

DOUGLAS AIRCRAFT COMPANY, INC.
5301 Bolsa Avenue
Huntington Beach, California
OVERMAN, ROBERT E.
HOLDEN, R. H.

3000 Ocean Park Blvd.
Santa Monica, California
ARCHER, F. E.

2560 Walnut Avenue
Culver City, California
MCDONALD, H. D. Dept. A-2-263

Bldg. 4481, Rm. 58
George C. Marshall Space Flight Center
Huntsville, Alabama
ARCHER, DOUGLAS
ARMIJO, TOM
GAUTHIER, GEORGE A.
SHEPARD, F. J.

GENERAL DYNAMICS/ASTRONAUTICS
P. O. Box 1128
San Diego, California 92112
AGUILERA, ENGIGUE P.
GRIMES, LARRY E.
PRINCE, W. A. Mail Zone 572-10
ROBERTS, P. W. Dept. 662-7

GENERAL ELECTRIC COMPANY
Advanced Technology Laboratories.
One River Road
Schenectady 5, New York
GITZENDANNER, L. G.

LEVY, S.
MARR, J. W.
RATHBUN, F. O., JR.
WALLACH, J.

Missile and Space Division
Valley Forge Space Technology Center
Box 8555
Philadelphia, Pennyslvania
BOYLE, E. H.

R-QUAL-AMM
George C. Marshall Space Flight Center
FERRITER, P. J.

GEOPHYSICS CORPORATION OF AMERICA
Bedford, Massachusetts
POSCHENRIEDER, WALTER

GRAY TOOL COMPANY
P. O. Box 2291
Houston, Texas
BOLLFRASS, C. A.
LATHAM, R. E.
LETLOW, ED

GRUMMAN AIRCRAFT ENGINEERING CORP.
Bethpage, N. Y.
MARX, H.
SCHLICHTIG, J.

HARRISON MAFG. COMPANY
Burbank, California
WILLIAMS, R. H.

HOKE, INC.
1747-C La Visita Rd.
Atlanta 6, Georgia
TRUNZO, C. A.

HYDRODYNE CORP., SKINNER SEAL DIVN.
7350 Coldwater Canyon Avenue
North Hollywood, California
JOHNSON, WILLIAM J.
WEST, CLARE E.

IIT RESEARCH INSTITUTE
Technology Center
10 W. 35th Street
Chicago 16, Illinois
BAVER, PAUL
BOWMAN, C. E.
GLICKMAN, MYRON
IWAISUKI, F.

JOHNS-MANVILLE
Division Headquarters
22 East 40th Street
New York 16, New York
BROWN, N. D.
DUNKLE, H. H.
800-101 Marietta Building
Atlanta 3, Georgia
ALFRIEND, W. J., JR.
P. O. Box 9066
Birmingham 13, Alabama
CROUCH, W. M.

LOCKHEED MISSILES AND SPACE COMPANY
7701 Woodley Avenue
Van Nuys, California
BIRTHRONG, J. E.
GILMOUR, R. B.

LOCKHEED GEORGIA COMPANY
Marietta, Georgia
YANG, HERMAN

LOCKHEED PROPULSION COMPANY
Division of Lockheed Aircraft Corporation
P. O. Box 11
Redlands, California
CAMPBELL, PHILLIP

MARTIN COMPANY - DENVER DIVISION
The Aerospace Division of Martin-Marietta
Denver 1, Colorado
ALLEN, H. N. P. O. Box 179, Mail No. 165
DAY, W. A.
FATINO, C. C.
HERBST, GEORGE F. Mail No. L-8, P. O. Box 179
MARCUS, J. P. Mail No. A-165
RUSCIO, D.
SCHROEDER, ROBERT L. P.O. Box 179, Mail No. A-130
SPRENGER, DON P.O. Box 1176, Mail No. C-188
TIMMONS, K. P. P. O. Box 179, Mail No. A-241
WERKMA, M. J.
ZIMMERMAN, J. A. Mail No. D-1

MARTIN COMPANY
Baltimore, Maryland
SNYDER, ROBERT O.

MCDONNELL AIRCRAFT CORPORATION
Lambert - St. Louis Municipal Airport
Box 516
St. Louis, Missouri 63166
ELDRIDGE, M. T.
JAHN, CHARLES
LAY, GEORGE R.
MCCANDLISH, E. C.
SNYDER, J. R.

NARMCO, R&D DIVISION, TELECOMPUTING CORPORATION
3540 Aero Court
San Diego 23, California
GOSNELL, R.
WILSON, F.

NATIONAL UTILITIES CORP.
135 East Railroad Avenue
Monrovia, California 91016
ABBOTT, MILES C.
HUNT, WYNN
MORROW, RAY

PARKER AIRCRAFT COMPANY
5827 West Century Blvd.
Los Angeles 9, California
BRAGG, K. R.
PICKETT, JAY

9400 Memorial Parkway, S. W.
Huntsville, Alabama
SCHLOEMER, P. G.
WARD, DAVID

PARKER-HANNIFIN CORP.
17325 Euclid Avenue
Cleveland 12, Ohio
RUSSELL, JOHN G.
SULLIVAN, H.

PARKER SEAL CO.
10567 Jefferson
Culver City, California
JELINEK, JERRY G.

RAYBESTOS-MANHATTAN, INC.
940 Rayman Street
Bridgeport 2, Connecticut
D'OLIER, GEORGE
EHMAN, J. M.
MCBREARITY, F.

REPUBLIC AVIATION CORPORATION
Farmingdale, New York
BERNARD, G. F.
SCHUTZMAN,

RESISTOFLEX CORPORATION
Roseland, New Jersey
BELYEA, H. M.
BROCK, F. H.
COZZENS, C. C.

ROCKETDYNE DIVISION OF NORTH AMERICAN AVIATION
6633 Canoga Avenue
Canoga Park, California
DANIELS, C. M.
TELLIER, G. F.
SMITH, HAMPTON MSFC

NAVAN PRODUCTS, INC.
1320 E. Imperial Highway
El Segundo, California
MORAN, ROBERT L.

NORTH AMERICAN AVIATION - LOS ANGELES DIVISION
International Airport, Los Angeles California
RUNFOLA, BENEDICT A.
SLOUGH, JAMES F., JR.

SPACE & INFORMATION SYSTEMS DIVISION
12214 Lakewood Blvd.
Downey, California
FIELD, W. E.
SMITH, STAN

COLUMBUS DIVISION
4300 East 5th Avenue
Columbus 16, Ohio
DEMARCHI, J. N. Dept. 63, GP453

NORTHRUP SPACE LAB.
6025 Technology Drive
Huntsville, Alabama
KOSFELD, OTTO R.
LIGOCKI, JEROME
MAJESKE, LEONARD M.

PRATT & WHITNEY COMPANY, INC.
COMOLLI, C. R.

RUSSELL ASSOCIATES, INC.
2516 N. Memorial Parkway
Suite E.
Huntsville, Alabama
STUART, RICHARD E.
STUART, ROBERT

SEALOL, INC.
P. O. Box 2158
Providence, Rhode Island 02905
BIELLO, S. J.
STEVENS, J. B.

P. O. Box 56
Mississippi City, Mississippi
ASH, TOM
BUSBY, K. D.

SPACE CRAFT, INC.
8620 Memorial Parkway, S.
Huntsville, Alabama
ARMSTRONG, ROBERT

THIOKOL CHEMICAL CORPORATION
Reaction Motors Division
Denville, New Jersey 07834
AITKEN, JAMES
MILLER, JACK
SOSSONG, HENRY

THOMPSON RAMO WOLLDRIDGE
Electro Mechanical Division
23555 Euclid Avenue
Cleveland 17, Ohio
ROWAN, J. W.
URICH, J. F.

TRW SPACE TECHNOLOGY LABORATORIES
One Space Park
Redondo Beach, California
HOWELL, GLEN W.
MOORE, DAVID E.

VOI-SHAN MANUFACTURING COMPANY
505 Seminary South Office Bldg.
Fort Worth, Texas
GATES, W.

8463 Higuera Street
Culver City, California
SCOTT, W. S.

WESTINGHOUSE ASTRONUCLEAR LABORATORY
P. O. Box 10864
Pittsburgh 36, Pennsylvania
HENGSTENBERG, T.
MANJOINE, M. J.

E. B. WIGGINS, INC.
3423 East Olympic Blvd
Los Angeles, California
CANNON, C. D.
THOMPSON, PAUL

WYLE LABS
7800 Governors Drive
Huntsville, Alabama
ANDRIULLI, J.
DE ANGELIS, H.

APPROVAL

PROCEEDINGS OF THE CONFERENCE ON DESIGN OF
LEAK-TIGHT SEPARABLE FLUID CONNECTORS
March 24, 25, 1964
Volumes I and II

The information in this report has been reviewed for security classification. Review of any information concerning Department of Defense or Atomic Energy Commission programs has been made by the MSFC Security Classification Officer. This report, in its entirety, has been determined to be unclassified.

C. C. Wood

C. C. WOOD
Conference Chairman